BEHAVIOUR OF RAMMED EARTH STRUCTURES: SUSTAINABLE MATERIALS AND STRENGTHENING TECHNIQUES

Dissertation

submitted to and approved by the

Department of Architecture, Civil Engineering and Environmental Sciences
University of Braunschweig – Institute of Technology

and the

Department of Civil and Environmental Engineering
University of Florence

in candidacy for the degree of a
Doktor-Ingenieurin (Dr.-Ing.) /
Dottore di Ricerca in Civil and Environmental Engineering

by

Federica, Loccarini
born 11.05.1986
from Senigallia (AN), Italy

Submitted on	28.02.2017
Oral examination on	09.05.2017
Professorial advisors	Prof. Giovanna Ranocchiai Prof. Harald Kloft

2017

To my free time

Abstract

In this thesis, a natural reinforcement method for earth structures is proposed. In particular, this research focused on the possibility of building and modeling a structural system made with rammed earth strengthened with jute fabric.

In recent years, research has turned the attention towards the materials obtained from renewable sources, biodegradable and easily recoverable at the end of use.

Earth is a natural traditional building material used all over the world and, as such, it has always been used in accordance with local traditions that are based on empirical knowledge. However, the preservation and enhancement of traditional earthen masonry, as well as the practice of construction with raw earth material for new buildings, needs a deep scientific knowledge of constructive techniques and of physical and mechanical properties of the material. The possibility of proposing earth material for new constructions is based on the use of reinforcement systems to yield appropriate renovations. Acting with suitable corrections and devices, earthen buildings can be used even in areas subject to seismic risk, guaranteeing acceptable safety. The aim of the reinforcement intervention is to increase resistance against the seismic actions and improve the ductility, both for the individual structural elements and for the construction. Artificial fiber composites are commonly used as reinforcement of masonry structures both in view of the seismic retrofitting of historical buildings and of the realization of new constructions which structural performances are adequate also in seismic areas. Correspondingly, biocomposites are being used as a reinforcement of earth buildings, being compatible with earth architecture from the point of view of environmental sustainability.

This research work fits in the research field of FRCs (Fiber Reinforced Composites) as reinforcement method for masonry structures with the aim to extend and adapt to natural fibers, test methods and procedures of data treatment, useful to interpret the parameters that rule the materials behaviour and the interaction between parts. In order to design a reliable experimental technique to determine the necessary properties for the successive step of designing a reinforcement system, preliminary tests were necessary to assess the materials characteristics. Mineralogical, geotechnical and mechanical earth's characteristics were investigated, even with the use of eco-friendly additive. Tensile tests on jute yarns and jute strips were carried out. Test results were organized and statistically analyzed in order to interpret the basic laws of scale effects which influence is necessary to account for in the successive use of mechanical parameters.

After materials characterization, the adhesion capacity of the reinforcement package composed by jute fabric and earth-gypsum matrix was investigated. Since the composite material strips, externally bonded to rammed earth supports, are generally subjected to peel and tangential loads on the bonding surface, the determination of the adhesion properties

was considered a fundamental issue to produce specific rules that adequately support designers. In particular, an experimental campaign of peeling tests of jute fabric strips applied on prismatic earth specimens was carried out to evaluate the adhesion properties of the strengthening system. The results are compared with those obtained from single lap joint tests and interpreted with existing analytical models. In order to improve the knowledge concerning this reinforcing technique, necessary to assess appropriate interventions on existing buildings, an experimental program was carried out concerning the analysis of the mechanical behaviour of this type of reinforcements applied to rammed earth arches loaded asymmetrically. The arches were subjected to asymmetric load condition increasing up to incipient collapse characterized by the opening of four hinges. To verify the results obtained from the experimental tests the ultimate loads of the arches were calculated by limit analysis. Subsequently the arches were strengthened with jute fabric and tested again in order to verify the reinforcing ability of the fabric. The biocompatible reinforcement made with jute fabric and earthen matrix showed that it is possible to significantly increase the bearing capacity and the kinematical ductility of structural elements made with rammed earth.

Acknowledgements

The experimental work was conducted partially at the University of Florence in Italy, partially at the TU Braunschweig in Germany and partially at the Universitat Politècnica de València. After three years of research work, it is not easy to list and thank all the people that have contributed to the realization of this work. Firstly, I would like to thank my supervisors, Professor Ranocchiai and Professor Kloft for their guidance over the last three years. Every meeting with Professor Ranocchiai was always very helpful and she was a really great support and guide during my PhD activity. The interest in this research topic of Professor Kloft allows me to continue working on earth constructions. I would like to thank my Italian co-tutor Professor Mario Fagone who helped me a lot with every technical and scientific matter, Spanih co-tutor José Ramón Ruiz Checa and also Pedro Antonio García, the technician who have helped me set up my laboratory work at the the Universitat Politècnica de València. Among my unofficial supervisors I want to thank also Professor Briccoli Bati (Italian tutor for the first year of my PhD) for the scientific and moral support and expert guidance she gave me during my PhD activity. I would like to thank Fabio Fratini of CNR ICVBC of University of Florence that performed the Mineralogical analysis on soils, Fabrizio Andriulo of CSGI of Florence for suggestions on the materials analysis; the architects Guido Morelli (co-author in our master degree thesis), Sara Samorè, Cecilia Lodi Rizzini and Andrea Piredda, from which thesis I used some data and results; the students Lorenzo Gili and Michele Ficeli who helped me in the construction of the third arch after it was accidentally destroyed.

A thank you goes to the PhD colleagues who have shared with me this path and to the German colleagues that always welcomed and helped me during my stays at the Institute of structural design of the TU Braunschweig. I would like to thank also Gabriele Mertz who took care of me during my stays in Germany.

Finally, I really want to express all my gratitude to all the people that have contributed indirectly to this work with their emotional support. First of all, to my family, who has always supported me in every choice, and to my friends, in particular Cecilia Lodi Rizzini, Stefano Dore, Rodrigo Patti, Irina Danieli, Paolo Privitera, Roberta Perria, Oskar Rojewski, Maria Diodato, Eleni Andreou, Elpiniki-Maria Pnevmatikou, Giulio Russo and Pina Nicoletta De Cicco that supported me in all the countries that I stayed.

Federica Loccarini

Florence, Italy, December 2016

Preface

This thesis was submitted to the Department of Civil and Environmental Engineering of the University of Florence in Italy and to the Department of Architecture, Civil Engineering and Environmental Sciences of the TU Braunschweig in Germany, as a partial fulfilment of the requirements to obtain the PhD degree. The work presented was carried out in the years 2013-2016 partially at the department of Civil and Environmental Engineering of the University of Florence under the supervision of Prof. Silvia Briccoli Bati (Italian tutor for the first year of my PhD), Prof. Giovanna Ranocchiai (Italian tutor) and Professor Mario Fagone (Italian co-tutor), partially at the Institute of Structural Design, University of Braunschweig under the supervision of Prof. Harald Kloft (German tutor) and partially at the Universitat Politècnica de València under supervision of Prof. José Ramón Ruiz Checa (Spanish co-tutor).

Objectives and thesis structure

The main objective of this work is to refine and tune test methods useful to analyze the natural material employed for the proposed reinforcement method of earth structures and to verify the effectiveness of a reinforcement system made with jute fabric and earth matrix. The intent is to give a contribution in research field of rehabilitation and new construction of earth structures. The practical purpose of the research brought to an across-the-board path, among different problems such as material characterization via experimental analysis, statistical data treatment, adhesion theories and the approach to the arch stability. For this reason, the structure of the thesis is organized to face a topic for each chapter starting with a relatively brief introduction to the argument, main conclusions and bibliography related to the treated problem.

In **Chapter 1** a general overview of the topic and the motivations behind this work is given. In the first part of the chapter, historical and general aspects of earth constructions, are presented. Regulations and material features are quickly presented. In particular, the review is focused on rammed earth techniques end methods to improve the material performances (stabilization processes). The most important previous works on the topic are summarized and discussed. The second part of the chapter is focused on possible applications of this material in the modern context in light of the new research about reinforcement systems already developed. Vulnerability of earth structures has proven to be one of the biggest open questions for these kinds of structures. Current studies on earth reinforced structures are reported. In the last part of the chapter the method proposed in this thesis is explained and the motivations behind it are given and explained. Note that

many of the cited papers have been written during the period in which this thesis was developed, showing the growing interest on the topics.

Chapter 2 shows how to approach to the research topic starting from the experimental campaigns for the materials characterization. In this chapter, the previous experiences are summarized in order to justify choices and define the starting point. The first section regards the analysis of soils used in this research work. In particular the mineralogical, geotechnical and mechanical characterization of the earth is reported. In the second part the experimental campaigns on jute yarns and jute fabric are presented and a statistical model able to analyze the obtained results is proposed. The goal of this chapter is to propose an approach useful to investigate these natural materials in view of the successive necessity of the design phase.

In **Chapter 3** the interaction between fabric reinforcement and substrate is studied and the adequate test procedures to determine the adhesion capacity are selected. In the first part of the chapter a brief introduction about composite materials and bio composites is reported, paying particular attention to the composites used as reinforcement system for masonry structures. The most important studies on the adhesion problem are summarized focusing on the model adopted to analyze the results of the experimental program. The design of test set-up is described. The results of lap joint tests and peeling tests of jute fabric applied on earth supports are reported and compared. The interface stress distribution is reported.

In **Chapter 4** the static theories of masonry arches are reported and the case study is described. A quick review on static theories of unreinforced arches and on the studies of reinforced arches is reported. The main problems and failure modes of reinforced masonry arches are briefly explained. The second part regards the experimental campaign on rammed earth arch models. The results of the load tests on unreinforced and reinforced arches are organized in data sheets following the chronological order with comments and description of the phenomena occurred during the test. In the last part of the chapter the results are interpreted in light of the conclusions arising out of the previous chapters.

In the **Chapter 5** conclusions about the PhD thesis are drawn. The main goals achieved in this thesis are summarized and suggestions for future developments of the work conducted are given

Contents

1 General overview on earth constructions

1.1 Historical and general aspects

In the current context of sustainable development, the renewed interest in raw earth as a building material derives from several qualities such as suitability to satisfy the need of low cost housing, self-build practice and preservation of natural resources (Pacheco-Torgal and Jalali 2012). Raw earth is one of the earliest and most widespread building materials in the world. It is estimated that one third of the world population, spread across six continents, lives or works in buildings made in rammed earth. Among the oldest earthen buildings in the world that still can be seen today the citadel of Ghazni in Afghanistan, the fortress of Paramonga in Peru, the Mosques of Mali, the Jesuit churches in Argentina, the tower houses of Yemen and, as shown in figure 1, the great walls of Marrakesh are mentioned.

Figure 1.1 - Walls of Marrakesh

Excluded from the list of building materials after the diffusion of steel and concrete in industrial countries, raw earth is back in use starting from the energy crisis of the 70's. Raw earth represents a sustainable construction practice because of low cost, local availability and recyclability, but also because it allows to satisfy environmental comfort, thermal and acoustic insulation of the interior, with minimum energy. These features make earth material and the corresponding construction techniques extremely competitive if compared to the conventional ones, not only in the developing countries.

Nowadays earthen architecture is no longer seen as exclusively inhabited by the poorest people: there are some very interesting examples of contemporary rammed earth buildings such as the Church of Reconciliation in Berlin shown in figures 2/3.

Figure 1.2/3 - Church of Reconciliation in Berlin (Martin Rauch, 1999)

Although earth exhibits extremely low values of the relevant mechanical parameters (Bui and Morel 2009), earthen constructions require high maintenance as they are prone to erosion under rainfall, spalling and damages due to salts transported by capillary action (Bui 2009). Rain and frost are the most destructive natural actions causing erosion and deterioration of the earth masonry. Abrasion is also a significant deterioration agent. The durability of earth constructions means the ability of the entire structure and the single elements to withstand the destructive action of weathering and other actions without degradation to the expected service life (Walker 2000; Keable 1994; Maniatidis and Walker, 2003).

Earthen buildings are also susceptible to fracturing under low tensile stress. In regions with high seismic risk, the intrinsically low resistance to dynamic actions of the earthen dwellings is further worsened by such durability issues (Miccoli et al. 2014). Moreover in absence of regulations, certain repair practices or the presence of heavy roofs, lack of continuity at corners and at wall junctions, and presence of roofs not connected to walls negatively affect earthen buildings and make them susceptible to huge damages even under low seismic actions (Vargas et al. 1986; Silva et al. 2014). Load bearing earth structures have developed over millennia completely in the absence of design standards and regulations.

Rules of thumb concerning geometric proportions derived by practical experience have proven sufficient to enable earth building to achieve enough resistance. However the majority of earthen buildings are low rise and consequently the stresses experienced by the

thick earth walls are generally within the modest capabilities of the material (Maniatidis and Walker, 2003).

Nowadays many technologically advanced and developing countries have set forth standards and codes defining the characteristics and usage limitations of the earth material and of buildings in which this is employed, for instance the SAZS 724:2001, Zimbabwe Standard, *ASTM E2392/E2392M-10,* New Mexico Building Code (2006) for adobe and rammed earth constructions, norma técnica de edification NTE E.80 of Perù for adobe constructions and the Indian standard IS 13827:1993 to improving earthquake resistance of earthen buildings. In particular the latter standards deal with the design and construction aspects for improving earthquake resistance of earth buildings, without using stabilizers such as lime, cement, bitumen, etc. In Germany DIN Standards relating to earth building were developed after World War II, in addition to the Lembau Regeln and recently improved (DIN 18945:2013-08; DIN 18945 Lehmsteine – Begriffe, Anforderungen, Prüfverfahren Earth blocks – Terms and definitions, requirements, test methods; DIN 18946 Lehmmauermörtel – Begriffe, Anforderungen, Prüfverfahren; Earth masonry mortar – Terms and definitions, requirements, test methods; DIN 18947 Lehmputzmörtel – Begriffe, Anforderungen, Prüfverfahren; Earth plasters – Terms and definitions, requirements, test methods). In Australia the first edition of Bulletin 5, a national reference document for earth building, was published by CSIRO in 1952 (Maniatidis and Walker, 2003).

The development of structural design codes and recommendations for earthen buildings have followed similar proposals developed for masonry construction in Australia, New Zealand and Spain (Standards Australia, 2002; MOPT, 1992, New Zealand Standard 4297:1998, Engineering design of earth buildings). Also, at its 31st session (New Zealand, 2007), the World Heritage Committee approved the initiation of the integrated World Heritage Programme on Earthen Architecture (2007-2017) in order to improve the conservation and management of sites of earthen architecture in the world. The projects included in the World Heritage Earthen Architecture Programme (WHEAP 2007-2017) allow you to identify best practices for the development and dissemination of methods and techniques appropriate for the conservation and management of the earthen architecture, encouraging scientific research to improve the know-how (Briccoli Bati et al. 2005). The possibility of recovering the existing buildings in areas subject to seismic activity and of proposing raw earth as a building material also for the new constructions in these areas is strongly influenced by the ability to develop a strengthening system able to withstand seismic actions.

As raw earth is a no tension material, it is necessary to combine it with a material able to compensate for its deficiencies. From these reflections the idea to produce a composite consisting of raw earth and natural fibers fabric was conceived.

1.2 Stabilized and non-stabilized rammed earth

Among all of earth construction techniques as adobe cob, torchis, CEB and rammed earth the attention was focused on the latter one. Cob and rammed earth are considered homogeneous (monolithic) constructions (Miccoli et al. 2014). Rammed earth is practiced on all continents and known as 'pisé' in French, 'Stampflehm' in German, 'tapial' in Spanish, 'taipa' in Portuguese and 'terra battuta' in Italian. The earth is ideally composed of sand, clay and gravel. These are mixed with a low moisture content, usually below the plastic limit of the earth and compacted inside temporary formworks (Bui et al.2014). The optimal moisture content depends on the clay and silt content but is usually around 10 % of the earth dry weight (Ciancio et al 2013).

The earth composition varies greatly and always includes clay but should not include any organic component. Clay acts as the binder between the grains, a mixture of silt, sand and gravel with diameter up to a few centimetres. Compaction is undertaken on material prepared to its optimum moisture in several layers of earth. The earth mixture is poured loose in layers into a timber or metal formworks, and is then rammed with a rammer (manual or pneumatic). The procedure is repeated until completion of the element. The compaction process of rammed earth produces a distinctive horizontal layering, for this reason a rammed earth wall cannot strictly be considered as "isotropic". The presence of interruptions in the formworks produces instead discontinuities in the masonry panel that can behave as a large blocks of masonry. According to New Zeeland Standard rammed earth as a construction material should have a minimum characteristic unconfined compressive strength of 1.3 MPa (Hall and Djerbib 2004).

For traditional rammed earth constructions, referred to as ''rammed earth'' or ''non-stabilized rammed earth'' the only binder is clay (Bui et al. 2014b). Small quantities of other binders can be added, such as cement, hydraulic or calcium lime and gypsum. In this case we speak of ''stabilized rammed earth'' (Isik. 2011; Miccoli et al., 2014). The main categories of additives used for earth constructions are Portland cement, other pozzolans (for clay soils), lime, gypsum, bitumen, natural fibers (broom, hemp, jute, flax, coconut etc) and chemical solutions such as silicates. The stabilization against the shrinkage can be done using short fibers inside the mixture (Binici et al. 2005). The fundamental difference between stabilization process and reinforcement system is that the first is able to improve the behaviour of the material the second the behaviour of the structures. The main advantage of stabilization is the increase in durability and mechanical performance (Briccoli Bati & Rovero. 2001). The authors Hejazi et al. (2012) review the history, features, applications and possible executive problems connected to the use of different types of natural and/or synthetic fibers in soil stabilization where soil stabilization means a technique to improve the engineering characteristics of soil in order to improve the parameters such as shear

strength, compressibility, density and hydraulic conductivity. The first testimonies of straw and other types of natural fibers added to mud bricks were discovered in Çatal Höyük settlement in southern Anatolia and according to archaeologists; date approximately back to 6500 BC, and in the ziggurats of Babylon where earth was reinforced using branches of trees to improve tensile strength. Other examples are the Great Wall of China built with reinforced earth or the mortars and plasters strengthened with animal fibers of ancient Romans. The use of stabilizers such as cement has derived out of a need to improve wet strength and erosion resistance in very exposed walls (Houben and Guillaud 2006). In Australia and USA, stabilization by cement has become common practice in rammed earth because it is relatively inexpensive; also European local traditions included adding lime to the earth when the clay content was too low and the grain size distribution was not optimal, as documented in many rammed earth buildings (Miccoli et al. 2014).

However, in many situations, the use of cement and other stabilizers can be replaced by good design, by a choice of the construction techniques appropriate to earth building and by natural devices; in fact it should be considered that the stabilization process usually increases the construction cost and/or environmental impact. Rammed earth material and a compatible reinforcement system are the focus of this research for two main reasons. Firstly, the heritage of rammed-earth buildings in the world, especially in the seismic areas is still important. Secondly, the use of non-stabilized rammed earth in new constructions is possible in several countries, particularly in the context of sustainable development.

1.3 Reinforcement solutions

Many of existing earth constructions are built in areas subjected to seismic hazard. As for other materials that exhibit low tensile strength, the possibility to recover existing buildings in seismic areas and to build new constructions made of earth as structural material, is determined by the ability to design a strengthening system capable to induce in the structure the capability to respond to horizontal actions. Masonry structures made of artificial or natural elements and mortar are often reinforced by devices or strengthening systems made of fiber-reinforced composite material that realize binding, ties or connections as seismic protection (Hejazi et al. 2012).

Recent destructive earthquakes like those of Erzinkan (Turkey 1992), Bam (Iran 2003), Pisco (Peru 2007), Concepciòn (Chile 2010) and Gansu (China 2013) showed the vulnerability of earthen structures that, in spite of their “green” appealing characteristics, reveal serious structural fragilities (Bui et al. 2011a; Liu and Wang, 2015). Indeed most of the collapsed constructions were rammed earth or adobe buildings which caused human losses devastating at the same time cultural heritage in these regions (Miccoli et al. 2014).

The maintenance of the earth heritage needs scientific knowledge on the material to assess appropriate renovations (Millogo et al. 2014; Illampas et al. 2013).

The seismic vulnerability combined with high expressive and environmental potential of this material justifies the research of efficient strengthening methods. Most of researches carried out in the field of the earthen constructions are related to architectural and historical aspects and to thermal and hygrothermal performances; only in the recent years the structural and/or mechanical problems have been considered. Some researchers developed various techniques to characterize soil and to identify the clay minerals composition. Recently other studies focused on manufacturing process optimization, compaction energy, environmental comfort, durability and mechanical behaviour of earthen constructions (Morel & Pkla. 2002) (Bui et al. 2009).

For years the Civil Engineering Department of Aveiro, University, in Portugal, has been developing several scientific studies on the behaviour of adobe structures and their constituent materials (Figueiredo et al, 2012). Dynamic behaviour on in-situ rammed earth constructions has been investigated (Bui et al. 2011) A research group from Catholic University of Peru (PUCP) is playing a fundamental role on the acquisition of scientific knowledge on earthen constructions behaviour and on the development of reinforcement solutions against earthquakes (Vargas et al. 1986; Vargas et al. 2005; Blondet et al. 2007; Blondet et al. 2011). Several reinforcement solutions for seismic retrofit of existing earth constructions have been studied with enveloping geosynthetic, plastic or metallic meshes (Figures 4), fiber reinforcement composites, anchor systems (Ginell et al 2000; Liu et al. 2015; Miccoli and Fontana, 2014; Oliveira et al 2012). The use of vertical canes and horizontal ropes was compared and assessed. Techniques to repair seismic cracks (Figure 5) by injecting a grout compatible with rammed earth has been studied by Silva et al. (2016), Silva et al (2012), Vargas et al. (2008).

Figure 1.4 - Synthetic meshes in adobe structures. (Blondet et al. 2007)

Figure 1.5 - Reparation with injection of mud grouts (Silva et al. 2016)

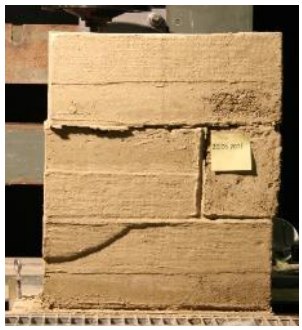

Figure 1.6 - Reinforced earth structural element. Degree thesis of Cecilia Lodi Rizzini 2015. University of Florence.

The following research work fits in this background, in particular in the research field of natural reinforcement systems that involved the University of Florence for years (Figure 6) and wants to be a contribution to the study of rammed earth as a building material and of environmentally friendly reinforcement techniques that can make earthen buildings suitable for seismic areas.

1.4 Bibliography

ASTM E2392/E2392M-10. In Standard Guide for Design of Earthen Wall Building Systems; ASTM International: West Conshohocken, PA, USA, 2010.

Binici, H., Aksogan, O., Shah, T.2005. “Investigation of Fibre Reinforced Mud Brick as a Building Material”. Construction and Building Materials, 19(4): 313–318. doi:10.1016/j.conbuildmat.2004.07.013

Blondet, M., Vargas, J., Tarque, N., Iwaki, C. 2011. “Construcción Sismorresistente en Tierra: la Gran Experiencia Contemporánea de la Pontificia Universidad Católica del Perú”. Informes de La Construcción, 63(523): 41–50. http://doi.org/10.3989/ic.10.017

Blondet, M., Aguillar, R. 2007.“Seismic Protection of Earthen Buildings”, International Conference of Seismic Engineering, Lima, Peru.

Briccoli Bati, B. “Riflessioni su di un Possibile Futuro delle Costruzioni in Terra”. In: La terra cruda nelle costruzioni: dalle testimonianze archeologiche all'architettura sostenibile, Caltanissetta, 29 Giugno 2007, 169-178, ISBN:9788876763793, 2007.

Briccoli Bati, B., Rovero, L. 2005. “Costruzioni in Terra Cruda” First International Research Seminar of Forum UNESCO - University and Heritage on "Architectural Heritage and Sustainable and Appropriate Development of Small and Medium Cities in South Mediterranean Regions. Research and cooperation. Results and strategies” Edizioni ETS Pisa, 619-629.

Briccoli Bati, S., Ranocchiai, G. 1997. “Le Tecniche Costruttive della Terra Cruda in Toscana, Calabria e Sardegna. In: AAVV. Le regioni dell'architettura in terra Culture e tecniche delle costruzioni in terra in Italia, pp. 113-127, G. Scudo, S. Sabbadini, URL, Maggioli Editore, Rimini, 1999

Bui, Q.-B., Hans, S., Morel, J.-C., Do, A.-P. 2011. “First Exploratory Study on Dynamic Characteristics of Rammed Earth Buildings”. Engineering Structures, 33(12): 3690–3695. http://doi.org/10.1016/j.engstruct.2011.08.004

Bui, Q. B. and Morel, J. C.2009. “Assessing the Anisotropy of Rammed Earth”. Construction and Building Materials, 23(9), 3005–3011. http://doi.org/10.1016/j.conbuildmat.2009.04.011

Bui, Q. B., Morel, J. C., Hans, S., Walker, P. 2014. “Effect of Moisture Content on the Mechanical Characteristics of Rammed Earth”. Construction and Building Materials, 54, 163–169. http://doi.org/10.1016/j.conbuildmat.2013.12.067

Bui, Q. B., Morel, J. C., Venkatarama Reddy, B. V., Ghayad, W. 2009a. “Durability of Rammed Earth Walls Exposed for 20 Years to Natural Weathering”. Building and Environment, 44(5), 912–919. http://doi.org/10.1016/j.buildenv.2008.07.001

Ciancio, D., Jaquin, P., Walker, P. 2013. Advances on the Assessment of Soil Suitability for Rammed Earth. Construction and Building Materials, 42, 40–47. http://doi.org/10.1016/j.conbuildmat.2012.12.049

Codispoti, R., Oliveira, D. V, Olivito, R. S., Lourenço, P. B., Fangueiro, R. 2015. “Mechanical Performance of Natural Fiber-Reinforced Composites for the Strengthening of Masonry”. Composites Part B: Engineering, 77(0): 74–83. Journal Article. http://doi.org/10.1016/j.compositesb.2015.03.021

DIN 18945:2013-08 (DIN 18945 Lehmsteine – Begriffe, Anforderungen, Prüfverfahren. Earth blocks– Terms and definitions, requirements, test methods; DIN 18946 Lehmmauermörtel – Begriffe, Anforderungen, Prüfverfahren. Earth masonry mortar – Terms and definitions, requirements, test methods; DIN 18947 Lehmputzmörtel – Begriffe, Anforderungen, Prüfverfahren.Earth plasters – Terms and definitions, requirements, test methods)

Figueiredo, A., Varum, H., Costa, A., Silveira, D., Oliveira, C. 2012. “Seismic Retrofitting Solution of an Adobe Masonry Wall”. Materials and Structures, 46(1–2): 203–219. http://doi.org/10.1617/s11527-012-9895-1

Galdieri, E. 1982. “Le Meraviglie dell’Architettura in Terra Cruda”, Laterza, Bari.

Ginell, W., and Tolles. E. 2000. “Seismic Stabilization of Historic Adobe Structures”. Journal of the American Institute of Conservation 39(1): 147–163

Hall, M., and Djerbib, Y. 2004. “Rammed Earth Sample Production: Context, Recommendations and Consistency”. Construction and Building Materials, 18(4): 281–286. http://doi.org/10.1016/j.conbuildmat.2003.11.001

Hejazi, S. M., Sheikhzadeh, M., Abtahi, S. M., Zadhoush, A. 2012. A Simple Review of Soil Reinforcement by Using Natural and Synthetic Fibers”. Construction and Building Materials, 30, 100–116. http://doi.org/10.1016/j.conbuildmat.2011.11.045

Houben H, Guillaud H. 2006. Traité de construction en terre. Parenthèses

Illampas, R., Ioannou, I., Charmpis, D. C.2013. “Overview of the Pathology, Repair and Strengthening of Adobe Structures”. International Journal of Architectural Heritage, 7(2): 165–188. http://doi.org/10.1080/15583058.2011.624254

Isik, Bilge. 2008. “Sustainable Housing in Island Conditions Using Alker-Gypsum-Stabilized Earth: a Case Study from Northern Cyprus”, Building and Environment.

Keable, J. 1994. Rammed Earth Standards. ODA Final Project Report R 4864C.

Liu, K., Wang, M., Wang, Y. 2015. “Seismic Retrofitting of Rural Rammed Earth Buildings Using Externally Bonded Fibers”. Construction and Building Materials, 100(December): 91–101. http://doi.org/10.1016/j.conbuildmat.2015.09.048

Maniatidis, V., Walker, P. 2003. “A Review of Rammed Earth Construction”. Developing Rammed Earth for UK Housing, (May), 109.

Miccoli, L., Fontana, P. 2014. “Bond Strength Performances of Anchor pins for Earthen Buildings. A Comparison Between Earth Block Masonry, Rammed Earth and Cob”. Proceedings of 9th International Conference on Structural Analysis of Historical Constructions, Mexico City, (October).

Miccoli, L., Muller, U., Fontana, P. 2014. “Mechanical Behaviour of Earthen Materials: A Comparison Between Earth Block Masonry, Rammed Earth and Cob”. Construction and Building Materials, 61, 327–339. http://doi.org/10.1016/j.conbuildmat.2014.03.009

Millogo, Y., Morel, J. C., Aubert, J. E., Ghavami, K. 2014. “Experimental Analysis of Pressed Adobe Blocks Reinforced with Hibiscus Cannabinus Fibers”. Construction and Building Materials, 52, 71–78. http://doi.org/10.1016/j.conbuildmat.2013.10.094

NZS (1998) New Zealand Standard 4297:1998, Engineering design of earth buildings. Standards New Zealand, Wellington.

Oliveira, C. F., Varum, H., Vargas, J. 2012. “Earthen Construction : Structural Vulnerabilities and Retrofit Solutions for Seismic Actions”. 15 Wcee, 1–9.

Pacheco-Torgal, F., Jalali, S. 2012. “Earth construction: Lessons from the Past for Future Eco-efficient Construction”. Construction and Building Materials, 29: 512–519. http://doi.org/10.1016/j.conbuildmat.2011.10.054

Silva R.A., Jaquin P., Oliveira D.V., Miranda T., Schueremans L., Cristelo N. 2014. “Conservation and new Construction Solutions in Rammed Earth”. Structural Rehabilitation of Ancient Buildings, A. Costa; J. Miranda; H. Varum (Eds), Springer, 77-108. ISBN 978-3-642-39685-4.

Silva, R. A., Oliveira, D. V., Schueremans, L., Miranda, T., Machado, J. 2016. "Effectiveness of the Repair of Unstabilised Rammed Earth with Injection of Mud Grouts". Construction and Building Materials, 127, 861–871. http://doi.org/10.1016/j.conbuildmat.2016.10.064

Silva R.A., Schueremans L., Oliveira D.V., Dekoning K., Gyssels T. 2012. “On the Development of Unmodified Mud Grouts for Repairing Earth Constructions: Rheology, Strength and Adhesion”. Materials and Structures 2012, 45 (10), pp. 1497-1512

Vargas, J., Bariola, J., Blondet, M., & Mehta, P. K. 1986. “Seismic Strength of Adobe Masonry”. Materials and Structures, 19(4): 253–258. http://doi.org/10.1007/BF02472107

Vargas J, Bariola J, Blondet M, Mehta PK. Seismic strength of adobe masonry. Mater Struct 1986;19(4):253–8.

Vargas J., Blondet M., Ginocchio F., Garcıa G. 2005. “35 Anos de Investigaciones en Sismo Adobe: la Tierra Armada”, International Conference SismoAdobe 2005: Architecture, Construction and Conservation of Earthen Buildings in Seismic Areas, Lima, Pontificia Universidad Catolica del Peru´,. Lima, Peru

Vargas J., Blondet M., Cancino C., Ginocchio F., Iwaki C., Morales K. 2008. “Experimental Results on the use of Mud-based Grouts to Repair Seismic Cracks on Adobe walls”. In proceedings of the VI International Conference on Structural Analysis of Historic Constructions, D’Ayala D. and Fodde E. Eds., Bath, UK, pp. 1095-1099.

Walker, P. 2000. “Review and Experimental comparison of Erosion Tests for Earth Blocks”, in Proceedings 8th International conference on the study and conservation of earthen architecture, 176-181, Torquay, May.

.

Chapter 2
Materials characterization

2.1 Earth characterization

Soil is basically a mixture of mineral particles, air and water, and its properties are defined by parameters such as Atterberg limits, clay content and chemical analysis and granulometry. The high variability of earth materials in terms of mechanical behaviour, is dependent on a number of parameters affecting physical and chemical bonds at microstructural level, i.e. particle size, clay content, compaction and moisture content (Miccoli, et al. 2014). Investigations were carried out at micro and macro structural levels to acquire a basic knowledge of the mechanical properties of the earth as well as that used for realization of the structural elements and to compare the general failure mechanisms. Soils used in earth construction are composed by clay, silt, sand and gravel. The latter three are sub-grouped into coarse, medium and fine. The relative proportions of these determine the suitability of the soil for a particular construction method (rammed earth, earth block masonry, cob). The earth referred to does not include the vegetation layer or top soil, that must be cleared and removed before material extraction takes place. The samples must be taken at least 50cm of depth. Clays act as binder in earth construction and confer the highest cohesive strength of all the soil grades and are typically made up of small, flat platelet shaped particles and are usually formed by the chemical weathering of silicate bearing rocks. The main groups are kaolinite, montmorillonite, illite, and chlorite-vermiculite. They are unstable against water characterized by different behaviour, may swell or shrink considerably with changing water content as shown by CRAterre (Figures 1 and 2). Silt is made of slightly larger, rounder particles. It has some cohesive strength and swells slightly when wet. Gravel and sand are still larger particles. They have no cohesive strength and do not swell when wet.

Principaux composants des sols et leurs propriétés physiques			
Désignation du groupe	Principaux minéraux présents	grosseur des grains	Propriétés physiques
Sable très pur Silice	Quartz	$>1\,\mu$	Sans cohésion, abrasif
Mica	Muscovite	$>1\,\mu$	sans cohésion
Carbonate	Calcite Dolomite	variable	
Sulfate	Gypse	$>1\,\mu$	susceptible d'attaquer cert. ciments
Argiles	Kaolinite	$\approx 1\,\mu$	pas de gonflement plasticité faible peu de cohésion
	Illites et Micas partiellement dégradés	variable	gonflement, plasticité moyenne
	Montmorillonites « bentonites » et interstratifiés	$\leq 1\,\mu$	très gonflante très plastique
	Chlorite Vermiculite	$\approx 0{,}1\,\mu$	gonflement limité
Matières organiques	ne sont pas des minéraux	aucune	dégradation rapide

Figure 2.1 – Soil principal components (CRAterre, Construire en terre, 1979)

ORDRE DES GRANDEURS DES GRAINS D'ARGILES			
$1\mu = 10^{-6}$ m	KAOLINITES	ILLITES	MONTMORILLONITES
Longueur μ et largeur μ	0,1 à 2	0,01 à 0,5	0,05
Epaisseur μ	0,005 à 2	0,005 à 0,05	0,001 à 0,02
Surface spécifique	5 à 10 m^2/g	80 m^2/g	80 à 800 m^2/g
COMPORTEMENT LIE AUX VARIATIONS D'HUMIDITE	TRES VARIABLE suivant la composition et la structure des feuillets		
	Les argiles naturelles sont des mélanges comportant souvent des minéraux mixtes (interstratifiés)		
	PLUTÔT STABLE	TRES SOUVENT INSTABLES (GONFLANTES)	

Figure 2.2 - Clay different grain size (CRAterre, Construire en terre, 1979)

Earth vary from one site to another and the major obstacle to the use of earthen construction is that earthen materials are classified as non-standard material. Geotechnical analyses were performed in order to classify the soil according to the CRAterre *(International Centre on Earthen Architecture in Grenoble, France)* recommendations and identify the right construction technique to use. For the sake of completeness, the mineralogical analysis was performed to better understand the clay composition. Despite X-ray diffraction analysis involves only fine-grain part of the soil, it can give us information about the shrink–swell capacity of the earth in relation to the clay components and their properties that influence the choice to eventually use additives for earth stabilization. Among clays, Illite is the most suitable for earth constructions, in fact, does not present the stiffness of kaolinite, or the excessive capacity to absorb water and therefore to swell of montmorillonite. The parameters useful to decide the technique are suggested by geotechnical analysis.

The earth employed in the experimental campaign described below comes from Seggiano (Grosseto, Italy). The results of analyses performed in the laboratories of Univeristy of Florence on soils taken from different Italian areas where the presence of earthen architecture is traditional will be reported in this section for two main reasons: first of all, the experimental campaign described in chapter 3 shows results of the lap joint on supports made with earth of Musciano (Pisa, Italy); secondly, to qualitatively assess the difference among soils taken from neighboring areas.

In recent years, the issue of earth construction has been addressed at the University of Florence and for completeness conclusions and observations, resulting from previous experiences will be reported in order to justify choices and define the starting point of this research.

2.1.1 Mineralogical analysis

The mineralogical composition was determined by X-ray diffractometry carried out at the Florence CNR "Istituto per la Conservazione e la Valorizzazione dei Beni Culturali" (ICVBC). In Table 2.1 the main mineralogical composition and clay minerals composition of different soils are listed, the earth employed in the present work are highlighted in bold.
Note the presence of a good percentage of Illite in both cases.

Main mineralogical composition %						
	Calabria			Tuscany		
	Lamezia	Altomonte1	Altomonte2	**Musciano**	Seggiano1	**Seggiano2**
Quartz (%)	25	42	38	**40**	16	**27**
Feldspar (%)	12	3	4	**20**	-	**-**
Calcite (%)	5	-	-	**-**	20	**25**
Clay minerals (%)	58	55	58	**40**	64	**48**
Clay minerals composition %						
Illite (%)	55	50	25	**35**	5	**40**
Kaolinite (%)	20	50	45	**20**	30	**20**
Chlorite (%)	15	-	-	**-**	-	**-**
Vermiculite (%)	-			**20**	-	**40**
Montmorillonite (%)	-	-	30	**-**	-	**-**
Illite-smectite (%)	-	-	-	**25**	40	**-**
Chlorite-Vermiculite (%)	10			**-**	25	**-**

Table 2.1. Main mineralogical composition and clay minerals composition of different soils (CNR), Florence.

2.1.2 Geotechnical analysis

To classify the soils, geotechnical tests, that is particle density γs, consistency limits, plasticity index according to EN 103103 and EN 103104, and linear shrinkage, were carried out in the Material and Structure Test Laboratory of the Architecture Department, University of Florence.
The determination of consistency limits (Atterberg limits) that is the water content that determines the transition of earth from solid to liquid and plastic state, were carried out following ASTM D4318 standard, the particle density was determined according to ASTM D854 and to BS 1377 Test 6A. The parameters in bold regard soils used in the following experimental campaigns.

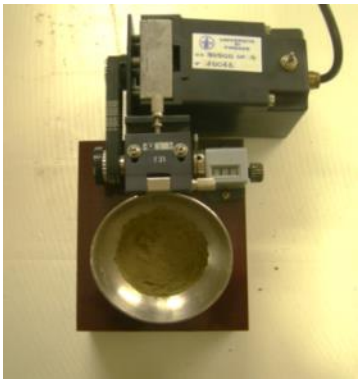

Figure 2.3 – sample for liquid limit determination

Figure 2.4 – sample for the plastic limit determination

	Bulk density γs (g/cm^3)	Liquid limit Wl (%)	Plastic limit Wp (%)	Plasticity index Ip (%)
Lamezia	2.55	31.80	22.87	8.93
Altomonte 1	2.64	33.53	17.79	15.83
Altomonte 2	2.67	44.00	18.43	25.58
Musciano	**2.28**	**31.83**	**20.8**	**11.03**
Seggiano1	2.66	36.6	21	15.6
Seggiano2	**2.31**	**43.42**	**19.72**	**23.7**

Table 2.2. Geotechnical parameters of different soils

The indices that allowed to classify the soil were determined considering the values of natural content of water (W_N) respectively equal to 15.98% for Musciano's earth and equal to 12.3% for earth of Seggiano2 (Table 2.3).

Soils	**Consistency index Ic**	**Liquidity index**
Musciano	1.44%	-0.44
Seggiano2	1.31%	-0.31

Table 2.3. Consistency index and liquidity index calculated from the Atterberg limits results of the two soils analyzed

According to the consistency indices Musciano earth is classified as a semi-solid, in fact on the Casagrande plasticity chart where an empirical boundary called the 'A' line, separates inorganic clays from inorganic silts and organic soils, it is located between the low plasticity inorganic clays and inorganic silts, instead the earth of Seggiano2 is carachterized by medium plasticity. Vertical subdivisions of the chart are made to distinguish differences in engineering properties such as compressibility, permeability and toughness (Figure 5).
Soils located within each area of the chart would be expected to behave similarly (Bain, 1971). In the figure 6 the envelope proposeded by CRAterre for rammed earth is reported with the position of the analyzed soils in the chart.

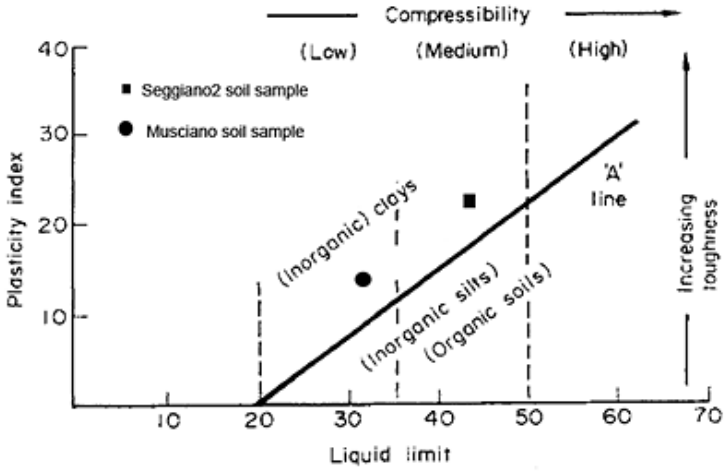

Figure 2.5 - Plasticity chart (Bain 1971)

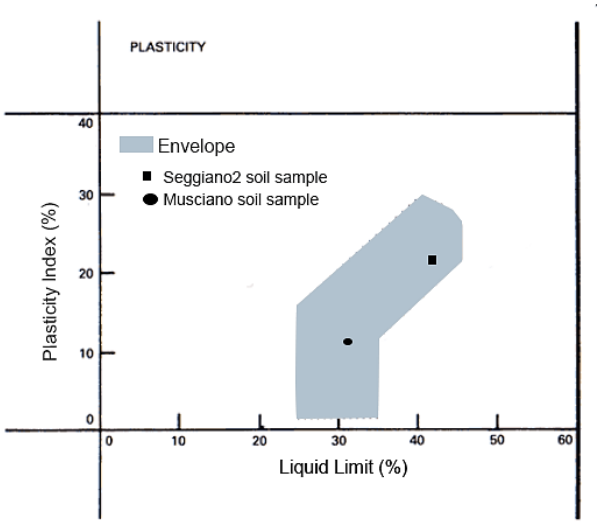

Figure 2.6 - Envelope for consistency parameters of soils recommended for rammed earth construction proposed by Houben and Guillaud (CRAterre)

The objective of the particle-size determinations is to classify, according to fixed classes of size, the particles that constitute the sample in order to determine the percentage size distribution. This analyses were conducted by dry method following ASTM D421 and showed that the soils of Musciano and Seggiano2 are predominantly large-grained (Figure 7).

Figure 2.7 ASTM sieves used for particle-size analysis

The particle size distribution curves of the soils are presented in Figure 8, where it is compared with the envelope of soils recommended for producing rammed earth. Houben and Guillaud 1996 of CRATerre-EAG recommend non-prescriptive parameters for a suitable rammed earth particle-size distribution. The red and blue curves represent the prticle size distribution of two different samples of Musciano's earth, in black the curve corrisponding to eath of Seggiano2 is illustrated.

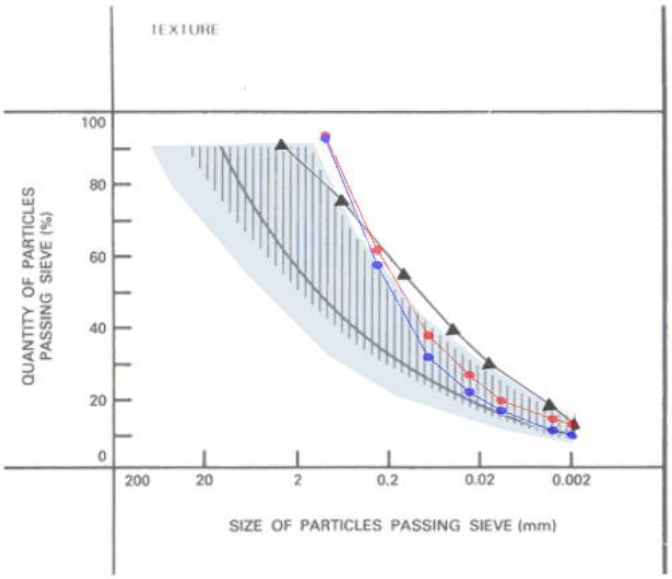

Figure 2.8 Comparison of the properties of the soils with the recommendations of CRAterre for rammed earth technique

As can be observed, the clay content respect the recommended range, as this standard discards the use of soils with clay content below 10%. A minimum percentage of clay is required to the soil in order to provide initial cohesion and enough strength.

Finally, the linear shrinkage was determined according to BS 1377 Test 5, both on raw earth and on specimens stabilized with gypsum powder in order to evaluate the influence of gypsum in the matrix used for strengthening system. The test specimens were made with different mixtures, each one containing a different percentage of water and gypsum powder. The percentage of water and gypsum added to each mixture was calculated by dry weight of the earth while the shrinkage was calculated on the initial length.

The analysis of the shrinkage test results shows that the addition of gypsum powder significantly decreases the percentage of the linear shrinkage up to almost zero for an amount of 25% of additive for the earth of Lamezia Terme (Table 2.4).

Soil	Gypsum (%)	Water (%)	Linear shrinkage (%)
Lamezia	-	30	8.25
Lamezia	-	60	8.32
Lamezia	10	60	5.53
Lamezia	15	30	2.26
Lamezia	25	60	0.45
Altomonte 1	-	25	6.79
Altomonte 2	-	40	11.39
Altomonte 2	15	40	8.32
Altomonte 2	25	40	6.99
Altomonte 2	30	40	3.18
Musciano	**-**	**30**	**9.37**
Musciano	**15**	**30**	**2.38**
Seggiano 1	-	30	8.24
Seggiano 1	15	30	2.75
Seggiano 2	**-**	**30**	**9.64**
Seggiano 2	**15**	**30**	**3.85**
Seggiano 2	**20**	**30**	**2.85**
Seggiano 2	**25**	**30**	**1.43**

Table 2.4 Linear shrinkage

Figure 2.9 – Specimens used for linear shrinkage determination (earth of Musciano)

The results confirmed that the addition of 15% by weight of gypsum powder (biocompatible stabilizer) greatly reduces the earth shrinkage. In general, limiting volume changes, the addition of gypsum powder is able to increase mechanical properties, stability, durability and resistance to weathering (Isik and Tulbentci 2008).

2.1.3 Mechanical characterization

In comparison to advances in research on stone and fired brick masonry, little is known on the material properties and failure mechanisms of earthen masonry and the few results are extremely scattered (Jaquin, et al. 2006), only in recent years, several studies have been carried out to investigate rammed earth mechanical properties (Hall and Djerbib 2004; Burroughs 2008; Jayasinghe and Kamaladasa 2007; Walker and Dobson 2001) and its anisotropic behaviour (Bui and Morel 2009). The heterogeneity of rammed earth and the challenge of manufacturing process which are representative of the rammed earth are discussed in different research works (Bui et al. 2008; Maniatidis and Walker, 2008).

For simplification purposes, most of these investigations are performed through tests on samples characterized by small dimensions: 8cm, 10cm, 15cm cubes or cylinders 20cm high and 10 cm in diameter (Lilley and Robinson 1995, Hamilton et al 2006, Briccoli Bati et al 2013).

Despite the differences between the results obtained with small samples and those obtained with samples closer to the real size of the structures, due to the difficulties in controlling the scale effect, laboratory tests on small samples are indispensable to understand the mechanical behaviour.

Miccoli et al. (2014) assembled literature results obtained for earth masonry specimens showing the large scatter of mechanical property values. This clearly is not only due to factors such as workmanship and weathering, but also to different testing procedures, for instance in the Young's modulus determination, especially in case of small specimens. The average values of elastic modulus calculated on specimens realized with rammed earth technique according to Miccoli et al. (2014) can vary from 60MPa to 750MPa. In many studies, the failure modulus is used rather than the elasticity modulus as a characteristic parameter of rammed earth specimens. The failure modulus is calculated using the ratio between the maximum stress and the deformation corresponding to this stress (Bui and Morell 2009). For rammed earth as a construction material, New Zealand standards recommend a minimum unconfined compressive strength of 1.3MPa, but as known, the strength values of rammed earth depend on many factors (Vargas-Neumann 1993): granulometry, clay content, moisture content, compaction energy, fibers or stabilizer content, which influence also the density and porosity, respectively. The optimum moisture content for rammed earth method is a fundamental issue in order to achieve maximum dry density, strength and durability of the material through compaction, in fact, Vargas-Neumann 1993, deduced that the amount of clay, water and compaction are the dominating influences on the resistance of rammed earth.

With a low water content, the soil cannot achieve the same level of compaction due to the greater degree of friction between the soil particles. On the contrary, too much water,

occupying the soil pore spaces, reduces the level of achievable compaction and influences the level of porosity of the manufactured product dried. Different studies show that the optimum moisture content for rammed earth can be individuated to a value between 7 and 11% of soil dry weight.

The laboratory production of rammed earth samples should reflect the on-site construction technique of rammed earth construction for test results to be meaningful and transposable. In this case, the aim was not to reproduce a real construction but make representative samples of the elements used in the experimental campaign described in the chapter 4. For this reason, a manually operated rammer was employed in order to replicate the type and nature of compaction forces that the earth would be subjected to during arches realization. New Zealand Standard NZS 4298: 1998 recommends a minimum of five rammed earth samples for compressive strength testing, and an aspect ratio correction factor of 0.7 to be applied to the compressive stress value obtained for a cuboid sample. The procedure used was similar to that of ASTM E 519, UNI 9724/3, 9724/8.

2.1.3.1 Monotonic compression tests and three point bending tests to assess the influence of gypsum

The mechanical behaviour of various combinations of earth - water - gypsum was determined with mechanical tests on specimens ad hoc made. The procedures followed for the mechanical tests are the same used for natural and artificial stones, that are no tension, heterogeneous and anisotropic materials, such as earth building material. Earth specimens of different size and composition were made to be subjected to uniaxial compression tests and three point bending test. Specifically, cubic specimens (8x8x8cm) were made for uniaxial compression tests while prismatic specimens (8x8x30cm) were made for three point bending tests (six for each series). All the tests were performed in a quasi-static process with a device able to proceed with controlled displacement. The results of the experimental tests were used to calculate compressive σ_c (the average stress on the upper load plate corresponding to the peak of the load path), tensile strength σ_f; conventional elastic modulus E was determined in the branch of equilibrium path that could reasonably be considered linear, note that the elastic modulus was calculated using the average deformation of the prism, calculated by the ratio of the relative displacement of the load plates and the height of the prism in the hypothesis of uniform deformation; kinematic ductility μ_c was determined as the ratio between the displacement corresponding to the peak load and the linear displacement corresponding at the break load; available kinematic ductility μ_{cd}, was calculated as the ratio of the displacement measured at the conventional ultimate load, conventionally established in two thirds of the peak load, and the linear

displacement corresponding to the peak load. Gypsum powder was used as a natural additive for the stabilization of earth because it is fully biodegradable and natural. Furthermore, it is even used to improve the quality of agricultural land for some crops, so it does not compromise the possibility of reusing earth for farming. For this specific survey Lamezia Terme and Musciano soils were employed; the gypsum powder, characterized by a very fine grain and by the ability to incorporate large quantities of water, was composed of hemihydrate (CaSO4 1/2H2O) with minor amounts of anhydrite (CaSO4). The cubic and prismatic specimens, six for each of four mixtures, were made with different percentages of gypsum powder. Table 2.5 presents the composition of the tested mixtures, the results of the compression tests and of the three point bending tests.

Gypsum (%)	Water (%)	σ_c (MPa)	E (MPa)	μ_c	μ_{cd}	σ_f (MPa)
-	20	1.503	955	1.31	1.44	0.328
		12.77%	35.03%	12.06%	6.72%	30.55%
10	25	1.888	1033	1.31	1.49	0.584
		17.74%	22.31%	8.85%	5.70%	27.17%
15	25	2.206	2479	1.18	2.02	0.91
		9.19%	8.78%	9.94%	15.95%	25.38%
25	30	1.526	1601	1.31	2.19	0.505
		11.48%	20.99%	22.84%	21.36%	18.60%

Table 2.5 Average mechanical parameters and coefficient of variation determined on six specimens made with the Lamezia earth and gypsum powder (six specimens for each series)

Gypsum powder used as an additive proved to be successful. In fact, it gave good results increasing both mechanical properties, without significantly altering the appearance and colour of the material. Just the amount of 10% of gypsum increases the strength of earth; the amount of 15% of gypsum increases the values of mechanical parameters 1.5-2 times with respect to specimens without additives. The test results show that, above a certain percentage, gypsum is no longer able to improve mechanical performance compared to mixtures of earth without additives and indicate that an addition of 15% of gypsum powder is the optimum value to improve the performance of the earth analysed. Compression tests previous carried out in the laboratory of University of Florence showed that a quantitative of gypsum powder equal to 15% and 30% of water produce an increase of mechanical behaviour in terms on strength. The recyclability as the most attractive feature of earth as building material led us to investigate on a possible change of the resistance concerning reused stabilized earth. For this investigation the stabilized specimens realized with earth from Musciano, and 15% of gypsum were tested in compression and subsequently

destroyed in order to reproduce with the same materials already stabilized six specimens with the same formwork (*8*x8x8cm). In tables 2.6, 2.7 and 2.8 the parameters of unstabilized earth, stabilized earth and reused stabilized earth are respectively reported.

	E (MPa)	σ_c (MPa)	μ_c
A.V.	294.32	3.76	1.21
S.D.P.	8.70	0.17	0.09
C.V. %	2.96	4.53	7.48

Table 2.6 Average values of the mechanical parameters determined by uniaxial compression test on unstabilized Musciano earth specimens (twelve specimens)

	E (MPa)	σ_c (MPa)	μ_c
A.V.	356	4.71	1.13
S.D.P.	11.21	0.20	0.03
C.V. %	3.14	4.25	2.65

Table 2.7 Average values of the mechanical parameters determined by uniaxial compression test on stabilized Musciano earth specimens (twelve specimens)

	E (MPa)	σ_c (MPa)	μ_c
A.V.	179.08	2.88	1.36
S.D.P.	49.63	0.25	0.21
C.V. %	27.71	8.69	15.70

Table 2.8 Average values of the mechanical parameters determined by uniaxial compression test on reused stabilized Musciano earth specimens (six specimens)

Regarding the effectiveness of the stabilizing throght gypsum powder, it seems that the stregth improving action is significant only if it is added to the soil at the time of the mixture, while in case of a reuse of material already stabilized, gypsum loses its mechanical characteristics and joints the aggregates or can be considered as extra aggregate. Gypsum hydrates during curing of the specimen compensating for the natural shrinkage of the earth and giving a contribution not so much in terms of cohesive capacity.

.

2.1.3.2 Monotonic and cyclic compression tests to study the anisotropic behaviour

Monotonic tests

The anisotropy of this material was studied performing monotonic uniaxial compression tests in two directions, both perpendicular and parallel to the layers on specimens made

with earth of Seggiano2. Unloading–reloading cycles were performed to study the non-elastic behaviour of this material.

With earth material and 11% of water, rammed earth specimens 8x8x8cm were prepared by compacting layers of about 1cm within a wooden framework. These were subjected to monotonic and cyclic uniaxial compression tests and the load path was analyzed to obtain the main mechanical parameters.

The main paramenters obtained by monotonic compression tests of rammed earth specimens in the directions perpendicular and parallel to the layers, are reported in tables 2.9 and 2.10 The parameters have been calculated with the same procedure already explained in section 2.1.3.1.

The difference between the compressive strengths obtained in the two directions, perpendicular and parallel to the layers, is about 11%; the elastic modulus measured with load parallel to layers is about 176% higher than the value obtained with the load applied in the perpendicular direction. The differences in the behaviour and crack pattern is evident also in case of specimens with small dimensions.

Figure 2.10 specimen after compression test perpendicular to layers

Figure 2.11 specimen after compression test parallel to layers

Load parallel to layers								
	h mm	A mm^2	Peak N	σ MPa	E MPa	μc	μcd (2/3)	μcd (1/3)
A.V.	78.5	5981.65	11444.55	1.91	244.90	2.06	2.17	2.94
dev.st.p.	0.49	122.06	1073.21	0.14	48.15	0.99	0.41	0.60
C.V %	0.63	2.04	9.38	7.58	19.66	47.76	18.71	20.45

Table 2.9 Average values of mechanical parameters determined by monotonic uniaxial compression test (six specimens)

	Load perpendiculr to layers							
	h mm	A mm^2	Peak N	σ MPa	E MPa	μc	μcd (2/3)	μcd (1/3)
A.V.	78.35	6022.93	12841.75	2.13	88.62	1.28	1.57	2.07
dev.st.p	0.69	58.13	1375.49	0.22	32.14	0.08	0.14	0.36
c.v. %	0.88	0.96	10.71	10.21	36.26	6.49	8.79	17.29

Table 2.10 Average values of mechanical parameters determined by monotonic uniaxial compression test (six specimens)

Cyclic tests

Despite the apparent layered structure of rammed earth the mechanical properties seem not to be distinctively anisotropic in terms of compressive strength, although the layered nature has an influence on crack mechanism and Young's modulus and must be taken into account when input data on mechanical properties of rammed earth from laboratory is used for design.

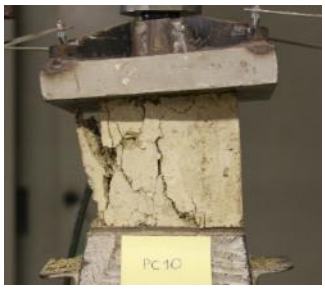

Figure 2.12 – Specimen PC10 after cyclic compression test with parallel to layers

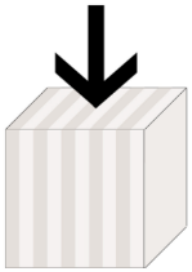

Figure 2.13 – Test scheme

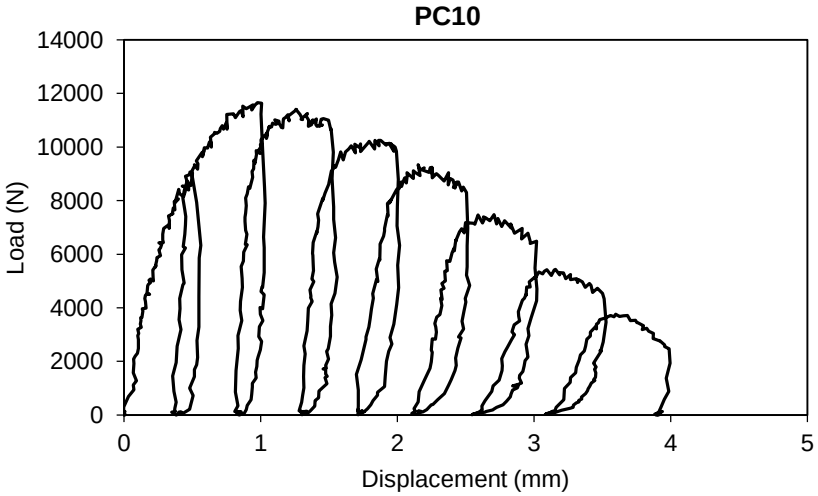

Figure 2.14 Load- displacement curve of specimen PC10 subjected by cyclic compression test parallel to layers

Load parallel to layers					
	h mm	A mm^2	Peak N	σ MPa	K N/mm
A.V.	78.6	5959.2	11422.15	1.91	16030.26
dev.st.p.	0.37	62.41	941.26	0.14	2359.34
C.V %	0.47	1.05	8.24	7.47	14.72

Table 2.11 Average values of mechanical parameters determined by cyclic uniaxial compression test (five specimens)

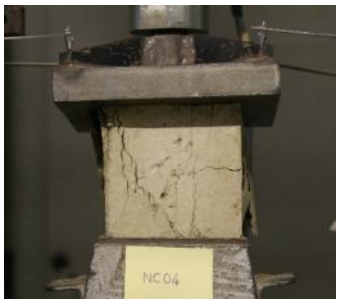

Figure 2.15 - Specimen NC04 after cyclic compression test with perpendicular to layers

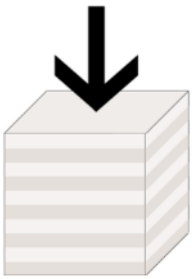

Figure 2.16 – test scheme

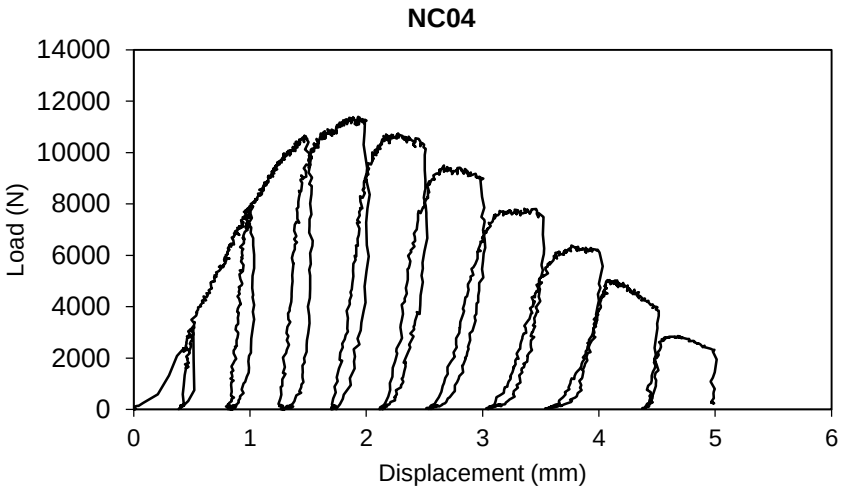

Figure 2.17 Load- displacement curve of specimen NC04 subjected by cyclic compression test perpendicular to layers

Load perpendicular to layers					
	h mm	A mm^2	Peak N	σ MPa	K N/mm
A.V.	78.5	6084.25	11564.34	1.89	6706.61
dev.st.p.	0.40	95.12	2878.15	0.45	1751.57
C.V %	0.50	1.56	24.89	23.75	26.12

Table 2.12 Average values of mechanical parameters determined by cyclic uniaxial compression test (five specimens)

These tests gave similar results for compressive strength, in both load directions; on the contrary, the stiffness calculated on the envelope curve of the specimens loaded parallel to layers is about 140% higher than the envelope stiffness of the specimen loaded perpendicular to layers.

If we compare the stiffness calculated on the envelope curve of the cyclic tests with the stiffness calculated on the monotonic tests, which average values are 18661N/mm and 6812N/mm for parallel and perpendicular loads respectively, it can be noted that the difference is within statistical error for the specimens loaded perpendicular to layers. The average stiffness of the specimens subjected to monotonic tests is about 16% higher than the envelope stiffness of the cyclic tests parallel to layers.

The average cycle stiffness of the first three cycles is about ten times higher than the envelope stiffness and than the monotonic stiffness in the perpendicular load condition and about five times higher in case of parallel load conditions due to the compacting effect of the load. The cycle stiffness decreases after four cycles as an obvious effect of damage. As seen from the monotonic test results rammed earth shows an isotropic behaviour in terms of strength, but not in terms of stiffness.

2.2 Jute characterization

2.2.1 Jute fabric as a reinforcement

Synthetic fiber fabrics are commonly adopted as masonry structures reinforcement, both for seismic retrofitting of historical buildings and for realization of new constructions in seismic areas. The scientific community focused on the use of fiber reinforced composites to strengthen masonry or reinforced concrete structures, producing a great deal of experimental results and of literature, including dedicated congresses; the technical fabric industry, together with the industry of adhesive and chemicals for building, offers a variety of products and systems; recommendations, guidelines and standards have been published by associations and authorities to suggest or prescribe use and design methods. Particularly, delamination of FRP composites on reinforced supports has been studied, (Yao, Teng, Chen 2005; Cottone and Giambanco 2009; Capozucca 2010; Fedele and Milani 2012; Basilio et al. 2014; Carloni and Focacci 2016; D'ambrisi, Feo, and Focacci 2013; Freddi and Sacco 2016; Pintucchi and Zani 2016; Speranzini and Agnetti 2015; Maruccio et al. 2014), this topic will be treated in the chapter 3. Anchorage devices have been developed to improve adhesion, on concrete, masonry support (Kalfat, et al., 2013; Fagone et al., 2014; Fagone, et al., 2015; Briccoli Bati, et al.,2014; Caggegi et al. 2014), as well as other materials as, for example, wood (Corradi et al. 2016); the effect of confining compressed concrete or masonry elements with CFRP was also studied (Alecci, et al. 2014; Alecci, et al. 2009) and special attention has been devoted to the modification or removal of the mechanisms on masonry structures subjected to seismic actions (Fagone, et al., 2016; Briccoli Bati et al., 2013).

Nowadays, petroleum-based fibers are considered inferior to natural ones in respect to physiological, hygienic, and health properties (Kostic, et al., 2008), that are perceived particularly important in the world of textile industry; from this point of view, using natural fiber as reinforcement of polymer matrix composites misses the opportunity of developing a bio compatible composite material (Gowda, et al.,1999; Doan, et al., 2006).

The idea of using natural fibers as substitute of synthetic ones in polymer matrix composites explains the abundant scientific literature on this topic. Natural fiber fabrics are appropriate to earth buildings reinforcement, being compatible from the point of view of environmental sustainability. The properties of natural materials are very scattered, for this reason, it was necessary to characterized jute fabric trough experimental campaign. The great variability of yarns behaviour and the difficulties in controlling the boundary conditions during the tests induced to perform statistical treatment of yarns mechanical properties.

Due to the sustainability of earth structures, it is necessary to define a reinforcement system that is eco-friendly; according to information taken from the literature, vegetal fibers, for

example broom, flax, hemp, jute fibers, or fibers taken from bamboo, pineapple and coconut, exhibit the necessary strength and adhesion properties to act as a reinforcement of masonry material. Borri, et al., (2013) studied the use of natural fibers as reinforcement of wood elements and Menna et al., (2015) used hemp fiber composite grid to strengthen tuff masonry and clay masonry panels, and demonstrated the contribution to improve shear performances of masonry. Moreover, in the recent years natural fibers were studied to replace the synthetic fibers used as a reinforcement in fiber reinforced composites (Codispoti et al. 2015b); in particular, jute fibers, as the second most common natural cellulosic fibers in the world (Sreenath et al. 1996), are attracting more attention for their characteristics. Jute fibers have strong physical and mechanical properties, especially when the jute fibers if treated with alkaline solution, Yunhai et al. (2014) investigated the influence of the treatment in relation to friction performance of jute fiber.

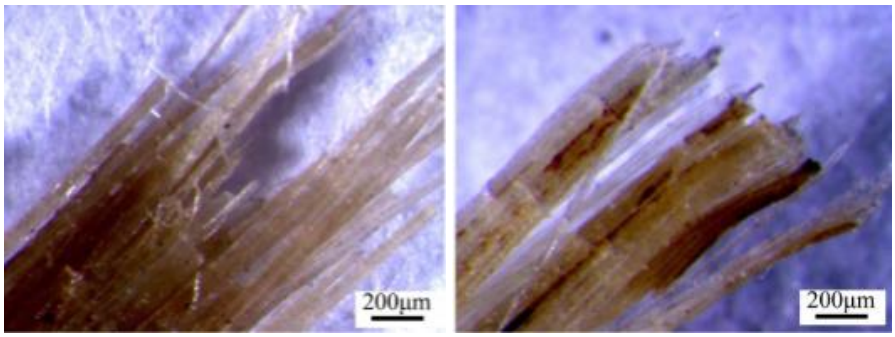

Figure 2.17 - Morphologies of tensile fracture of the untreated jute fiber and the jute fiber treated with alkaline solution (Yunhai et al. 2014).

Preliminary tests already carried out in the Laboratory of University of Florence (S Briccoli Bati et al. 2014; S Briccoli Bati et al. 2013) showed that, among the types of vegetable fibers mentioned before, jute yarns are particularly apt to produce reinforcement for earth structural elements even using a mud matrix. Jute exhibits good mechanical properties and exceptional adhesion to rammed earth material (Figure 19).

	Elongation (%)	Tensile strength (MPa)	Elastic modulus (GPa)
Untreated jute fiber	1.7	40.6	17.8
Alkaline treated jute fiber	1.3	67.4	25.3

Figure 2.18 - test results of mechanical properties of jute fiber (Yunhai et al. 2014)

Figure 2.19 - three point bending test on earth prismatic specimen reinforced with jute fabric (Loccarini and Morelli master degree thesis)

The use of earth mud, both as matrix and as adhesive, permits to obtain a compatible reinforcement system in which only jute fabric contribute to strength and stiffness of the strengthening system.

Effectively, the earth mixture used as adhesive only adds some negligible layer to the support and consequently negligible contribution to its strength. Jute is a natural biodegradable fiber characterized by good tensile strength and good thermal conductivity. Jute fiber is obtained by the stem of plans in the genus Corchorus, classified with the family Malvaceae; it is abundantly grown in Bangladesh, China, India and Thailand. Recently, due to the improvement of people's living standards and need for environmental protection, the demand of natural biodegradable and eco-friendly fibers is rising worldwide.

Jute fiber is a bast fiber obtained by degumming the jute plant stem; it contains three main categories of chemical compounds: cellulose (58~63%), hemicellulose (20~24%) and lignin (12~15%), and some other small quantities of fats, pectin, aqueous extract. Lignin and hemicellulose act like cementing agents to give tenacity and flexibility to the fiber, and make it quite coarse and hard to produce refined textiles (Joko et al., 2002; Pan et al., 1999). The weight per unit length of individual fibers varies from 0.7 to 5.5 tex but the average is between 1.9 and 2.2 tex (Yeşildal et al., 2011). Approximately one thousand varieties of jute have been identified by the raw jute division of the Indian Jute Institute Research Association (IJIRA), Calcutta (Gowda et al., 1999). Thus, one has very little control over the properties and characteristics of jute fabric as it arrives on the market. The retting process influences also the strength and the color that can vary from brown to white. Jute yarns are obtained by simple spinning of jute fibers; being made of a single twisted ply of jute fibers (coarse and hard in nature), jute yarns are very coarse and have very irregular transverse

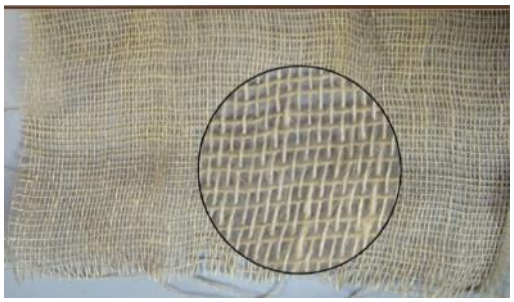

Figure 2.20 - jute fabric

sections. Moreover, there is no clearly defined average fiber length: any sample of jute yarns contains large numbers of short fibers and few long ones.

Jute fibers are roughly interlocked in yarns connected one another by friction, producing a new material whose properties are clearly lower than the properties of single fibers, and sensitive to the yarn length. On the other hand, the coarse structure of jute yarns facilitate the mechanical connection with rammed earth (Figure 20).

Jute fabric is a textile made of plain weaving of jute yarns; while flax, hemp and other vegetable fibers have been used as textile materials, historically, jute fabric has been only considered for packaging because of its coarser structure.

In order to acquire necessary information to develop a strengthening system for rammed earth structures based on the use of jute fabric, it was necessary at first to investigate on the mechanical properties of jute fabric and yarns, as they arrive on the market. For this reason, tensile tests on jute fabric and on jute yarns were carried out. The extreme variability of data obtained from the early tests and the size effect that was observed, however, make it difficult both to define and to use some average results, unless statistical methods are employed to process and utilize them. Indeed jute fibers, due to their nature, to their length and to the spinning in single ply yarns, constitute wires which properties need to be defined from a macroscopic point of view. This is obviously not the case of CFRP usually employed for the strengthening of structures, that combine polymer matrix with synthetic fibers characterized by regular geometry and properties.

It is necessary to define a sufficiently simple test method to determine reliable properties of strength and stiffness of jute fabric, which results do not depend on the specimen size. For this reason, a successive campaign of tensile tests on jute yarns was performed on different length specimens, so to highlight the dependence of experimental strength on yarn length. Mechanical properties of jute fibers and their statistical distribution have already been studied, for example, by (Xia et al., 2009) in order to collect the necessary information for the design of new composites where vegetable fibers substitute synthetic ones. The Weibull statistic, already used to study vegetable fibers, was used to describe the statistical properties of yarns. The results were compared with the results of tensile tests performed on jute fabric strips, pointing out some inconsistency and suggesting the possibility of intrinsic difficulties in the test method.

Following, the results of tensile tests on jute strips and jute yarns are described, organized and statistically analyzed in order to interpret the basic laws of size effects involved.

An overview of the statistical approach is reported, together with the reasons for which such distribution model is generally employed when analyzing such materials; tests are described and tests results are reported; the treatment of data for the determination of the statistical parameters is described.

2.2.2 Strength of heterogeneous specimens and Weibull distribution

It is widely known that results of mechanical experiments are strongly influenced by heterogeneities of the specimen. The hypothesis of homogeneity on which continuum theories are based is sometimes far from reality, also within the size of laboratory specimen. For this reason, the precaution is generally taken that the size of laboratory specimens for compression tests is 7 times the maximum defect dimension (see for example concrete cubic specimens), in order to minimize the consequences of non-uniform load distribution. Successively, statistical analysis is necessary to interpret the experimental results affected not only by experimental errors but also by intrinsic scattering among the specimens that constitute the statistical sample. These precautions are sufficient if the differences of properties from one point to another are small enough with respect to their average value, or when the characteristic size of the heterogeneity is small enough. Otherwise, that is when the specimen is small and heterogeneity is sharp, the assumption of homogeneity on heterogeneous specimens can produce evident size effects on results; that is, the measured property does in fact depend somehow on the size of the laboratory specimen.
On the other hand, Weibull statistical distribution supplies a tool for the analysis and description of data samples affected by size effects, that is profitably employed for handling strength results obtained on materials that are particularly sensitive to the presence of defects, due to the small fracture energy and plastic asset (Weibull, 1951; Zhang et al., 2002; Xia et al., 2009), as for example glass. In fact, Weibull model was conceived to represent size effect of unidimensional structure, that is the dependence of strength from length, via the so called Weibull parameter and can be a fortiori used to interpret the results of tensile tests of slender specimens.
Weibull probability distribution function was built imagining a unidimensional structure, as a chain made of a series of rings having different strength, subjected to tensile load; it identifies the cumulative probability distribution function of rupture as the probability $P(X \leq x)$ that only one link, the weakest, breaks, due to a force less or at least equal to x.

$$P(X \leq x) = 1 - e^{-n\left(\frac{x}{x_0}\right)^m} \qquad (2.1)$$

Here, x_0 is the strength of some reference link; m is called Weibull (shape) exponent; n represents the number of rings forming the chain specimen. When using Weibull statistical model to describe the strength of a continuous unidimensional yarn, it is useful to substitute n with the ratio of the specimen length L to the reference length L_0 (that is the length of the specimen having average strength equal to x_0). We have:

$$P(X \leq x) = 1 - e^{-\frac{L}{L_0}\left(\frac{x}{x_0}\right)^m} \qquad (2.2)$$

Weibull distribution function, in the form represented in eq. (2) has three characteristic coefficients: Weibull exponent *m* that is also referred to as shape parameter, the characteristic length L_0 and the reference parameter x_0. It must be noted that among these, the independent parameters are only two because the characteristic length has been introduced to express the ratio L/L_0 in place of the number of links of the discrete chain model.

Weibull distribution function can be represented in a simplified form, in which the specimen characteristic length L_0 and the reference parameter x_0 are not directly represented, but it is embodied in the so called scale parameter a as follows:

$$P(X \leq x) = 1 - e^{\frac{-L}{a} x^m} \qquad (2.3)$$

where

$$a = L_0 x_0^m \qquad (2.4)$$

The expected value of the Weibull distribution is:

$$\bar{x} = E(x) = x_0 \left(\frac{L}{L_0}\right)^{-\frac{1}{m}} \Gamma\left(1 + \frac{1}{m}\right) \qquad (2.5)$$

Starting from the expected value it is possible to obtain the scale law:

$$\bar{x} = x_0 \left(\frac{L}{L_0}\right)^{-\frac{1}{m}} = \left(\frac{a}{L}\right)^{\frac{1}{m}} \qquad (2.6)$$

It can be easily shown that x_0 is the average value of the *x* parameter as obtained from the reference length specimen L_0. If the dependence on specimen length has to be highlighted, eq. (2)

Weibull statistical distribution function has been applied to the interpretation of mechanical tests on brittle materials and, recently, on vegetable fibers, and has been enriched introducing other parameters (Xia et al., 2009). Due to the huge non uniformity of jute yarns, a strong variability of properties in the length can be supposed. For this reason, tensile tests on jute yarns for the statistical analysis of strength data were performed on different length specimens and the apparent dependence of strength on length was interpreted by means of the Weibull distribution.

2.2.3 Experimental campaign

For the experimental investigation, jute fabric from Bangladesh was used, purchased from Deyute Consortium, an international organization that deals with the distribution of jute products. This investigation involves:

- Tensile test on twenty jute strips 7cm width

- Tensile test on five series of jute yarns with different length performed in the Material and Structure Test Laboratory of the Architecture Department, University of Florence. The results of this experimental campaign have been statistically treated
- Tensile tests on nine series of jute yarns carried out in the Department of Structural Design of University of Braunschweig.

The tissue analyzed was employed for the experimental campaigns on the reinforced prismatic elements (Chapter 3) and reinforced arches (Chapter 4).

2.2.3.1 Tensile tests on jute fabric

The fabrics most used to produce composite materials are 2D fabrics. For this research work, a fabric in which warp and weft directions are aligned forming a simple cross pattern was employed. In order to determine the mechanical properties of this fabric, 20 strips 7 cm wide and 20cm long were cut from a bold of jute fabric along the warp, having weight of 150g/m^2 and average spacing between wires of 4.292mm. In a previous experimental investigation carried out in the Material and Structure Test Laboratory of the Architecture Department, University of Florence on a different type of jute fabric in terms of density and provenience, half the specimens were immersed in potable water for some ten minutes, then were left to dry for 24 hours. In fact, as the jute fabric has to be applied as reinforcement on earth masonry with a plaster of soil, water and, eventually, gypsum, it inevitably gets in touch with water and it was necessary to evaluate if this could someway affect its properties. The results obtained on the two series of specimens (dry and wet) are almost equal, and the differences can be considered within the experimental variability. Instead, tests already carried out in order to assess the difference between warp and weft showed that the warp is generally stronger than the weft result observed also by others authors (Codispoti et al., 2015). Therefore, it was decided to perform this experimental investigation only employing dry jute and cutting specimens in the warp direction. In the chapter 3 and 4 the jute fabric used as a reinforcement on rammed earth elements is applied in the same direction.
Top and bottom of the jute strips were fixed into steel plates with latex topping to improve adherence (figure 21) and were subjected to tensile tests with a press made of a rigid frame equipped with a screw jack.

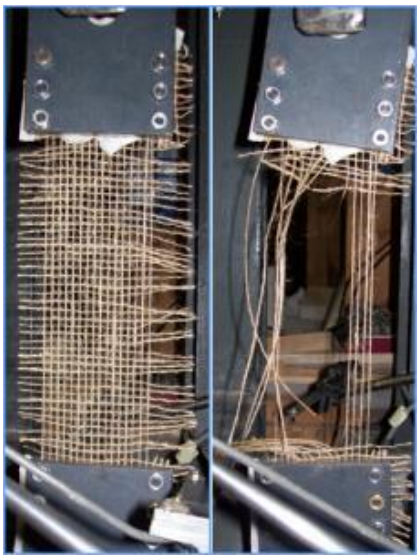

Figure 2.21 – Tensile test on jute strips (master degree thesis Piredda)

The steel clapping plates at the edges of the specimens guarantee that the warp yarns are subjected to uniform relative displacement and the rotation is effectively avoided. A load cell having a capacity of 500kg was put in series with the specimen and the jack, and total deformation was evaluated with four displacement transducers constrained at the basis of the specimen and lent on the top. Load was applied with a rate of about 500 N/min. Average values of strength and stiffness are reported in table 2.13, referring to one single yarn, in order to make the results comparable. In fact, handling the specimens often caused the detachment of some yarns, so that the specimens subjected to tests were characterized by different numbers of yarns, ranging from 14 to 16.In particular, maximum load reached during the test P, strip stiffness K, P_{yarn} and K_{yarn} respectively maximum load and stiffness, divided by the number of yarns of the specimens, maximum load for strip unit where s is the average spacing between yarns equal to 4.292mm and Young modulus for a strip of unit width and of the unit thickness Eh are listed in the table 2.13. An example of load-displacement curve of jute strip is depicted in figure 22.

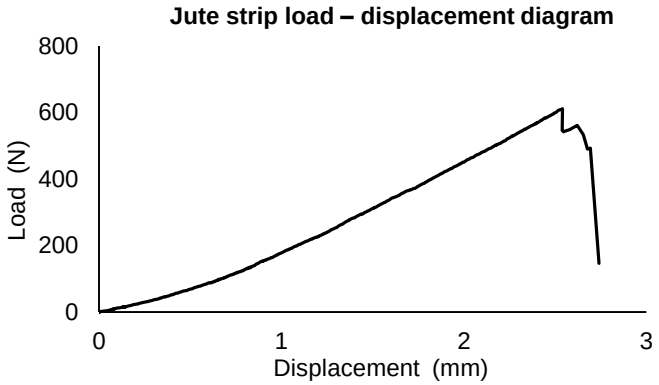

Figure 2.22 – Load displacement diagram of specimen 07(master degree thesis Piredda).

	P (N)	K (N/mm)	P_{yarn} (N)	K_{yarn} (N/mm)	P_{yarn}/s (N/mm)	E h (N/mm)
Average	476.5	221.6	31.25	14.57	7.28	679.0
St. dev.	82.75	37.99	3.74	1.97	0.87	91.88
c%	17.37	17.14	11.96	13.53	11.96	13.53

Table 2.13: Main mechanical parameters of 20 specimens of jute fabric, (approximate length 20 cm). The values reported have been divided by the yarn number due to the not regular width of specimens.

The great variability of the jute yarn cast some doubts on the meaning of yarn strength as obtained on tensile tests on fabric specimens, mainly because of the difficulty to control the boundary conditions in the test device.

Due to the relatively wide spacing among wires (4.292 mm) only few yarns could be contained in a fabric specimen (about 15 yarns), so that the heterogeneity of the specimens was obvious. The stiffness centroid of the specimen can be significantly far from the geometric centroid in which load is applied. For this reason, the boundary condition implemented by the constraint system is crucial; if any rotation is possible to the edge boundaries, also in an initial stage of the test, it can significantly affect the specimen behaviour.

The great heterogeneity of material can cause the weaker yarn that is able to absorb the higher share of force to influence the behaviour of the strip. The distribution of the forces among the parallel yarns is determined by the different stiffness values and by the kind of boundary conditions that it was possible to produce in the experiment. Moreover, such distribution changes when a single yarn fails. It is presumable that the test results will depend on the specimen width and the constraint system. (Such problem deserve attention and makes it necessary to define a reference test procedure in order to obtain the same results among different laboratories.)

For this reason, tensile tests on yarns were performed, as, in this case, the realization of the constraint in the laboratory experiment is simpler. The results of tests on yarns permit to analyze the statistical character of material and to better understand the difficulties involved in the realization of tests on fabric

To better understand the phenomenon of stress distribution in the tests and interpret the global behaviour of the fabric when put in place as a reinforcement of earth structures, it was necessary to perform extensive experimental analysis of jute yarns in order to successively analyze the statistical behaviour of test results.

2.2.3.2 Tensile tests on jute yarns for the statistical analysis of strength data

In order to analyze the statistical properties of strength of jute yarns and highlight the size effect of yarn strength with specimen length, an experimental campaign was performed in which the length of specimens was varied to verify the presence of size effect and to assess effective influence. The sampling procedure was a tricky task as the reliability of the statistical analysis is conditioned by the ability to produce a representative sample of the population of fabric yarns. For this reason, 30 yarns 200 cm long were taken from a fabric portion. From each of these yarns, five pieces were cut with the following lengths: 20cm, 30cm, 40cm, 50cm and 60cm. It was paid specific attention to random alternate the yarn length. All the specimens were tied with a reef knot on themselves as to form rings that were successively subjected to tensile test with a press made of a rigid frame equipped with a screw jack. A load cell having a capacity of 500kg was put in series with the specimen and the jack (Figure 23). The deformation of the specimens was not registered. A test machine was used not equipped for the registration of displacements because in those days it seemed not important to analyze wire stiffness. The test results obtained on the five series of 30 specimens are reported in table 2.14. The trend of strength to decrease with length is apparent.

Figure 2.23 tensile test on jute yarn

	I series (30 yarns.)	II series (30 yarns.)	III series (30 yarns.)	IV series (30 yarns.)	V series (30 yarns.)
Wires length (cm)	20	30	40	50	60
Specimens average length (cm)	9.87	14.68	19.45	24.54	29.76
St. dev.	0.21	0.25	0.26	0.24	0.29
Average maximum load (N)	46.77	46.29	46.12	42.35	39.18
St. dev.	6.34	6.18	5.52	6.52	5.61

Table 2.14. Results of tensile test on five series of different length of jute yarns

It must be noted that the values of strength determined on yarns and reported in table 2.14 are definitely higher than the strength per yarn determined on the jute fabric specimens (Table 2.13). This can be connected to the influence of the statistical scattering of jute yarns properties in the fabric specimens that can approximately be described as an elastic system of springs arranged in parallel; the weakest yarn is able to influence the global behaviour of the specimen. In order to better comprehend the influence of statistical scattering and of size effects on the experimental results, a statistical analysis was carried out of the data collected with the experimental campaign described previously. In particular, as described in the next section, yarns strength values determined were used to calibrate the Weibull type models (3).

2.2.3.3 Statistical analysis of test results

Determination of the parameters of Weibull distribution for strength results on jute yarns.

The experimental tensile strength values obtained on 150 jute yarns of different length, as described in previous section, were statistically analyzed via Weibull distribution, using the probability density functions.

Manipulating equation (3) and taking the natural logarithm twice, this can be transformed in a linear equation:

$$ln\left(-ln\left(1-P(X\leq x)\right)\right)=m\,ln(x)+ln(L)-ln(a) \qquad (2.7)$$

This equation has been used to fit the experimental values of tensile strength referring both to the single length (five series of 30 specimens) and to all the experimental values interpreted as a whole. Starting from Weibull distribution through a fitting process it is possible to obtained the values of the statistical parameters m and $\mathfrak{a}$, where m is Weibull exponent and $\mathfrak{a}$ is the relation between characteristic length and the characteristic strength of this material. The Weibull parameters obtained by the fitting procedure are reported:

$$m = 7.11471$$

$$a = 2.65273 * 10^{13}$$

Choosing a length it is possible to determine the characteristic strength of this length.
Strength values, treated as a whole, were interpolated using the probability density function taking into account the effective length of specimens.
In The figure 23 the cumulative distribution function of strength represented in the plane of L (specimen length) and strength is showed. The points corresponding to the experimental results are reported in red.

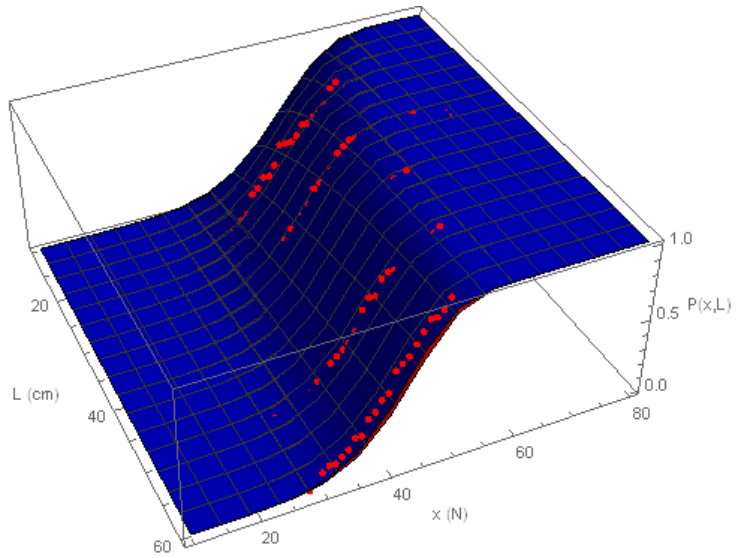

Figure 2.24 Cumulative probability of the whole data sample (150 specimens)

Figure 25 (a. to e.), representing vertical sections with planes parallel to P and x axes of the plot in figure24, reports the cumulative probability densities of the five data series compared with the corresponding Weibull probability distribution function.

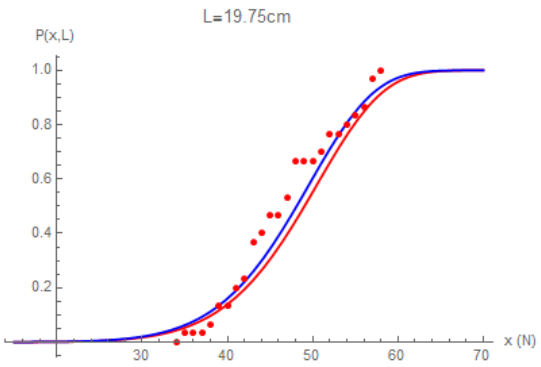

a

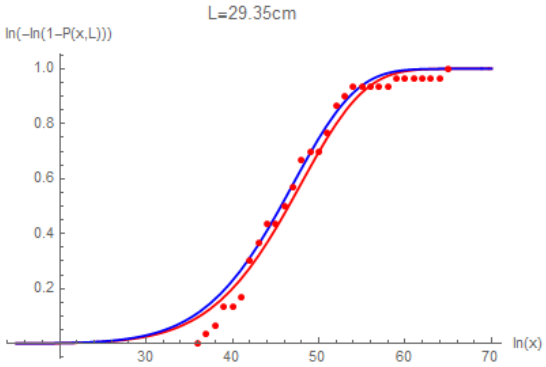

b

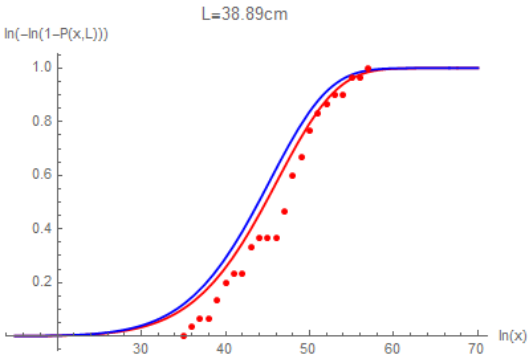

c

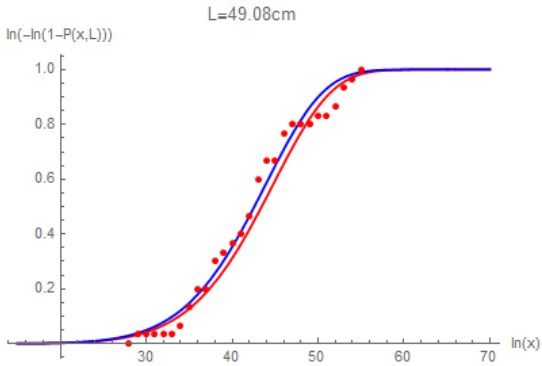

d

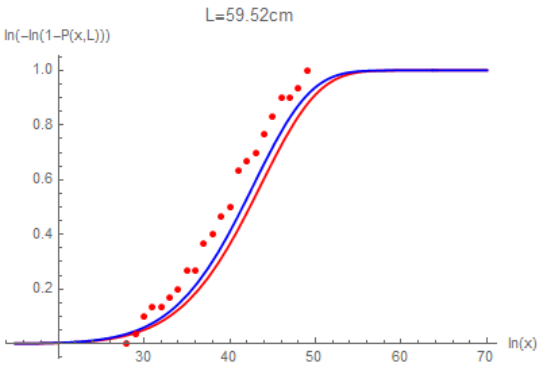

e

Figure 2.25 - Distribution functions corresponding to the five series, compared with the experimental points (in red).

It is apparent that the described procedure produce reliable representations of the experimental data. Given the average experimental value x_0 of a yarn corresponding to the length L_0 the expected value $\bar{x}$ of yarn of length L can be calculated via equation (6).

2.2.3.4 Tensile tests on jute yarns (University of Braunschweig)

Nine series of tensile test on jute yarns (thirty for each series) with different lengths were performed using Zwick Z50 kN Testing Machine (Figure 2.26) and TestXpert II simulation software (DIN EN13895) in the department of structural design of University of Braunschweig in order to deeply investigate the possibility to statistically correlate strength and stiffness.

Some specimens failed near the clamping area and these results have been excluded. In order to analyze the correct strength of yarns only the specimens that broke at their middle length have been considered. In the table 2.15 the maximum load and the average tensile elongation for each series are reported

	I series	II series	III series	IV series	V series	VI series	VII series	VIII series	IX series
Specimens length (cm)	5	7.5	10	12.5	15	17.5	20	22.5	24
Average max. load (N)	75.57	72.84	70.10	64.41	60.92	57.94	55.73	56.94	56.32
St. dev. pop	11.82	12.59	12.16	11.05	9.15	9.69	9.13	7.82	8.56
Average tensile elongation (%)	6.72	4.71	5.21	2.89	3.12	2.46	2.66	2.27	2.36
St. dev. pop	2.34	1.89	1.48	0.70	0.96	0.54	0.55	0.31	0.47

Table 2.15 Results of tensile test on nine series of different length of jute yarns

Figure 2.26 – Tensile test on jute specimen

2.3 Conclusions

In the light of studies conducted on the use of gypsum as a stabilizer it was decided to use the 15% of gypsum powder to reduce the shrinkage of the reinforcement matrix. The matrix is composed by sieved earth and 30% water for easy application. This amount of water leads to a linear shrinkage of 9% (Table 2.4) which can be greatly reduced by using 15% of gypsum. In view of the results obtained from the compression tests with load parallel and perpendicular to the layers it is evident that the substantial difference between the two load conditions is in terms of elastic modulus and not of compression strength. Natural materials, especially if rough due to specific processing techniques, deserve particular attention in the tuning of test methods for the definition of mechanical properties, due to the high scattering of results, to the size effects induced by heterogeneities and to the resulting uncertainties. For these reasons it was necessary to define test methods and possible modes to use of the obtained parameters through statistical analysis of the resulting data (Fagone et al. under review).

Insofar as it is possible to understand in this stage, tests on yarns seem to be simpler and more reliable and recommend these experiments as the reference ones could be useful in order to evaluate the mechanical and statistical parameters of jute to be employed for the design of strengthening systems. Statistical analysis is, in this phase, a necessary tool to obtain mechanical parameters to be used for the correct design of earth construction strengthening systems.

Further research is necessary to examine in depth the capability of describing the statistical character of test results with different statistical models and it is interesting to deeply analyze the stiffness using the results obtained by tensile tests performed on august 2016 at the University of Braunschweig.

In a successive step, it is necessary to define some rules that permit to use the material parameters, whose variability has a definitely statistical behaviour, in a proper way when dealing with the design of a strengthening system for rammed earth constructions.

2.4 Bibliography

Alecci V, Briccoli Bati S, Ranocchiai G. 2014. “Concrete Columns Confined with CFRP wraps”. Mater Struct Constr 47:397–410. doi:10.1617/s11527-013-0068-7.

Alecci V, Briccoli Bati S, Ranocchiai G. 2009. “Study of Brick Masonry Columns Confined with CFRP composite”. J Compos Constr 13:179–87. doi:10.1061/(ASCE)1090-0268(2009)13:3(179).

Bain, J. A. 1971.”A Plasticity Chart as an Aid to the Identification and Assessment of Industrial Clays”. Clay Minerals 9: 1–17. doi: 10.1180/claymin.1971.009.1.01

Basilio I, Fedele R, Lourenço PB, Milani G. 2014. “Assessment of Curved FRP-Reinforced Masonry Prisms: Experiments and modeling”. Constr Build Mate 51:492–505. doi: org/10.1016/j.conbuildmat.2013.11.011.

Borri A, Corradi M, Speranzini E. 2013. “Reinforcement of wood with natural fibers”. Compos Part B Eng 53:1–8. doi:10.1016/j.compositesb.2013.04.039.

Borri A, Corradi M, Speranzini E. 2013. “Bending tests on natural fiber reinforced fir wooden elements” 778: 537–44. doi:10.4028/www.scientific.net/AMR.778.537.

Briccoli Bati S, Fagone M, Rotunno T. 2013. “Lower Bound Limit Analysis of Masonry Arches with CFRP Reinforcements: A Numerical Method”. J Compos Constr 17:543–53. doi:10.1061/(asce)cc.1943-5614.0000350.

Briccoli Bati S, Fagone M, Loccarini F, Ranocchiai G. 2014. “Jute Fabric to Improve the Mechanical Properties of Rammed Earth Constructions”. Mileto C, Vegas F, Garcìa L, Cristini V, editors. Versus 2014, Valencia, Spain: CRC Press: 55–60.

Briccoli Bati S, Fagone M, Loccarini F, Ranocchiai G. 2013. “Analysis of Rammed Earth Arches Strengthened with Natural Fibers”. Iványi BHVT and P, editor. Fourteenth Int. Conf. Civil, Struct. Environ. Eng. Comput., vol. Proceeding, Cagliari: 1–16. doi:10.4203/ccp.102.78.

Briccoli Bati S, Fagone M, Ranocchiai G. 2014. “The Effects of Mortar Joints on the Efficiency of Anchored CFRP Sheets Reinforcements of Brick-Masonry”. Mech. Mason. Struct. strengthened with Compos. Mater. Model. testing, Des. Control, Ravenna: 575–83. doi:10.4028/www.scientific.net/KEM.624.575.

Bui QB, Morel JC, Hans S, Meunier N. 2008. “Compression Behaviour of Nonindustrial Materials in Civil Engineering with Three Scale Experiments: the case of Rammed Earth”. Mater Struct: doi:10.1617/s11527-008-9446-y.

Bui, Q. B., & Morel, J. C. 2009. “Assessing the Anisotropy of Rammed Earth”. Construction and Building Materials, 23(9): 3005–3011 doi:10.1016/j.conbuildmat.2009.04.011

British standards institute (BSI). BS 1377-2: 1990 soils for civil engineering purposes – part 2: classification. London: BSI, 1990

Burroughs S. 2008. “Soil Property Criteria for Rammed Earth Stabilization”. J Mater Civil Eng: 20 (3):264–73.

Caggegi C, Pensee V, Fagone M, Cuomo M, Chevalier L. 2014. “Experimental Global Analysis of the Efficiency of Carbon Fiber Anchors Applied over CFRP Strengthened Bricks”. Constr Build Mater 53:203–12. doi:10.1016/j.conbuildmat.2013.11.086.

Carloni C, Focacci F.2016. “FRP-Masonry Interfacial Debonding: an Energy Balance Approach to Determine the Influence of the Mortar Joints”. Eur J Mech - A/Solids 55: 122–33. doi:10.1016/j.euromechsol.2015.08.003.

Capozucca R. 2010. “Experimental FRP/SRP-historic masonry delamination”. Compos Struct 92:891–903. doi: 10.1016/J.Compstruct.2009.09.029.

Codispoti R, Oliveira D V, Olivito RS, Lourenço PB, Fangueiro R. 2015. “Mechanical Performance of Natural Fiber-Reinforced Composites for the Strengthening of Masonry”. Compos Part B Eng 77:74–83. doi: 10.1016/j.compositesb.2015.03.021.

Corradi M, Borri A, Castori G, Speranzini E. 2016. “Fully Reversible Reinforcement of Softwood Beams with Unbonded Composite Plates”. Compos Struct 149:54–68. doi:10.1016/j.compstruct.2016.04.014.

Cottone, A., Giambanco G. 2009. “Minimum Bond Length and Size Effects in FRP-Substrate Bonded Joints. Eng Fract Mech 76:1957–76. doi:10.1016/J.Engfracmech.2009.05.007.

D’Ambrisi A, Feo L, Focacci F. 2013. “Experimental and Analytical Investigation on Bond Between Carbon-FRCM Materials and Masonry”. Compos Part B-Engineering 46:15–20. doi:Doi 10.1016/J.Compositesb.2012.10.018.

Doan T-T-L, Gao S-L, Mäder E. Jute/polypropylene composites I. Effect of matrix modification. Compos Sci Technol 2006;66:952–63. doi:10.1016/j.compscitech.2005.08.009.

Fagone, M., Loccarini, F., Ranocchiai, G. Under review. “Strength Evaluation of Jute Fabric for the Reinforcement of Rammed Earth Structures”. Submitted to Composites part B

Fagone M, Ranocchiai G, Caggegi C, Briccoli Bati S, Cuomo M. 2014. “The efficiency of Mechanical Anchors in CFRP Strengthening of Masonry: An Experimental Analysis”. Compos Part B Eng 64:1–15. doi:10.1016/j.compositesb.2014.03.018.

Fagone M, Ranocchiai G, Briccoli Bati S. 2015. “An Experimental Analysis about the Effects of Mortar Joints on the Efficiency of Anchored CFRP-to-Masonry Reinforcements”. Compos Part B-Engineering 76:133–48. doi:10.1016/j.compositesb.2015.01.050.

Fagone M, Rotunno T, Briccoli Bati S. 2016. “The Groin Vaults of St. John Hospital in Jerusalem: An Experimental Analysis on a Scale Model”. Int J Archit Herit. doi:10.1080/15583058.2016.1158331.
Fedele R, Milani G. “Assessment of Bonding Stresses between FRP Sheets and Masonry Pillars during Delamination Tests”. Compos Part B Eng 2012;43:1999–2011. doi:http://dx.doi.org/10.1016/j.compositesb.2012.01.080.

Freddi F, Sacco E. 2016. “An Interphase Model for the Analysis of the Masonry-FRP Bond”. Compos Struct 138:322–34. doi:10.1016/j.compstruct.2015.11.041.

Gowda TM, Naidu ACB, Chhaya R. 1999. “Some Mechanical Properties of Untreated Jute Fabric-Reinforced Polyester Composites”. Compos Part a-Applied Sci Manuf 30:277–84.

Hall M, Djerbib Y. 2004. “Rammed Earth Sample Production: Context, Recommendations and Consistency”. Constr Build Mater 18:281–6.

Hamilton HR, McBride J, Grill J. 2006. “Cyclic Testing of Rammed Earth Walls Containing Post-Tensioned Reinforcement. Earthquake Spectra 22(4):937–59

Hejazi SM., Sheikhzadeh M., Abtahi SM., Zadhoush A. 2012. “A Simple Review of Soil Reinforcement by Using Natural and Synthetic Fibers. Constr Build Mater;30. doi:10.1016/j.conbuildmat.2011.11.045.

Houben H, Guillaud H. 2008. Earth construction: a comprehensive guide. CRATerre-EAG, Intermediate Technology Publication, London

Houben H, Guillaud H. 2006. Traité de construction en terre. Parenthèses

Isik, B., Tulbentci, T. 2008. “Sustainable Housing in Island Conditions Using Alker-gypsum-stabilized earth: A Case Study from Northern Cyprus”. Building and Environment, 43(9), 1426–1432. doi: 10.1016/j.buildenv.2007.06.002

Jayasinghe C, Kamaladasa N. 2007. “Compressive Strength Characteristics of Cement- Stabilized Rammed Earth Walls”. Constr Build Mater 21(11):1971–6.

Jaquin PA, Augarde CE, Gerrard CM. 2007. “Historic Rammed Earth Structures in Spain: Construction Techniques and a Preliminary Classification”. Proc int symposium on earthen structures 327-33.

Joko K, Tokuda S, Kikumoto N, Sugai J, Hayashi T, Arai M. 2002. “Enzymatic Function on Jute Fiber with Various Commercial Enzymes”. Sen’i Gakkaishi 58:22–8. doi:10.2115/fiber.58.22.

Kalfat R, Al-Mahaidi R, Smith ST. 2013. “Anchorage Devices Used to Improve the Performance of Reinforced Concrete Beams Retrofitted with FRP Composites: State-of-the-Art Review”. J Compos Constr 17:14–33. doi:10.1061/(Asce)Cc.1943-5614.0000276.

Kostic M, Pejic B, Skundric P. 2008. “Quality of Chemically Modified Hemp Fibers”. Bioresour Technol 99:94–9. doi:10.1016/j.biortech.2006.11.050.

Lilley DM, Robinson J. 1995. “Ultimate Strength of Rammed Earth Walls with Openings. Proc – ICE: Struct Build 110(3):278–87.

Maniatidis V, Walker P. 2008. “Structural Capacity of Rammed Earth in Compression”. J Mater Civil Eng 20(3):230–8.

Maruccio C, Basilio I, Oliveira D V, Lourenço PB, Monti G. 2014. “Numerical Modelling and Parametric Analysis of Bond Strength of Masonry Members Retrofitted with FRP”. Constr Build Mater 73:713–27. doi:10.1016/j.conbuildmat.2014.09.082.

Menna C, Asprone D, Durante M, Zinno A, Balsamo A, Prota A. 2015. “Structural Behaviour of Masonry Panels Strengthened with an Innovative Hemp Fibre Composite Grid”. Constr Build Mater 100:111–21. doi:10.1016/j.conbuildmat.2015.09.051.

Miccoli, L., Muller, U., Fontana, P. 2014. “Mechanical Behaviour of Earthen Materials: A Comparison between Earth Block Masonry, Rammed Earth and Cob”. Construction and Building Materials, 61, 327–339. http://doi.org/10.1016/j.conbuildmat.2014.03.009

Miccoli, L., Oliveira, D. V., Silva, R. a., Müller, U., & Schueremans, L. 2014. “Static Behaviour of Rammed Earth: Experimental Testing and Finite Element Modelling”. Materials and Structures, 3443–3456. doi: 10.1617/s11527-014-0411-7

Muray R. Spiegel, John J. Schiller RAS. Probability and Statistics. 2009.

Pacheco-Torgal, F., Jalali S. 2011. “Earth Construction: Lessons from the Past for Future Eco-Efficient Construction”. Constr Build Mater 29:512–9. doi:10.1016/J.Conbuildmat.10.054

Pan NC, Day A, Mahalanabis KK.1999 “Chemical Composition of Jute and its Estimation”. Man-Made Text India 42:467–73

Pintucchi B, Zani N. A. 2016. “Simple Model for Performing Nonlinear Static and Dynamic Analyses of Unreinforced and FRP-Strengthened Masonry Arches”. Eur J Mech A/Solids 59:210–31. doi:10.1016/j.euromechsol.2016.03.013.

Raviolo, P.L.1993. “Il laboratorio geotecnico: procedure di prova, elaborazione, acquisizione dati”, Editrice Controls, Milano

Speranzini E, Agnetti S. 2015. “Flexural Performance of Hybrid Beams made of Glass and Pultruded GFRP. Constr Build Mater 94:249–62. doi:10.1016/j.conbuildmat.2015.06.008.

Sreenath HK, Shah AB, Yang VW, Gharia MM, Jeffries TW. 1996. “Enzymatic Polishing of Jute/Cotton Blended Fabrics”. J Ferment Bioeng 81:18–20. doi:10.1016/0922-338X(96)83113-8.

Standards New Zealand. NZS 4298: 1998 Materials and work- manship for earth buildings – incorporating amendment no. 1. Standards New Zealand, Wellington, New Zealand, 1998.

Vargas-Neumann J. 1993. “Earthquake Resistant Rammed Earth (tapial) Buildings”. Proc. 7a conferencia internacional sobre e estudo e conservação da arquitectura de terra140-51.

Walker P, Dobson S. 2001. “Pullout Tests on Deformed and Plain Rebars in Cement- Stabilized Rammed Earth. J Mater Civil Eng 13 (4):291–7.

Weibull W. 1951. “A Statistical Distribution Function of Wide Applicability”. J Appl Mech 18:293-7.

Xia ZP, Yu JY, Cheng LD, Liu LF, Wang WM. 2009. “Study on the Breaking Strength of jute Fibres using Modified Weibull Distribution. Compos Part a-Applied Sci Manuf 40. doi:10.1016/j.compositesa.2008.10.001.

Yao J., Teng J.G., Chen J.F. 2005. “Experimental Study on FRP to Concrete Bonded Joints”. Compos Part B-Engineering 36:99–113. doi:10.1016/j.compositesb.2004.06.00l.

Yeşildal S, Önal M, Özes Ç, Neşer G. 2011. “Green Materials and Their Use in Pleasure Craft” Construction: An Experimental Case Study on Jute Fibres. 1st Int. Symp. Nav. Archit. Marit 111–8.

Zhang YP, Wang XG, Pan N, Postle R. 2002. “Weibull Analysis of the Tensile Behavior of Fibers with Geometrical Irregularities”. J Mater Sci 37:1401–6. doi: 10.1023/A:1014580814803.

Chapter 3
Interaction between jute reinforcement and earth substrate

3.1 Composite materials

Composite materials are required in many fields to satisfy needs that cannot be fulfilled by substances or materials that can be considered homogeneous at the microscale (molecular). Therefore, composite materials are designed to satisfy different requests basing on a synergetic use of components. Composites are all those materials obtained by overlapping or mixing different materials with the intent to obtain a complex which has better mechanical and chemical characteristics than those of the two components. Starting from this definition, any two-phase material can be considered a composite material. The two-phase materials possess many of the mechanical and physical characteristics that are typical of composites.

The practice of combining materials with additives to increase performance and to reduce the shrinkage during the drying and curing is an ancient practice (stabilization process of rammed earth has been treated in chapter 1); in particular fibers were used to reinforce brittle materials since Egyptian and Babylonian civilization. Glass, steel, textile, and other kinds of fibers are widely used to improve performance of concrete from about one hundred years. The main role of fibers is to bridge the cracks that develop in concrete due to shrinkage and increase the ductility of concrete elements (Brahma Chari, 2015).

The reinforcement fibers can be cut, aligned and placed in different ways to affect the properties of the resulting composite (Campbell 2010). Fiber-reinforced composites are made of two phases; the matrix, acting as a binder, and the reinforcement fibers, continuous/discontinuous and filiform, that determine mainly the mechanical characteristics of the composite. We define discontinuous fiber composites as materials in which the organic or inorganic matrix is reinforced with one or more fibrous materials of short length. The fibers can be linear or bent, dispersed in the matrix in all directions, thereby creating a distributed multidirectional texture, which improves the composite in terms of performances such as resistance against fire, thixotropy, ductility and abrasion resistance.

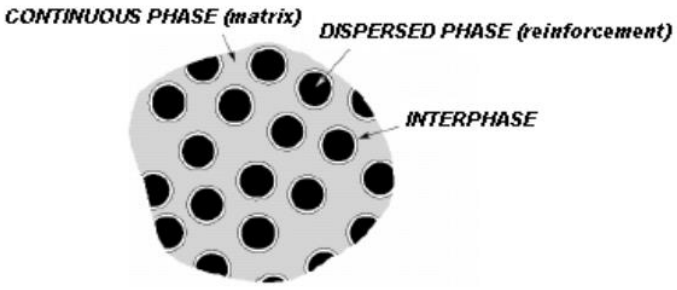

Figure 3.1 - Representation of phases in a FRP composite. (CNR-DT 200_R1_2013).

In general, the fibers addition impairs the material workability, so it is necessary to take account of this effect. The continuous fiber composite materials represent an evolution of the discontinuous-fiber composite applications. In fact if in the first category, the fibers have the task of improving the matrix characteristics or of conferring new properties on it, in the continuous-fiber composites the fiber plays the role of structural reinforcement. Also in these cases, matrix can be of organic and inorganic nature and generally presents as an isotropic continuous and has the objective to fix the fibers, to confer compressive strength to the composite and to ensure the geometrical stability of the material. The fabric is the main component of the composite and has the aim to absorb the most of the actions applied to the material. The fibers used for the production of fabrics for composite materials are thin continuous filaments and are considered one-dimensional elements and they are available in different forms: monofilament, tow, spun yarn, rowing. The unidirectional tissue is characterized by fibers all oriented in the direction of the length, the bidirectional fabric is made of an orthogonal weft-warp weaving and the multiaxial tissue is characterized by fibers oriented in different directions. Through adhesion or friction, the matrix distributes the stress among the fibers, enclosing them so that they can act independently and protecting them from weathering or abrasion.

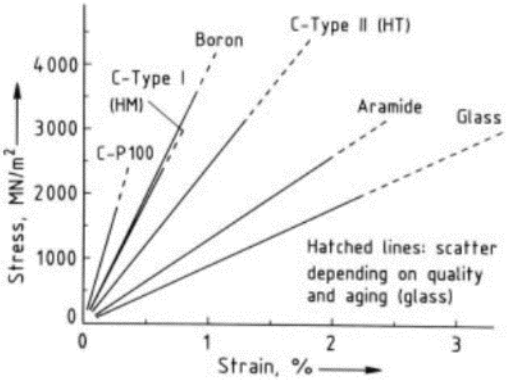

Figure 3.2 - Stress–strain diagram of some inorganic fibers (Clauß and Fitzer, 2012)

It can easily be noted that the long fiber composite will have directionality depending on the direction in which the fibers are laid out in the composite. FRCs are available in several geometries raging from laminates with regular surfaces to bi-directional fabrics that are easily adaptable to the shape of the member being strengthened. In particular, when there is a single ply or a lay-up in which all of the layers or plies are stacked in the same orientation, the lay-up is called a lamina. When the plies are stacked at various angles, the lay-up is called a laminate. Continuous-fiber composites are normally laminated materials in which the individual layers, plies, or laminae are oriented in directions that will enhance the strength in the primary load direction (Campbell 2010). Although all materials can be

used for the production of fibers in principle, in practice this succeeds only with a limited number of materials which have mechanical characteristics valid for applicative purposes.
Over the last decades, the evolution of the concept of sustainable development combined to the sustainability objectives definition are producing the essential driving principles, such as the use renewable resources in preference to nonrenewable resources, for the development of innovative materials and technological solutions in the construction industry (Hill and Bowen 1997). In the case of FRP composites, questions remain regards to the feasibility of FRP composites within the framework of a sustainable environment. Environmental concerns appear to be a barrier to consider them as sustainable materials. In addition, the ability to recycle FRP composites is limited and, unlike steel and timber, structural components cannot be reused to perform a similar function in another structure. On the other hand, it is important to note that the best way to minimize use of resources is find solutions which seek to extend the service life of existing structures and develop new structures that achieve superior service life with minimal maintenance. This is the primary role of Fiber Reinforced Composites as a structural reinforcement system avoiding the environmental, social, and economic impacts associated with replacement and new construction of buildings. (Lee and Jain, 2009; Menna et al., 2015).
Among possible sustainable solutions, natural fibers appear a valid alternative to produce reinforcing composite materials for structural applications thanks their good mechanical properties in agreement with sustainability prerequisites (Madsen et al., 2007; Codispoti et al., 2015; Faruk et al., 2012; Asprone et al. 2011).

3.1.1 Biocomposite

A new generation of materials has been developed focusing sustainability and eco-efficiency with products derived from biodegradable plastics and natural polymers obtained by renewable crops and using biomass as raw materials. Glass, carbon, boron and kevlar are being used as reinforcing materials in FRCs in which have been widely accepted as materials for structural and non-structural applications. However, these materials are prohibitively expensive and their use is not justified in several cases. The development of new materials which enhance optimal utilization of natural resources, and particularly, of renewable resources shifts the focus to natural fibers as jute, pineapple leaves, sisal, kenaf, coir, flax, bamboo, hemp and sisal (Dweib et al. 2004). The interest in Innovative composite materials made of continuous natural fibers embedded in different matrices is increasing both in international research and in advanced applications. Natural fiber reinforced composites, are gaining more space especially in the construction field for externally bonded reinforcement of masonry structures (Asprone et al. 2011; Menna et al. 2015; Codispoti et al. 2015; Satyanarayana et al. 1990; Liu and Wang 2015)

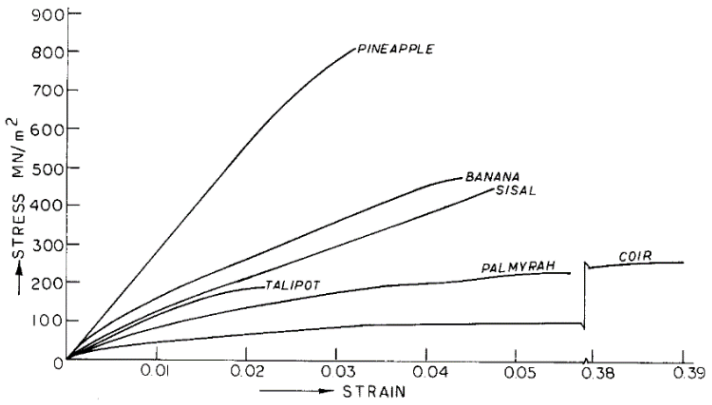

Figure 3.3 - Stress-strain curves of natural fibers (Satyanarayana K. G. et al, 1990)

Starting from the basic concept of FRP i.e. three-dimensional combination between a polymer resin and a reinforcing fiber, instead of exploiting materials of synthetic origin, arising from the processing of petroleum they employ totally or at least in part, elements of plant origin. These composites are going to find more and more application in the near future, especially in Europe, where pressure from both legislation and the public is rising (Faruk et al. 2012). The literature regarding combination of natural fibers with polymer matrix (NFRP) or with cementitious (NFRCM) to produce competitive solutions in strengthening application than the synthetic composite materials shows that their production requires more attention in particular in what concerns the interface between bio fiber and matrix and more articulated stages of processing.

Fiber	Tensile strength (MPa)	Young's modulus (GPa)	Elongation at break (%)	Density [g/cm^3]
Abaca	400	12	3–10	1.5
Bagasse	290	17	–	1.25
Bamboo	140–230	11–17	–	0.6–1.1
Flax	345–1035	27.6	2.7–3.2	1.5
Hemp	690	70	1.6	1.48
Jute	393–773	26.5	1.5–1.8	1.3
Kenaf	930	53	1.6	–
Sisal	511–635	9.4–22	2.0–2.5	1.5
Ramie	560	24.5	2.5	1.5
Oil palm	248	3.2	25	0.7–1.55
Pineapple	400–627	1.44	14.5	0.8–1.6
Coir	175	4–6	30	1.2
Curaua	500–1150	11.8	3.7–4.3	1.4

Figure 3.4 - Physico-mechanical of natural fibers (Faruk et al., 2012)

Three typologies of natural fiber composites were investigated by Codispoti et al. (2015); through tensile tests on reinforcement packages they show how the biocomposite properties are influenced by a number of variables, as the fiber and matrix type, (where the plant fiber are sourced), processing methods, and any modification of the fiber. They conclude that the epoxy resin is the most suitable matrix. Faruk et al. (2012) in their comprehensive review of literature from 2000 to 2010 summarize the mostly readily utilized

natural fibers and biopolymers paying attention on characteristics of reinforcing fibers used in biocomposites, including source, type, structure, composition, as well as mechanical properties.

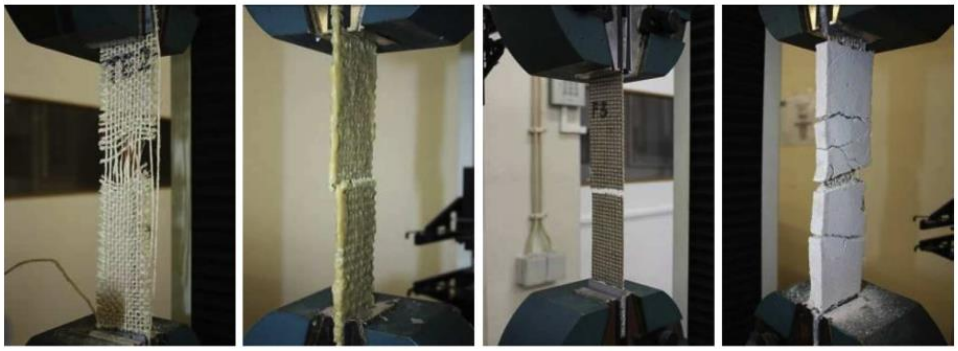

Figure 3.5 - Typical failure mode observed (Codispoti R. et al., 2015)

The so-called biocomposites are evolving using natural fibers with natural polymers derived from renewable resources such as cellulose plastics, starch, plastics derived from starch, polyhydroxyalkanoates (bacterial polyesters), soy-based plastics. Normally biocomposites materials are divided into three categories: agglomerated composite, fibrous composite and porous materials. Many biocomposites materials employ recycled materials or fibers derived from fast-growing plants. They can be recyclable or biodegradable. They also reduce the need for products derived from the petrochemical industry or other fossil fuels, as they generally use natural binders, and favor the use of local products, thus also reducing the cost of transport. They can ensure an increase in the welfare housing, coming to be fire-resistant, thermally efficient, but sufficiently permeable to avoid the occurrence of mold inside the built and at the same time ensure a better indoor air quality. As other materials used in sustainable buildings, the biocomposites help in getting the LEED Certification (Leadership in Energy and Environmental Design).

Despite the significantly advantageous properties and benefits of biocomposite reinforced with natural fibers and/or biopolymers, like biodegradability, low cost, low density yielding relatively light weight, high specific strength and renewable nature further research is required to overcome obstacles such as durability, moisture absorption, inadequate toughness, and reduced long-term stability for outdoor applications. In particular, different weathering conditions, such as temperature, humidity, and UV radiation all affect the service life of the product (Ahmed and Vijayarangan 2008; Shah and Lakkad 1981).

Mechanical properties of natural fibers are scattered and lower than those of synthetic fibers so the failure mechanisms would be different. Another disadvantage of natural fiber composites, which makes them less attractive, is the poor resistance to moisture absorption. Studies in order to assess mechanical behaviour of the bond between fibers and matrices of different nature are known in literature (Asprone et al. 2011; Hejazi et al. 2012). Ghavami et al. (1999) analyze the adhesion between fibers and earth material,

concerning the application of sisal and coconut fibers in conjunction with three types of soil for the production of composite reinforced soil blocks (short-fiber reinforced). They show how reinforcing fibers in the soil matrices prevent cracking by adhesion or bonding to the soil. The main factors, which affect the adhesion between the reinforcing fibers and soil, are the cohesive properties of soil, the compression friction forces appearing on the surface of the reinforcing fiber due to shrinkage of the soil and the shear resistance of the soil, due to the surface form and roughness of the fibers. The dimensional changes of natural fibers due to moisture and temperature variation influence all three adhesion characteristics. During mixing and drying of the soil, the fibers absorb water and expand.

Jute fibers, as the second most common natural cellulosic fiber in the world (Sreenath et al., 1996) appears to be a promising material because it is relatively inexpensive; it has higher strength and modulus than plastics and, more importantly, as its only application in packaging is constantly threatened by synthetics, an additional area of application would be highly desirable. Some studies have been conducted to investigate the use of jute as a reinforcement for plastics or hybrid laminates fiber reinforced polymer or in structural retrofitting of reinforced concrete beams (Shah and Lakkad 1981; Sen and Jagannatha Reddy, 2013).

Jute fiber has a multicellular structure composed of microfibrils and the cross-section is highly non-uniform. Most commonly reported problems include the large scattering in mechanical and physical properties, as for other natural materials, influenced by the highly non-uniform cross-section, their growing conditions geographic origin, climatic growth conditions, fiber processing technique and, as for other fiber types, by the fineness of the fiber and sample test-length. (Ahmed and Vijayarangan, 2008; Gassan and Bledzki, 1999). (Munikenche Gowda et al., 1999) analyze the mechanical properties of jute/polyester laminates, which have better strengths than wood composites and some plastics.

Islam and Iwashita (2010) adopt natural fibers (straw, hemp and jute) with cement and gypsum as strengthening methods to improve strength and ductility of adobe constructions. They conclude that jute seems to be the most effective among the selected fibers since jute improves both the ductility and toughness with slight decreases in compressive strength. The authors suggest an optimal jute content and jute length, which are 2.0% by weight and 2cm, respectively. The higher flexibility, friction to soil, and the tensile strength of the jute fiber might be the reason for its best performance among the selected fibers. The choice to use jute fabric derived to previous experiences. Preliminary tests already carried out in the Laboratory of University of Florence showed that, among the types of vegetable fibers mentioned before, jute wires are particularly apt to produce reinforcement for earth structural elements, as they exhibit good mechanical properties and exceptional adhesion to rammed earth material (Briccoli Bati et al., 2013; Briccoli Bati et al., 2015).

3.2. Fiber-reinforced strengthening of masonry structures

The main reasons for the interest in FRCs as reinforcement of structures is due to their outstanding mechanical properties as high specific modulus, high stiffness to weight ratio, the high strength to weight ratio compared to conventional materials, the lightness, the limited invasiveness, the relative reversibility and ease of installation (Munikenche Gowda, Naidu et al., 1999). The low density causes the specific resistance values (strength/density ratio) and specific elastic modulus (elastic modulus/density ratio) to be higher than those of traditional building materials. These features suggest the choice of FRCs in the case of structural interventions of old structures, since at the same strength, entails a load increase on the existing structure decidedly lower in comparison to other materials; they become competitive compared to other types of traditional intervention for both applications in modern buildings, and to recover the historical heritage when the aesthetic preservation of the original structures is required (buildings of historic or artistic interest) or when traditional strengthening techniques cannot be effectively employed (CNR-DT200 R1 2013).

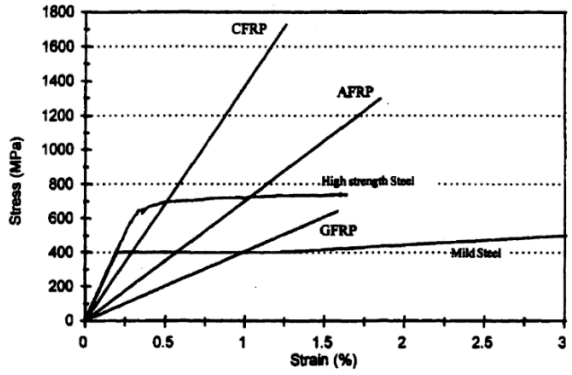

Material	Density (kg/m3)	E (GPa)	σ_t (GPa)	ϵ_t (%)	α 10^{-6}/°C
E-glass (GFRP)	2500	70	1.5 – 2.5	1.8 – 3.0	5.0
S-glass (GFRP)	2500	86	4.8	--	--
High-Modulus Carbon (CFRP)	1950	380	2.0	0.5	-0.6 – -1.3
High-Strength Carbon (CFRP)	1720	240	2.8	1.0	-0.2 – -0.6
Carbon (CFRP)	1400	190	1.7	--	--
Kevlar 49 (AFRP)	1450	60 – 130	2.9	--	--

Figures 3. 6/7 - Material properties of various FRP fibers and stress-strain behaviour of FRP bars (Shehata E. et al, 2000)

Commonly fiber composite materials used for traditional masonry are made of glass, carbon, boron, aramid fibers embedded in a resin (polyester, vinyl, epoxy, phenolic) or cementitious matrix. In the following figures, stress-strain diagram of fibers and matrix and stress-strain diagram in relation to the volumetric fraction for FRP are reported.

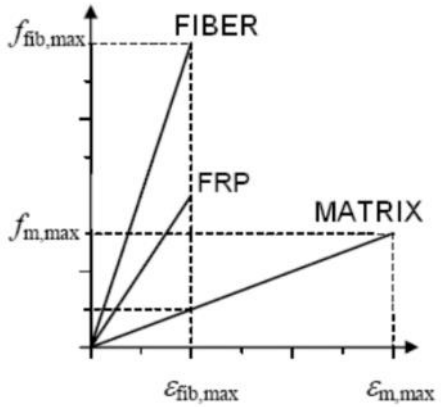

Figure 3. 8 - Stress-strain diagram of fibers and matrix (CNR-DT 200_R1_2013).

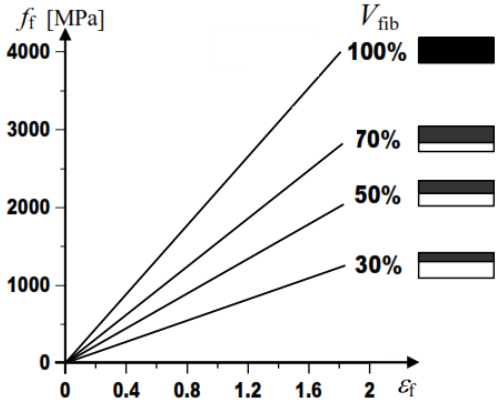

Figure 3. 9 - Stress-strain diagram in relation to the volumetric fraction (CNR-DT 200_R1_2013).

The type of fiber and matrix used in the FRCs (fiber reinforcement composites) determine the main characteristics. The materials are classified and named according to the component:

- FRCM (Fiber Reinforced Cementitous Matrix)
- CFRP (Carbon Fiber Reinforced Polymers)
- GFRP (Glass Fiber Reinforced Polymers)
- AFRP (Aramid Fiber Reinforced Polymers)
- Bio-derived Polymers or Biocomposites

The choice of materials for different reinforcing systems is a critical process based on the principle of synergy of the materials used.

The adhesion between the two phases is an important aspect, normally promoted from the interphase. The interphase is a very thin layer, often monoatomic that makes the fiber compatible with the organic matrix. The fiber matrix interface is one of the points of greater criticality of the system and the lack of adhesion between the two phases constitutes a major cause of structural composite failure.

Each system is unique in the sense that the components i.e. fibers and matrix are designed to work together. This means that a matrix suitable for a specific system could work not in an appropriate manner for another system. It is necessary that the resin guarantees the adhesion with the substrate as well as the fiber-resin bond.

In general, the aim of the reinforcement systems is to increase the load bearing capacity against the thrusting action and the displacement values at the collapse, both for structural elements and for the entire construction. The practice of consolidation techniques based on the use of composite materials as reinforcement of concrete and masonry structures, is more and more widespread in the structural rehabilitation and retrofitting of existing buildings (Fagone et al., 2015).

For masonry constructions, they are usually applied in order to avoid collapse mechanisms due to seismic actions, as overturning of masonry panels and in order to connect them each other.

The reinforcing intervention should provide as much as possible solutions capable of ensuring physical-chemical and constructive-mechanical compatibility, durability and reversibility. These aspects are crucial parameters for the intervention assessment. The compatibility regards the relation between the strengthening materials and the manufacture on which they are applied and can have different meanings. The mechanical compatibility regards the possible alterations in the structural system that are introduced by the intervention, for example, resistance or stiffness concentrations. The chemical-physical aspect concerns the relationship between the existing and applied materials as mixtures for injections and adhesives and matrix in case of fiber-reinforced. Another type of compatibility regards buildings of historical interest, is the compatibility of the intervention with the values to be protected in the abstract sense. The Charter of Krakow 2000 underlines the importance of protecting traditional building techniques and this implies the preservation of the original material.

The intervention durability is connected to the behaviour of materials in time and constitutes one of the critical points of the innovative technical applications. In what concern fiber-reinforced composite materials tests were conducted in the laboratory with the aging simulation machines, but the effectiveness of the simulation constitutes a critical point of these experiments (Micelli et al., 2001). The reversibility of the strengthening device is another key requirement in what concern applications on buildings of historic and artistic interest, as to be often considered a discriminating factor. In terms of structural behaviour, the use of Fiber Reinforcement Composites is able to significantly enhance the tensile strength and global ductility of masonry structures as widely reported in literature.

Since the entry into force of the new Technical Regulations on Construction (NTC, DM 14.01.2008) and related instructions (Circular n. 617/2009 of 02.02.2009), the regulations and recommendations framework for the design, calculation and control of reinforcement, seismic coverage and retrofitting by using FRP materials has been significantly modified. The National Research Council (CNR), in the period 2004-2013, has drafted the guidelines thank to scientific interest of several researchers working in the fields of structural mechanics, construction, structural rehabilitation and of seismic engineering. The Technical Standards for Construction include contents of important technical documents issued by the CNR:

CNR DT 200/2004 - Istruzioni per la Progettazione, l'Esecuzione ed il Controllo di Interventi di Consolidamento Statico mediante l'utilizzo di Compositi Fibrorinforzati - Materiali, strutture in c.a. e in c.a.p., strutture murarie:

CNR DT 201/2005 - Studi preliminari finalizzati alla redazione di Istruzioni per Interventi di Consolidamento Statico di Strutture Lignee mediante l'utilizzo di Compositi Fibrorinforzati.

CNR DT 202/2005 - Studi preliminari finalizzati alla redazione di Istruzioni per Interventi di Consolidamento Statico di Strutture Metalliche mediante l'utilizzo di Compositi Fibrorinforzati.

CNR DT 203/2006 - Istruzioni per la progettazione, l'esecuzione ed il controllo di strutture di calcestruzzo armato con barre di materiale composito fibrorinforzato.

CNR DT 205/2007 - Istruzioni per la Progettazione, l'Esecuzione ed il Controllo di Strutture realizzate con Profili Pultrusi di Materiale Composito Fibrorinforzato (FRP).

CNR DT 200 R1 2013 – Guide for the design and construction of externally bonded FRP systems for strengthening existing structures.

These documents are considered guidelines for design and application of FRP, technology suited to the needs expressed by the anti-seismic regulations. The cited Technical documents represent the synthesis between Italian and International scientific research, including Japanese Instructions (JSCE - 1997), Canadian ISIS 2001, American (ACI 440-2008) and European (FIP-CEB - 2007) ones.
It is worth noting that, in the recent years, bio-composites as structural reinforcing materials are attracting increasing attention (Munikenche Gowda et al., 1999). These materials use, totally or in part at least, elements of vegetable origin as flax, hemp, bamboo, or jute instead of exploiting synthetic origin materials deriving from petroleum processing, improving sustainability and eco-efficiency.

3.3 The Adhesion Problem

When the composite is used as a strengthening system for masonry structures, the study of adhesion between fiber-composite sheets and quasi-brittle substrates is essential. The bond capacity of the external FRCs reinforcement to the substrate is responsible of stress transfer between substrate and laminate in order to develop composite reinforcement action.

The application of adhesives is common in several engineering sectors. Adams and Wake (1984) show typical classifications of joint, which are commonly found in engineering practice. Any joint occurring in practice is designed to carry a given set of loads. Most of the adherends are loaded in tension and the subsequent loads on the adhesive are then a function of the geometry of the joint.

The loading system is often prescribed by the function, but the skill of engineer is to use the best available materials and design techniques to arrive at the suitable and cost-effective solution (Adams and Wake, 1984).

Different approaches were employed to predict the mechanical behaviour of bonded composite joints and assemblies. The models reported in the literature describe, in some extent, different aspects of the adhesion phenomenon depending on the specific problem addressed such aluminum profile connection, strengthening of concrete beams, polymer adhesive tapes on metals and composite material connection (Campilho et al., 2011; Banea and da Silva, 2009).

Volkersen (1938) introduce the concept of differential shear and analyzes the tangential stress distribution of a single lap shear joint in which the adhesive deforms elastically only in shear. However, this analysis does not account for the bending effect caused by the eccentric load of single lap joint. The solution is more representative of a double lap joint than a single lap joint since in a double lap joint the overall bending of the adherends is not as significant as in the single one. Goland and Reissner (1944), enrich the model of single lap joint taking into account the flexural deformability of the adherends and evaluating also the influence of the cleavage stress. They took into account the effect of large deflections of the adherends with an infinitely thin adhesive layer. It can be seen that Goland and Reissner and Volkersen, for the same single lap joint, give similar adhesive shear stress distributions, but the Goland and Reissner solution predicts higher adhesive shear stress at the ends of the overlap. This is because the peel stresses cause an additional shear stress.

Hart-Smith (1973) extends the shear theory including adhesive plasticity and adherend stiffness imbalance. He considers the individual deformation of the upper and lower adherends in the overlap, thus not neglecting the adhesive layer. Hart-Smith (1973) presents an alternative expression for Goland and Reissner's bending moment factor. In

these analyses, it is assumed that the adhesive joints are in a state of plane stress or plane strain in the plane perpendicular to the width direction. Volkersen's analysis well describes the phenomenon if the joint bending is not severe and the adhesive is brittle. However, if there is adherends bending and substantial peeling is present, a more complex model is necessary. Johnson et al, (1971) analyze the influence of surface energy on the contact between elastic solids and Kendall (1975a); Kendall (1975b) applies the energy balance to the evaluation of the strength of an adhesive strip on a rigid substrate, proving that the force that produces delamination is related to the interfacial fracture energy and pave the way to the application of interfacial fracture analysis.

The energy balance theory of peeling reported by Kendall (1975a) do not takes into account any interfacial properties and the properties of the substrate is able to describe the total value of peeling force but not the distribution of interfacial stress.

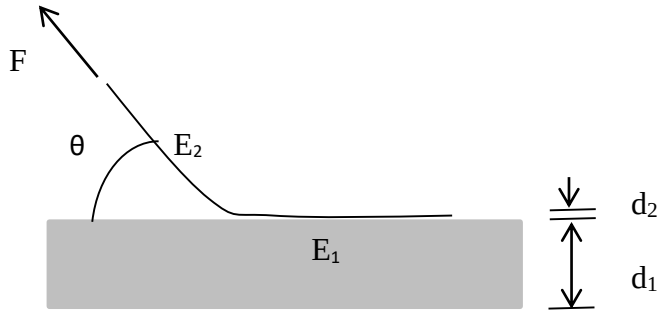

Figure 3.10 – Peel test general scheme (Kendall 1975)

Using the peeling test scheme (Figure 10), referring to a linear elastic flexible strip bonded to a linear elastic substrate, it can be proved that the force F that produces delamination is related to the interfacial fracture energy R by the following equation:

$$\left(\frac{F}{b}\right)^2 \frac{1}{2d_2E_2} + \frac{F}{b}(1-\cos\theta) - R = 0 \qquad (3.1)$$

where the meaning of the symbols are reported in Figure 9 and b is the width of the strip. In the eq. (1) the influence of E_1 and d_1 has been neglected as they are negligible if their product is significantly higher than the product E_2d_2. When $\theta = \pi/2$, the first term of the sum becomes negligible as well, and F/b represents the interfacial fracture energy R.

$$R = \frac{F}{b} \qquad (3.2)$$

On the contrary, in case a lap joint adhesion test is performed, $\theta = 0$ and the second term of the summation disappears. In this case, it can be easily shown that the delamination

force at the same interfacial fracture energy R, reaches considerably higher values of delamination strength F/b.

$$\left(\frac{F}{b}\right)^2 \frac{1}{2d_2 E_2} - R = 0 \qquad (3.3)$$

For this reason, the use of a peeling test permits not only to obtain results for the delamination strength of a reinforcement of low strength capacity in peeling, but also to evaluate in an approximate way, the delamination force in the lap joint condition.

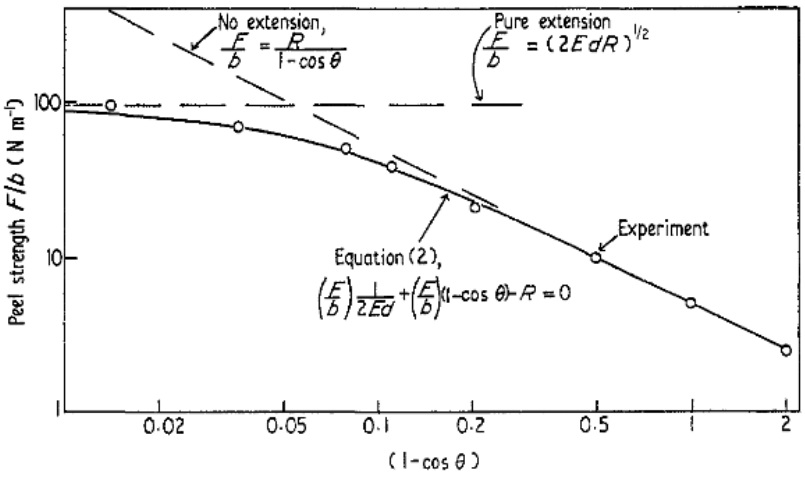

Figure 3.11 - Dependence of peel strength on peel angle (Kendall 1975)

The solution form for shear transfer presented by Kim and Kedward, (2001) is analogous to the tension-loaded lap joint case attributed to Volkersen. They analyze the in-plane shear and tension-loaded cases as uncoupled from each other. For simultaneous shear and tension loading, they present a multicomponent shear stress state in the adhesive by superimposing the two solutions. Although employing simplifying assumptions in the structures geometry, materials behaviour, loading, and boundary conditions, efficient elasticity solutions for the local fields in the adhesive region have been, formulate. According to the Kaelble (1960) we can have two modes of failure interface propagation due to failure mechanisms identified as boundary cleavage and boundary shear. Cleavage stresses are normal to the bond plane and highly localized at the bond boundary where the flexible member undergoes a sudden transition from maximum to zero curvature. The shear stresses are parallel to the bond plane and distributed throughout the bond (Kaelble, 1960; Kaelble, 1965).

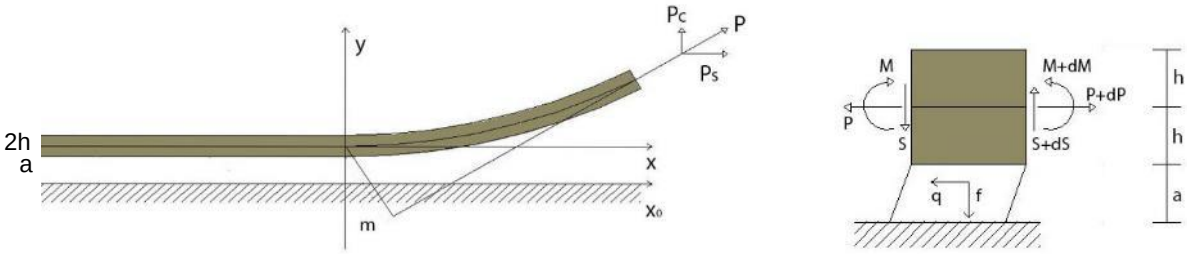

Figure 3.12 - External forces acting on the flexible member (Kaelble 1960)

In what concern the cleavage stresses the assumption of Spies (1953) and Bikerman (1957) are adopted. These models used to interpret the results starting from the hypothesis of rigid substrate. This model will be discussed later.

The failure mechanism of the interfacial bond between a thin plate and a quasi-brittle substrate under mode-II loading (the interface is subjected to shear stress and the force is distributed on the effective anchoring surface) has been analyzed both with experiments and theories based on analytical and numerical methods, among others, by De Lorenzis et al, 2001; Kafkalidis and Thouless (2002). These investigations have described the possible responses of a bonded joint subjected to predominant shear stresses, starting from the linear-elastic stage up to the final delamination. An example is given by fiber-reinforced polymer (FRP) strips bonded to concrete or masonry where debonding failure typically occurs by cohesive mode-II fracture of the substrate (in a macroscopic sense) due to high-strength adhesives (De Lorenzis and Zavarise 2008).

Anyway, it was clear that the influence of peeling, that is of cleavage stresses perpendicular to the joint, was crucial for the mechanical behaviour of the connection. Mixed-mode conditions take place at a variety of bonded interfaces existing in practice, between thin plate and curved support or in case of arches strengthened with thin bonded plates (De Lorenzis et al., 2006; Yang and Thouless 2001; De Lorenzis and Zavarise, 2010). In these cases, the interface is subjected to normal and shear stress. The peeling stress distribution (cleavage stress) is mainly controlled by the flexural stiffness of the thin plate and is distributed in a limited area, so the force required to delaminate is greatly reduced. The tangential stress distribution is mainly controlled by the axial stiffness of the adherend and by the shear stiffness of the adhesive (mode II fracture energy according to the fracture mechanics approach).

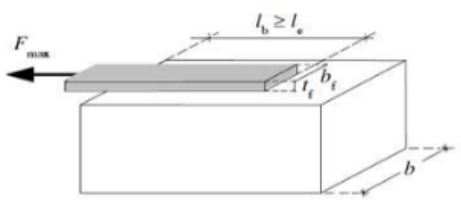

Figure 3.13 – Mode II

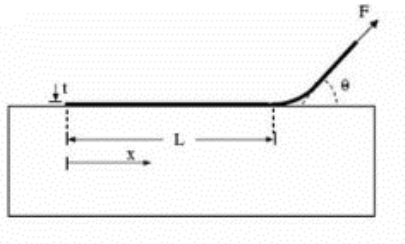

Figura 3.14 - Mode I + mode II

There are not experimental investigations on the evaluation of delamination force for natural fabric on rammed earth supports. Therefore in order to evaluate the adhesion capability, the bonding length and to develop adequate adhesion test method for FRC made with jute fabric, an experimental campaign on strengthened prismatic specimens was carried out referring to test procedures, theories and models developed for the adhesive joint.
Standard test procedures for either fatigue or fracture behaviour of adhesive-bonded joints made from FRP composites have been established.
Examples are standard tests which have been specified to provide the determination of the metal-to-metal peel strength of adhesive joints (ASTM D3166; EN15190; ASTM D3167 − 10 standard test method for floating roller peel resistance of adhesives). Fatigue of FRP composites under tension-tension loading is standardized in ASTM D3479/D3479M. A tensile shear fatigue standard for structural adhesives (ISO 9664) notes that the results are dependent on specimen geometry. The guidelines on the use of results from single-lap shear tests of adhesives (ASTM D4896) specify the range of applicability. The standard ISO 25217 is on the determination of adhesive-fracture energy under tensile opening loading that includes adhesively-bonded FRP composite beams as adherends (Mode I).
In general, the methodologies and the applicability of the test results are important issues that deserve detailed consideration. In particular, the transferability of laboratory-scale tests to engineering structures is of fundamental importance in their design, or in the estimating service life. Strengthening systems are able to prevent the collapse for horizontal bending or, acting as wraps, connect the structural panels each other; in so doing, the strengthening package is subject, in turn, to tangential loads and peeling.
The experimental campaign includes single lap-joint tests and peeling tests of jute fabric strips applied on prismatic earth specimens to reproduce the condition in which reinforcement is subjected in the two common cases of failure mechanisms.

3.4. Experimental program

In the field of masonry structures, many studies exist on the use of fiber composites as a strengthening method. The strengthening system is aimed to increase the load bearing capacity of each structural member as well as the global capacity of the structure; in particular it bears the tensile forces within the structural members or between adjoining members, confines the columns for enhancing their resistance, connects different structural parts, stiffens the horizontal elements and limits the crack width. The adhesion between support and the reinforcement package is fundamental for the efficiency; unlike concrete elements, masonry constructions have commonly irregular external surfaces due to the presence of blocks and mortar. This makes particularly thorny the application procedure and for this reason, there are many studies about that. Starting from the concept that each

geographical area is characterized by different typologies of masonry that use local materials and apply typical construction techniques, the earth masonry (adobe, pisè, cob) can be considered one of these traditional masonry typologies (see chapter 1). The lack of research on the development a strengthening method for rammed earth masonry leads to the absence of a scientific basis to define the correct design procedure and application methodologies of reinforcement systems for this kind of construction.

The experimental study proposed in this work has been designed to analyze the effectiveness of natural fabric applied on rammed earth element as a reinforcement and to define a test procedure useful to define parameters that rule the interaction between these raw materials. The reinforcement is made of jute fabric in earth matrix. The matrix is made of the very same earth used for the realization of the raw earth support (pisé) except that only the fine fraction has been used to enhance workability, and that gypsum has been added to reduce shrinkage and improve the mechanical performance of earth.

A quick review of the main mechanical characteristics of employed materials is reported in the following tables for the sake of thoroughness; these have been obtained respectively by uniaxial compression tests on earth cubic specimens and tensile tests on jute strips and jute yarns deeply described in the chapter 2.

In particular, compressive strength σc, Young's modulus E and kinematic ductility μc, of the earth material are reported in Table 1 and 2. P is the maximum load reached during the tensile test on jute strips and K is the strip stiffness; their values, divided by the number of wires, are respectively P_{yarn} and K_{yarn} in table 3. The nominal strength and Young modulus for a strip of unit width and of the unit thickness h respectively P/s and E h for jute strips are reported in the table 3. Finally the maximum load reached during the tensile test on different lengths of jute wires are showed in the table 4.

	h mm	A mm^2	P N	σ_c MPa	E MPa	μ_c
A.V.	78.7	6189.75	23273.46	3.76	294.32	1.21
St. dev.	0.43	120.34	1007.53	0.17	8.70	0.09
C.V %	0.55	1.94	4.33	4.53	2.96	7.48

Table 3.1. Average values of the mechanical parameters determined by uniaxial compression test on Musciano earth specimens (Loccarini and Morelli master degree thesis, 2012).

	h mm	A mm^2	P N	σ_c MPa	E MPa	μ_c
A.V.	78.35	6022.93	12841.75	2.13	88.62	78.35
St. dev.	0.69	58.13	1375.49	0.22	32.14	0.69
C.V %	0.88	0.96	10.71	10.21	36.26	0.88

Table 3.2. Average values of the mechanical parameters determined by uniaxial compression test on "Seggiano2" earth specimens (Chapter 2).

	P N	K N/mm	P_{yarn} N	K_{yarn} N/mm	P_{yarn}/s N/mm	E h N/mm
A.V	476.5	221.6	31.25	14.57	7.28	679.0
St. dev.	82.75	37.99	3.74	1.97	0.87	91.88
c%	17.37	17.14	11.96	13.53	11.96	13.53

Table 3.3. Average values of the mechanical parameters determined by tensile test on twenty jute strips, about 7 cm wide (Chapter 2).

	I series (30 w.)	II series (30 w.)	III series (30 w.)	IV series (30 w.)	V series (30 w.)
Wires length (cm)	20	30	40	50	60
Specimens average length (cm)	9.87	14.68	19.45	24.54	29.76
St. dev.	0.21	0.25	0.26	0.24	0.29
Average maximum load (N)	46.77	46.29	46.12	42.35	39.18
St. dev.	6.34	6.18	5.52	6.52	5.61

Table 3.4. Average values of the mechanical parameters determined by tensile test on jute wires (Chapter 2).

As it is known, the detachment of reinforcement from the support (debonding) is a critical failure mode for FRP strengthening systems in masonry structures, because it occurs when the tensile stress in the reinforcement composite is smaller than its tensile capacity. This phenomenon is normally ruled by some physical parameters: the fracture energy, the effective bond length and the design bond strength. The fracture can be adhesive, cohesive and mixed. Adhesive fracture takes place in the interface between adhesive and support material. Cohesive fracture takes place inside the support. Mixed fracture is registered when

both cohesive and adhesive failure happen. The study of debonding was faced with this experimental campaign with the aim to verify if the same phenomena and failure mechanisms occur when reinforcing earth material with jute fabric and earth matrix, and which parameters play a fundamental role. The support has been realized in order to reproduce a surface of pisè construction, which is the most common typology all over the world with almost uniform characteristics. In fact, despite the type of soil, the rammed earth constructive technique used to build the walls is similar in all the regions. Moreover, the use of this "base" typology for the realization of the experimental tests of earth masonry, without additives or devices to increase the materials behaviour, could be a significant starting point on the field of performances reinforcement technique evaluation. The experimental program proposed consists in four progressive series of tests realized, in part, in collaboration with the Laboratorio de Polìmeros of the Universitat Politècnica de València. These are, in chronological order:

I series _ **Lap Joint** test on 25 specimens carried out in the Material and Structure Test Laboratory of the Architecture Department, University of Florence, using a steel frame and displacement controlled screw jack (Samorè master degree thesis, 2013).

II series _ **Peeling** test carried out in the Material and Structure Test Laboratory of the Architecture Department, University of Florence. (Lodi Rizzini master degree thesis, 2015)

- Steel frame and displacement controlled screw jack
- Displacement rate equal to six millimeters per minute.
- Jute strip length = 22cm
- Fabric average wires spacing = 4.292mm
- Number of symmetric tests = 6

III series _ **Peeling** test carried out in Laboratorio de Polìmeros, Universitat Politècnica de València

- Materials testing machine INSTRON 5960, program Bluehill 3 test Method Development
- Displacement rate equal to six millimeters per minute
- Jute strip length =22cm
- Fabric average wires spacing = 4.292mm
- Number of symmetric tests = 8

IV series _ **Peeling** test carried out in Material and Structure Test Laboratory of the Architecture Department, University of Florence.

- Steel frame and displacement controlled screw jack

- Displacement rate equal to six millimeters per minute.
- Strip length = 10cm
- Fabric average wires spacing = 4.292mm
- Number of symmetric tests = 7

3.4.1 Specimens

Prismatic earth specimens of about 24x12x6cm have been made with earth material taken in Musciano (Pisa, Italy) for the shear tests and in Seggiano (Grosseto, Italy) for the peeling test with the same formworks and realization process.
The prisms have been realized manually using pisè technique, filling formworks with soil material after a simple sieving and 11% of water by the method of compacting layer by layer. The largest particle size of the earth used is seven times smaller than the shorter side of the test specimen.

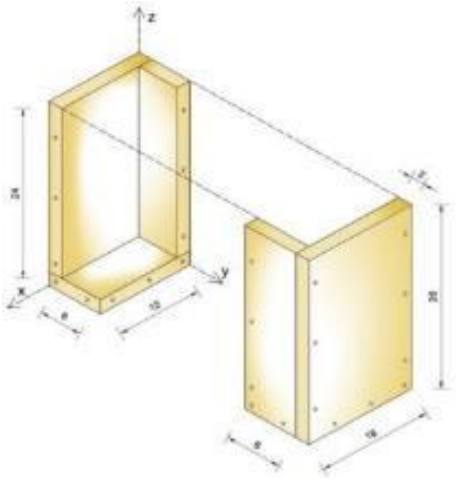

Figure 3.14 – Specimens formwork of 24x12x6cm

The reinforcement package has been characterized by two phases, which are jute fabric as continuous reinforcement and matrix constituted by earth material and 15% of gypsum. Gypsum powder is normally used as an additive of earth in order to limit shrinkage that high

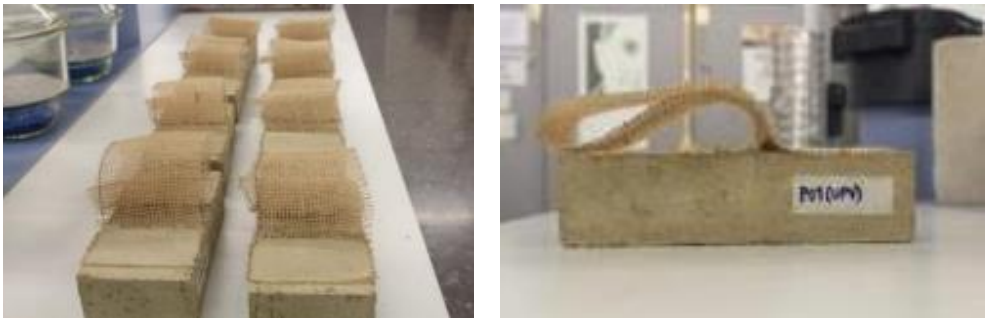

Figure 3.15/16 – Specimens for peeling test (Universitat Politècnica de València)

water content usually confers during the curing. In fact, it was shown that gypsum powder is a good natural additive increasing mechanical properties, without significantly altering the appearance and color of the material (Isik and Tulbentci 2008).
The fabric employed is made of jute yarns in warp and weft. In so doing, a reinforcement system is obtained in which the two phases are both biocompatible materials. (See chapter 2 for the description of the materials employed).
The strips were applied mixing the constituents of the matrix (earth and gypsum powder) with 30% of water. Higher water content is necessary to lend better workability and to allow the infiltration of earth matrix in the empty spaces between the fabric wires.
The use of earth mud, both as matrix and adhesive, permits to obtain a compatible reinforcement system in which only jute fabric contribute to strength and stiffness of the strengthening system. Effectively, the earth mixture used as adhesive only adds some negligible layer to the support and consequently negligible contribution to its strength.

3.4.2 Adhesion test

3.4.2.1 Single Lap Joint Test

The single-lap joint is one of the commonly occurring joints and is the configuration most often used for testing adhesives.
Lap joint shear tests subject the interface between reinforcement and substrate to pure shear; with this procedure, the tensile force is applied to the free jute fabric while a contrast system prevents the sliding of the brick in the load direction as shown in the figure 17.

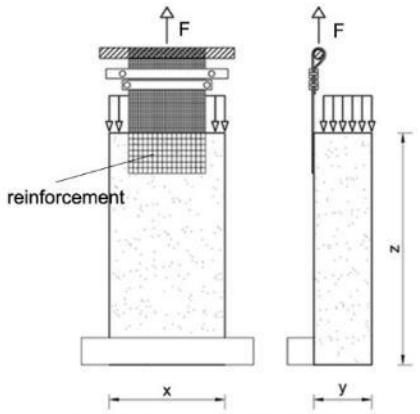

Figure 3.17 - test scheme single lap joint test

For the present study, concerning the delamination capacity of jute fabric applied to rammed earth supports, twenty-five tests were carried out with different methodologies on specimens differing for type of jute fabric used, type of specimen anchorage to the test machine and for displacement rate. Rammed earth prismatic specimens were reinforced

with jute fabric strips, obtained by cutting in a direction parallel to the warp, applied on one of the wide surfaces of the samples with a matrix composed by earth material, 15% of gypsum and 30% of water. Although the test procedure was changed many times, the lap joint test proved to be not useful for the determination of the bond strength of jute fabric reinforcement. Bond strength seems to be higher than the load capacity of the fabric. Delamination never took place and the specimens failed due to the rupture of fabric except in one case (figure 18) as shown in the table 5.

Specimen	Anchoring surface cm^2	Peak load N	Load velocity mm/min	Failure modes
T.D.01	288	4.812	2	wires rupture
T.D.02	288	4.435	2	wires rupture
T.D.03	288	8.467	2	wires rupture
T.D.04	40	4.350	2	wires rupture
T.D.05	20	5.950	0,5	wires rupture
T.D.06	20	4.897	0,5	wires rupture
T.D.07	40	6.007	2	wires rupture
T.D.08	**40**	**4.678**	**3**	**Delamination**
T.D.09	60	4.880	3	wires rupture
T.D.10	60	4.988	4	wires rupture
T.D.11	80	5.044	4	wires rupture
T.D.12	80	5.632	4	wires rupture
T.D.13	16	1.715	2	wires rupture
T.D.14	32	1.609	3	wires rupture
T.D.15	32	1.313	3	wires rupture
T.D.16	32	0.811	3	wires rupture
T.D.17	16	2.918	3	wires rupture
T.D.18	32	2.037	3	wires rupture
T.D.19	48	3.988	3	wires rupture
T.D.20	64	6.399	3	wires rupture
T.D.21	48	6.814	3	wires rupture
T.D.22	192	1.776	3	wires rupture
T.D.23	194	0.752	3	wires rupture
T.D.24	32	2.176	3	wires rupture
T.D.25	48	4.112	3	wires rupture

Table 3.5. Results of Lap joint test (Samorè master degree thesis, 2013)

Figure 3.18 - specimen T.D.08 after test (Samorè master degree thesis, 2013)

The conclusion was drawn from the tests, that the adhesion capability of the strengthened package is higher than the load capacity of the fabric. For this reason, in order to evaluate the reinforcement capacity of this composite material, a peel test experimental campaign was carried out. It was noted that Liu and Wang (2015) in their study used the double shear test in order to measure the adhesiveness of fiber materials bonded to rammed earth blocks. They tested combinations with bamboo, canvas and tarpaulin, embedded in sodium silicate, epoxy, and NFcompound matrices. Interface debonding was observed only using NFcompound as adhesive.

3.4.2.2 Peeling Test

The peel test is a mechanical test that has been extensively studied and adopted to measure adhesion strength, i.e. the force required to separate a flexible strip from the substrate, and it has been widely used to characterize the bond behaviour of the adhesives for joint design purposes (Kim and Aravas, 1988), for measuring the adhesion of flexible laminates and of coatings (Kendall, 1975a; Bikerman, 1957; Adams and Wake, 1984; Kendall, 1994; Gialamas et al., 2014; Begley et al., 2013; Ghatak et al., 2005; Pesika et al., 2007; Sauer 2011; Williams and Kauzlarich, 2005; Georgiou et al., 2003; Molinari and Ravichandran, 2008; Gent and Hamed 1975). This test method covers the determination of the relative peel resistance of adhesive bonds between one rigid adherend and one flexible adherend when tested under specified conditions of preparation and testing (ASTM D3167). In this test, a thin plate bonded to a substrate is pulled from it at a ‘‘peel angle” and the ‘‘peeling force” needed to produce debonding is measured. In this configuration the interface is subjected to shear and normal stresses, hence debonding occurs by mixed-mode fracture.
On these bases, test procedures have been defined in order to determine the main characteristic parameters of the reinforcement package.

It is known that the peel force is by far lower than the force necessary to delaminate a shear joint. The most common test procedure is the asymmetric one, but in the research field also the symmetric test mode is used (Gent and Kaang, 1986; Williams, 1997).

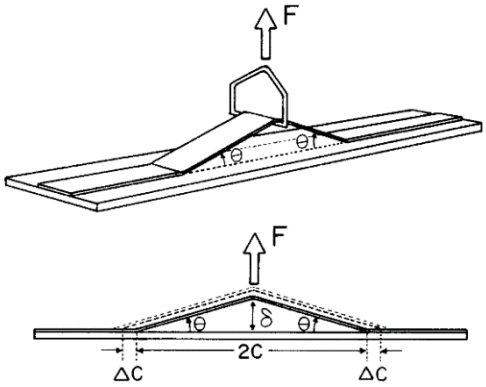

Figure 3.19 - Sketch of the pull-off experiment (Gent and Kaang, 1986)

Rammed earth prismatic specimens of about 24x12x6cm were strengthened with jute fabric strips of about 60cm for the second and third series and of about 40 cm for the fourth series. The strips were applied symmetrically on one of the wide surfaces of the specimens, leaving free from adhesion the central part, according to the scheme reported in fig. 19. The strip was pulled with a displacement rate of about 1mm/10sec.

Although the specimens were prepared in Florence, at the Material and Structure Test Laboratory of the Architecture Department, the jute reinforcement was applied for the second and the fourth series in Florence, where they were tested with a displacement controlled device made of a screw jack in a stiff frame, in series with a load cell (500N); the third series of the specimens was strengthened with jute fabric in Valencia at the Laboratorio de Polímeros of the Polytechnic University of Valencia, where they were tested with an Instron 5960 Dual Column Testing Systems for Tensile, Compression, Flexure, Peel testing controlled by Bluehill software (5000N).

The fourth series of tests differs from the others by the length of the strip applied; in fact, it was decided to perform the last series in chronological order in order to evaluate the variation of the peel angle using the photo sequence. in the tables 3.6, 3.7 and 3.8 the main mechanical parameters are reported for the specimens tested in Florence and in Valencia respectively, in particular: the yarns number, peak load, equivalent delamination load obtained starting from the dissipated energy (equivalent area below the graph), equivalent delamination force F (equivalent delamination load/2); in order to obtain values of bond strength the equivalent delamination force was divided by the number of yarns and by nominal width of the strip. Nominal width is obtained by multiplying the specimen wires number by the fabric average spacing between wires equal to 4.292mm. Only the

specimens that exhibited a symmetrical behaviour at rupture were reported in the data sheets organized at the end of this chapter, while five specimens (three tested in Florence and two in Valencia) were excluded from the analysis, as their fracture process was not symmetrical, probably due to some imperfections in the bonding procedure.

	y. number	Peak load (N)	Equivalent delamination load (N)	F equivalent delamination force (N)	F/y. number (N)	F/nominal strip width (N/mm)
A.V	26	62.356	44.933	22.467	0.873	0.203
St. dev.	2.236	5.961	5.454	2.727	0.145	0.034
c%	8.600	9.559	12.138	12.138	16.660	16.660

Table 3.6. Results of II series of peel test (Lodi Rizzini master degree thesis, 2015)

	y. number	Peak load (N)	Equivalent delamination load (N)	F equivalent delamination force (N)	F/y. number (N)	F/nominal strip width (N/mm)
A.V	26.625	53.739	35.793	17.896	0.672	0.157
St. dev.	0.696	7.869	6.699	3.349	0.128	0.030
c%	2.614	14.643	18.716	18.716	18.979	18.979

Table 3.7. Results of III series of peel test

	y. number	Peak load (N)	Equivalent delamination load (N)	F equivalent delamination force (N)	F/y. number (N)	F/nominal strip width (N/mm)
A.V	26.143	66.594	52.584	26.292	1.007	0.235
St. dev.	1.125	11.430	7,31726	3.659	0.138	0.032
c%	4.303	17.163	13,91539	13.915	13.732	13.732

Table 3.8. Results of IV series of peel test

It can be noted that the values obtained in Valencia are slightly lower than the results obtained in Florence. This can be due to different ambient conditions (for example lower moisture) or to some damage produced on the specimens during the transportation. In what follow, you can find the test data sheets for each specimen containing the corresponding load path, the linearized load-displacement diagram obtained starting from dissipated energy. In the fourth test series data sheets, the linearized graph obtained taking into account the angle variation is also inserted.

3.5 Analysis of the results

Since the bond capacity of fiber composite sheets used for the reinforcement of masonry structures, with respect to in-plane loads, is generally lower than the composite tensile strength, the lap joint test method was chosen, at first, to study the failure mechanisms of jute fabric and earth matrix reinforcement on rammed earth masonry.

The first attempts in measuring the adhesion properties of jute reinforcement to rammed earth substrate did not give good results as the fabric failure occurred before debonding, due to the low strength of jute wires with respect to the bond strength of jute fabric reinforcement package. Therefore, a different test setup was necessary to evaluate the bond capacity of the reinforcement system, designed on the model of the peeling test. The procedure applied for the symmetric peeling tests has proved to be helpful to achieve quantitative evaluation of adhesion strength. In the table 3.9 the average results of all the three series of peeling test are reported, in particular the value of the nominal bond strength in the seventh column used for the follow analysis.

	y. number	Peak load (N)	Equivalent delaminatio n load (N)	F equivalent delamination force (N)	F/y. number (N)	**F/nominal strip width (N/mm)**
A.V	26.286	60.486	44.002	22.001	0.841	**0.196**
St. dev.	1.452	10.395	9.691	4.845	0.197	**0.046**
c%	5.525	17.186	22.023	22.023	23.443	**23.443**

Table 3.9. Average value of the three series of peeling test

The results have been interpreted using the theory of Kaelble, (1960); though based on the linear elastic analysis of a peeling test, it is apt to interpret the peeling tests of jute fabric on rammed earth support as it describes the stress distribution before any detachment occurs; starting from the assumptions of Spies, (1953) and Bikerman, (1957) of a rigid plate as substrate and homogenous adhesive (hookean solid) under the hypothesis of concentrated elasticity system.

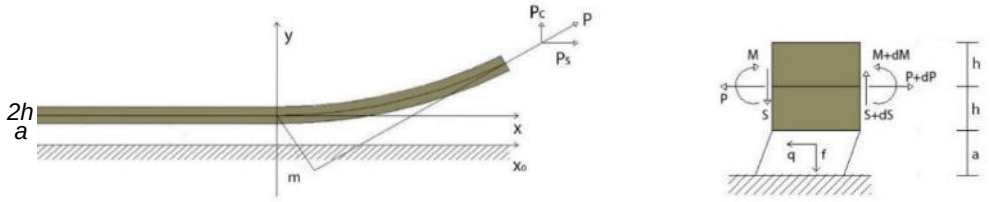

Figure 3.20 - External forces acting on the flexible member (Kaelble, 1960)

$$\begin{cases} dS - f = 0 \\ dP - q = 0 \\ dM + Sdx - qh = dMc + dMs + Sdx - qh = 0 \end{cases}$$

Under small flexural deformation and small curvatures hypothesis, introducing the relation for bending defamation of the sheet $Mc = EJ(\frac{d^2y}{dx^2})_c$ in which the bending moment is related to the Young's modulus E, the moment of inertia J of the flexible sheet and the curvature and deriving twice and substituting the shear force of the bending sheet, we obtain:

$$EJ\frac{d^4y}{dx^4} = -\frac{dS}{dx} \quad (3.4)$$

From the first equilibrium equation and expressing the normal stress in the adhesive via the Yung modulus and the relative displacement:

$$dS = f = E_A\frac{y}{a}bdx \quad (3.5)$$

Where E_A is the Young's modulus of the adhesive, a is the thickness of the adhesive and b is the width of the reinforcement strip.

$$\frac{d^4y}{dx^4} + \left(\frac{E_Ab}{EJa}\right)y = 0 \quad (3.6)$$

Solving the linear differential equation (6), axial stress (boundary cleavage) normal to the bond plane can be evaluated.

$$\sigma = \frac{2M}{b}\alpha^2e^{\alpha x}(\cos\alpha x + \sin\alpha x) + \frac{2P\sin\vartheta}{b}\alpha e^{\alpha x}\cos\alpha x \quad (3.7)$$

in which

$$\alpha = \sqrt[4]{\frac{E_Ab}{4EJa}}$$

Applying the second condition of equilibrium:

$$dp - q = 0 \quad (3.8)$$

$$q = \tau dxb$$

$$dP = 2hbd\sigma u$$

The tangential stress in the adhesive is $\tau = G\gamma = \frac{Gu}{a}$

$$q = G\frac{u}{a}\,bdx \quad (3.9)$$

$$\frac{d\sigma}{dx} = \frac{Gu}{2ha} \quad (3.10)$$

Deriving we obtain:

$$\frac{d^2\sigma}{dx^2} - \left(\frac{G}{2haE}\right)\sigma = 0 \quad (3.11)$$

Solving the linear differential equation (10), we can evaluate (boundary shear) parallel to the bond plane at the interface

$$\tau = \frac{P\cos\theta}{b}\beta e^{\beta x} \quad (3.12)$$

In which

$$\beta = \sqrt{\frac{G}{2hEa}}$$

Using this model, we can calculate the axial stress (boundary cleavage) normal to the bond plane and tangential stress (boundary shear) parallel to the bond plane at the interface

using the elastic modulus and shear modulus obtained by experimental tests on the materials employed (see chapter 2).

For this analysis, we consider a unit reinforcement strip thickness of 1mm (h=0.5mm), unit strip width b=1 mm and the unit adhesive thickness a. The interface stress diagrams at the variation of peel angle, reported in the paths in figures 21/22, in which the experimental average peel force P = 0.196N/mm, Young's modulus of earth material E_A=88.621N/mm^2, earth shear modulus G =40.282N/mm^2 (Poisson coefficient = 0.2) and the elastic modulus of the jute fabric E=679 N/mm^2.

The maximum axial stress calculated in the peeling condition is equal to 0.567MPa and the tangential stress in the lap joint condition is equal to 2.263MPa. The former is, evidently, the normal stress able to delaminate the composite package from the substrate in peeling condition while the latter is the maximum tangential stress registered during lap joint test at break of the fabric (with P = 10.75N/mm), evidently not enough to delaminate in lap joint condition (Figure 23). 10.75N/mm is the nominal break force obtained by tensile test on jute wires of 40cm dividing the peak load by the average spacing between wires equal to 4.292mm.

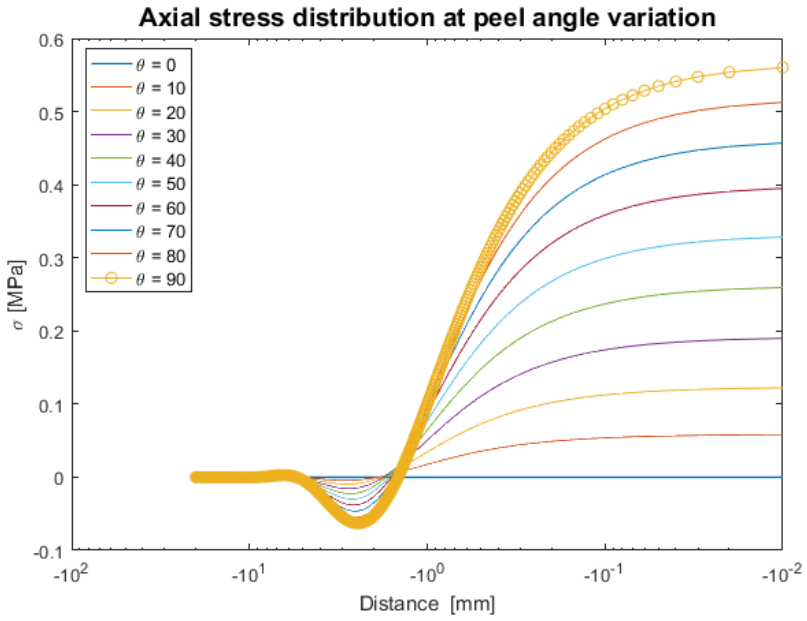

Figure 3.21 – Axial stress distribution at the peel angle variation calculated with the force necessary to delaminate in peeling condition equal to 0.196N/mm

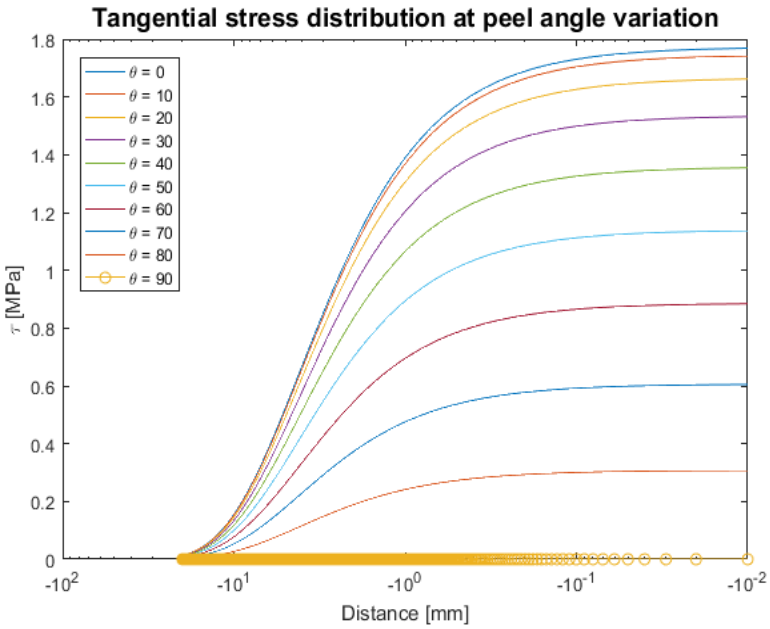

Figure 3.22 – Tangential stress distribution at the peel angle variation calculated with the force necessary to delaminate in peeling condition equal to 0.196N/mm

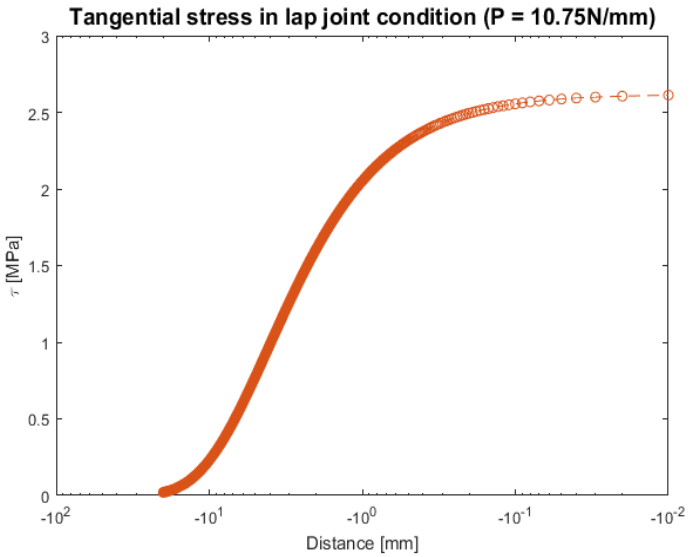

Figure 3.23 – Tangential stress distribution at the peel angle equal to 0 (lap joint condition) evaluated with the jute nominal break force equal to 10.75N/mm

Figure 3.24 – Lap joint test (wires rupture)

For this type of reinforcement system, the effective bond length is not a critical parameter. In fact, in the lap joint condition crisis occurs in any case for low resistance to traction of the fabric. You notice that the axial stress due to peeling are already substantial for very small angles. As we can see from the curves reported in the figure 25, with a peel angle of 8° the boundary cleavage has the same influence of the boundary shear.

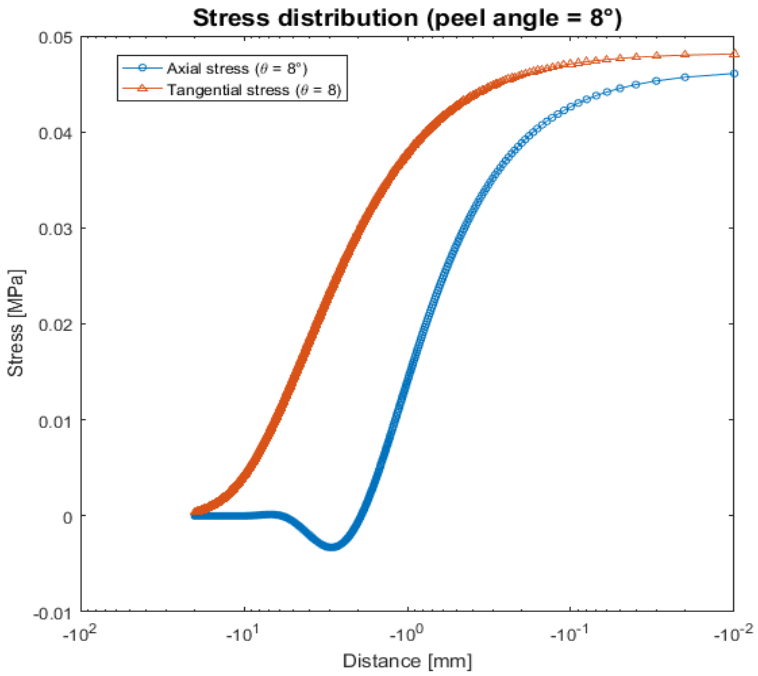

Figure 3.25 – Stress distribution at peel angle of 8° calculated with the force necessary to delaminate in peeling condition equal to 0.196N/mm

In the design phase it is important to consider that this type of reinforcement works well in the lap joint condition; for this reason it is fundamental to arrange it so that it is not subject to peeling, and to dimension the reinforcement on the reinforcement strength. Furthermore, the small length of adhered reinforcement involved in the process has to be noticed.

The elastic model used to analyze the results is based on some elastic parameters whose values have been determined on earth specimens with some approximations. For this reason, the Kealble model has been applied with different values of earth Young modulus, in order to evaluate the possible variations that could be obtained with different earth properties or in case of errors in the determination of mechanical parameters (Figures 27 and 28).

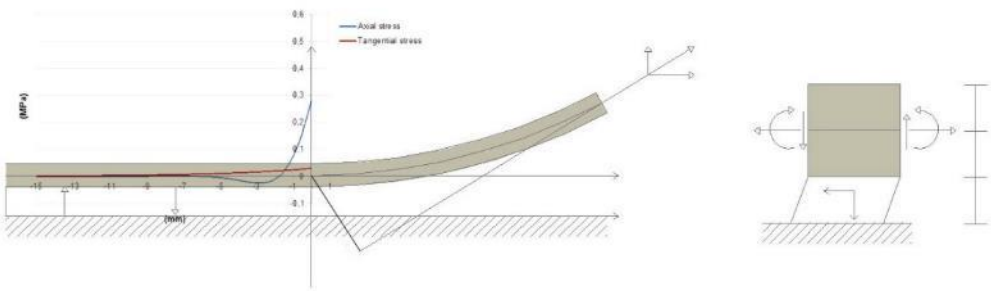

Figure 3.26 – Stress distribution at peel angle of 45° calculated with the force necessary to delaminate in peeling condition equal to 0.196N/mm

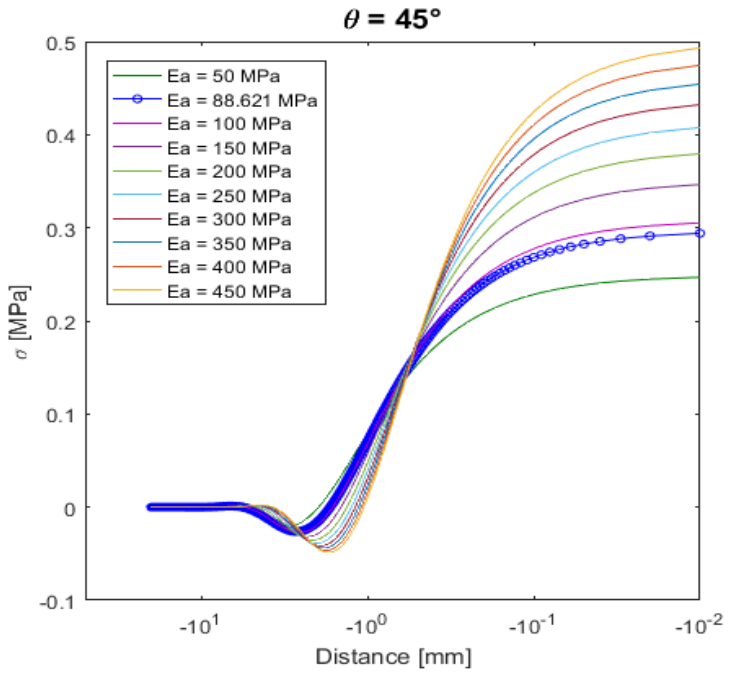

Figure 3.27 – Axial stress distribution at peel angle of 45° calculated with different values of Young's modulus

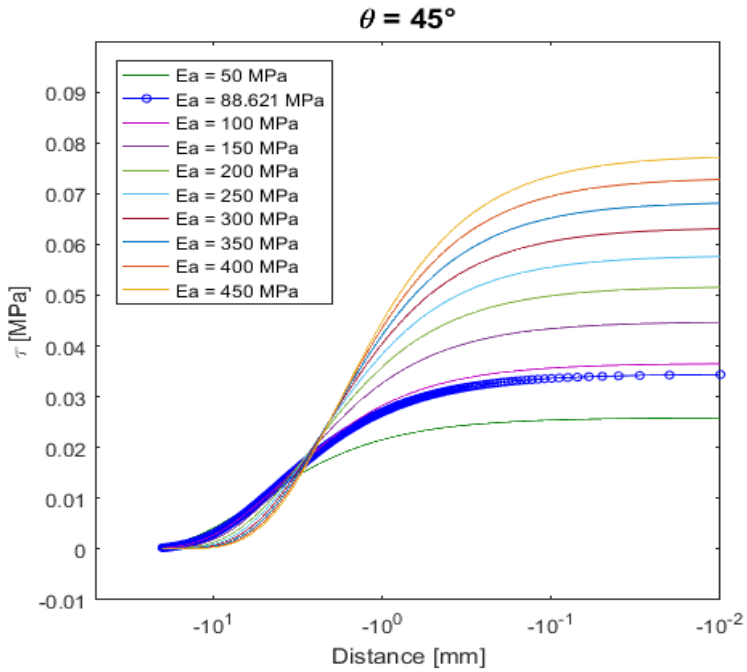

Figure 3.28 – Tangential stress distribution at peel angle of 45° calculated with different values of Young's modulus

The effective bond length does not change significantly varying the Young modulus. We consider a range of the variation able to cover all the values obtained from compressive test on cubic specimen of 8x8x8cm and 15x15x15cm of different stabilized or not stabilized soils taken in Tuscany region during 10 years of experimental investigations on earth construction field carried out in the Material and Structure Test Laboratory of the Architecture Department, University of Florence.

Note that according to Kendall model (1975) reported above, if we compute the value of R (that is F/b) from the average of the sets of results obtained in Florence and in Valencia (7th column in Table 1.9) we can obtain the experimental value of 0.196N/mm. Using the value of Eh obtained by the tests on jute fabric reported in Table 1.3, we can calculate the corresponding value of F/b, that is the force on unit width able to delaminate a jute strip from rammed earth support in a lap joint condition. The result is 16.31N/mm that is about 52% higher than the strength of a unit width strip 10.75N/mm calculated starting from the results of tensile test on jute wires of 40cm. It is evident that the lap joint test cannot give information about the delamination strength of jute reinforcement as jute itself breaks when subjected to a significantly lower force.

Note that the energy balance theory of peeling reported by Kendall (1975) is able to describe the total value of peeling force and not the distribution of interfacial stress.

Supposing that the earth interface has the same mechanical properties of the earth substrate, we can compare the interface axial stress 0.567MPa in peeling condition calculated using Kealble model with the mechanical properties of raw earth. The results obtained from the indirect tensile tests on different soils carried out in the Laboratory of university of Florence provided a range of tensile strength of earth from 0.22MPa to 0.58MPa in agreement with the value obtained with a peeling force equal to 0.196N/mm. The adhered interface strip involved in the peeling and subjected to normal stress is about 1.5 millimeter long. As it is known, the peeling condition is more severe than the lap joint condition because of the concentration of stress on the delamination line due to the flexibility of the adherent strip, in this case jute fabric strip.

3.6 Data sheets of symmetric tests

In the following the data sheets of the peeling test series are listed that include peeling test scheme adopted, the information about rammed earth specimens, the information about jute fabric and test results. Only the tests with symmetric behaviour have been reported.

P.P.01

Rammed earth specimen	
date of realization	20-09-2014
weight (kg)	3.44
length x,y,z (cm)	23x11.5x6
Jute fabric	
strip width (cm)	11.5
strip length (cm)	61.28
longitudinal wires number	22
Test data	
test date	24-10-2014
displacement rate (mm/sec)	1/10
peak load (N)	61.279
equivalent delamination force F (N)*	22.175
F/ wires number (N)	1.008
F/ strip nominal width (N/mm)**	0.235

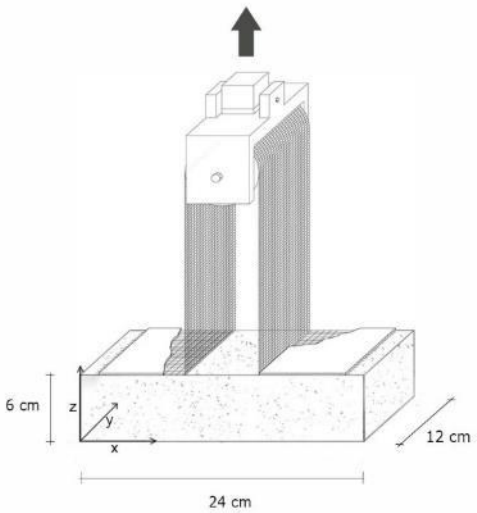

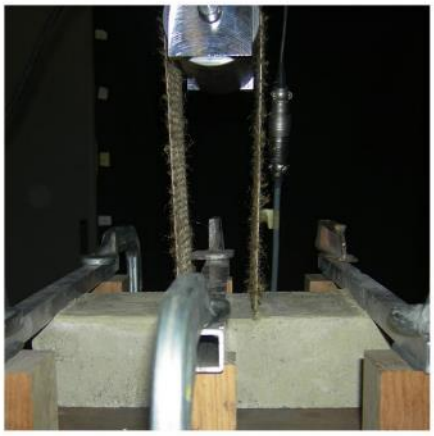

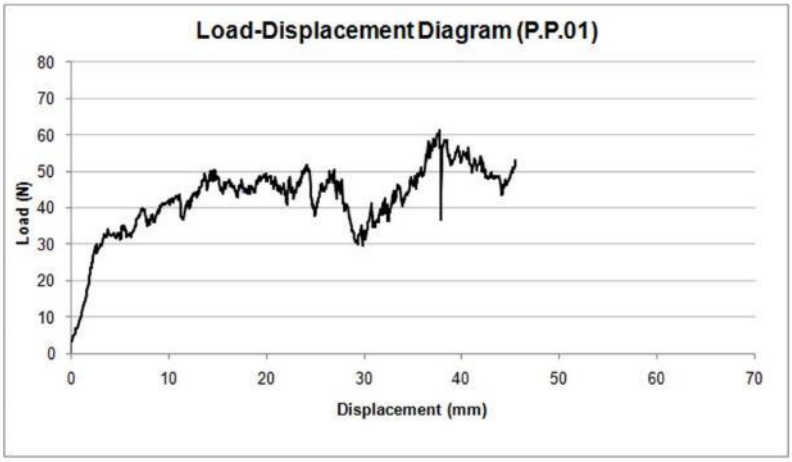

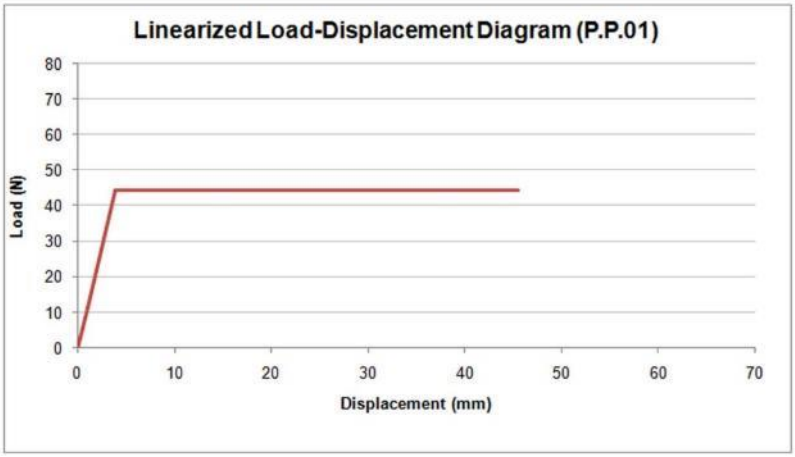

* Equivalent delamination force was determined starting from dissipated energy (equivalent area below the graph):
F = equivalent delamination load/2).

** Nominal width is obtained by multiplying the specimen wires number by the fabric average wires step equal to 4.292 mm.

.

P.P.05

Rammed earth specimen	
date of realization	22-11-2014
weight (kg)	3.50
length x,y,z (cm)	23x11.5x6.1
Jute fabric	
strip width (cm)	11.5
strip length (cm)	62
longitudinal wires number	24
Test data	
test date	13-01-2015
displacement rate (mm/sec)	1/10
peak load (N)	70.503
equivalent delamination force F (N)*	26
F/ wires number (N)	1.083
F/ strip nominal width (N/mm)**	0.252

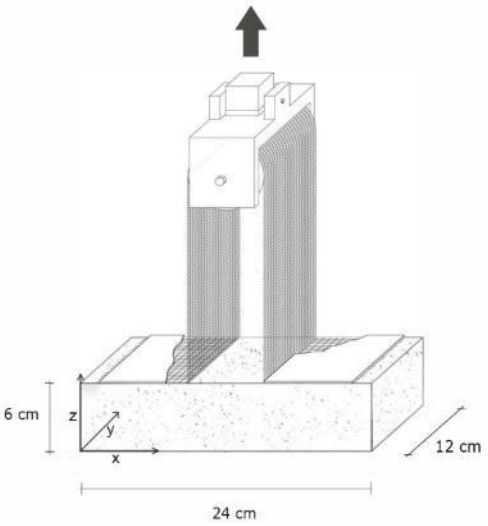

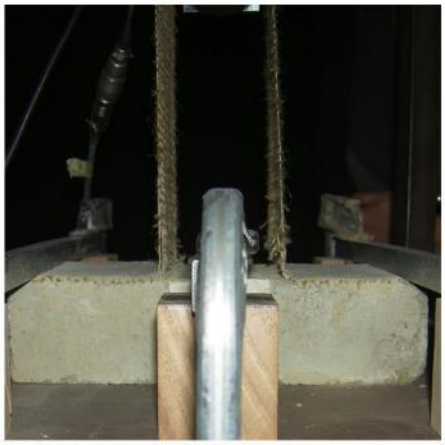

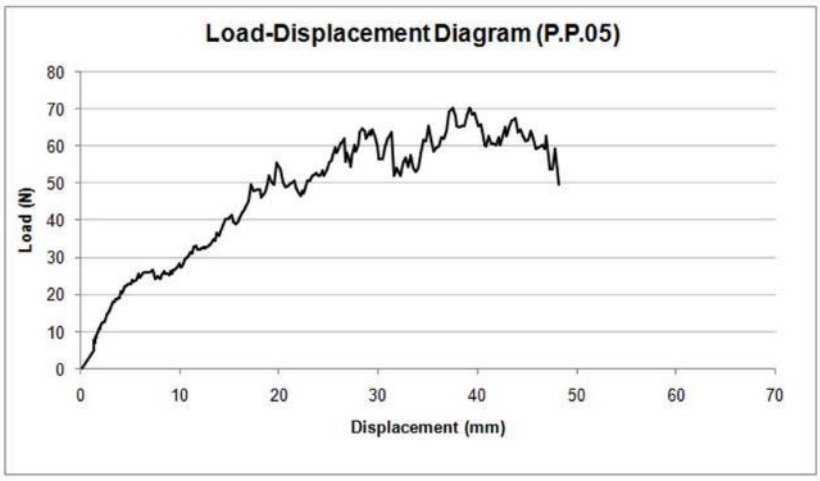

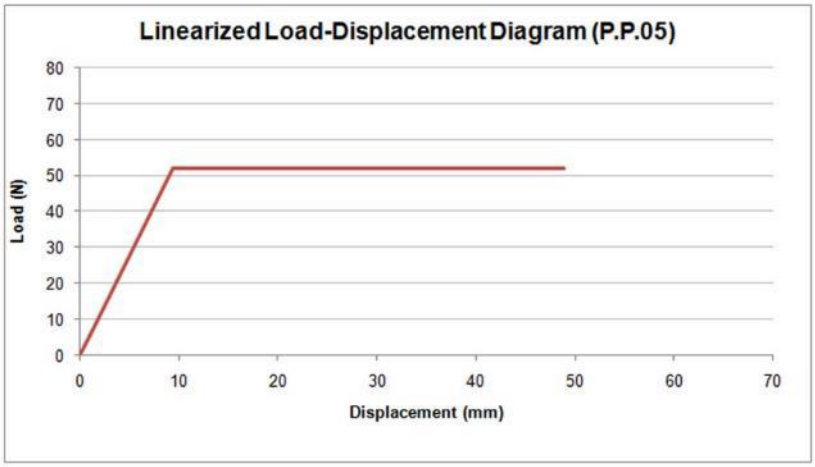

* Equivalent delamination force was determined starting from dissipated energy (equivalent area below the graph):
F = equivalent delamination load/2).

** Nominal width is obtained by multiplying the specimen wires number by the fabric average wires step equal to 4.292 mm.

.

P.P.06

Rammed earth specimen	
date of realization	20-09-2014
weight (kg)	3.44
length x,y,z (cm)	23x11.5x6
Jute fabric	
strip width (cm)	11.5
strip length (cm)	62
longitudinal wires number	27
Test data	
test date	24-02-2015
displacement rate (mm/sec)	1/10
peak load (N)	55,670
equivalent delamination force F (N)*	17,306
F/ wires number (N)	0,640
F/ strip nominal width (N/mm)**	0,149

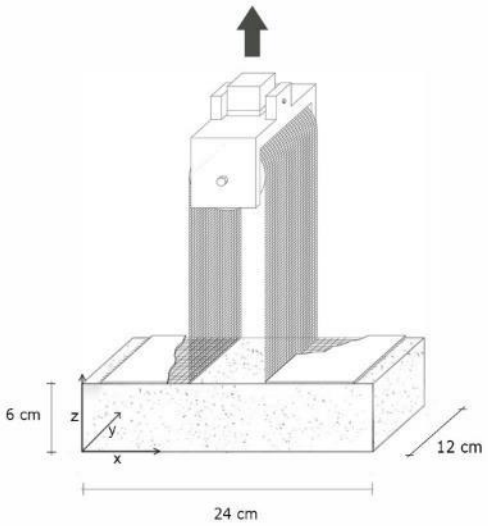

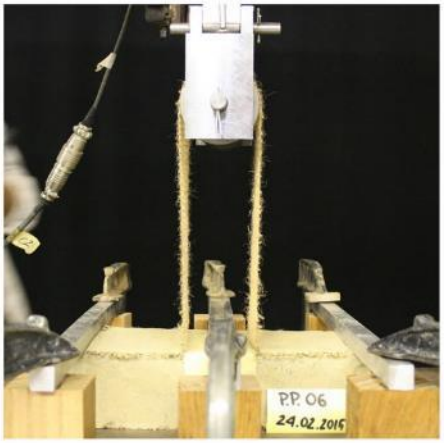

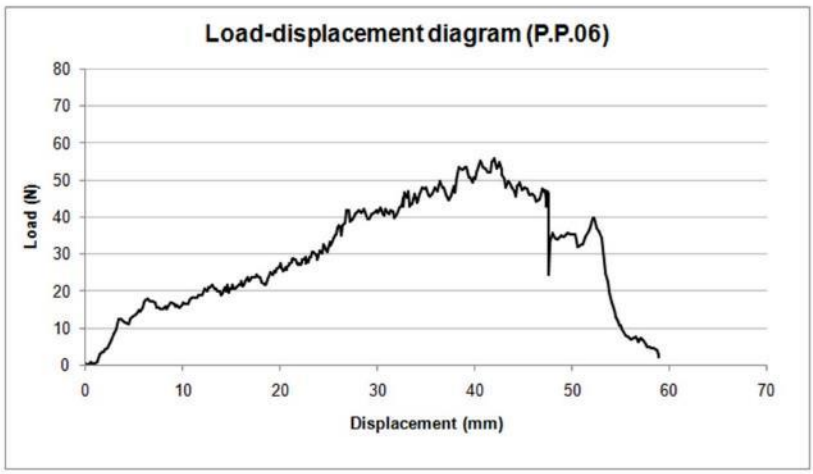

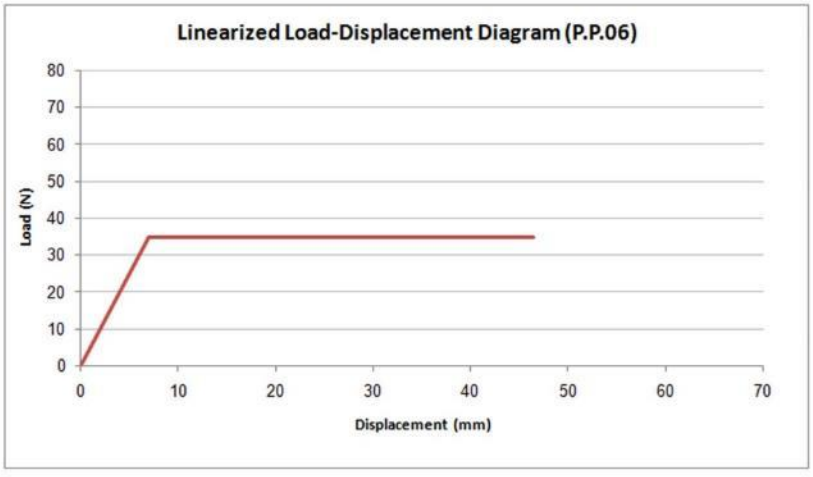

* Equivalent delamination force was determined starting from dissipated energy (equivalent area below the graph):
F = equivalent delamination load/2).

** Nominal width is obtained by multiplying the specimen wires number by the fabric average wires step equal to 4.292 mm.

.

P.P.07

Rammed earth specimen	
date of realization	16-09-2014
weight (kg)	3.64
length x,y,z (cm)	23.7.x11.8x6
Jute fabric	
strip width (cm)	11.8
strip length (cm)	62
longitudinal wires number	28
Test data	
test date	24-02-2015
displacement rate (mm/sec)	1/10
peak load (N)	69.913
equivalent delamination force F (N)*	24.437
F/ wires number (N)	0.873
F/ strip nominal width (N/mm)**	0.203

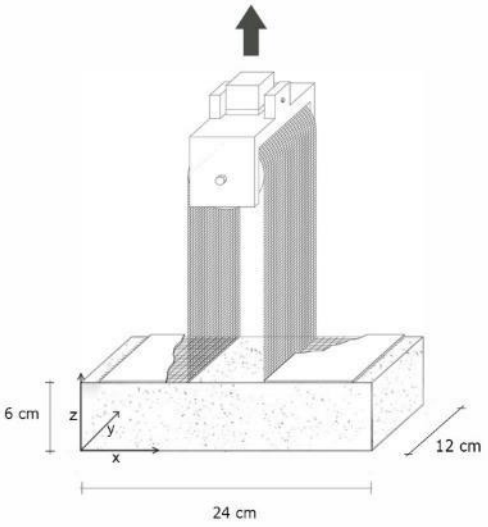

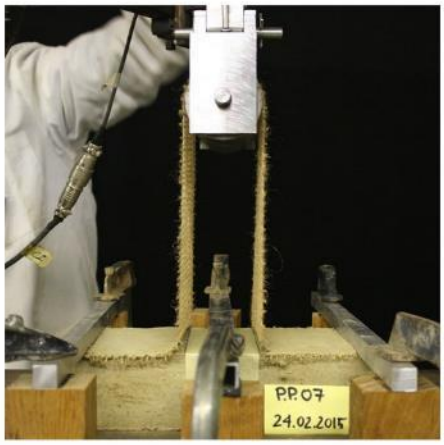

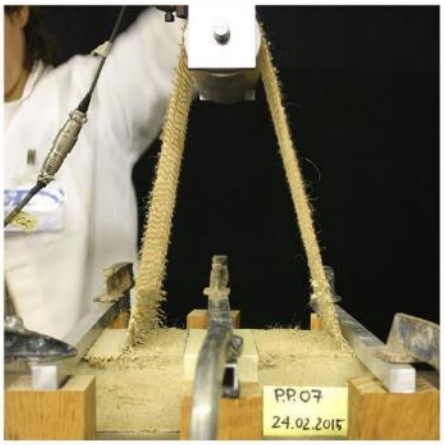

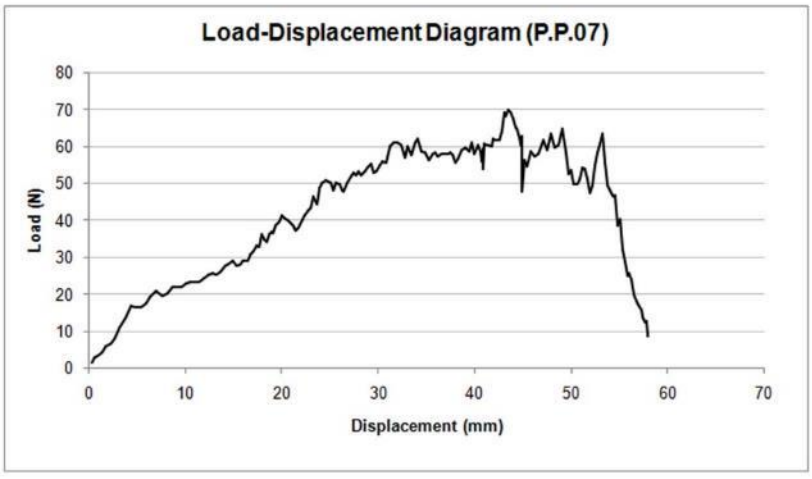

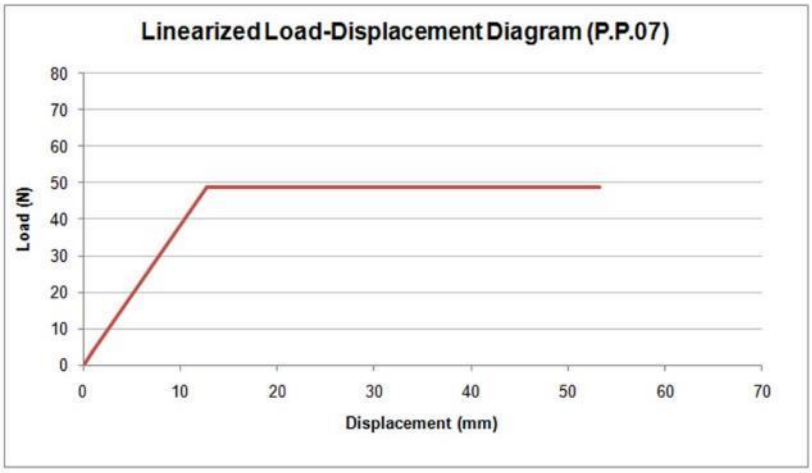

* Equivalent delamination force was determined starting from dissipated energy (equivalent area below the graph):
F = equivalent delamination load/2).

** Nominal width is obtained by multiplying the specimen wires number by the fabric average wires step equal to 4.292 mm.

.

P.P.08

Rammed earth specimen	
date of realization	20-09-2015
weight (kg)	3.77
length x,y,z (cm)	23.8.x11.8x6.2
Jute fabric	
strip width (cm)	11.8
strip length (cm)	60
longitudinal wires number	28
Test data	
test date	24-02-2015
displacement rate (mm/sec)	1/10
peak load (N)	55.91
equivalent delamination force F (N)*	21.56
F/ wires number (N)	0.770
F/ strip nominal width (N/mm)**	0.179

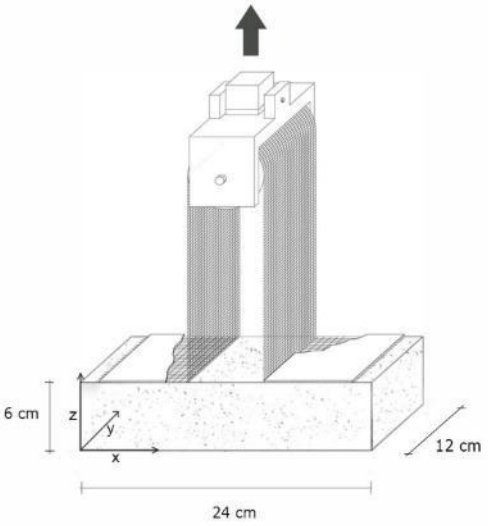

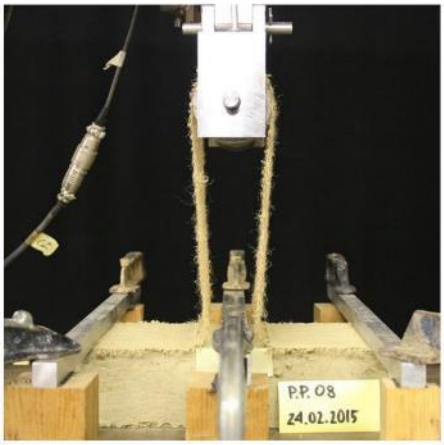

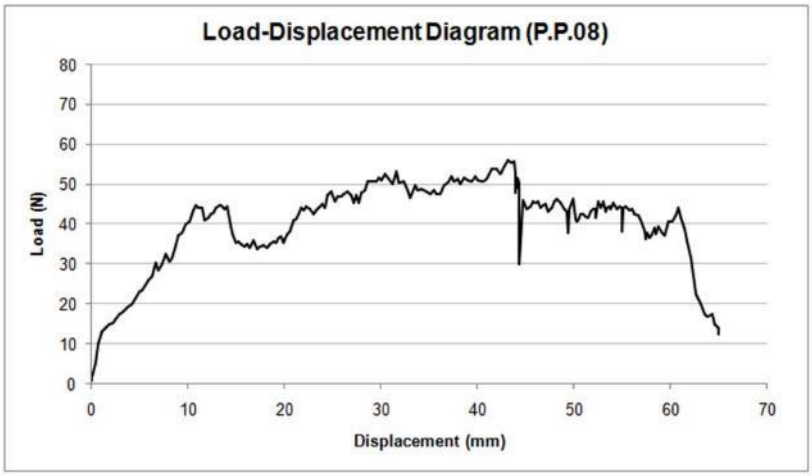

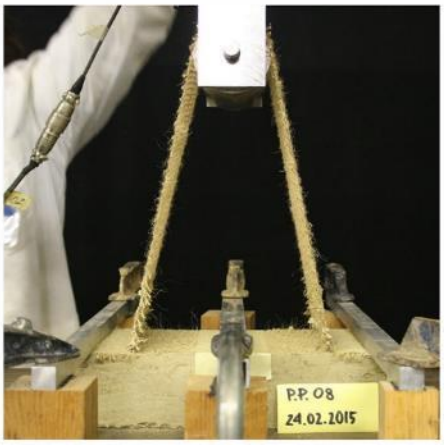

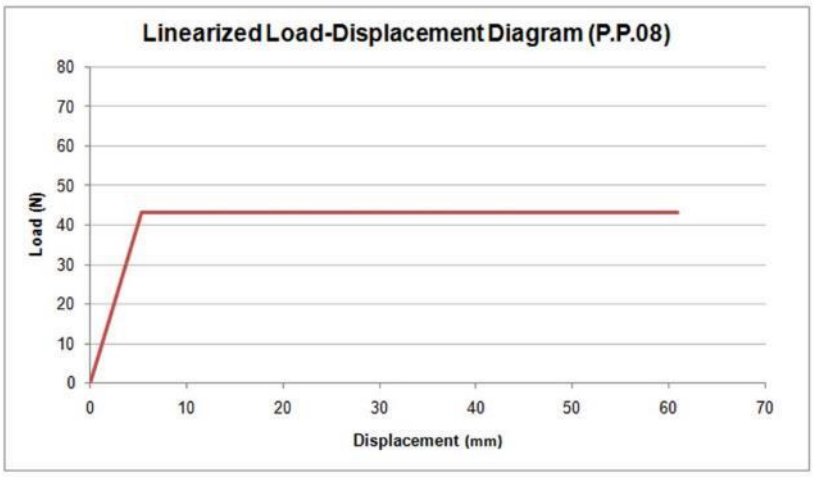

* Equivalent delamination force was determined starting from dissipated energy (equivalent area below the graph):
F = equivalent delamination load/2).

** Nominal width is obtained by multiplying the specimen wires number by the fabric average wires step equal to 4.292 mm.

.

P.P.10

Rammed earth specimen	
date of realization	22-11-2014
weight (kg)	3.50
length x,y,z (cm)	23.x11.5x6.1
Jute fabric	
strip width (cm)	11.5
strip length (cm)	62
longitudinal wires number	27
Test data	
test date	17-03-2015
displacement rate (mm/sec)	1/10
peak load (N)	60.863
equivalent delamination force F (N)*	23.3177
F/ wires number (N)	0.863
F/ strip nominal width (N/mm)**	0.201

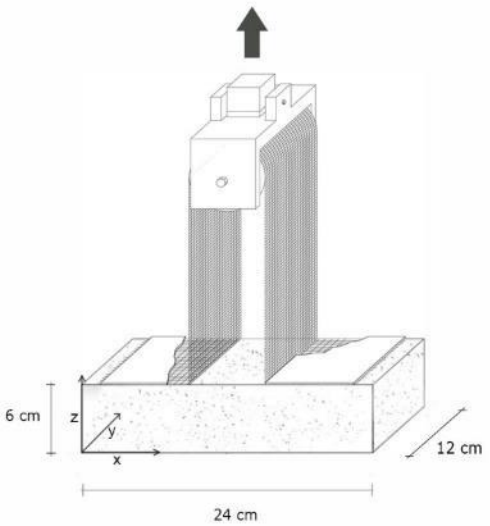

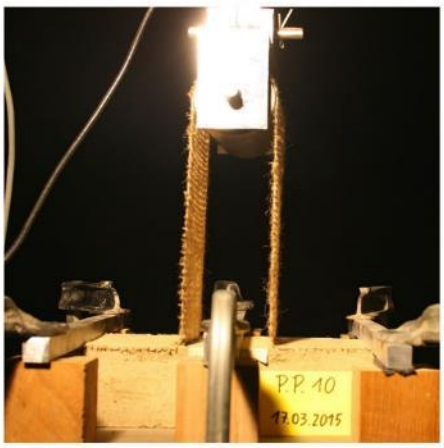

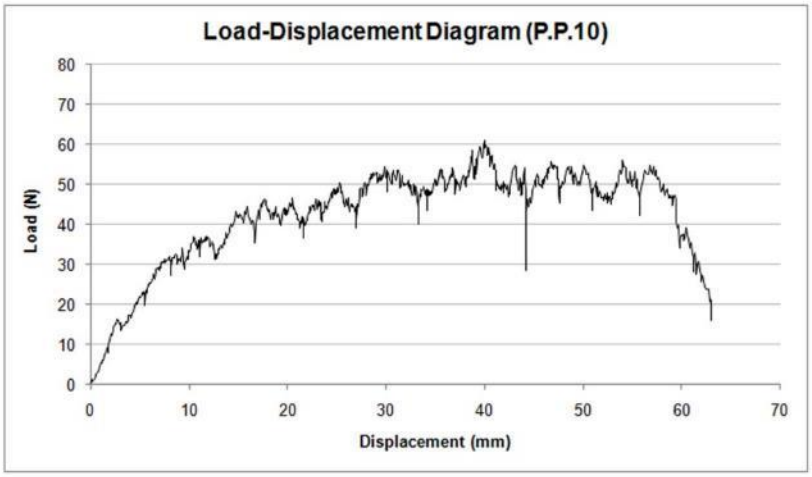

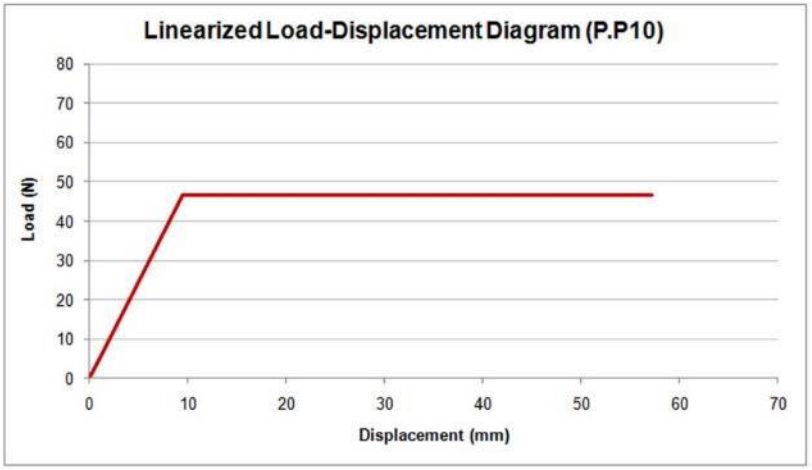

* Equivalent delamination force was determined starting from dissipated energy (equivalent area below the graph):
F = equivalent delamination load/2).

** Nominal width is obtained by multiplying the specimen wires number by the fabric average wires step equal to 4.292 mm.

.

P.01 (UPV)

Rammed earth specimen	
date of realization	17-01-2015
weight (kg)	3.61
length x,y,z (cm)	23.8x11.8x5.9
Jute fabric	
strip width (cm)	11.5
strip length (cm)	61.28
longitudinal wires number	27
Test data	
test date	22-05-2015
displacement rate (mm/sec)	1/10
peak load (N)	57.52
equivalent delamination force F (N)*	20.523
F/ wires number (N)	0,760
F/ strip nominal width (N/mm)**	0.177

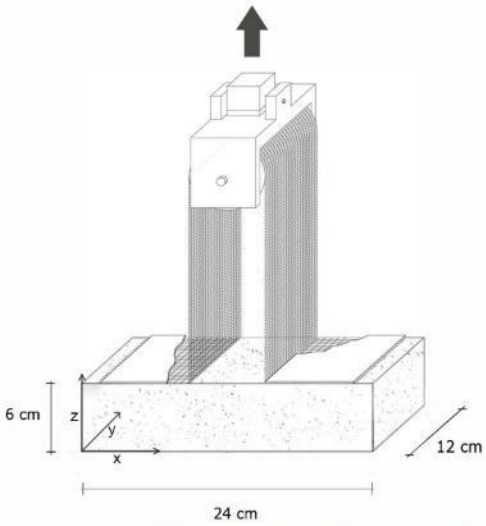

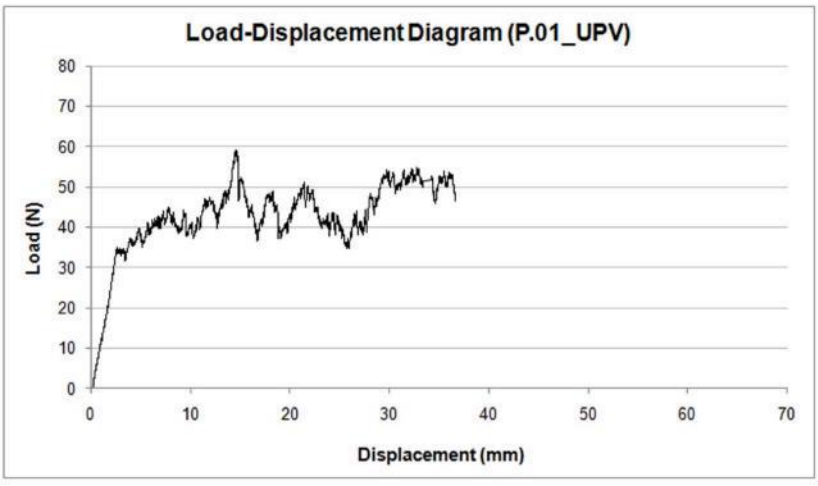

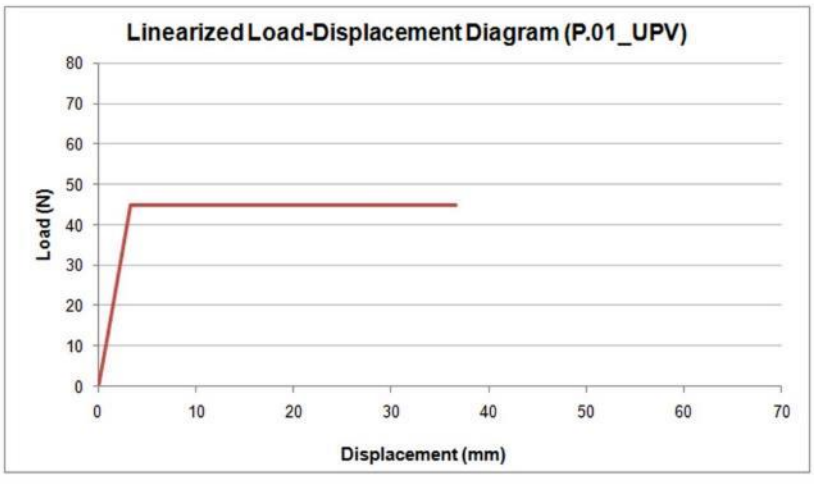

* Equivalent delamination force was determined starting from dissipated energy (equivalent area below the graph):
F = equivalent delamination load/2).

** Nominal width is obtained by multiplying the specimen wires number by the fabric average wires step equal to 4.292 mm.

.

P.02 (UPV)

Rammed earth specimen	
date of realization	06-02-2015
weight (kg)	3.61
length x,y,z (cm)	23.8x11.8 x5.9
Jute fabric	
strip width (cm)	12
strip length (cm)	62
longitudinal wires number	28
Test data	
test date	27-05-2015
displacement rate (mm/sec)	1/10
peak load (N)	66.72
equivalent delamination force F (N)*	22.916
F/ wires number (N)	0.881
F/ strip nominal width (N/mm)**	0.205

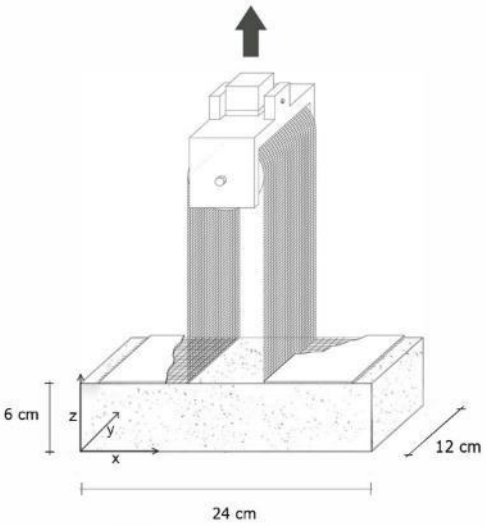

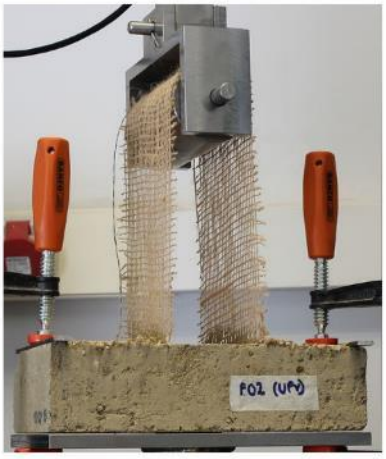

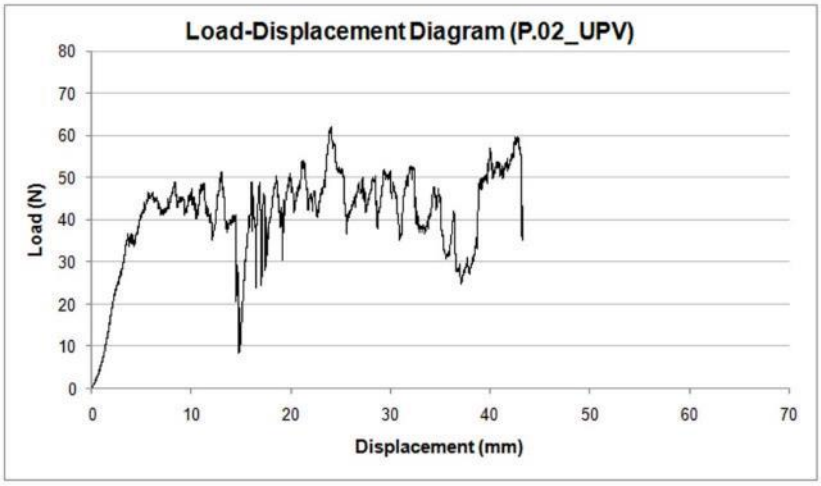

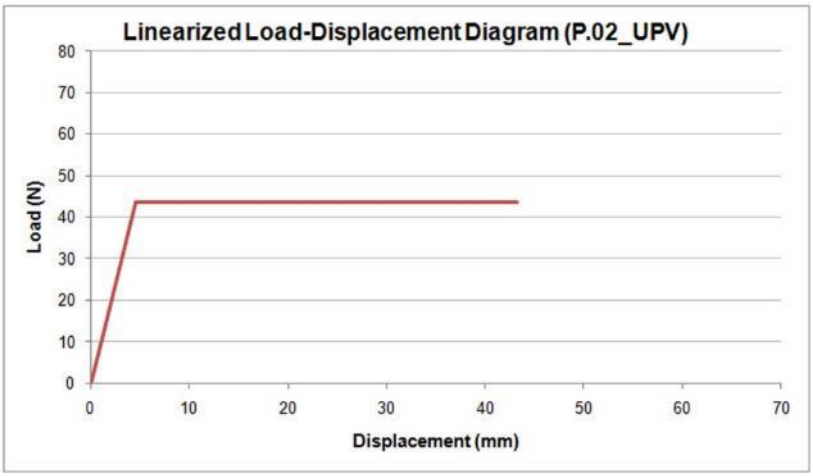

* Equivalent delamination force was determined starting from dissipated energy (equivalent area below the graph):
F = equivalent delamination load/2).

** Nominal width is obtained by multiplying the specimen wires number by the fabric average wires step equal to 4.292 mm.

.

P.03 (UPV)

Rammed earth specimen	
date of realization	09-02-2015
weight (kg)	3.61
length x,y,z (cm)	23.6x11.7x5.8
Jute fabric	
strip width (cm)	11.5
strip length (cm)	62
longitudinal wires number	26
Test data	
test date	26-05-2015
displacement rate (mm/sec)	1/10
peak load (N)	55.69
equivalent delamination force F (N)*	19.827
F/ wires number (N)	0.762
F/ strip nominal width (N/mm)**	0.177

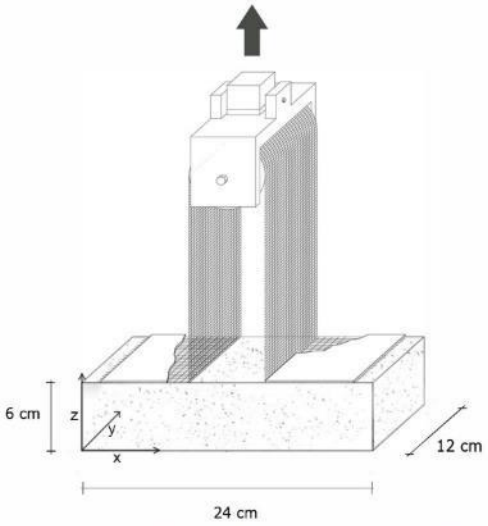

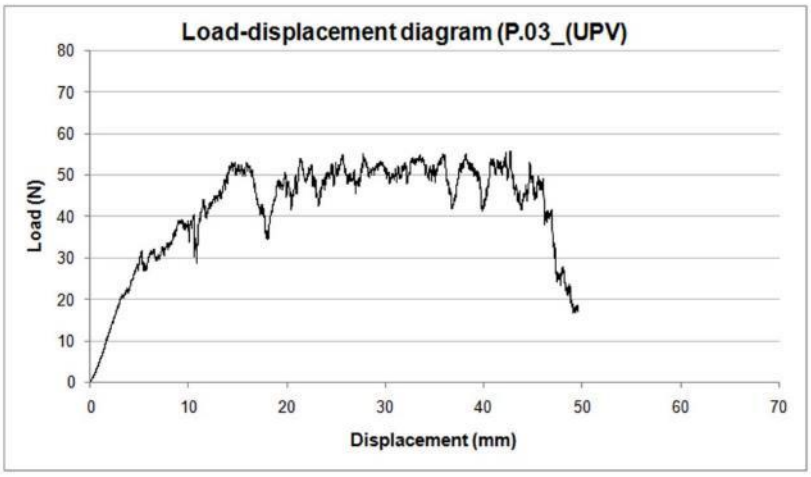

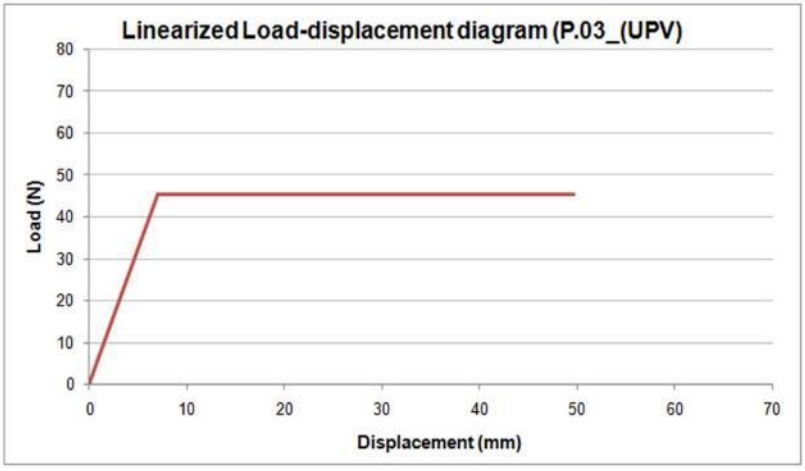

* Equivalent delamination force was determined starting from dissipated energy (equivalent area below the graph):
F = equivalent delamination load/2).

** Nominal width is obtained by multiplying the specimen wires number by the fabric average wires step equal to 4.292 mm.

.

P.04 (UPV)

Rammed earth specimen	
date of realization	28-01-2015
weight (kg)	3.61
length x,y,z (cm)	23.7x11.7x5.9
Jute fabric	
strip width (cm)	11.1
strip length (cm)	62
longitudinal wires number	26
Test data	
test date	26-05-2015
displacement rate (mm/sec)	1/10
peak load (N)	41.97
equivalent delamination force F (N)*	13.582
F/ wires number (N)	0.522
F/ strip nominal width (N/mm)**	0.121

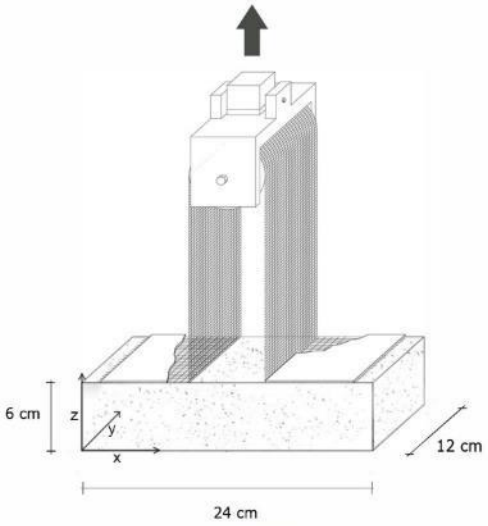

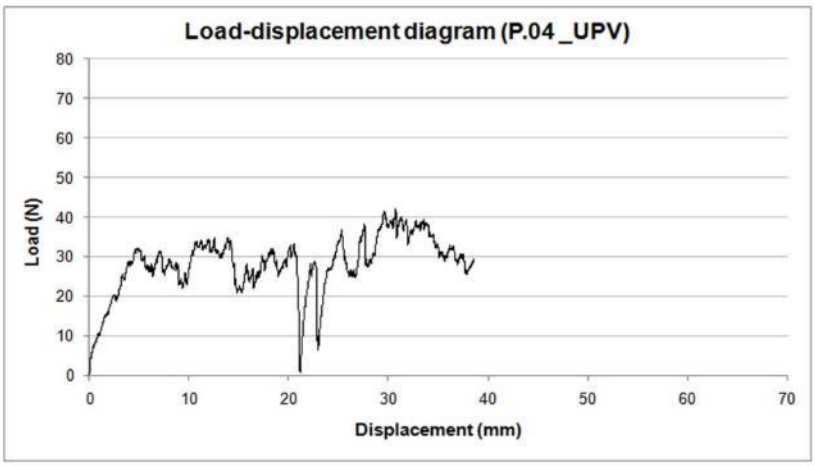

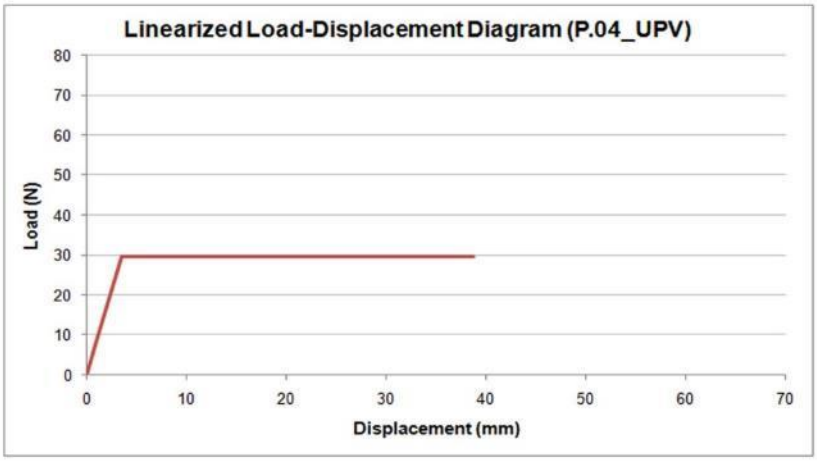

* Equivalent delamination force was determined starting from dissipated energy (equivalent area below the graph):
F = equivalent delamination load/2).

** Nominal width is obtained by multiplying the specimen wires number by the fabric average wires step equal to 4.292 mm.

.

P.05 (UPV)

Rammed earth specimen	
date of realization	02-02-2015
weight (kg)	3.61
length x,y,z (cm)	23.7x11.8x5.8
Jute fabric	
strip width (cm)	11.1
strip length (cm)	62
longitudinal wires number	26
Test data	
test date	26-05-2015
displacement rate (mm/sec)	1/10
peak load (N)	49.47
equivalent delamination force F (N)*	16.716
F/ wires number (N)	0.642
F/ strip nominal width (N/mm)**	0.149

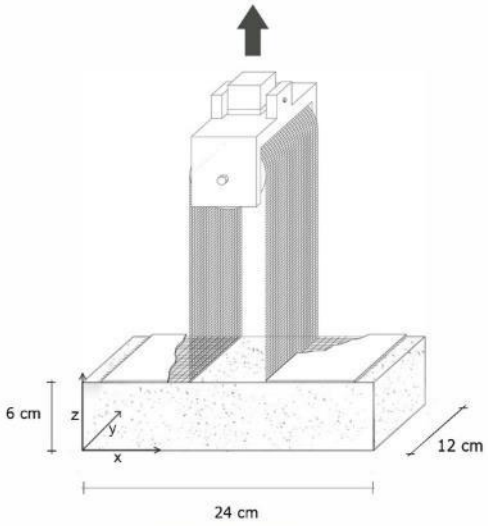

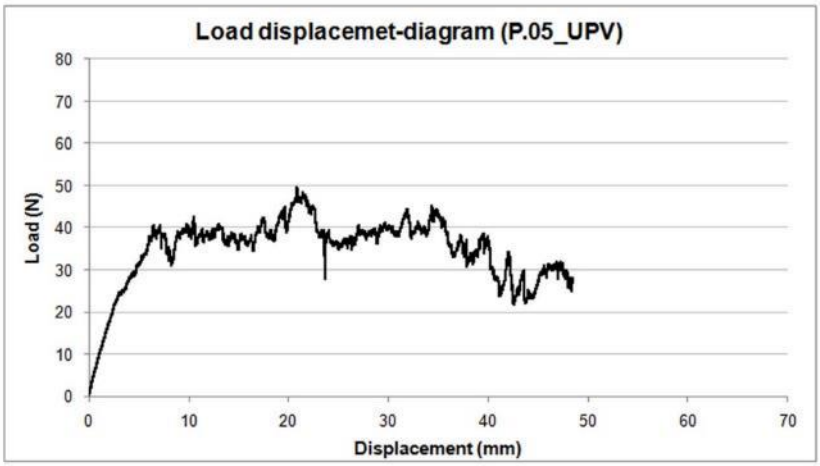

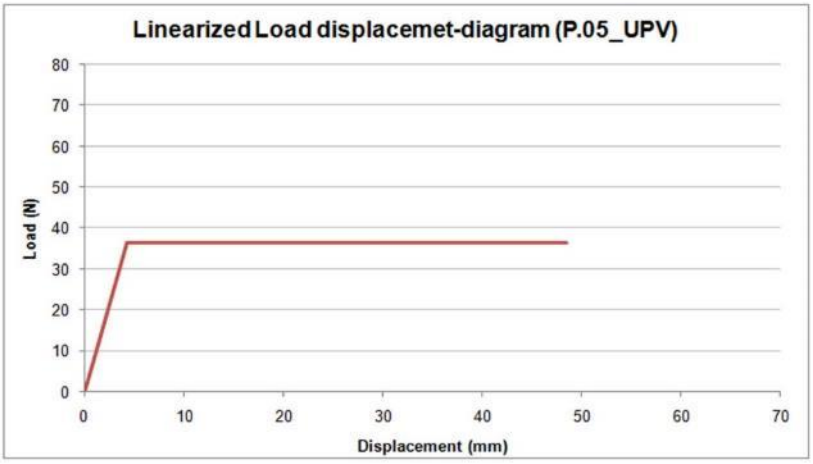

* Equivalent delamination force was determined starting from dissipated energy (equivalent area below the graph):
F = equivalent delamination load/2).

** Nominal width is obtained by multiplying the specimen wires number by the fabric average wires step equal to 4.292 mm.

.

P.06 (UPV)

Rammed earth specimen	
date of realization	11-02-2015
weight (kg)	3.61
length x,y,z (cm)	23.7x11.7x5.9
Jute fabric	
strip width (cm)	11.5
strip length (cm)	62
longitudinal wires number	27
Test data	
test date	27-05-2015
displacement rate (mm/sec)	1/10
peak load (N)	51.34
equivalent delamination force F (N)*	17.594
F/ wires number (N)	0.651
F/ strip nominal width (N/mm)**	0.151

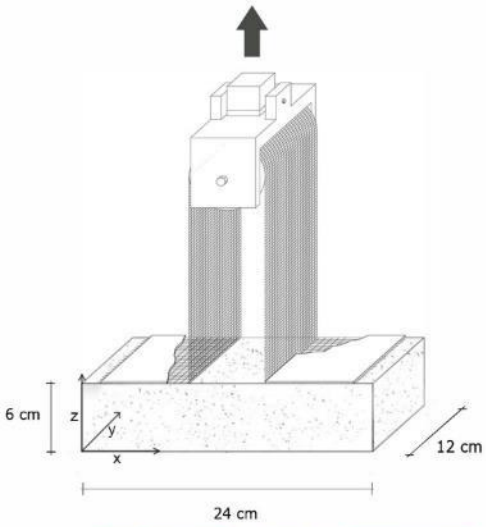

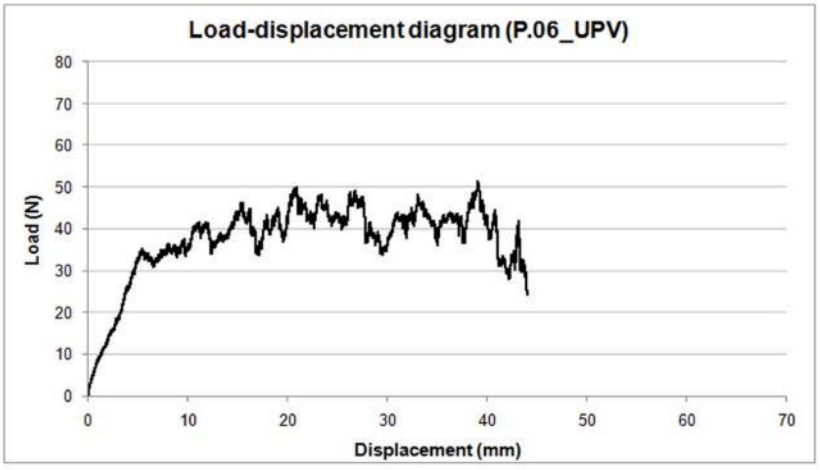

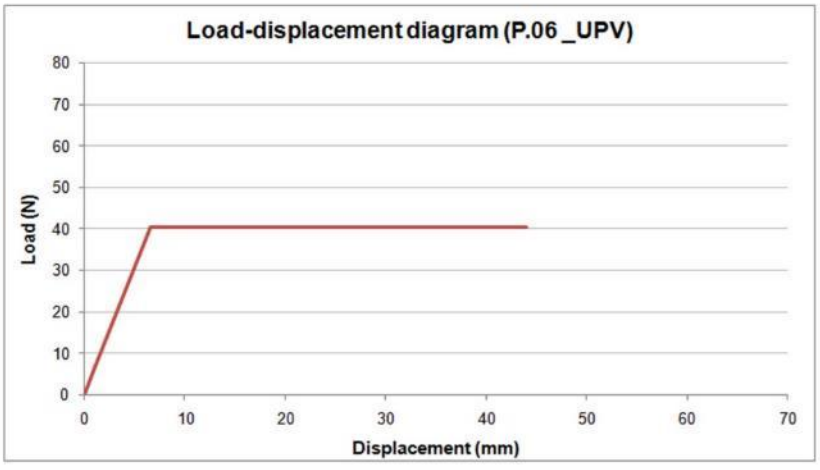

* Equivalent delamination force was determined starting from dissipated energy (equivalent area below the graph):
F = equivalent delamination load/2).

** Nominal width is obtained by multiplying the specimen wires number by the fabric average wires step equal to 4.292 mm.

.

P.07 (UPV)

Rammed earth specimen	
date of realization	12-02-2015
weight (kg)	3.61
length x,y,z (cm)	23.7x11.8x6.0
Jute fabric	
strip width (cm)	11.1
strip length (cm)	62
longitudinal wires number	26
Test data	
test date	26-05-2015
displacement rate (mm/sec)	1/10
peak load (N)	62.15
equivalent delamination force F (N)*	19.658
F/ wires number (N)	0.702
F/ strip nominal width (N/mm)**	0.163

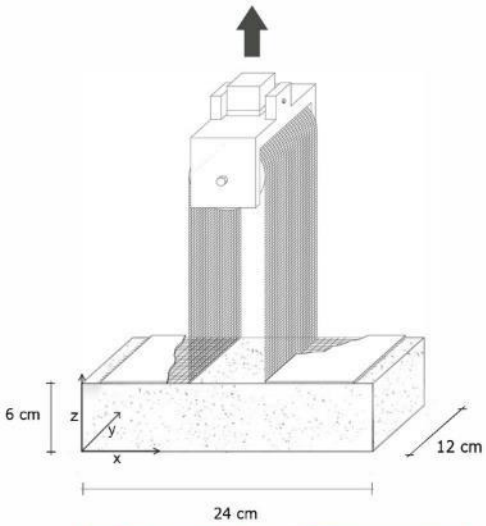

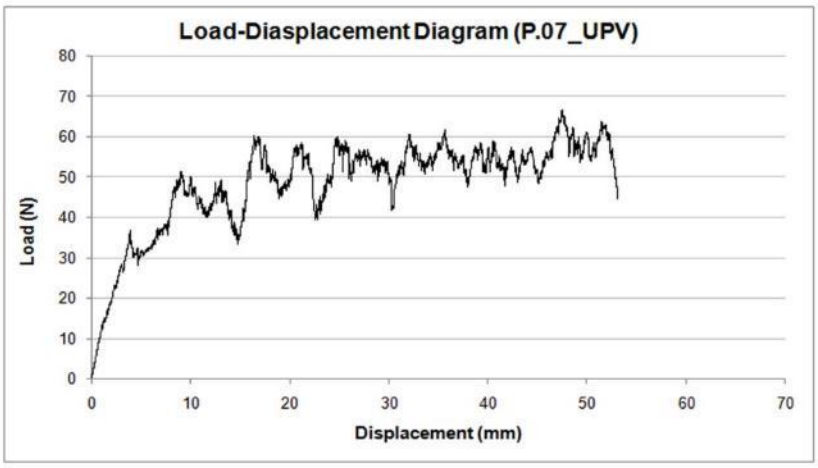

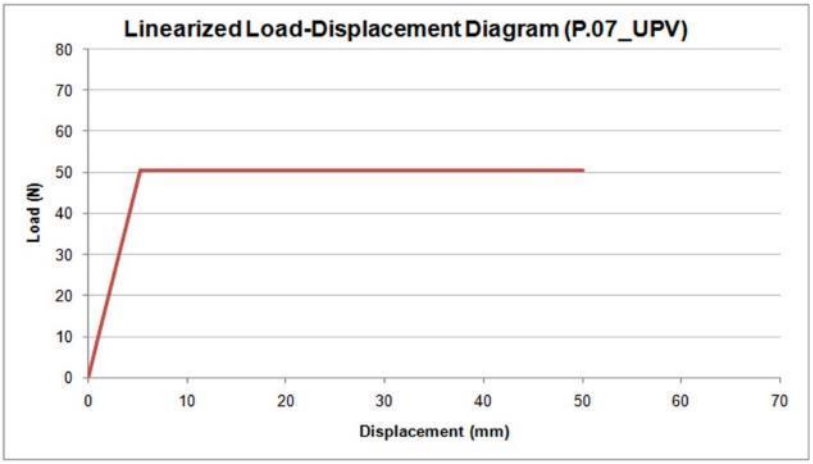

* Equivalent delamination force was determined starting from dissipated energy (equivalent area below the graph):
F = equivalent delamination load/2).

** Nominal width is obtained by multiplying the specimen wires number by the fabric average wires step equal to 4.292 mm.

.

P.08 (UPV)

Rammed earth specimen	
date of realization	04-02-2015
weight (kg)	3.61
length x,y,z (cm)	23.8x11.8 x5.7
Jute fabric	
strip width (cm)	11.5
strip length (cm)	62
longitudinal wires number	27
Test data	
test date	27-05-2015
displacement rate (mm/sec)	1/10
peak load (N)	45.05
equivalent delamination force F (N)*	12.353
F/ wires number (N)	0.457
F/ strip nominal width (N/mm)**	0.106

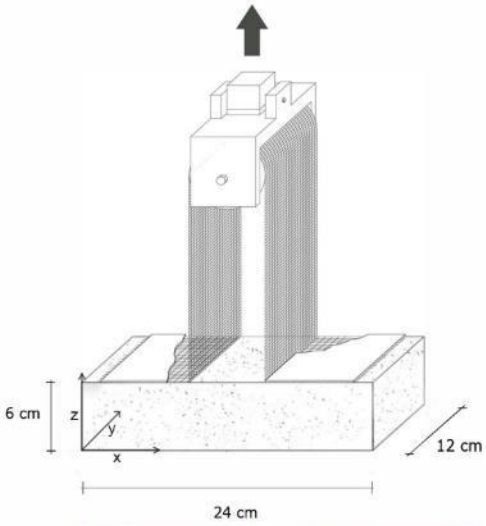

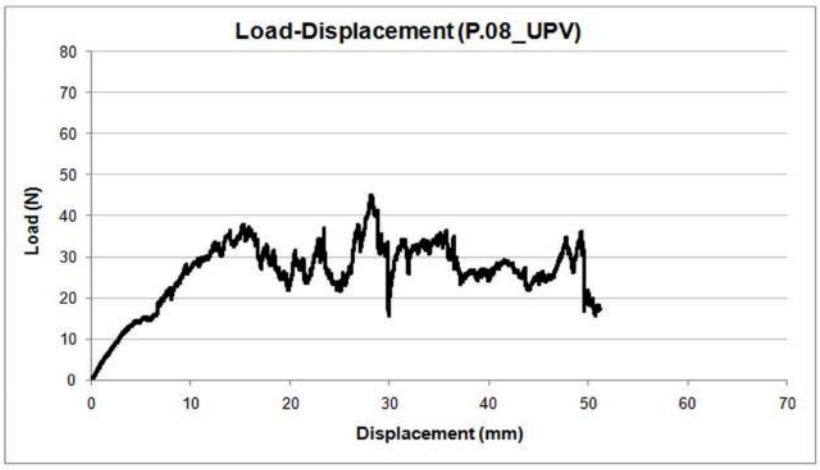

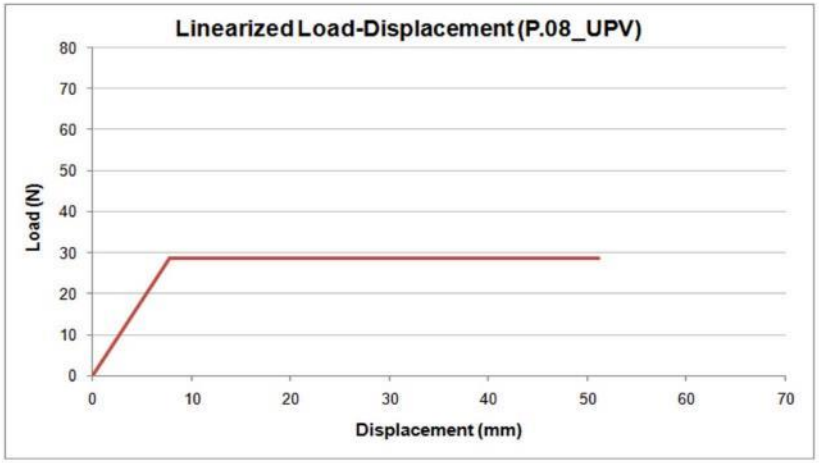

* Equivalent delamination force was determined starting from dissipated energy (equivalent area below the graph):
F = equivalent delamination load/2).

** Nominal width is obtained by multiplying the specimen wires number by the fabric average wires step equal to 4.292 mm.

.

P.01.10

Rammed earth specimen	
date of realization	17-01-2015
weight (kg)	3.60
length x,y,z (cm)	23.8x11.8 x5.9
Jute fabric	
strip width (cm)	11.5
strip length (cm)	40
longitudinal wires number	27
Test data	
test date	17-07-2015
displacement rate (mm/sec)	1/10
peak load (N)	92.170
equivalent delamination force F (N)*	33.875
F/ wires number (N)	1.254
F/ strip nominal width (N/mm)**	0.292

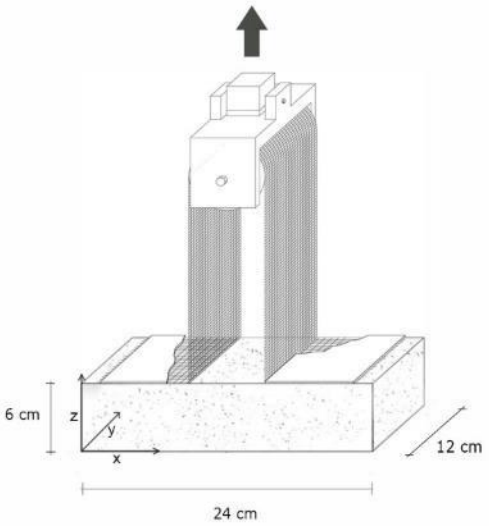

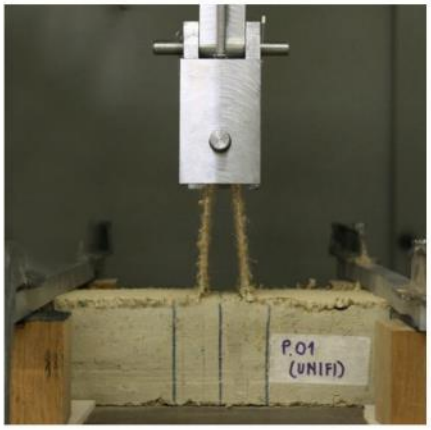

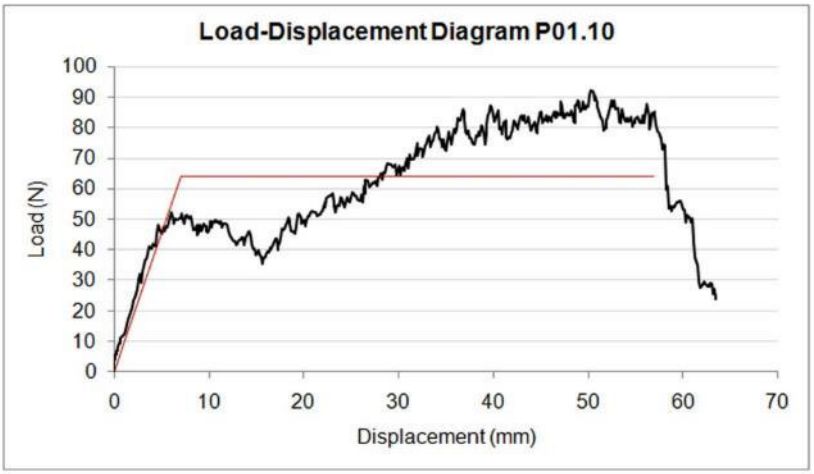

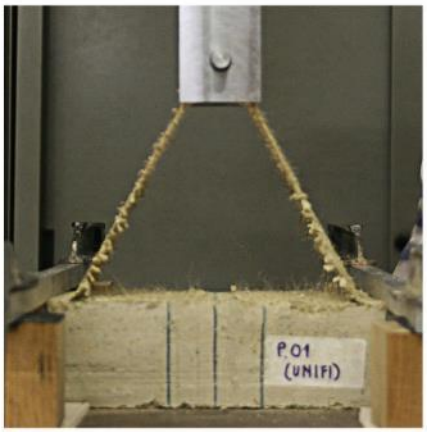

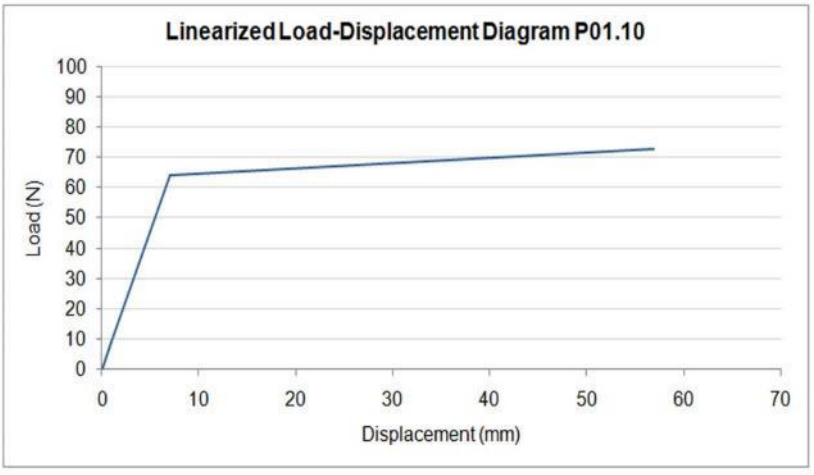

* Equivalent delamination force was determined starting from dissipated energy (equivalent area below the graph):
F = equivalent delamination load/2).

** Nominal width is obtained by multiplying the specimen wires number by the fabric average wires step equal to 4.292 mm.

.

P.02.10

Rammed earth specimen	
date of realization	06-02-2015
weight (kg)	3.60
length x,y,z (cm)	23.8x11.8 x5.9
Jute fabric	
strip width (cm)	12
strip length (cm)	40
longitudinal wires number	28
Test data	
test date	17-07-2015
displacement rate (mm/sec)	1/10
peak load (N)	62.145
equivalent delamination force F (N)*	24.856
F/ wires number (N)	0.920
F/ strip nominal width (N/mm)**	0.214

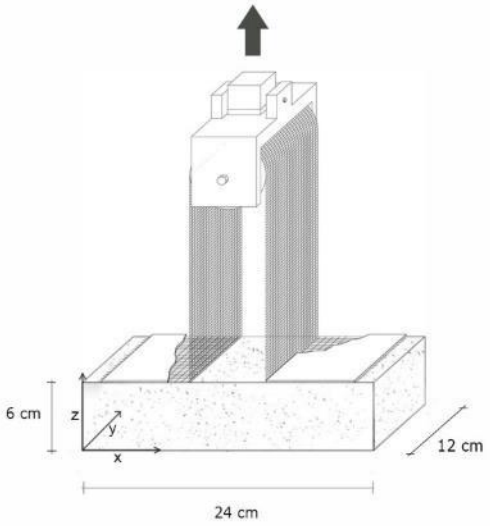

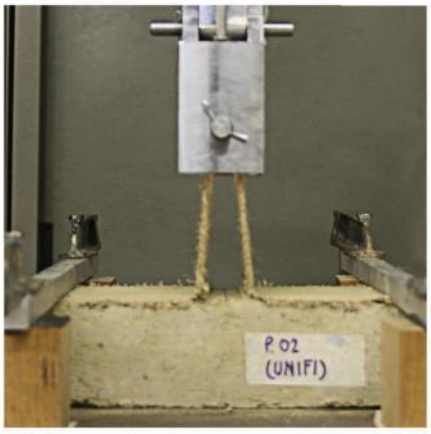

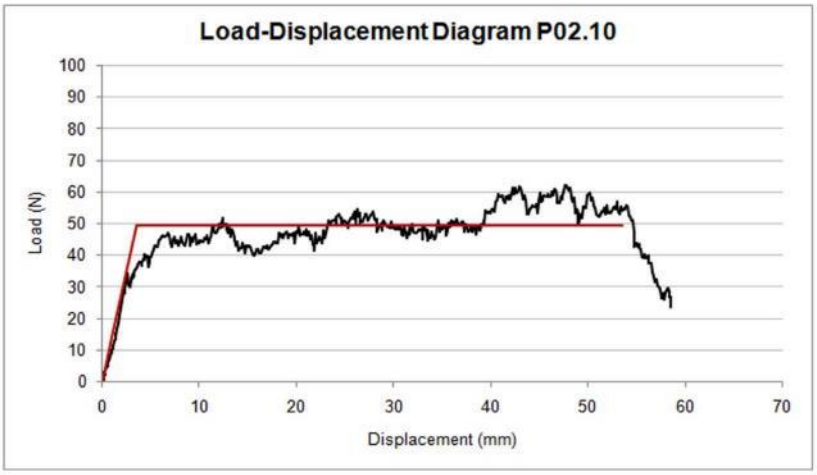

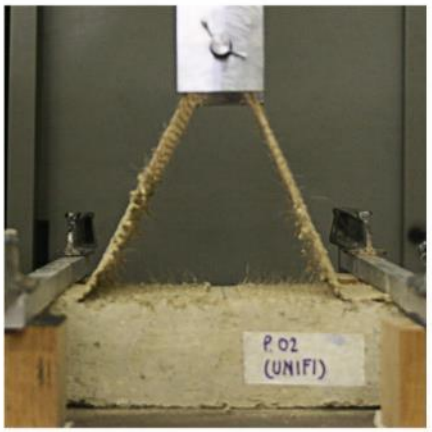

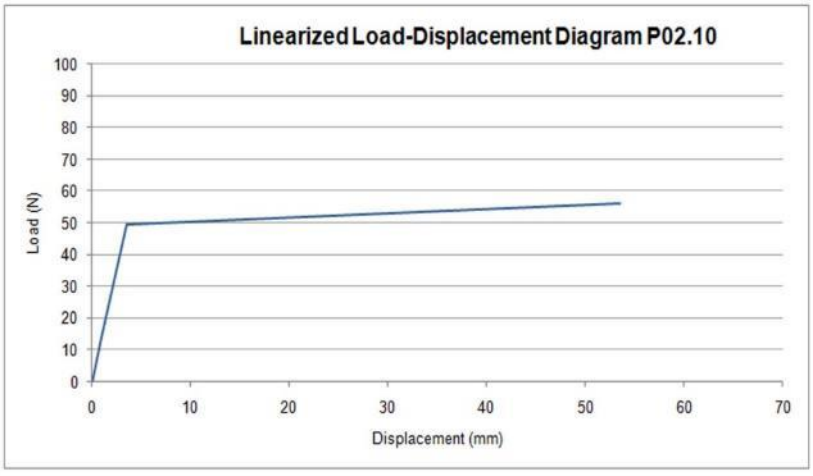

* Equivalent delamination force was determined starting from dissipated energy (equivalent area below the graph):
F = equivalent delamination load/2).

** Nominal width is obtained by multiplying the specimen wires number by the fabric average wires step equal to 4.292 mm.

.

P.03.10

Rammed earth specimen	
date of realization	09-02-2015
weight (kg)	3.60
length x,y,z (cm)	23.6x11.7x5.8
Jute fabric	
strip width (cm)	11.1
strip length (cm)	40
longitudinal wires number	26
Test data	
test date	17-07-2015
displacement rate (mm/sec)	1/10
peak load (N)	92.170
equivalent delamination force F (N)*	33.875
F/ wires number (N)	1.254
F/ strip nominal width (N/mm)**	0.292

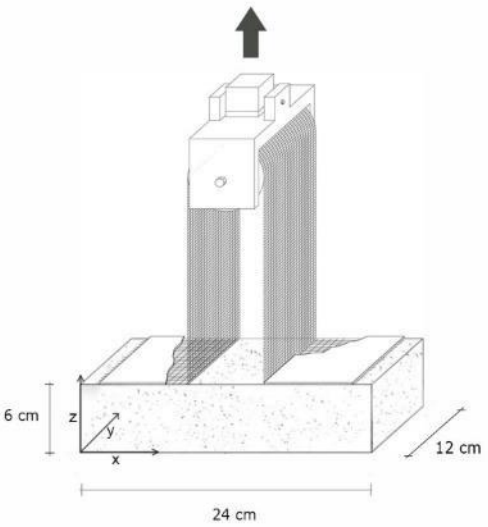

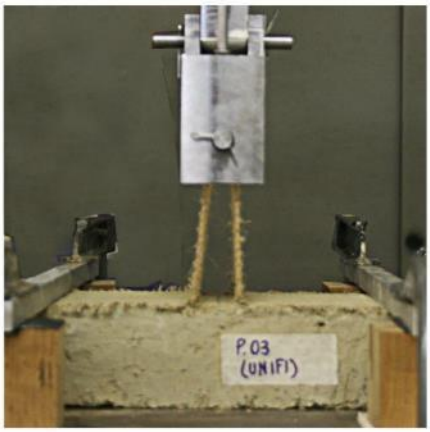

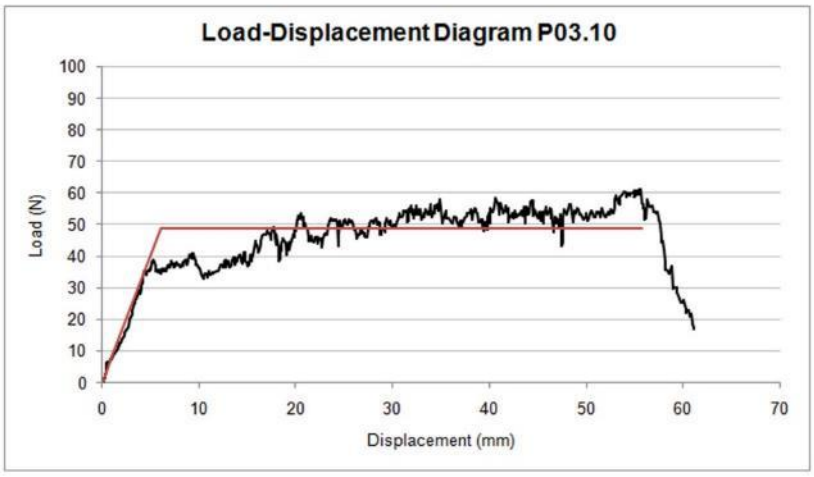

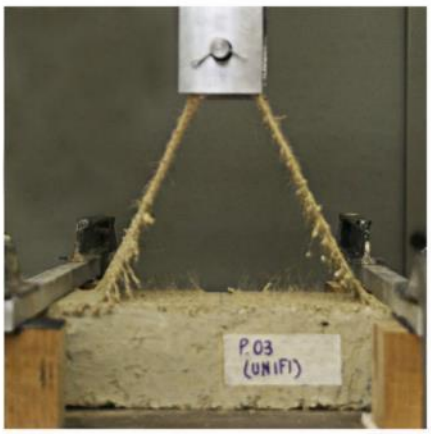

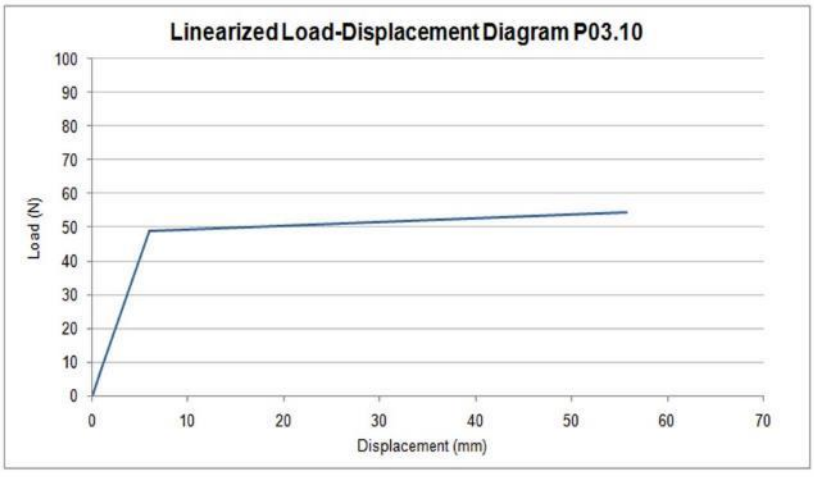

* Equivalent delamination force was determined starting from dissipated energy (equivalent area below the graph):
F = equivalent delamination load/2).

** Nominal width is obtained by multiplying the specimen wires number by the fabric average wires step equal to 4.292 mm.

.

P.04.10

Rammed earth specimen	
date of realization	28-01-2015
weight (kg)	3.60
length x,y,z (cm)	23.7x11.7x5.9
Jute fabric	
strip width (cm)	11.1
strip length (cm)	40
longitudinal wires number	26
Test data	
test date	17/07/2015
displacement rate (mm/sec)	1/10
peak load (N)	69.798
equivalent delamination force F (N)*	26.714
F/ wires number (N)	1.113
F/ strip nominal width (N/mm)**	0.259

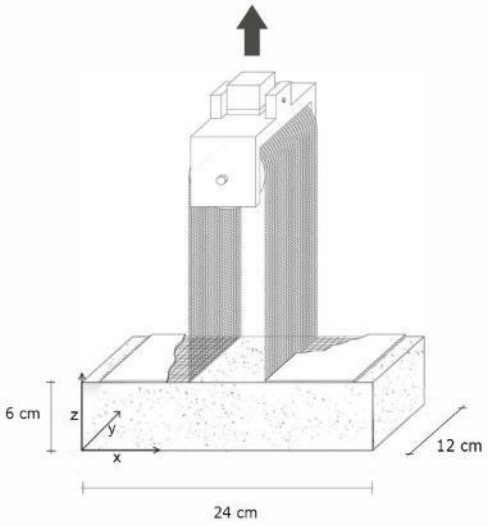

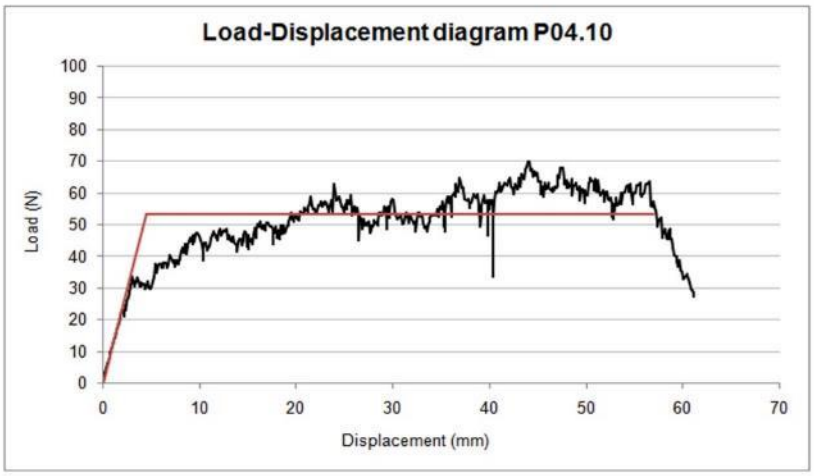

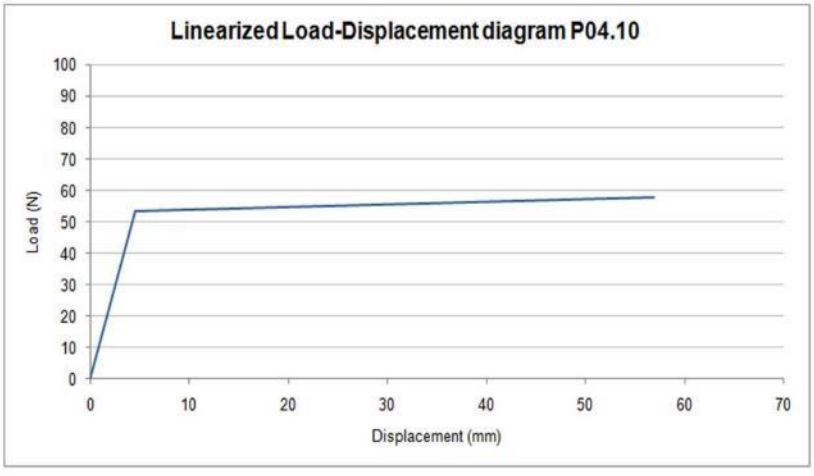

* Equivalent delamination force was determined starting from dissipated energy (equivalent area below the graph):
F = equivalent delamination load/2).

** Nominal width is obtained by multiplying the specimen wires number by the fabric average wires step equal to 4.292 mm.

.

P.05.10

Rammed earth specimen	
date of realization	02-02-2015
weight (kg)	3.60
length x,y,z (cm)	23.7x11.8x5.8
Jute fabric	
strip width (cm)	11.1
strip length (cm)	40
longitudinal wires number	26
Test data	
test date	17/07/2015
displacement rate (mm/sec)	1/10
peak load (N)	54.428
equivalent delamination force F (N)*	21.251
F/ wires number (N)	0.787
F/ strip nominal width (N/mm)**	0.183

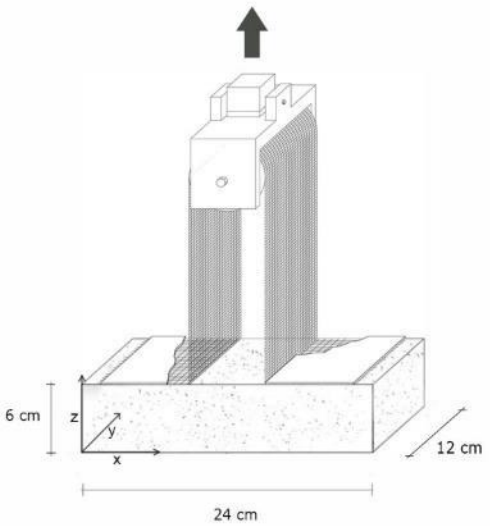

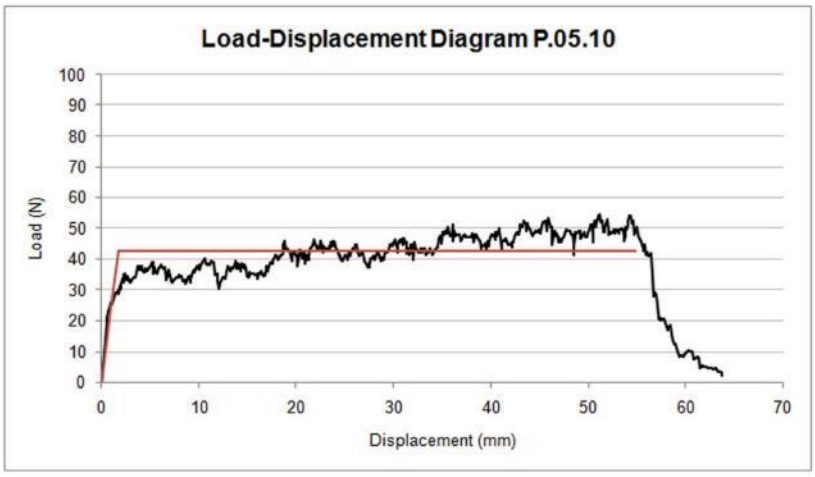

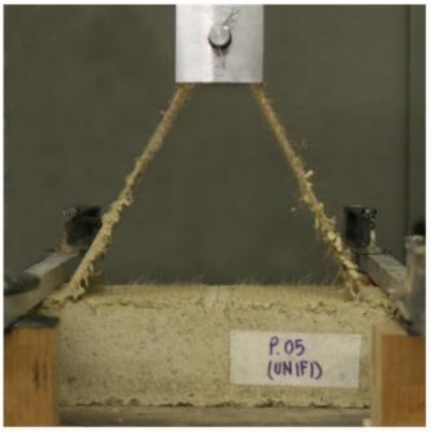

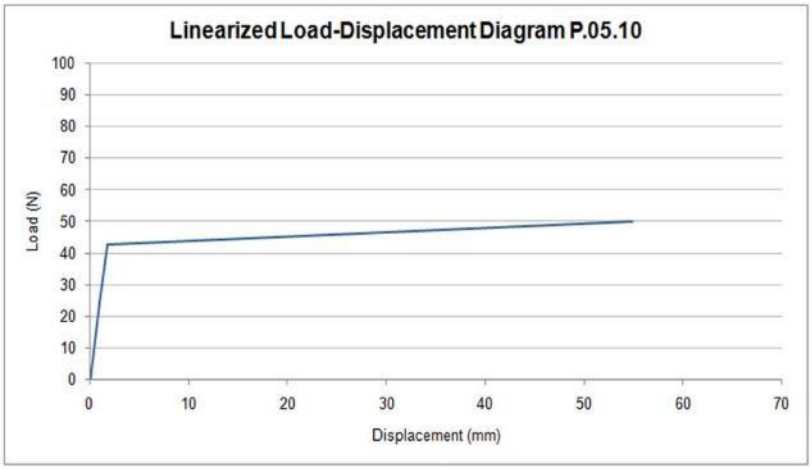

* Equivalent delamination force was determined starting from dissipated energy (equivalent area below the graph):
F = equivalent delamination load/2).

** Nominal width is obtained by multiplying the specimen wires number by the fabric average wires step equal to 4.292 mm.

.

P.06.10

Rammed earth specimen	
date of realization	11-02-2015
weight (kg)	3.60
length x,y,z (cm)	23.7x11.7x5.9
Jute fabric	
strip width (cm)	11.5
strip length (cm)	40
longitudinal wires number	27
Test data	
test date	17-07-2015
displacement rate (mm/sec)	1/10
peak load (N)	67.064
equivalent delamination force F (N)*	28.052
F/ wires number (N)	1.039
F/ strip nominal width (N/mm)**	0.242

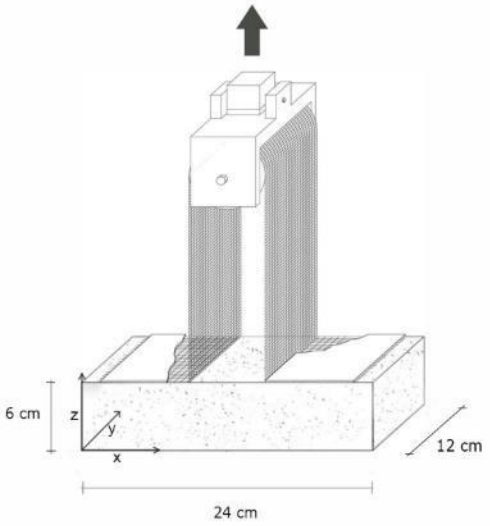

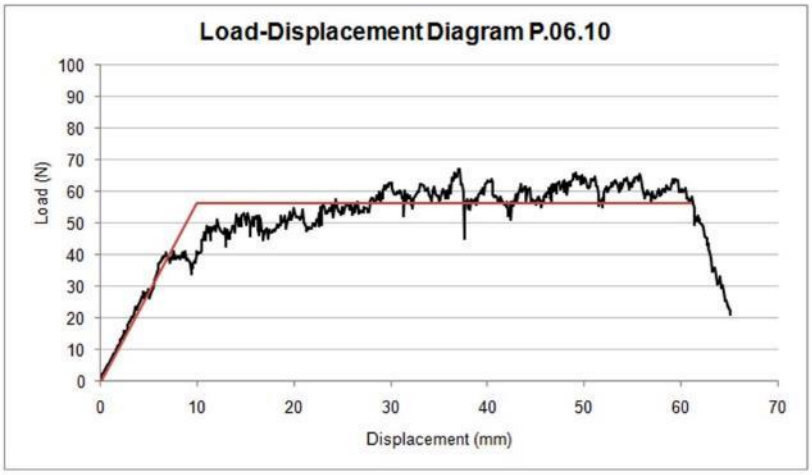

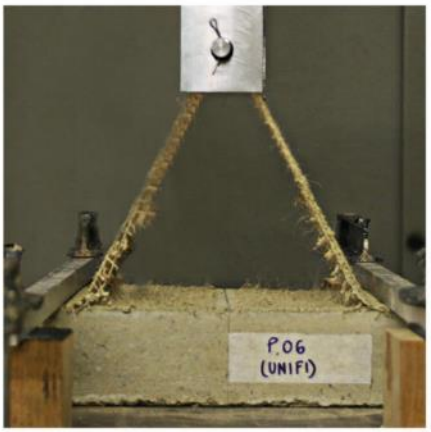

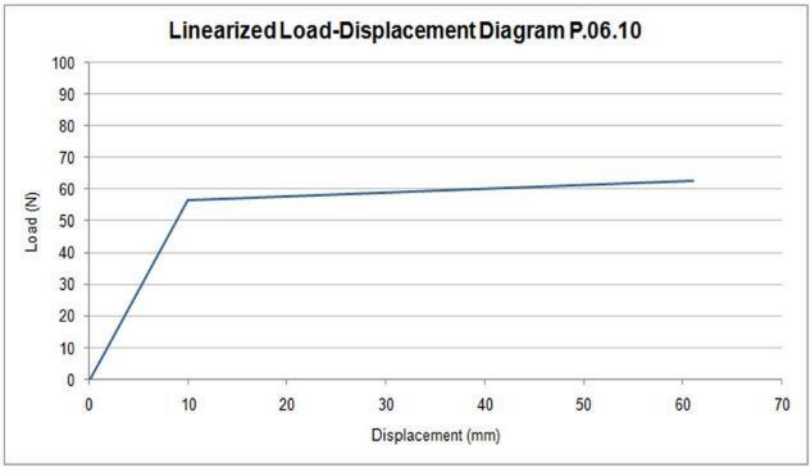

* Equivalent delamination force was determined starting from dissipated energy (equivalent area below the graph):
F = equivalent delamination load/2).

** Nominal width is obtained by multiplying the specimen wires number by the fabric average wires step equal to 4.292 mm.

.

P.07.10

Rammed earth specimen	
date of realization	12-02-2015
weight (kg)	3.60
length x,y,z (cm)	23.7x11.8x6.0
Jute fabric	
strip width (cm)	11.1
strip length (cm)	40
longitudinal wires number	26
Test data	
test date	17-07-2015
displacement rate (mm/sec)	1/10
peak load (N)	59.213
equivalent delamination force F (N)*	24.501
F/ wires number (N)	0.942
F/ strip nominal width (N/mm)**	0.219

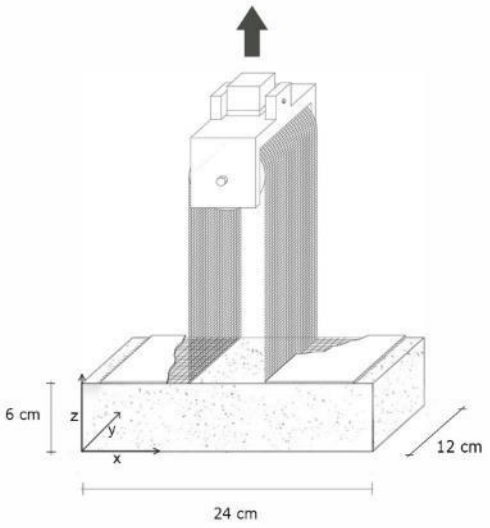

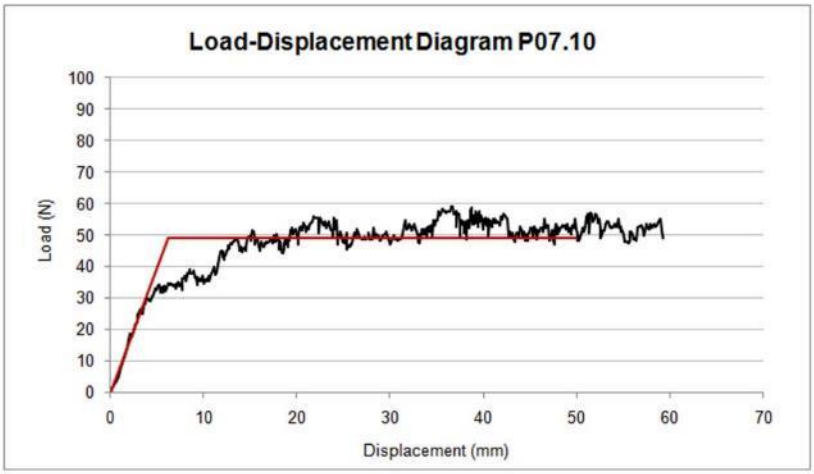

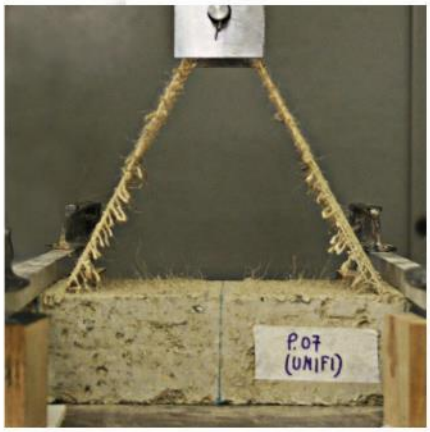

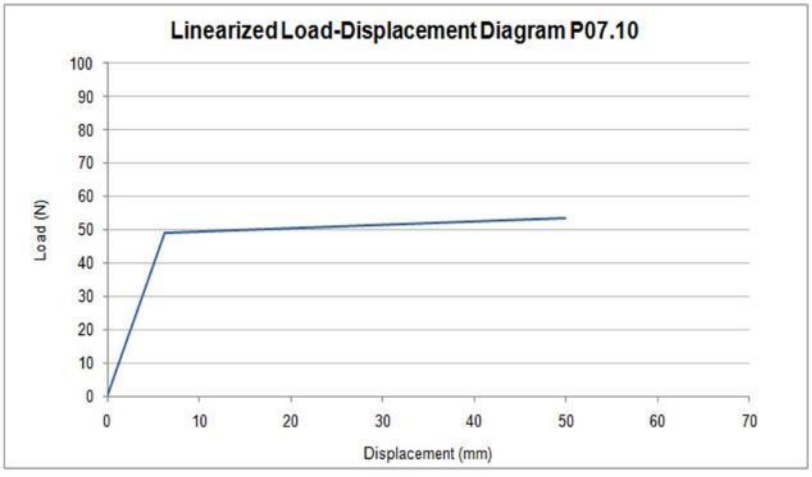

* Equivalent delamination force was determined starting from dissipated energy (equivalent area below the graph):
F = equivalent delamination load/2).

** Nominal width is obtained by multiplying the specimen wires number by the fabric average wires step equal to 4.292 mm.

.

3.7 Bibliography

ACI Committee 440. Guide for the design and construction of externally bonded FRP systems for strengthening concrete structures ACI 440.2R-08, Farmington Hills, MI.2008.

Adams, R.D., Wake, W.C. 1984. Structural Adhesive Joints in Engineering. Elsevier applied science publisher London and New York. ISBN 0-85334-263-6

Ahmed, K. S., Vijayarangan, S. 2008. "Tensile, Flexural and Interlaminar Shear Properties of Woven Jute and Jute-Glass Fabric Reinforced Polyester Composites." Journal of Materials Processing Technology 207 (1–3): 330–35.doi:10.1016/j.jmatprotec.2008.06.038.

Asprone, D., Durante, M., Prota, A., Manfredi, G. 2011. "Potential of Structural Pozzolanic Matrix-Hemp Fiber Grid Composites." Construction and Building Materials 25 (6). Elsevier Ltd: 2867–74. doi:10.1016/j.conbuildmat.2010.12.046.

ASTM, "Standard Test Method for Apparent Shear Strength of Single-Lap Joint Adhesively Bonded Metal Specimens by Tension Loading," D1002, 1994.

ASTM, "Standard Test Method for Strength Properties of Adhesives in Shear by Tension Loading of Single-Lap Joint Laminated Assemblies," D3165, 1991.

Banea, M. D., da Silva, L. F. M. 2009. Adhesively bonded joints in composite materials: an overview. Proceedings of the Institution of Mechanical Engineers, Part L: Journal of Materials: Design and Applications, 223(1), 1–18. http://doi.org/10.1243/14644207JMDA219

Begley, M. R., Collino, R., Israelachvili, J. N., McMeeking, R. M. 2013. "Peeling of a Tape with Large Deformations and Frictional Sliding." Journal of the Mechanics and Physics of Solids 61 (5). Elsevier: 1265–79. doi:10.1016/j.jmps.2012.09.014.

Bikerman, J. J. 1957. "Theory of Peeling through a Hookean Solid." Journal of Applied Physics 28 (12): 1484–85. doi:10.1063/1.1722682.

Briccoli Bati S., Fagone M., Loccarini F., Ranocchiai G. 2013. "Mechanical behavior of structural elements in rammed earth reinforced with jute fabric". In: Cornelia Theimer Gardella (Editor), "proceedings for the Seventh International Earth building Conference", Earth USA 2013 – Adobe in Action, Santa Fe, New Mexico, USA, 2013, ISBN 978-0-9824660-3-2.

Briccoli Bati S., Fagone M., Loccarini F., Ranocchiai G. 2014. "Jute fabric to improve the mechanical properties of rammed earth constructions". In: Mileto C, Vegas F, Garcìa L, Cristini V, editors. Versus 2014 – Earthen Architecture, Valencia, Spain: CRC Press. 55–60.

Briccoli Bati S., Fagone M., Loccarini F., Ranocchiai G. 2013. "Analysis of rammed earth arches strengthened with natural fibers". In: Iványi BHVT and P, editor. Fourteenth Int. Conf. Civil, Struct. Environ. Eng. Comput., vol. Proceeding, Cagliari: 2013. 1–16. doi:10.4203/ccp.102.78.

Campbell, F. C. 2010. "Structural Composite Materials". ASM International

Campilho, R. D S G, Banea, M. D., Pinto, A. M. G., da Silva, L. F. M., de Jesus, A. M. P. 2011. "Strength Prediction of Single- and Double-Lap Joints by Standard and Extended Finite Element Modelling." International Journal of Adhesion and Adhesives 31 (5). Elsevier: 363–72. doi:10.1016/j.ijadhadh.2010.09.008.

Brahma Chari, K. J. 2015. "Investigation on Mode – I Fracture Parameters Using Steel Fibers in High Strength Concrete" 3 (11): 110–16.

Clauß, B., Fitzer, E. 2012. "Fibers, 11. Inorganic Fibers, Survey." Ulmann's Encyclopedia of iIndustrial Chemistry 15 (January 2012): 735–68. doi:10.1002/14356007.a11.

CNR.Guide for the design and construction of externally bonded FRP systems for strengthening existing. Materials, RC and PC structures, masonry structures. CNR – Advisory Committee on Technical Recommendations for Construction; 20013.CNR-DT 200 R1/2013.

Codispoti, R., Oliveira, D. V., Olivito, R. S., Lourenço, P. B., Fangueiro, R. 2015. “Mechanical Performance of Natural Fiber-Reinforced Composites for the Strengthening of Masonry.” Composites Part B: Engineering 77 (November): 74–83. doi:10.1016/j.compositesb.2015.03.021.

Concrete Society. Design guidance on strengthening concrete structures using fibre composite materials. Technical Rep. No. 55, London 2004.

Corradi, M., Borri, A., Vignoli, A., 2003. “Experimental Study on the Determination of Strength of Masonry Walls.” Construction and Building Materials 17 (5): 325–37. doi:10.1016/S0950-0618(03)00007-2.

Corradi, M., Antonio B., Castori G., Coventry, K. 2015. “Experimental Analysis of Dynamic Effects of FRP Reinforced Masonry Vaults.” Materials 8 (12): 8059–71. doi:10.3390/ma8125445.

De Lorenzis, L., Teng, J. G., Zhang, L. 2006. Interfacial Stresses in Curved Members Bonded with a Thin Plate. International Journal of Solids and Structures, 43(25-26), 7501–7517. doi:10.1016/j.ijsolstr.2006.03.

De Lorenzis, L., Miller B., Nanni A. 2001. “Bond of Fiber-Reinforced Polymer Laminates to Concrete.” ACI Materials Journal 98 (3): 256–64.

De Lorenzis, L., Zavarise, G. 2008. “Modeling of Mixed-Mode Debonding in the Peel Test Applied to Superficial Reinforcements.” International Journal of Solids and Structures 45 (20): 5419–36. doi:10.1016/j.ijsolstr.2008.05.024.

De Lorenzis, L., Zavarise, G. 2010. Debonding analysis of thin plates from curved substrates. Engineering Fracture Mechanics, 77(16), 3310–3328. doi:10.1016/j.engfracmech.2010.08.013

Dweib, M.A., Hu, B., O’Donnell, A., Shenton, H.W., Wool, R.P. 2004. “All Natural Composite Sandwich Beams for Structural Applications.” Composite Structures 63 (2): 147–57. doi:10.1016/S0263-8223(03)00143-0.

Fagone, M., Ranocchiai, G., Briccoli Bati, S. 2015. “An Experimental Analysis about the Effects of Mortar Joints on the Efficiency of Anchored CFRP-to-Masonry Reinforcements.” Composites Part B: Engineering 76 (November 2016). Elsevier Ltd: 133–48. doi:10.1016/j.compositesb.2015.01.050.

Faruk, O., Bledzki, A. K., Fink, H. P., Sain, M. 2012. “Biocomposites Reinforced with Natural Fibers: 2000-2010.” Progress in Polymer Science 37 (11). Elsevier Ltd: 1552–96. doi:10.1016/j.progpolymsci.2012.04.003.

FIB. FRP reinforcement in RC structures. Fib Task Group 9.3, Lausanne, fib bulletin 40, 1–147 2007.

Gassan, J., Bledzki, A. K. 1999. “Possibilities for Improving the Mechanical Properties of Jute / Epoxy Composites by Alkali Treatment of fibres” 59: 1303–9.

Gent, A. N., Hamed G. R. 1975. “Peel mechanics”. The journal of Adhesion 7(2):91-95. doi:10.1080/00218467508075041

Gent, A. N., Kaang, S. 1986. “Pull-off Forces for Adhesive Tapes.” Journal of Applied Polymer Science 32 (4): 4689–4700. doi:10.1002/app.1986.070320433.

Georgiou, I., Hadavinia, H., Ivankovic, A., Kinloch, A. J., Tropsa, V., Williams, J. G. 2003. “Cohesive Zone Models and the Plastically Deforming Peel Test.” The Journal of Adhesion 79 (3): 239–65. doi:10.1080/00218460309555.

Ghatak, A., Mahadevan, L., Chaudhury, M. K. 2005. “Measuring the Work of Adhesion between a Soft Confined Film and a Flexible Plate.” Langmuir 21 (4): 1277–81. doi:10.1021/la0484826.

Ghavami, K., Toledo Filho, R. D., Barbosa, N. P. 1999. “Behaviour of Composite Soil Reinforced with Natural Fibres.” Cement and Concrete Composites 21 (1): 39–48. doi:10.1016/S0958-9465(98)00033-X.

Gialamas, P., Völker, B., Collino, R. R., Begley, M. R., McMeeking, R. M. 2014. “Peeling of an Elastic Membrane Tape Adhered to a Substrate by a Uniform Cohesive Traction.” International Journal of Solids and Structures 51 (18). Elsevier Ltd: 3003–11. doi:10.1016/j.ijsolstr.2014.04.001.

Goland M and Reissner E., The Stresses in Cemented Joints, Trans. ASME, Journal of Applied Mechanics, 11, A17-A27, 1944.

Hart-Smith, L J. 1973. “Adhesive-Bonded Single-Lap Joints.” Technical report, National Aeronautics and Space Administration, NASA CR 112236.

Hejazi, S. M., Sheikhzadeh, M., Abtahi, S. M., Zadhoush, A. 2012. “A Simple Review of Soil Reinforcement by Using Natural and Synthetic Fibers.” Construction and Building Materials 30. Elsevier Ltd: 100–116. doi:10.1016/j.conbuildmat.2011.11.045.

Hill, R. C., Bowen, P. A. 1997. “Sustainable Construction: Principles and a Framework for Attainment.” Construction Management and Economics 15 (3): 223–39. doi:10.1080/014461997372971.

Isik, B., Tulbentci, T. 2008. “Sustainable Housing in Island Conditions Using Alker-Gypsum-Stabilized Earth: A Case Study from Northern Cyprus.” Building and Environment 43 (9): 1426–32. doi:10.1016/j.buildenv.2007.06.002.

ISIS Canada. Strengthening reinforced concrete structures with externally-bonded fibre reinforced polymers. ISIS Canada design manual no. 4, Canada. 2001

Islam, M. S., Iwashita, K. 2010. “Earthquake Resistance of Adobe Reinforced by Low Cost Traditional Materials.” Journal of Natural Disaster Science 32 (1): 1–21. doi:10.2328/jnds.32.1.

Johnson, K. L., Kendall, K., Roberts, A. D. 1971. Surface Energy and the Contact of Elastic Solids. Proceedings of the Royal Society A: Mathematical, Physical and Engineering Sciences, 324(1558), 301–313. doi:10.1098/rspa.1971.0141

Kaelble, D. H. 1960. “Theory and Analysis of Peel Adhesion: Bond Stresses and Distributions.” Journal of Rheology 4 (1): 45. doi:10.1122/1.548868.

Kaelble, D. H. 1965. “Peel Adhesion: Micro-Fracture Mechanics of Interfacial Unbonding of Polymers.” Journal of Rheology 9 (2): 135. doi:10.1122/1.549022.

Kafkalidis, M. S., Thouless, M. D. 2002. “The Effects of Geometry and Material Properties on the Fracture of Single Lab-Shear Joints.” Int. J. Solids and Stucts. 39: 4367–83. doi:10.1016/S0020-7683(02)00344-X.

Kendall, K. 1975a. “Thin-Film Peeling - The Elastic Term.” Journal of Physics D: Applied Physics 8: 1449–52. doi:10.1088/0022-3727/8/13/005.

Kendall, K. 1975b. “Transition between Cohesive and Interfacial Failure in a Laminate.” Proceedings of the Royal Society A: Mathematical, Physical and Engineering Sciences 344 (1637): 287–302. doi:10.1098/rspa.1975.0102

Kendall, K. 1994. “Adhesion: Molecules and Mechanics.” Science 263 (5154): 1720–25. doi:10.1126/science.263.5154.1720.

Kim, H., & Kedward, K. T. 2001. Stress Analysis of Adhesively-bonded Joints Under In-plane Shear Loading. The Journal of Adhesion, 76(1), 1–36. doi:10.1080/00218460108029615

Kim, K-S., Aravas, N. 1988. “Elastoplastic Analysis of the Peel Test.” International Journal of Solids and Structures 24 (4): 417–35. doi:10.1016/0020-7683(88)90071-6.

Lee, L. S., Jain, R. 2009. “The Role of FRP Composites in a Sustainable World.” Clean Technologies and Environmental Policy 11 (3): 247–49. doi:10.1007/s10098-009-0253-0.

Kai, L. and Wang, M. 2015. “Seismic Retrofitting of Rural Rammed Earth Buildings Using Externally Bonded Fibers.” Construction and Building Materials 100 (December). Elsevier Ltd: 91–101. doi:10.1016/j.conbuildmat.2015.09.048.

Madsen, B., Hoffmeyer, P., Lilholt, H. 2007. “Hemp Yarn Reinforced Composites - II. Tensile Properties.” Composites Part A: Applied Science and Manufacturing 38 (10): 2204–15. doi:10.1016/j.compositesa.2007.06.002.

Menna, C., Asprone, D., Durante, M., Zinno, A., Balsamo, A., Prota, A. 2015. “Structural Behaviour of Masonry Panels Strengthened with an Innovative Hemp Fibre Composite Grid.” Construction and Building Materials 100. Elsevier Ltd: 111–21. doi:10.1016/j.conbuildmat.2015.09.051.

Micelli, F., Nanni, A. La Tegola, A. "Effects of Conditioning Environment on GFRP Bars," 22nd SAMPE Europe International Conference, CNIT Paris, March 27-29, 2001.

Molinari, A., Ravichandran, G. 2008. “Peeling of Elastic Tapes: Effects of Large Deformations, Pre-Straining, and of a Peel-Zone Model.” The Journal of Adhesion 84 (12): 961–95. doi:10.1080/00218460802576995.

Munikenche Gowda, T., Naidu, A.C.B., Chhaya, R. 1999. “Some Mechanical Properties of Untreated Jute Fabric-Reinforced Polyester Composites.” Composites Part A: Applied Science and Manufacturing 30 (3): 277–84. doi:10.1016/S1359-835X(98)00157-2.

Pesika, N. S., Tian, Y., Zhao, B., Rosenberg, K., Zeng, H., McGuiggan, P., Autumn, K., Israelachvili, J. N. 2007. “Peel-Zone Model of Tape Peeling Based on the Gecko Adhesive System.” The Journal of Adhesion 83 (4): 383–401. doi:10.1080/00218460701282539.

Satyanarayana, K.G., Sukumaran, K., Mukherjee, P.S., Pavithran, C., Pillai, S.G.K. 1990. “Natural Fibre-Polymer Composites.” Cement and Concrete Composites 12 (2): 117–36. doi:10.1016/0958-9465(90)90049-4.

Sauer, R. A. 2011. “The Peeling Behavior of Thin Films with Finite Bending Stiffness and the Implications on Gecko Adhesion.” The Journal of Adhesion 87 (7–8): 624–43. doi:10.1080/00218464.2011.596084.

Sen, T., Jagannatha Reddy, H.N. 2013. “Strengthening of RC Beams in Flexure Using Natural Jute Fibre Textile Reinforced Composite System and Its Comparative Study with CFRP and GFRP Strengthening Systems.” International Journal of Sustainable Built Environment 2 (1): 41–55. doi:10.1016/j.ijsbe.2013.11.001.

Shah, A.N., Lakkad, S.C. 1981. “Mechanical Properties of Jute-Reinforced Plastics.” Fibre Science and Technology 15 (1): 41–46. doi:10.1016/0015-0568(81)90030-0.

Shehata, E., Morphy, R., Rizkalla, S. 2000. “Fibre Reinforced Polymer Shear Reinforcement for Concrete Members: Behaviour and Design Guidelines.” Canadian Journal of Civil Engineering 27 (5): 859–72. doi:10.1139/l00-004.

Spies, G.J. 1953. “The Peeling Test on Redux-bonded Joints.” Aircraft Engineering and Aerospace Technology 25 (3): 64–70. doi:10.1108/eb032268.

Sreenath, H. K., Shah, A. B., Yang, V. W., Gharia, M. M., Jeffries, T. W. (1996). Enzymatic polishing of jute/cotton blended fabrics. Journal of Fermentation and Bioengineering, 81(1), 18–20. doi:10.1016/0922-338X(96)83113-8

Volkersen, O., "Die Niektraftverteilung in Zugbeanspruchten mit Konstanten Laschenquerschritten," Luftfahrtforschung, 15:41-47, 1938.

Williams, J. G. (1997). Energy release rates for the peeling of flexible membranes and the analysis of blister tests. International Journal of Fracture, 87(3), 265–288. doi:10.1023/A:1007314720152

Williams, J. A., Kauzlarich, J. J. 2005. “The Influence of Peel Angle on the Mechanics of Peeling Flexible Adherends with Arbitrary Load–extension Characteristics.” Tribology International 38 (11–12): 951–58. doi:10.1016/j.triboint.2005.07.024.

Yang, Q. D., Thouless, M. D. 2001. “Mixed-Mode Fracture Analyses of Plastically-Deforming Adhesive Joints.” International Journal of Fracture 110 (2): 175–87. doi:10.1023/A:1010869706996.

Chapter 4
Case study: Earth arch structures

In the recent years, the practice of strengthening masonry structures with Fiber Reinforced Composites (FRCs) has become very common. The reinforced masonry provides a different collapse mechanism with respect to the unreinforced one. Indeed, the unreinforced masonry collapses for the activation of mechanisms due to the negligible tensile strength. On the contrary, reinforced masonry structures collapse for the activation of different failure modes as opening of cracks for tensile stresses, masonry crushing, shear failure of the masonry, sliding, failure of the reinforcement, rupture of the fabric and debonding or peeling of the reinforcement sheets (Briccoli Bati and Rovero, 2007; Briccoli Bati et al., 2013; Foraboschi, 2004). The delamination of the reinforcement sheet in masonry reinforced with CFRP plays fundamental role in the overall behaviour of the structure and arched structures are commonly used to assess the effectiveness of a fiber reinforcement system of masonry structures by experimental investigations.

The arch is a fundamental architectural element; thanks its load-bearing and ornamental functions it represents the most interesting “invention” to span a void with a no-tension material. The equilibrium is achieved through the geometry (Huerta 2001; Block et al., 2006). The arch structure is easily reproducible in the laboratory overcoming problems of scale effect. The experimental work presented in this chapter was designed to attain knowledge about the effectiveness of the reinforcement system made with jute fabric and earth matrix.

Through load tests on arch structures reinforced at the intrados and extrados, we can evaluate at the same time, different conditions in which the reinforcement package works and we can assess the behaviour of the strengthening solution in different situations. Starting from the awareness that the earthen structures can be consider masonry constructions (that is material with good compression strength, weak in tension and not incline to slide) we can adopt the same theories used to assess the latter ones. The choice to build rammed earth arches instead of adobe arches, as normally happen, has a purely speculative nature. The aim is to build a structure as close as possible to a continuous material structure, without weak joints between different materials.

4.1 Static theories of the arch

The Romans used systematically arch structures because of its intuitive static behaviour. Vitruvio, identified the main characteristics of the arch in the books De Architectura and discussed about the presence of the thrust of the vault on the supports. The theory and the

practice of construction were reported in his books, suggesting that strong and massive supports should be realized in order to contrast the thrust of the arches and vaults.
In the Middle-Age, more refined theories were developed, characterized by the approximation of the arch shape by the thrusts line, and some geometrical rules were given to determine the piers thickness. Leon Battista Alberti in the 13th century presented in the De Re Aedificatoria the motivations about the use of arched structures in order to increase both the bearing capacity and the span covered. This theory was the only respected during the Renaissance. Leonardo Da Vinci (1452 - 1519) through his ideas and intuitions inspired theories of three centuries later.

> *"Arco non è altro che una fortezza causata da due debolezze, imperocchè l'arco negli edifizi è composto di due quarti di circulo, i quali quarti circuli, ciascuno debolissimo per sé desidera cadere, e opponendosi alla ruina l'uno dell'altro, le due debolezze si convertano in unica fortezza (…) l'arco non si romperà se la corda dell'archi di fori non toccherà l'arco di dentro".*

LEONARDO DA VINCI (Roberto Marcolongo, Studi Vinciani, VII, pp. 237-239, Napoli, 1937)

During the centuries, many studies were proposed on the more appropriate shape of the arch, but only in the 17th century a static theory of the arch was developed.
The first important masonry arch studies were performed by applying the technique of the funicular polygon by Hooke (1635-1733) and Poleni (1683-1761) who recognized the analogy between the arch and the inverted catenary.
Between the seventeenth and eighteenth century, the geometric and the empiric rules reported in the ancient treatises were replaced by a real static theory on the stability of the arches.
The first significant model regarding the collapse approach is attributed to Philippe De La Hire (1670-1718). In the Traitè De Mécanique (1695), De La Hire highlighted the wedge mechanism of the arch. This model was the first approach in the static theory to the collapse analysis of the masonry arch, modeled as a system of rigid voussoirs geometrically defined under their own weight.
The Académie Royale des Sciences published in 1731 and 1732 "De la poussé des voutes" and Seconde partie de l'éxamen de la poussé des voutes" written in 1729 by Claude Antoine Couplet (1642 1722). Here Couplet face the problem of friction among voussoirs that had been neglected by De La Hire and was later faced by Coulomb in the 1773. Coulomb enumerated the possible failure mechanisms of the arch.
In the 1785, Mascheroni considered two distinct mechanisms, the first of which had already been examined by La Hire and a second mechanism characterized by the formation of intrados cracks at key, of extrados cracks at springers and of intrados cracks at piers

extremities. In his book *"la scienza delle costruzioni e il suo sviluppo storico"* Edoardo Benvenuto quotes also the studies of the mathematician Leonardo Salimbeni "*Degli archi e delle volte"* (1787) and the historical essay on the equilibrium theories on vaulted structures written by J. V. Poncelet (1788-1867).

Early method characterized by a collapse analysis was developed by Mery in the 1840. The applicability of this method is linked to the hypothesis of symmetric semicircular shape loaded symmetrically, made with homogeneous material and characterized by constant thickness, and it is applicable only if the assumed collapse mechanism occurs.

Once determined the loads acting on the blocks, the resultant is determined and the thrust line can be obtained applying the parallelogram rule. In the 1833, Moseley enounced *the principle of least pressure* and applying this principle to arch structures he established that the actual thrust must be the minimum.

In the 1835, Moseley expressed rigorously the concept of the dependence of the form of line of thrust on the geometry of the arch (Huerta, 2001).

Mery and Moseley transformed the thrust line into an eloquent tool for representing the stability condition of the arch. Winkler in 1879 applied the elastic approach to masonry arch analysis and suggested to control the position of the line of thrust positioning internal hinges during the construction. The attempts to adapt the elastic theory to the masonry arch were not very successful. The turning point ~~of~~ was the introduction of the theorems of limit analysis which proved to suit or to be appropriate to determine of the collapse load of masonry arches.

Pippard and Ashby determined in1939 the load required to cause a mechanism in a two-hinged arch. These procedures guaranteed that an equilibrium configuration exists for the considered structural model. (Pippard and Chitty, 1951)

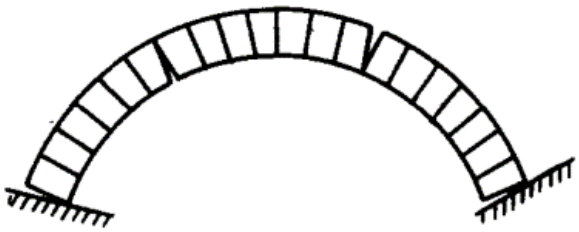

Figure 4.1 - Collaps of voussoir arch after Pippard and Baker (Heyman 1966)

In 1952, Kooharian applied to the voussoir arches the limit analysis already pointed out for the elasto-plastic structures.

According to the collapse approach, in the 1966 Heyman explained for the first time the applicability of ultimate load theory for any masonry load-bearing structure. He described the application of limit principles, derived from the plastic analysis of steel structures, to the

masonry arch. He formalizes clearly the hypotheses on the material which formed the basis for the calculation of the arches. These assumptions enabled Heyman to formulate the safe theorem (Heyman 1966; Heyman 1969; Heyman 1982).

4.1.1 Limit Analysis

The limit analysis allows to directly assess the ultimate bearing capacity of a structure, or the ultimate limit state, which is the last stage of the elastic plastic incremental analysis or the plastic collapse, considering the structure only in relation to its ultimate state, using few material parameters and neglecting the initial stress state.
The collapse multiplier is neither dependent on any constraint states nor on the stiffness of the structural elements therefore provides a much more reliable and synthetic assessment of the safety degree of a structure than the analysis in the elastic range. The value of the collapse multiplier is independent on the load history and the presence of failures, residual stresses and states of constraint. The limit Analysis was born in the fifties from the Plastic theory (Kooharian, 1953; Livesley, 1978) and subsequently proposed to analyze masonry arches behaviour by demonstrating that the safe theorem of plasticity can be applied to curved masonry structures through assumptions clearly expressed by Jaques Heyman (1966-1982).
In *"The Masonry Arches"* Heyman (1982) enounced the safe theorem of the limit analysis particularized to the masonry arches. The first hypothesis is that masonry is a no tension material. This assumption is true for masonry made by dry-stone blocks or joint using weak mortar, it does not respect always the reality but it represents a safety benefit. Frequently the adhesion between mortar and masonry blocks is negligible because of mortar decay.
The second assumption is the masonry infinite compression strength. With the hypothesis of infinite compression strength, it is accepted that, in general, bending is the only force capable of producing the collapse of the structure by producing a mechanism for activation.
The third hypothesis states that the sliding failure does not occur. Friction between the voussoirs is sufficient to prevent from losing cohesion and sliding. This implies that the shear stress component exerted between two contiguous voussoirs does not exceed the friction resistance between. Starting from these three assumptions, Coulomb first proposed as the only possible failure mechanism, the formation of opening hinges for relative rotation of the rigid blocks, and Kooharian demonstrated the applicability of the limit analysis theorems to the arched structures. The safe theorem of limit analysis remedying the uncertainty connected to the determination of the true line of thrust among infinite possibilities. It is impossible to know the actual line of thrust, but this is unimportant, as we can calculate the safety of the structure without making assumptions about its actual state (Huerta 2001). The thrust line must be drawn within the arch boundaries. It is necessary to determine at least

one line of thrusts contained inside the thickness of the arch to ensure that the structure is safe. On the other hand, it is sufficient a small variation in the position of the line of thrust, i. e. caused by loading increase, to allow the formation of localized cracks.

As consequence, a kinematical mechanism can activate with the progressive formation of hinges corresponding to the points where the thrust line is tangent to the intrados or extrados of the arch. In particular, the crisis is connected with the formation of the fourth hinge that produces an instability failure (O'Dwyer 1999). The four hinges open in alternating configuration at the intrados and extrados, following a path in function of the arch shape and the load conditions. The upper and the lower limits can be fixed.

Fundamental theorems of plastic analysis:

- Upper bound theorem or Kinematic theorem.

For any arbitrarily assumed mechanism, the corresponding load multiplier λ will always be greater or equal to the limit value λ_c corresponding to the actual collapse mechanism

- Lower bound theorem or Static theorem.

Defined a distribution of bending moments which does not exceed the value of the plastic moment in any section and is in equilibrium with the external loads in correspondence of a load factor λ, then the multiplier must be less than or at most equal to the true value of the collapse load factor or the collapse load λ_c.

- Uniqueness theorem.

One and only one collapse load λ_c exists.

Regarding masonry arches, it is possible to apply the theorems of plastic limit analysis if it is possible to find a system of forces which is in equilibrium with the loads on the structure and which is contained within the masonry envelope. Once any system of forces can be found which lies within the structure and which is in equilibrium with the external loads acting on the structure then the structure is safe.

4.2 Reinforced arch

The seismic vulnerability of unreinforced masonry arches increased the interest of the scientific community towards new retrofitting and strengthening solutions to improve their load bearing capacity and ductility.

Scientific literature reports experimental results on the structural capacity of arches and vaults strengthened by FRCs (Fiber Reinforced Composites) strips (Alecci et al., 2016; Borri et al., 2009; Briccoli Bati and Rovero, 2007; Briccoli Bati, et al., 2011; Oliveira, et al., 2010). Unreinforced masonry arches generally collapse predominantly by the opening of four hinges. Usually, the crack pattern of masonry arches is characterized by extremely localized damages producing structural hinges and, as we know, if the number of three hinges is exceeded a failure mechanism occurs. The presence of reinforcement sheets, bonded at the intrados or extrados surface of vaulted structures, modifies their collapse mechanism, and consequently increases the corresponding load carrying capacity e ductility. The fundamental aspect characterizing masonry structures strengthened with fiber reinforcement strips is the capacity that they acquire to bear tensile stresses. Therefore, the structural behaviour of reinforced arches under load~~ing~~ becomes completely different from that of unreinforced ones. Indeed, the presence of the reinforcement changes both the value of the collapse load and the corresponding failure mechanism. Foraboschi (2004), Valluzzi et al. (2001), Borri et al. (2009), Briccoli Bati and Rovero (2007), Oliveira et al. (2010) among others, identify in the FRP debonding from the masonry, in the masonry compressive failure and in the shear failure (sliding along the mortar joints) the most common failure modes of arches strengthened with FRP. Delamination from curved support produces a mixed-mode interfacial fracture. De Lorenzis and Zavarise (2010), Milani et al. (2009a), Milani et al., (2009b), Borri et al. (2011) show how the FRP plates with anchor spikes may overcome problems of intrados delamination.

In the research work conducted by De Lorenzis, et al. (2007), strengthening through FRPs at the intrados is proved to be able to reduce the minimum lateral abutment thrust of arches and vaults. Recently externally bonded fiber reinforced cementitious matrix (FRCM) materials have been proposed in the field of structure strengthening masonry (Prota et al., 2006; Papanicolaou et al., 2007; Briccoli Bati, 2001). Also in this regard, the key issue is the bond between the strengthening and the support.

4.3 Experimental program on segmental arch models

The experimental investigation was carried out at the Official Laboratory for Testing of Materials and Structures of University of Florence. Three half-scaled arches models were designed, with skew back angles of 30 degrees, 150cm span and characterized by 86.7 cm internal radius, 15cm width and 15cm thickness as illustrated in the figure 3. The construction technique adopted was pisè technique (already described in chapter 1) and earth material already characterized in the chapter 2 was employed. In particular, the earth taken from Seggiano, Monte Amiata (GR), the properties of which are reported in table 1.

	h mm	A mm^2	P N	σ_c MPa	E MPa	μ_c
A.V.	78.35	6022.93	12841.75	2.13	88.62	1.28
St. dev.	0.69	58.13	1375.49	0.22	32.14	0.08
C.V %	0.88	0.96	10.71	10.21	36.26	6.49

Table 4.1. Average values of the mechanical parameters determined by uniaxial compression test on "Seggiano2" earth specimens (Chapter 2).

All arches were built in the exact position in which they would have been tested, under the testing frame, on two rigid triangles fixed to the steel beam as supports. The use of scaled models to represent reality usually requires the adoption of certain similarity laws, selected taking into account the principal scope of the investigation and the forces related with the phenomenon under analysis.

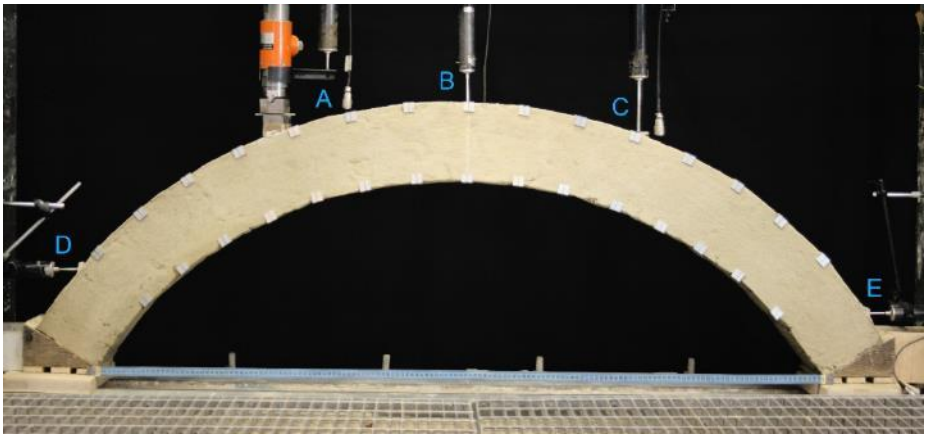

Figure 4.2 Unreinforced arch2 with transducer positions

These similarities usually have important consequences on the test setup because it is necessary to add mass to the scale model in order to fulfill the specific mass scale.
However, the purpose of this experimental work is not to perform a study on the collapse mechanism of rammed earth arches, but to achieve more information about the composites used as reinforcement. Moreover, the realized arches do not represent any existing structures, in fact arches are not a traditional element of pisé architecture. Only, attention has been paid to select the particle size so that it was not larger than 1/7 times the width of the arch.
Due to the particular shape of the formwork, the models were manually built. For this reason, it was possible to build a limited number of models and some difficulties were met in the control of initial constraints. Moreover, the arch models could not be built in series out to the steel frame, as it was not possible to move them; so they were realized directly into the test position. The arches were subjected to vertical asymmetric point load at one quarter span up to incipient collapse. Vertical displacement was applied in order to describe also the softening branch of the load path, with a device made of a screw jack controlled through a flywheel.

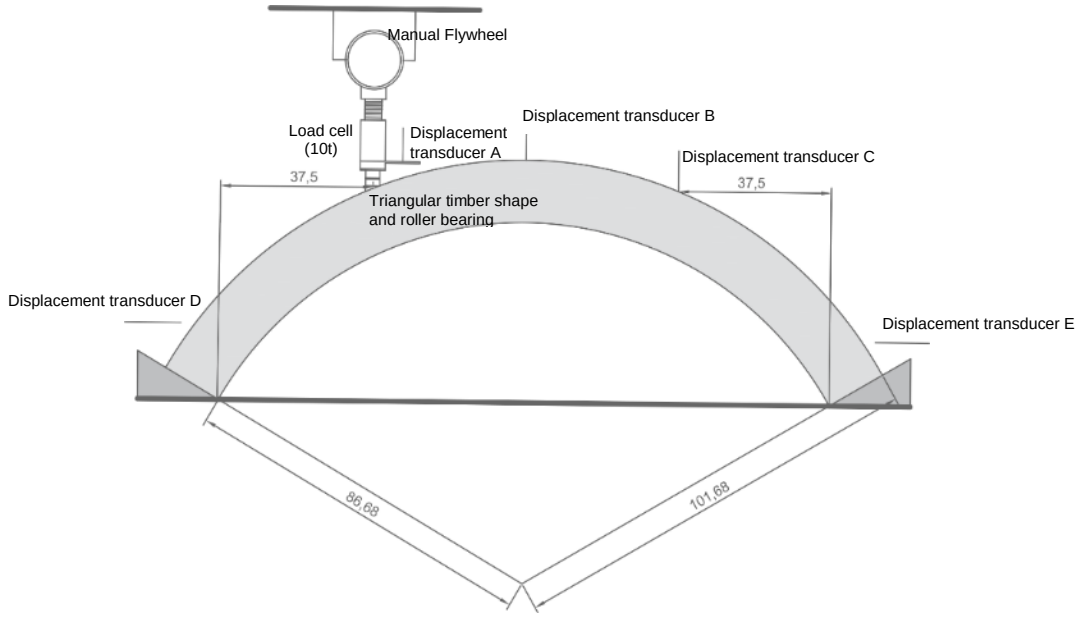

Figure 4.3 - Testing arch set up

The force was measured through a load cell with a capacity of 10t (tension/compression load cell). The arches deformation was monitored by five displacement transducers positioned in relevant locations as shown in figures 3 and 4: two displacement transducers

at the abutments with range of ±50mm (D and E) to register horizontal displacements; one near the key of the arch with a range of ±50mm (B); one in correspondence of the application point of the load and one symmetrically to it, both of them with a range of ±100mm (A and C). The last three displacement transducers were oriented to record vertical displacements. The transducers and the load cell were connected to a computer through an electronic control unit of recorded data, displaying the load–displacement curve. Tests were stopped previously to the occurrence of uncontrolled failure. Successively the aches were strengthened with the eco-compatible reinforcement previously pointed out and were tested again with the same testing set up. During each test, visual inspection was carried out in order to individuate the succession of hinges formation, cracking patterns, and debonding phenomena.

The strengthening composed by jute fabric was applied on the whole arches extrados and intrados on the arch width. The matrix was prepared according to the percentages used in the chapter 3 for the adhesion tests. The substrate surfaces were accurately moistened subsequently a first layer of matrix was manually applied and the jute textile was positioned on the first matrix layer; then a second matrix layer was applied over the fabric reaching a final thickness of about 1-1.5mm. The strengthening was always made of two equal strips of about 33/34 yarns for each arch, the different number of wires applied at the intrados and extrados is caused by the major difficulties in the application of the strip at the intrados with consequent loss of yarns.

Figure 4.4 – Reinforcement application

The experimental campaign includes seven tests, three on unreinforced arches and four on reinforced structures. Indeed, as it can be seen in what follows, the third reinforced arch was tested two times with different reinforcement configurations. In order to face the problem of the detachment of the fabric from the substrate at the intrados it was decided to use jute strips anchors of 15cm width. The four strips of 15cm width were bonded perpendicular to the direction of the reinforcement in the load proximity as to wrap the arch for a length 40cm.

Experimental tests:

ARCH1

Test I_ asymmetric point load on unreinforced Arch1 (UA1)

Test II_ asymmetric point load on reinforced Arch1 (RA1)

ARCH2

Test I_ asymmetric point load on unreinforced Arch2 (UA2)

Test II_ asymmetric point load on reinforced Arch2 (RA2)

ARCH3

Test I_ asymmetric point load on unreinforced Arch3 (UA3)

Test II_ asymmetric point load on reinforced Arch3 (RA3)

Test III_ asymmetric point load on reinforced Arch3 with anchor (AA3)

4.3.1 "Centering – Formwork" design

The stability condition of the arch is achieved by the joint action of its own weight and the vertical loads, which consolidate various parts, favoring mutual support. The arch structure "becomes" self-supporting only when the keystone is placed. During realization, it needs a temporary structure for the support able to discharge its weight gradually increasing on resistant elements. For this reason, a scaffolding was necessary to build the rammed earth

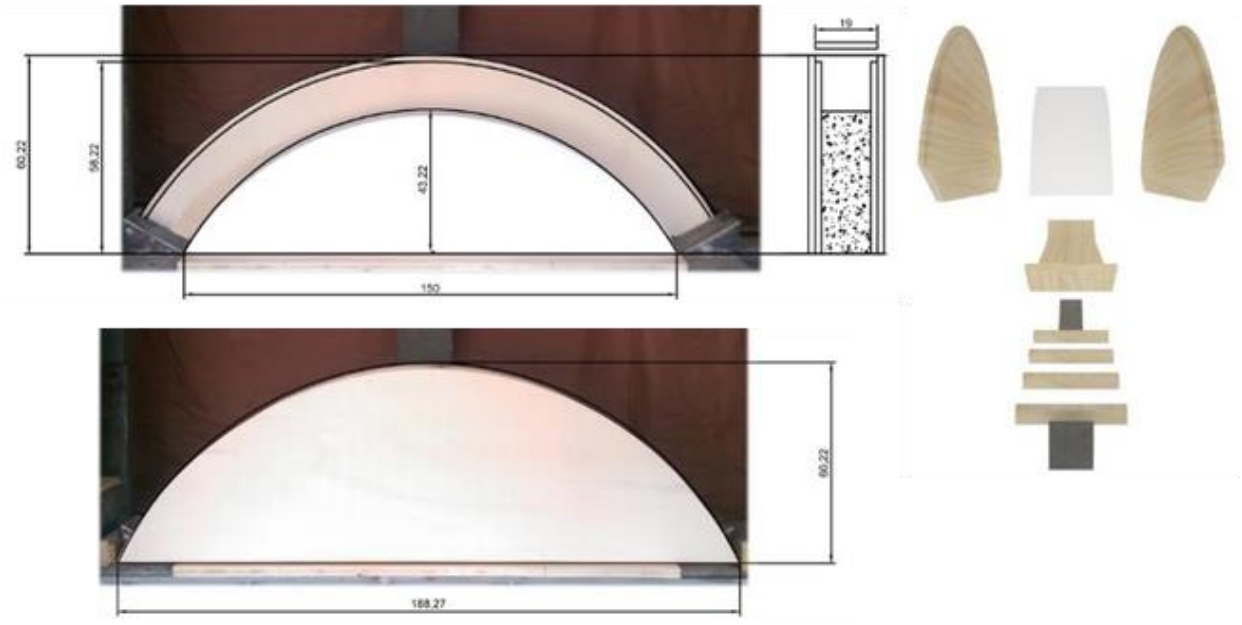

Figure 4.5 – "Centering-formwork"

arch models that, besides acting as temporary support, had the characteristics of a "centering-formwork". Building arches with rammed earth needs some forward planning.
The construction must proceed simultaneously as much as possible from both sides to avoid eccentric loads on the "centering-formwork" and to better distribute the effects of shrinkage. From the need to combine the support function of the centering and the containing function of the formwork the idea was born of a timber enclosure capable of confining the earth material until it has reached enough solidity.
The “centering-formwork” was composed by a 150cm long and 15cm wide board base connected at the ends to two rectangular wooden elements which, once anchored to steel supports, will constitute the supports with skew back angles equal to 30°respect to the horizontal beam of the steel test frame where the structure will be built. The true centering was a polystyrene removable circular segment of 15cm thick with span of 150cm and a rise of 43.2cm, cut to the shape of the intrados of the arch. Two circular segment plywood sides containing the centering but with a 15cm larger radius were cut to the shape of the curve. These ply faces are characterized by two guides situated on the arc edge inner side, which allow controlling the shape of the extrados during the ramming process by sliding specially sized wood elements 10x15x2cm.
The centering - formwork thus constituted is anchored to the steel triangular supports 150cm away from each other, resting on the wooden battens previously placed on the steel frame beam which, once removed, allow the lowering of the centering in the dismantle.

4.3.2 Realization

Each scale model was built using approximately 96kg of raw earth, sieved with sieve ASTM 8mm, and 11% of water on the dry weight of the earth, that is sufficient to allow a good workability and ensures a good strength. It has been calculated that the residual humidity after 30 days of curing is about 2%.
Ramming has been performed by successive layers of about 5cm parallel to the cross section of the arch up to approximately 20cm from the key where the layers have been rammed parallel to the ground.

Figure 4.6 – Key of the arch

When typing has been completed and stability has been achieved the arches were disarmed. The arches showed a significant shrinkage after 30 days of curing, and two intrados hinges formed at the supports except in the third case as shown in the pictures 7, 8 and 9.

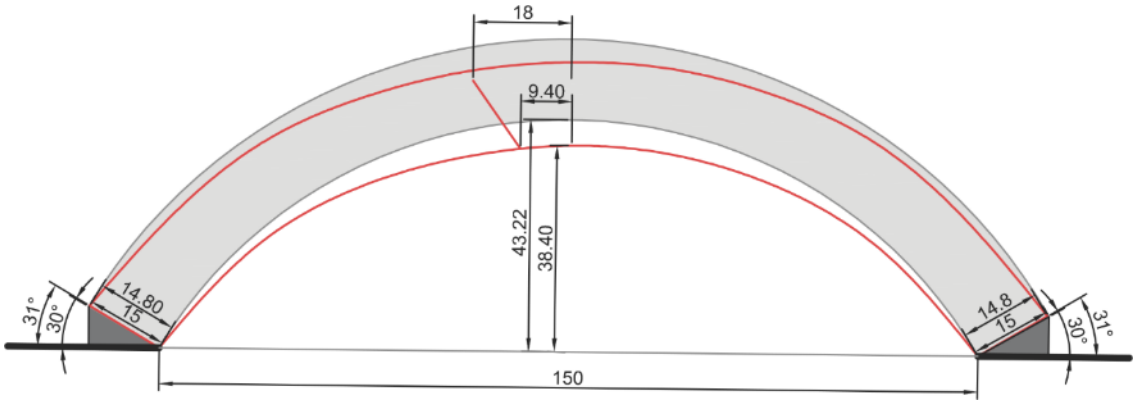

Figure 4.7- Arch1 after curing (red) and original shape (grey)

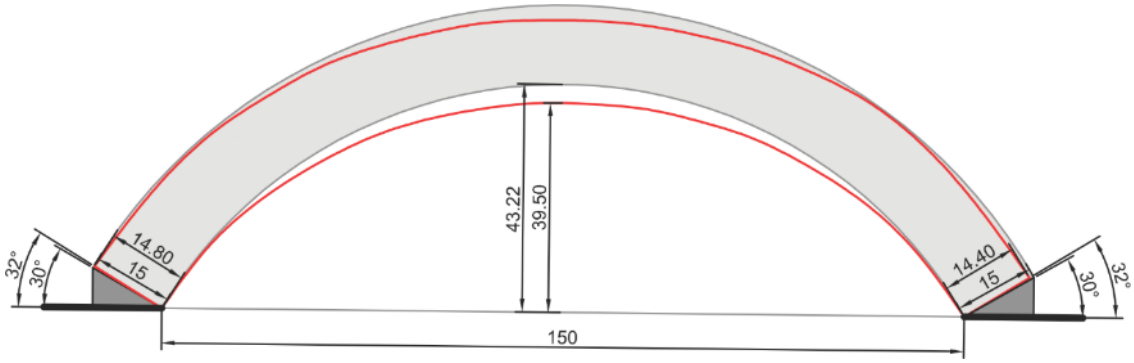

Figure 4.8 - Arch2 after curing (red) and original shape (grey)

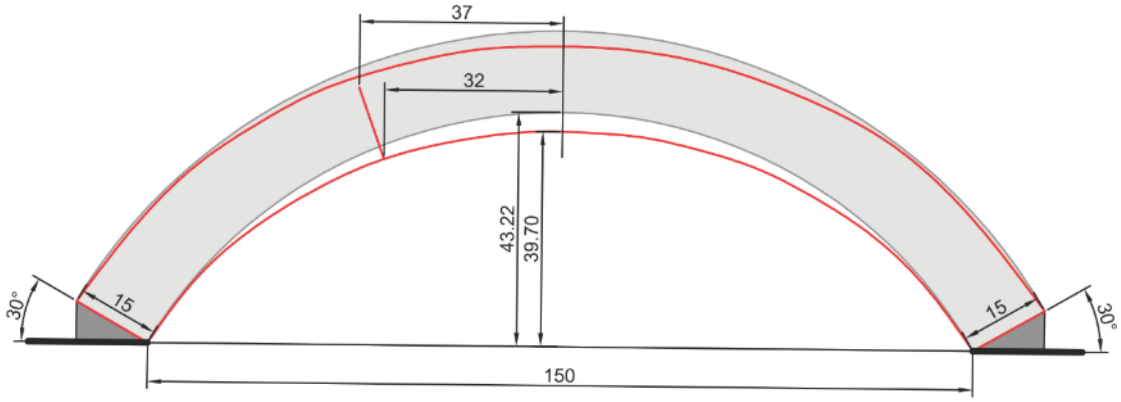

Figure 4.9- Arch3 after curing (red) and original shape (grey)

The third arch underwent a lower shrinkage than the others and the geometry was almost close to the initial one. In this case, there were not visible hinges at the supports, but a fracture at 32cm to the key (intrados) was evident. The same happened in the first arch at

the distance of 9.40cm from the key (intrados). There are many factors which influence the formation of fractures during curing phase, as the compaction energy that cannot be controlled, the stratification, the presence of defects and the air moisture and temperature that influence the shrinkage velocity and the consequent formation of fractures. The upper bound theorem and the lower bound theorem of limit analysis were applied in the design phase in order to predict the experimental results of the tests on unreinforced arches (Figures 10-11).

The calculated loads λ are respectively equal to 1307.70N as upper bound and about 1300N as lower bound considering the initial geometry and a specific weight equal to 0.00217kg/cm^3. The same analyses performed with the average geometry of the three arches after 30 days of curing restituted a load of about 1108N as an upper bound and 1070N as a lower bound.

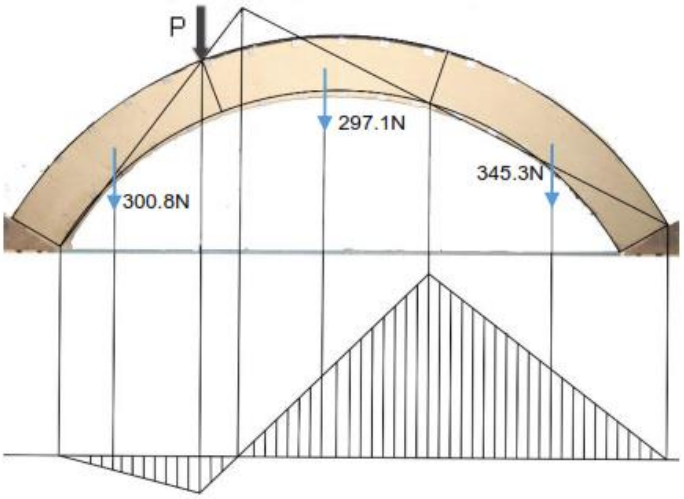

Figure 4.10-Limit analysis (Upper bond theorem)

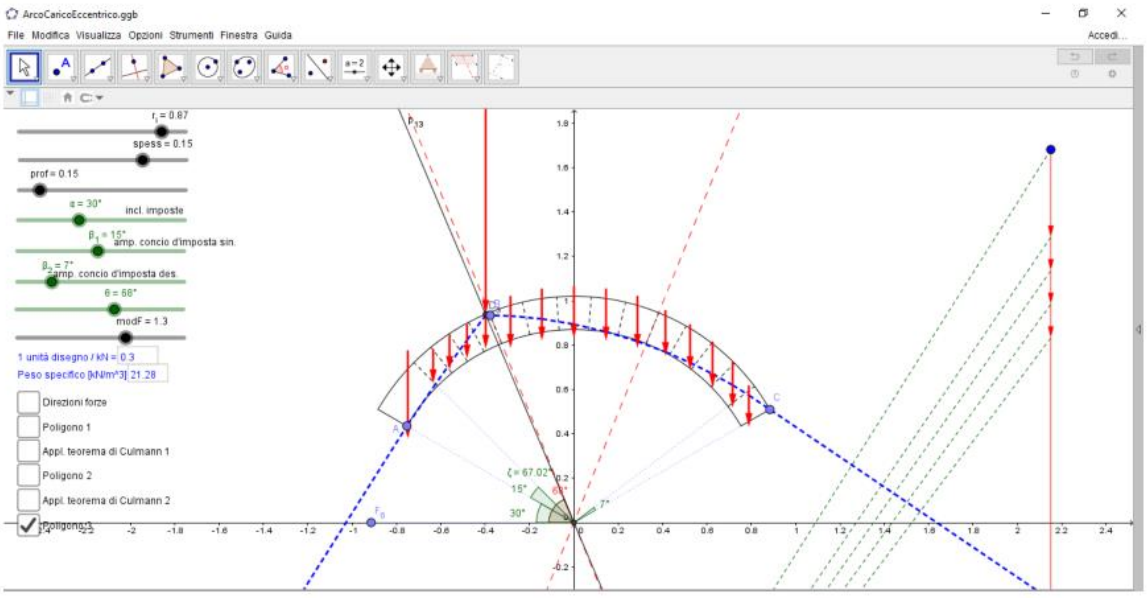

Figure 4.11- Limit analysis (Lower bond theorem performed using a program developed by Prof. M. Fagone).

4.4. Experimental results and data sheets

In the following the results are reported and discussed of the tests on the behaviour of rammed earth arches, with and without jute strengthening arrangements, carried out at University of Florence.

The tests were carried out on three unreinforced and reinforced half-scaled models subjected to an increasing vertical displacement applied at the quarter span and up to incipient collapse as previously described. This experimental work was designed aiming at understanding and clarifying the effect of the jute reinforcement system on the structural behaviour of the arches at both local and global levels.

***Objectives**:*

- Contribution to the establishment of a database on the experimental behaviour of jute strengthening applied on earth curved support, useful for future calibration of both analytical and numerical tools.
- Characterization of the structural behaviour of unreinforced and reinforced earth arches loaded, including softening regime.
- Assessment of the efficiency of the compatible strengthening strategy on the mechanical behaviour and failure mechanisms in terms of load capacity, ductility, and failure modes.

The choice of organize the tests description in chronological order is not casual. Indeed, we are not aware of literature references regarding experimental campaigns on rammed earth arches performed with the same dimensions and set-up. All the tests have been used to interpret and eventually modify the subsequent one simply paying attention to phenomena previously neglected, but fundamental in our case. Data sheets include load displacement curves corresponding to the five transducers A, B, C, D, E with markers that highlight the main phenomena. In the photo-sequence on the right of the sheets the transducers position is reported and the numbers represent the damage phenomena the position of which is reported in the photo and the corresponding equilibrium point is reported in the load path. The events are described in the text.

4.4.1 UA1 - RA1

UA1	
Start of realization	15-12-2015
End of realization	30-12-2015
Disarm	5-12-2015
Total dry weight soil (kg)	97
Total water (l)	10.78
Specific weight of the arch (kg/cm^3)	0.00217
Test data	
Test date	2-03-2016
Maximum Load (N)	885.67

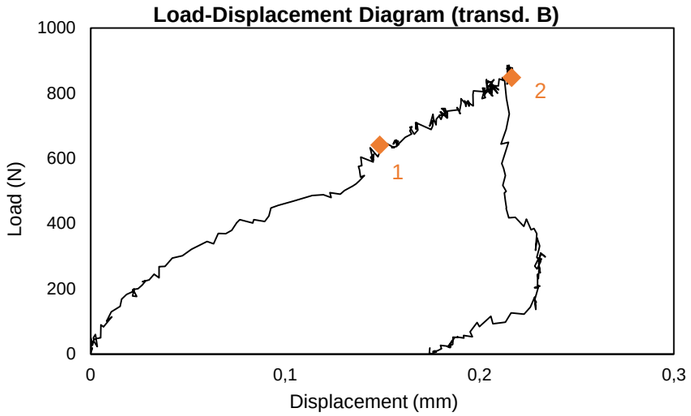

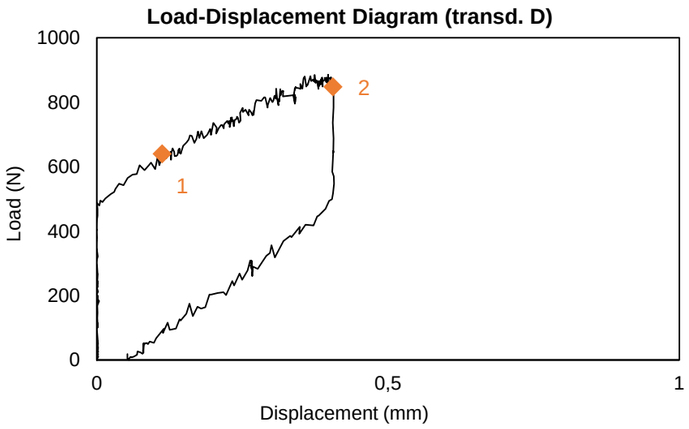

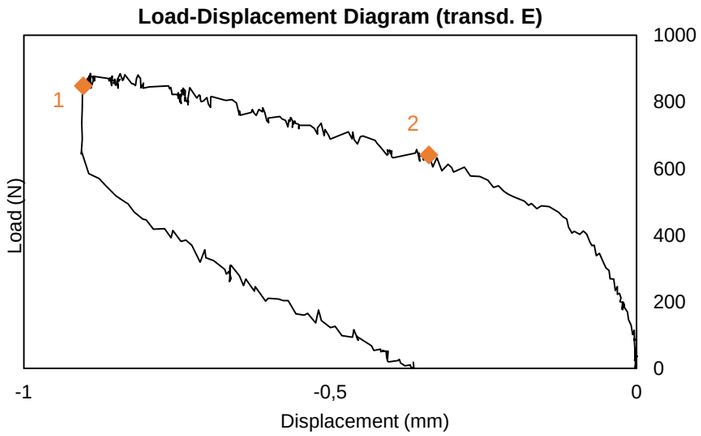

At the beginning of the load test two hinges at the supports had formed at the end of curing, both of them at the intrados.

The maximum load reached during the asymmetric load test was 885.67N evidently lower than the load factor calculated using the Lower Bound Theorem.

This happened because the test was stopped after the formation of hinge 2 approximately corresponding to 1.76mm of displacement (transd. A) and 848N of load, not considering that the hinge at the right support was still "moving" towards extrados of the arch.

The four alternating hinges mechanism was not activated. This consideration is very important for the successive tests on unreinforced arches

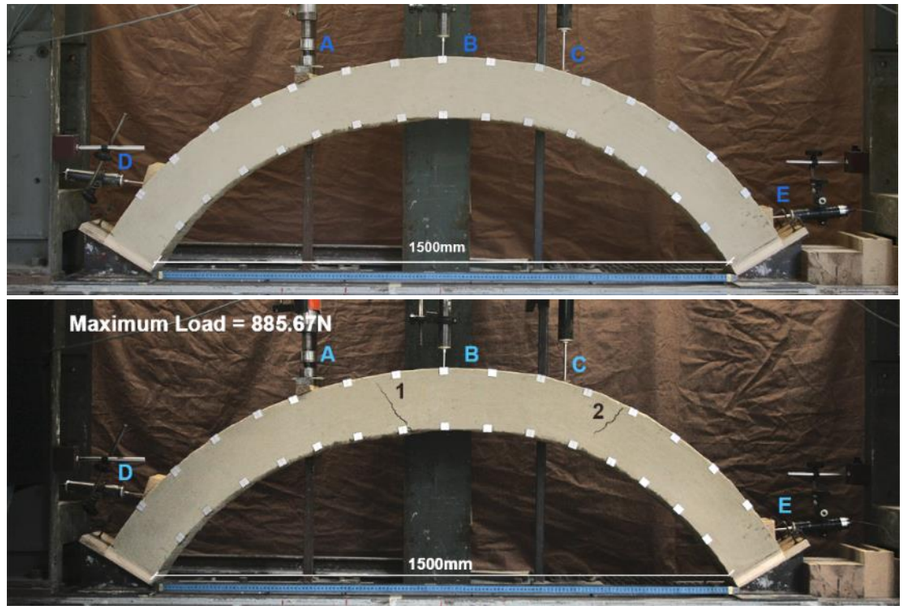

Crack pattern of unreinforced arch model after asymmetric point load test (02-03-2016)

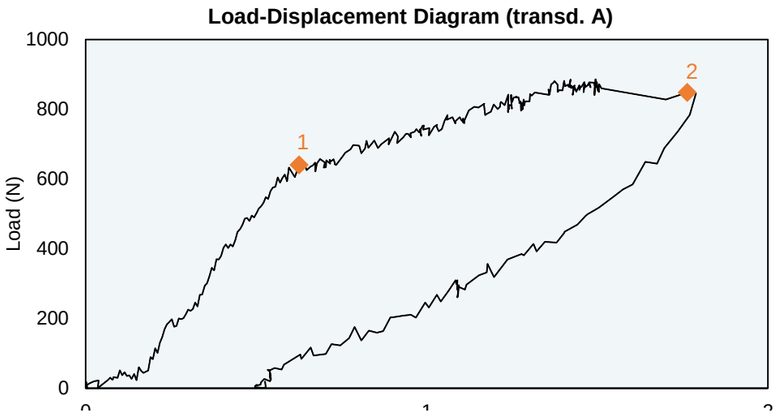

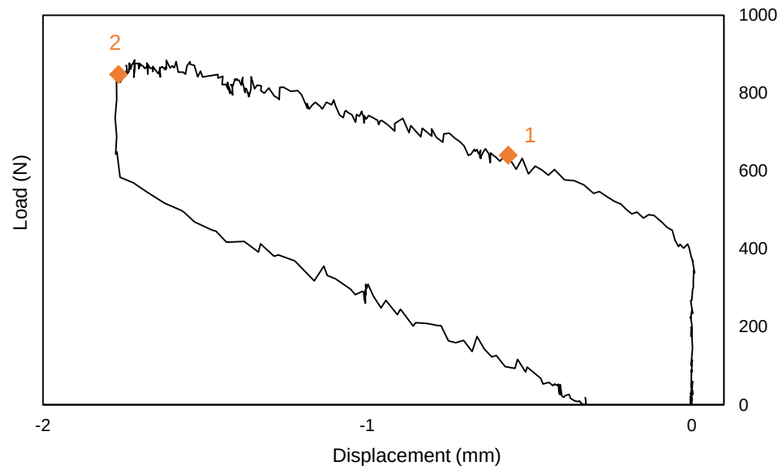

RA1	
Start of realization	15-12-2015
End of realization	30-12-2015
Disarm	5-12-2015
Total dry weight soil (kg)	97
Total water (l)	10.78
Specific weight of the arch (kg/cm^3)	0.00217
Reinforcement	
Date of reinforcement application	4-03-2016
Number of wires at the intrados	32
Number of wires at the extrados	34
Average spacing between wires (mm)	4.292
Test data	
Test date	8-03-2016
Maximum Load (N)	2594.8

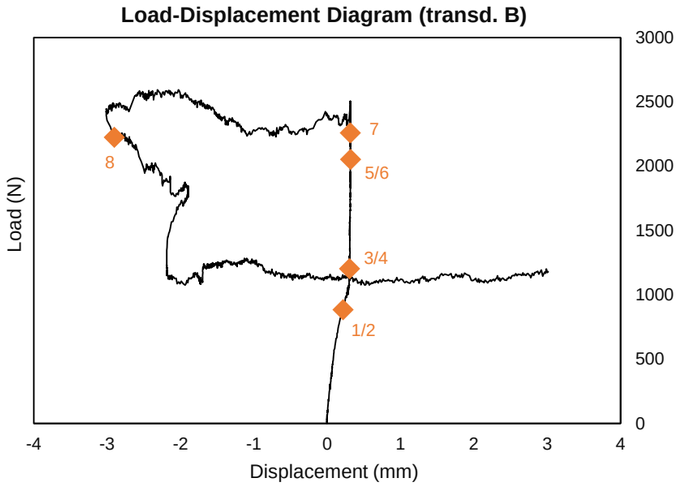

In the photo-sequence and in the load displacement curves the numbers, which identify different phenomena occurred are reported:

1/2_Fractures reopening corresponding to the hinges of the previous test

3_Crack development that lead to the formation of a hinge located on the boundary of the load cross section and debonding at the intrados

4_Hinges at the supports become evident (intrados at the left support and extrados at the right support)

5-9_Fractures

10 Fabric rupture at the extrados

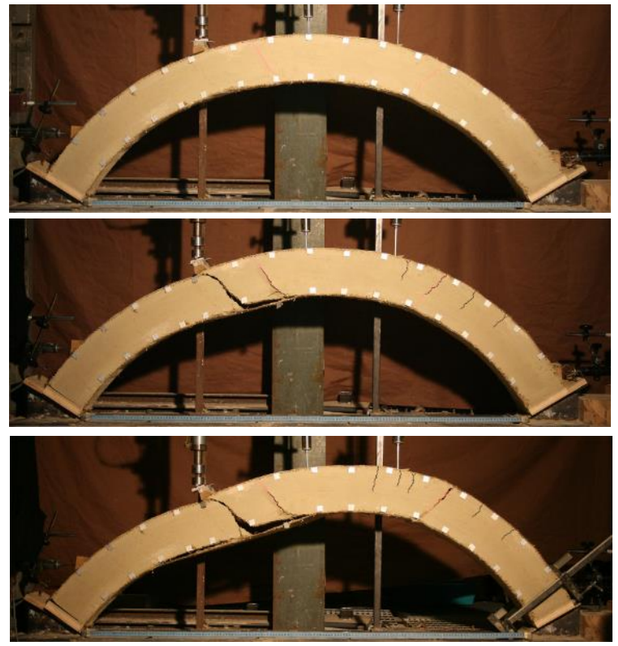

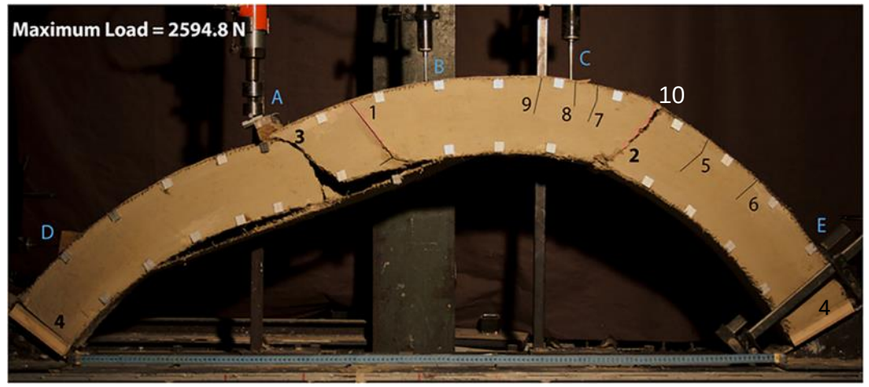

Crack pattern of reinforced arch model after asymmetric point load test (04-03-2016)

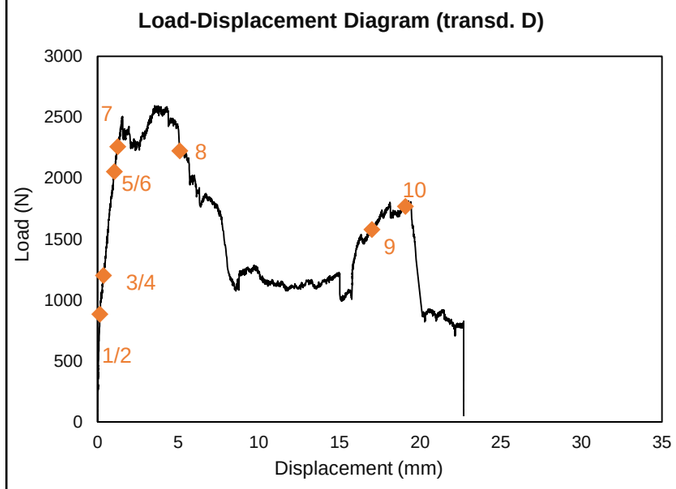

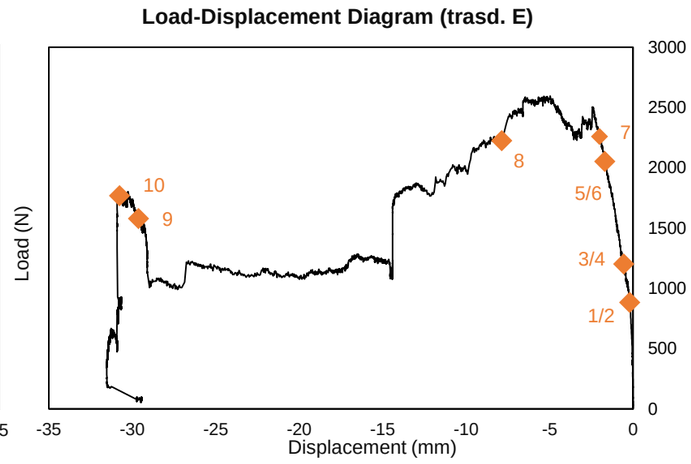

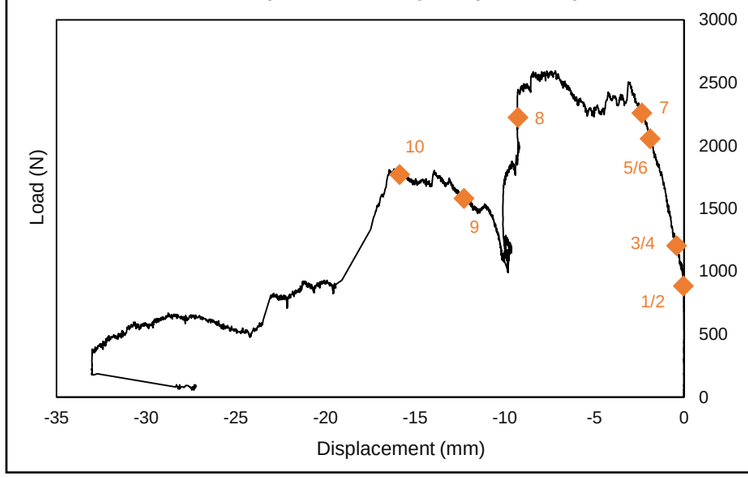

This test was affected to the sliding of the right support as we can note in the diagrams. Referring to the load-displacement curves obtained from the transducer A and E, the plateau in the graphs generated from the sliding is evident (from 20mm to 40mm of vertical displacement and from 15mm to 30mm of horizontal displacement).

The transducer C stopped recording at about 33mm of vertical displacement due to a sliding of the piston.

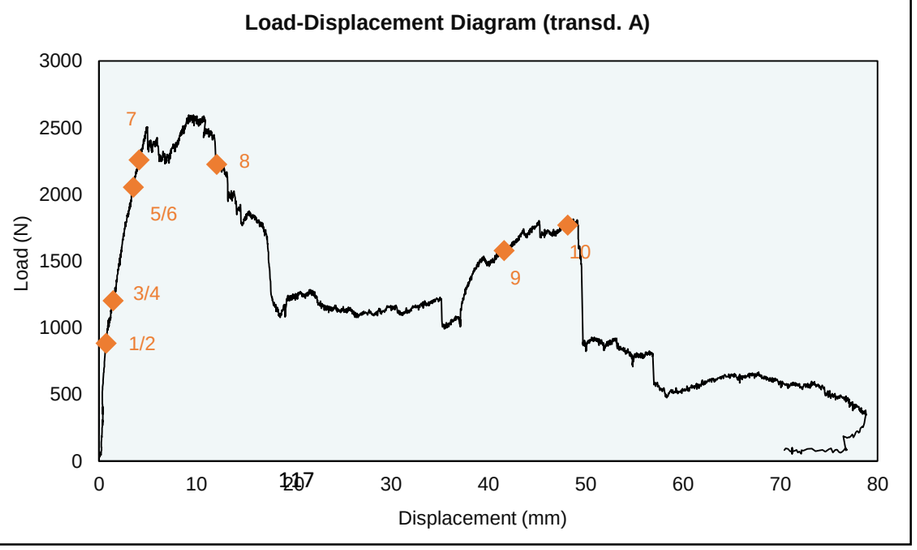

4.4.1.1 Comparison UA1 RA1

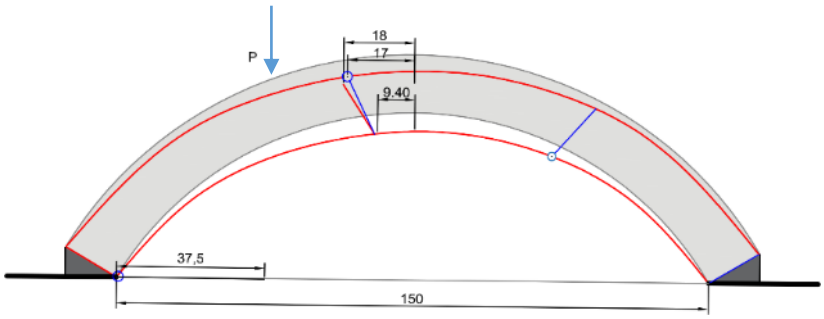

Figure 4.12 – comparison between the initial condition and the condition at the end of the first test

The unreinforced arch1 at the disarm presented a fracture to about 18cm left from the key as shown in red in the figure 12. During the first load test the hinge has been opened approximately at the same point (blue). In figure 12 the hinges at the end of the first test are reported in blu and the initial condition is reported in red, instead the grey shape represent the original geomerty. The experimental test was stopped before the opening of the fourth hinge at the right support.

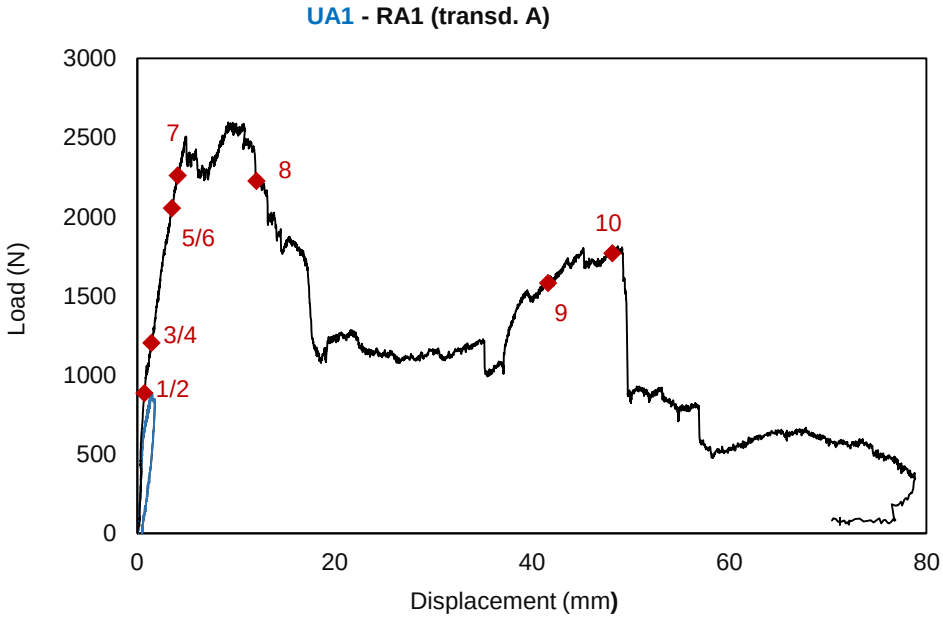

Figure 4.13 – Load displacement curves of unreinforced arch1 in blue and reinforced arch1 in black.

In figure 13 curves obtained from the two experimental tests in comparison are reported, even if the test on unreinforced arch1 was not led up to incipient collapse we can make a first comparison. An increase of the load bearing capacity and ductility is evident, although considering the sliding of the right support uncontrolled during the test on reinforced arch. Analyzing the reinforcement action, we can simultaneously evaluate the reinforcement

package action placed to work into two different conditions (mixed mode at the intrados and mode II at the extrados) as we can see in the figures 14 and 15.
As described in the chapter 3, the peeling condition is more severe than the shear condition and in case of mixed mode the component of the axial stress, perpendicular to the interface is considerable for small angles. In the RA1 delamination in proximity of the area under load starts from very low load. When the load reached the value of 1700N, delamination close to the crack 3 involved a length of 30cm to the right of the fracture.

Figure 4.14 - Fabric delamination (mixed mode)

Figure 4.15 - Fabric rupture

4.4.2 UA2 – RA2

UA2	
Start of realization	11-03-2016
End of realization	22-03-2016
Disarm	23-03-2016
Total dry weight soil (kg)	96
Total water (l)	10.55
Specific weight of the arch (kg/cm^3)	0.00217
Test data	
Test date	27-04-2016
Maximum Load (N)	1524.7

Load-Displacement Diagram (transd. B)

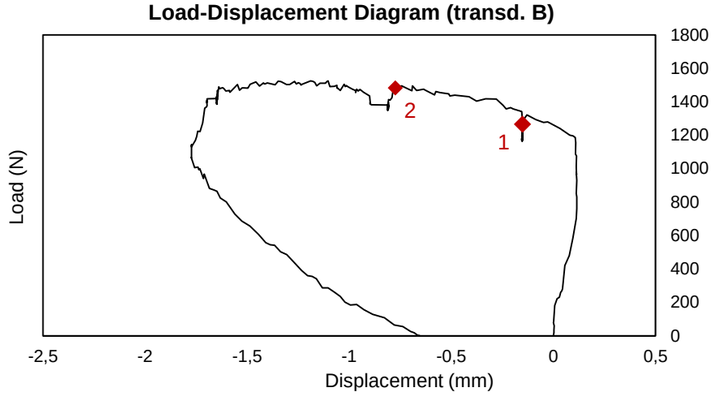

At the beginning of the load test two hinges at the supports had formed at the end of curing, both of them at the intrados.

The maximum load reached during the asymmetric load test was 1524.7N

Load-Displacement Diagram (transd. D)

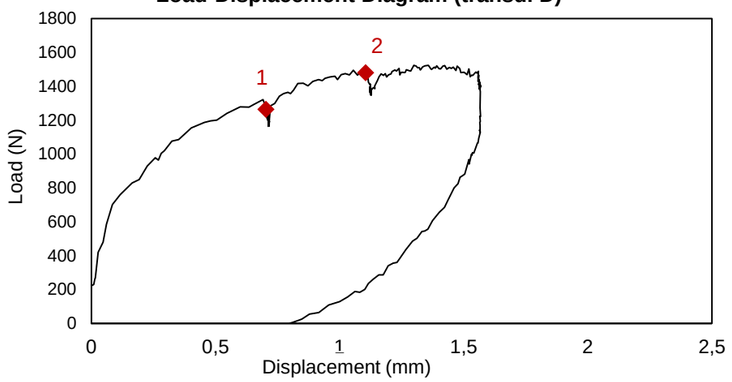

Load-Displacement Diagram (transd. E)

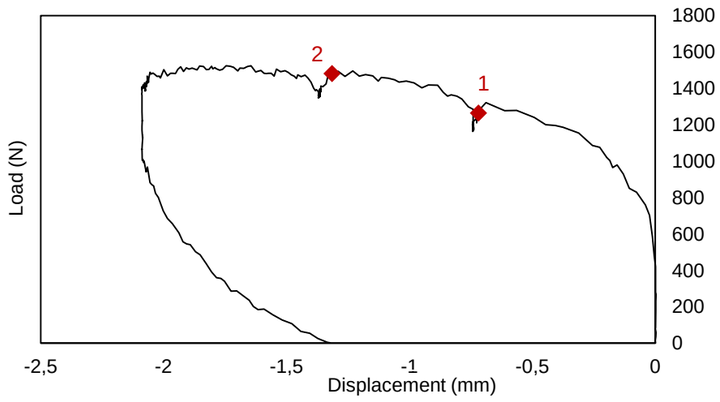

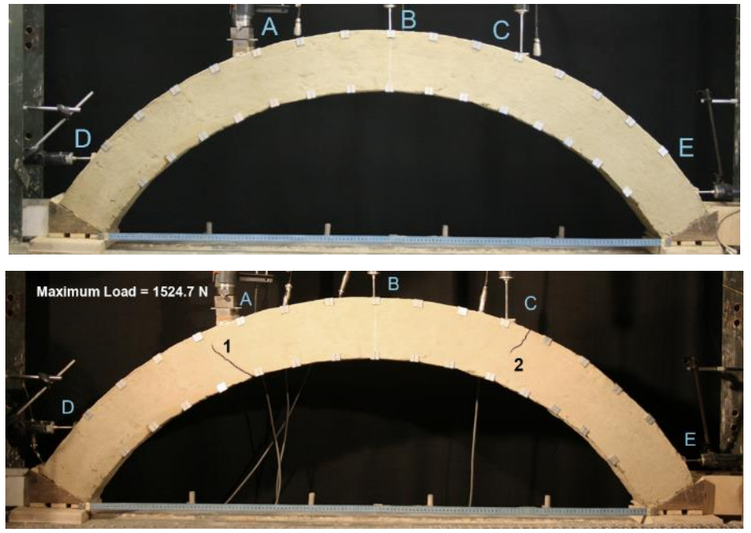

Crack pattern of unreinforced arch model after asymmetric point load test (02-03-2016)

Load-Displacement Diagram (transd. A)

Load-Displacement Diagram (transd. C)

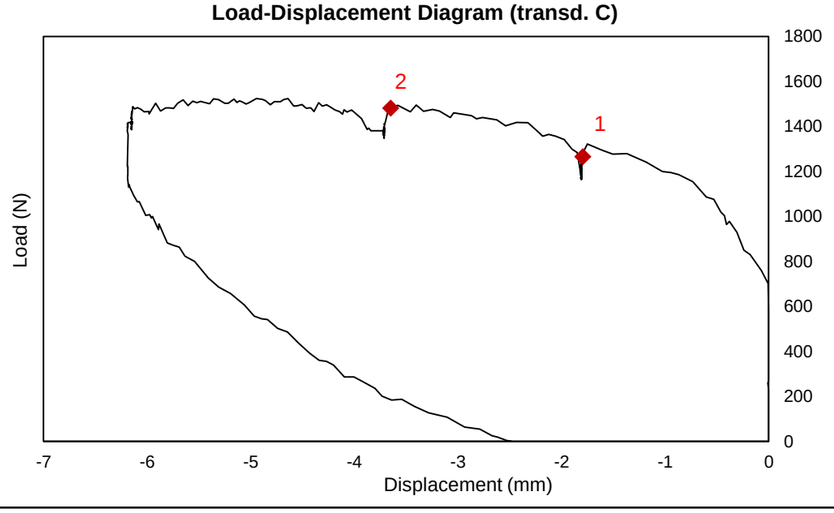

RA2	
Start of realization	11-03-2016
End of realization	22-03-2016
Disarm	23-03-2016
Total dry weight soil (kg)	96
Total water (l)	10.55
Specific weight of the arch (kg/cm^3)	0.00217
Reinforcement	
Date of reinforcement application	28-04-2016
Number of wires at the intrados	32
Number of wires at the extrados	33
Average spacing between wires (mm)	4.292
Test data	
Test date	2-05-2016
Maximum Load (N)	3312

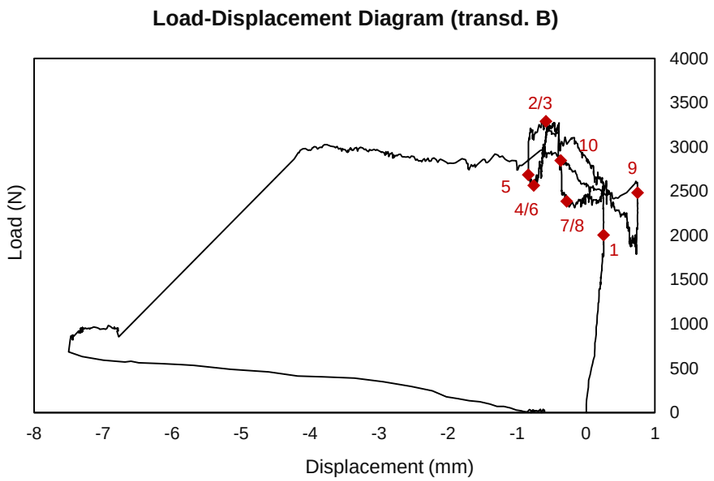

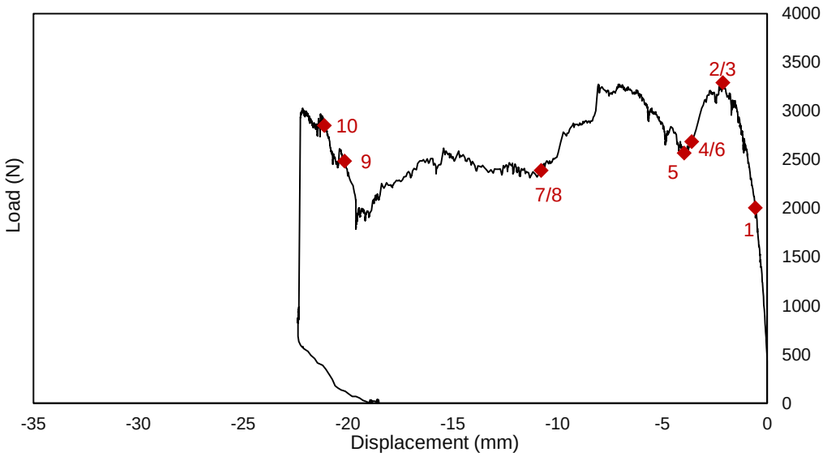

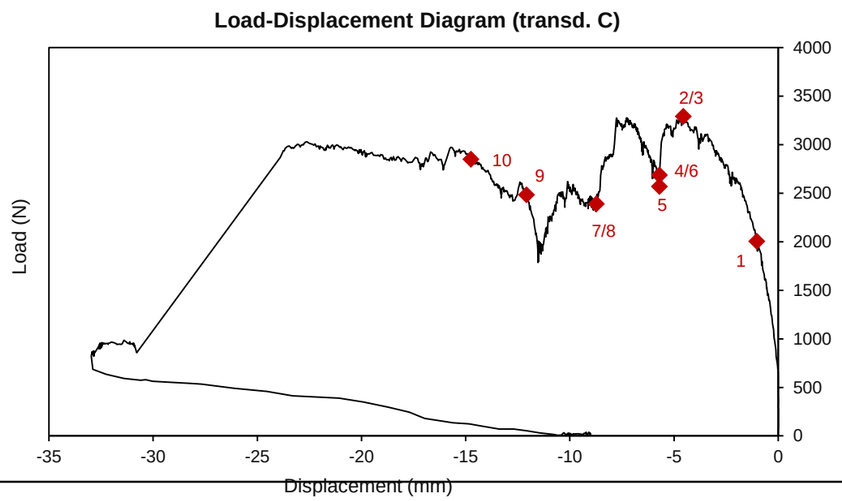

1 and 2_Fracture reopening corresponding to the hinges of the previous test
3_Fabric detachment
4_Radial fracturing
5_Hinges at the supports become evident (intrados at the left support and extrados at the right support)
6-10_ Radial Fractures

The maximum load reached during the asymmetric load test was 2594.8N. The load-displacement diagram referred to the transducer D is not reported for recording data problem identified during the test.

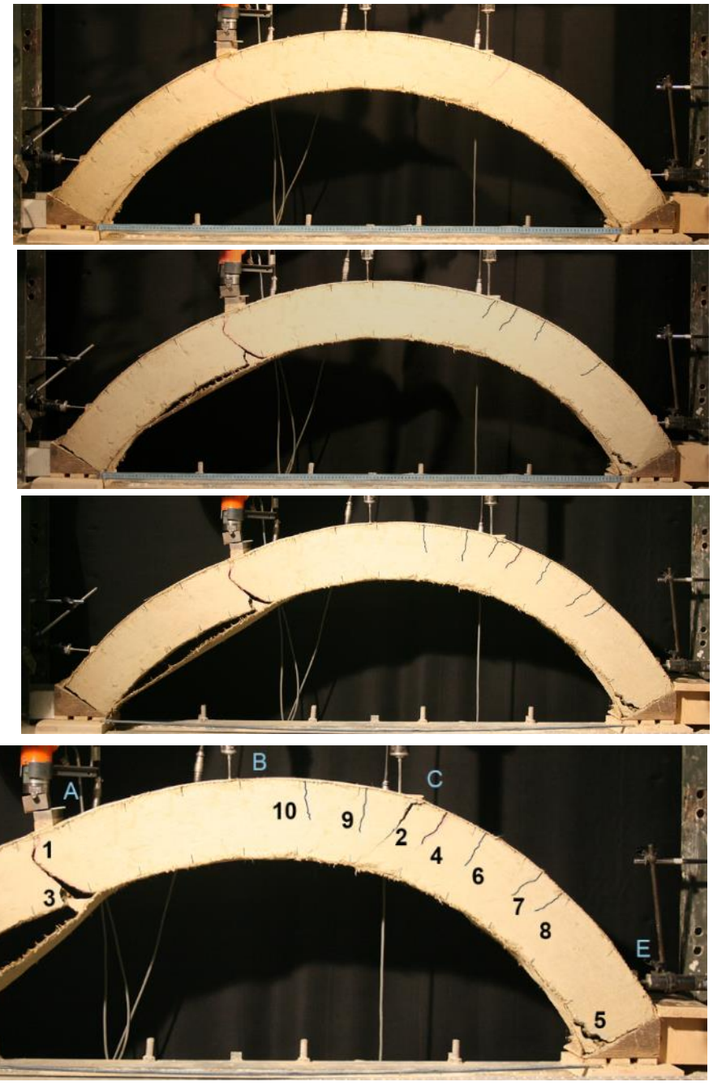

Crack pattern of reinforced arch model after asymmetric point load test (02-05-2016)

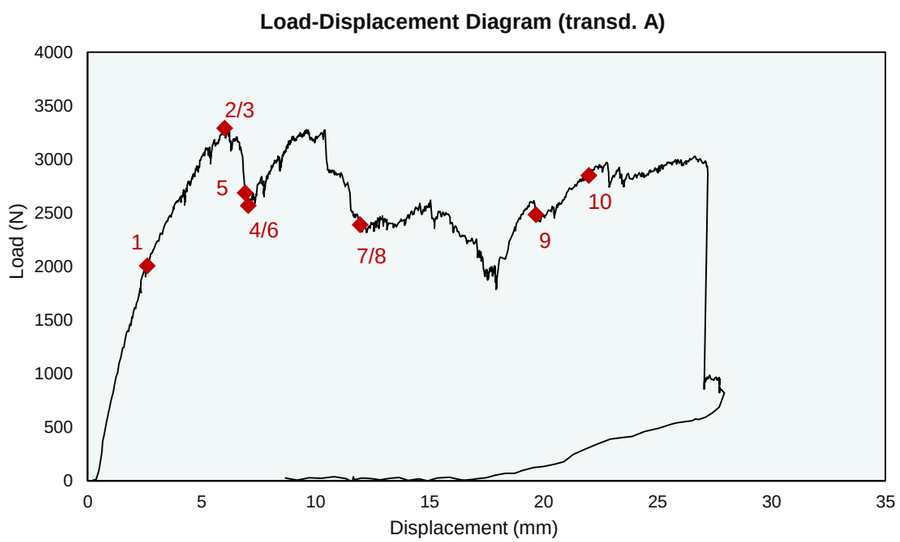

4.4.2.1 Comparison UA2 RA2

Apparently, the strengthening did not increase the initial stiffness. Regarding the global load-displacement response, a noticeable increase in terms of load bearing capacity is possible, as illustrated by the curves depicted in figure 16. In the reinforced arch, the abrupt drops in load due to the debonding at the intrados and rupture at the extrados took place for very large deformations.

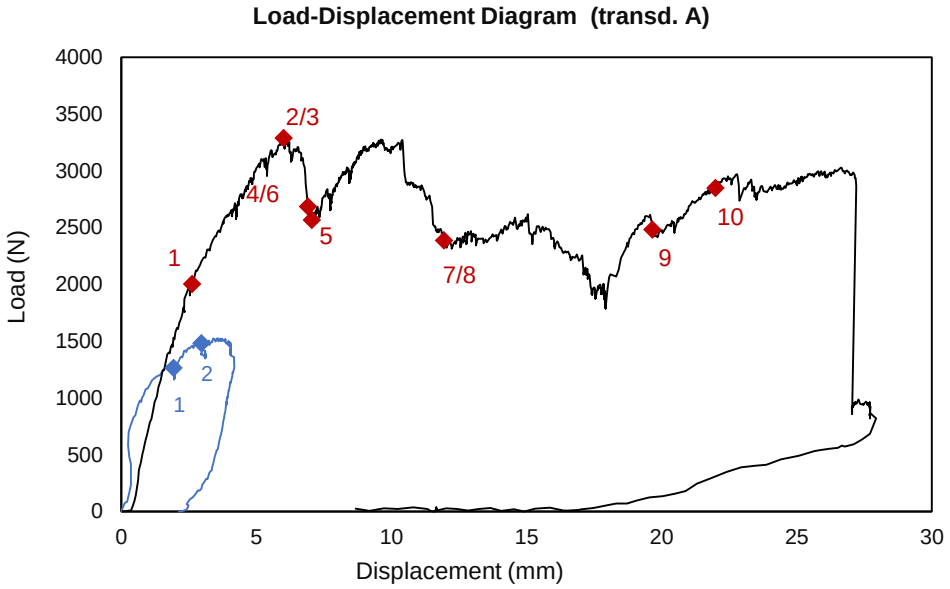

Figure 4.16 – Load displacement curves of unreinforced arch2 in blue and reinforced arch2 in black.

For the unreinforced one the alternating four-hinges mechanism occurred. The reinforcement increased the load capacity by 117% thanks to the reinforcement capacity to spread tensile stresses as we can see in the crack pattern characterized to diffusion cracks. The sustained displacement was about 20 times greater than the displacement corresponding to the unreinforced arch.

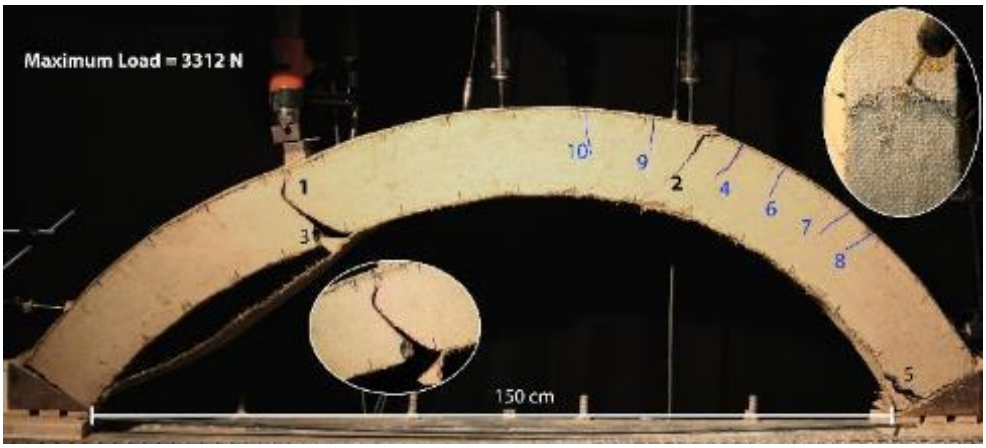

Figure 4.17 - Crack pattern of reinforced arch2 after asymmetric point load test (02-05-2016)

Failure mechanism of the strengthened arch was led by the progressive debonding at the intrados and involved the ripping of a portion of the earth material as shown in figure 17 and the failure occurred with the rupture of the fabric at the extrados. In the RA2 delamination in proximity of the area under load starts from approximately 2000N.

4.4.3 UA3 – RA3 – AA3

UA3	
Start of realization	29-06-2016
End of realization	6-07-2016
Disarm	23-03-2016
Total dry weight soil (kg)	96
Total water (l)	10.60
Specific weight of the arch (kg/cm^3)	0.00217
Test data	
Test date	5-10-2016
Maximum Load (N)	1237.7

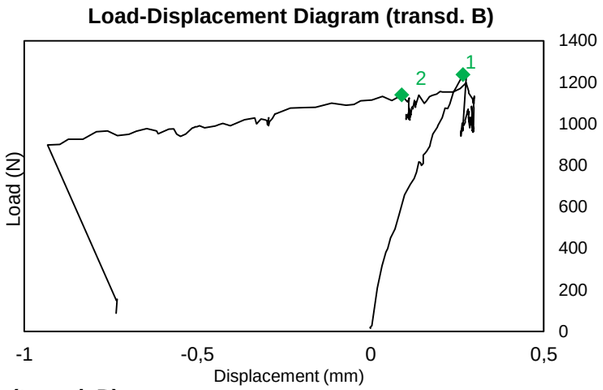

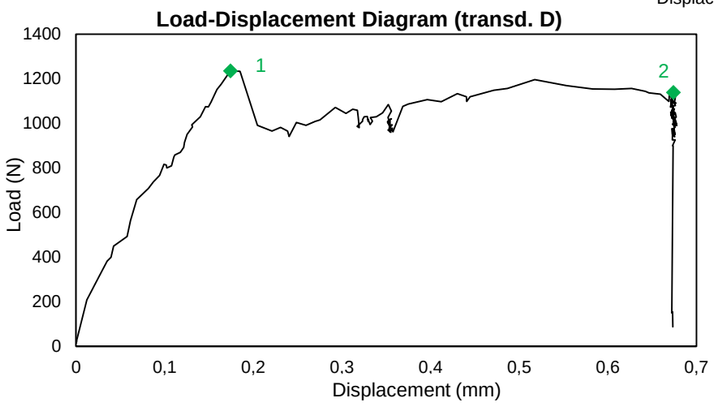

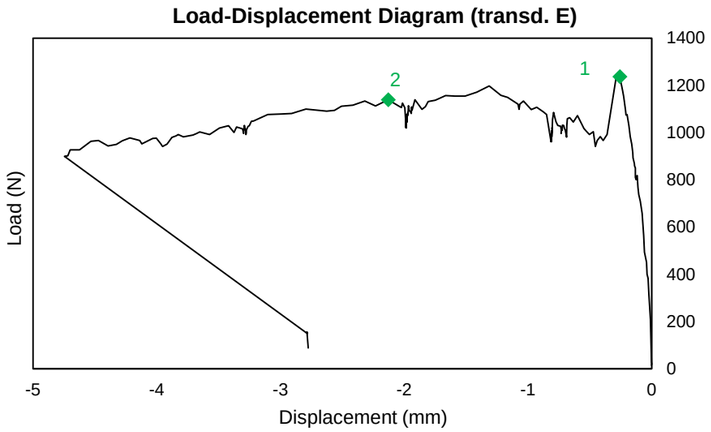

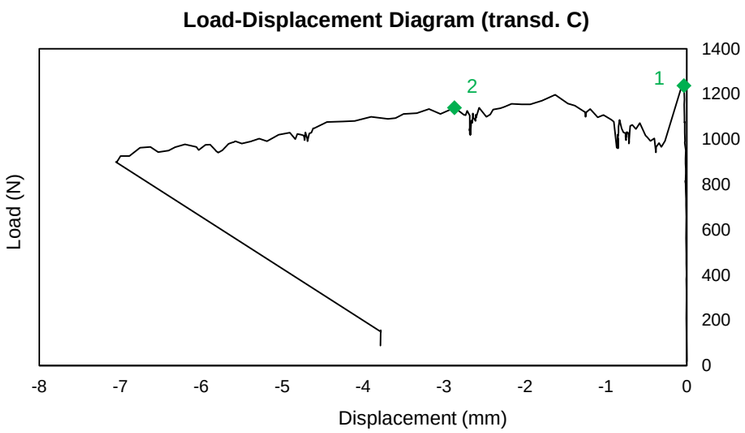

At the beginning of the test were not visible the two hinges at the support and the strengthening crack at 37cm to the key of the arch was closed by injection of mud. The maximum load reached during the experiment was 1237N and the structure appeared to be severely damaged.

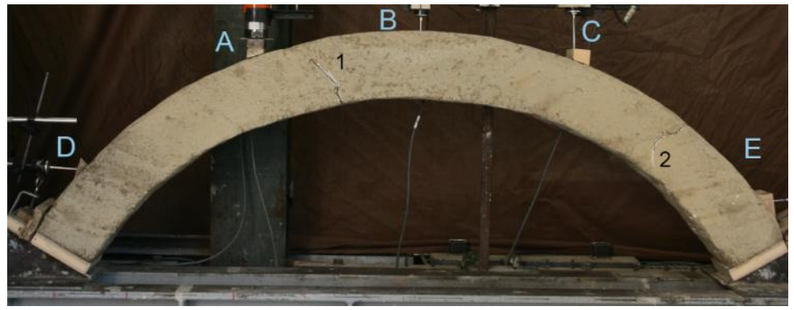

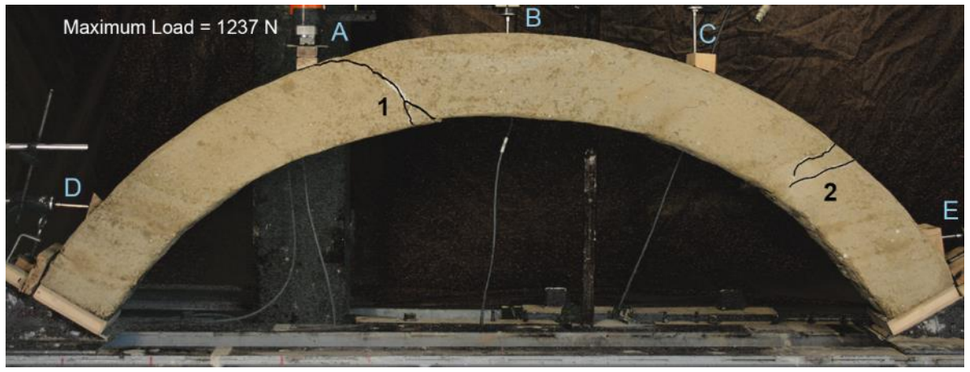

Crack pattern of unreinforced arch model after asymmetric point load test (05/10/2016)

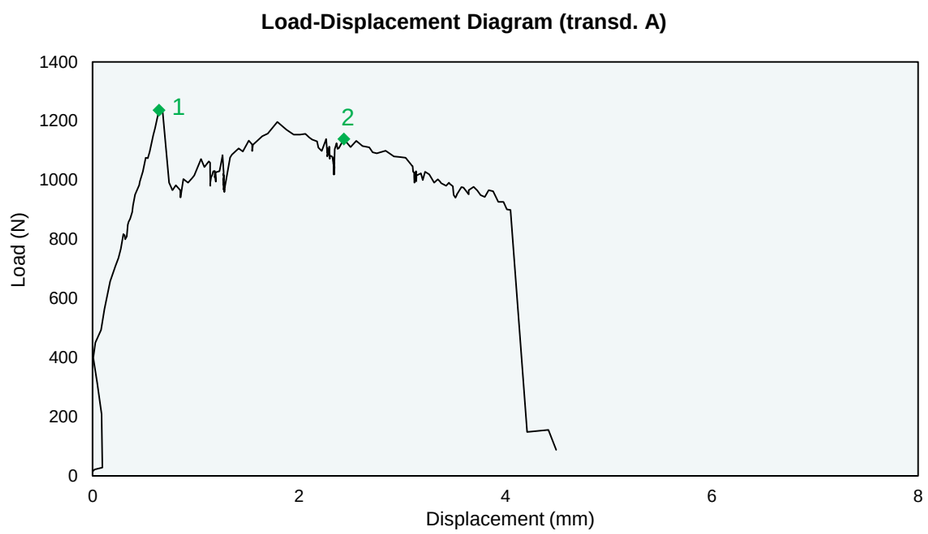

RA3	
Start of realization	29-06-2016
End of realization	6-07-2016
Disarm	23-03-2016
Total dry weight soil (kg)	96
Total water (l)	10.60
Specific weight of the arch (kg/cm^3)	0.00217
Reinforcement	
Date of reinforcement application	7-10-2016
Number of wires at the intrados	31
Number of wires at the extrados	34
Average spacing between wires (mm)	4.292
Test data	
Test date	11-10-2016
Maximum Load (N)	1428.7

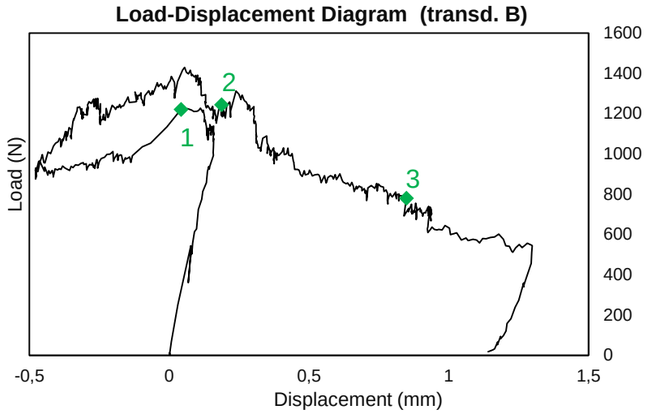

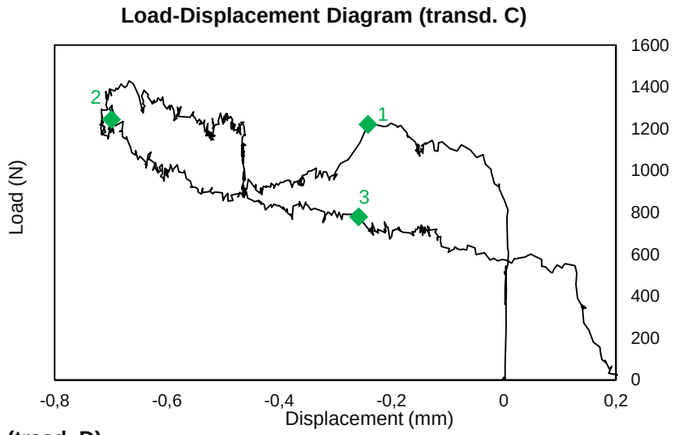

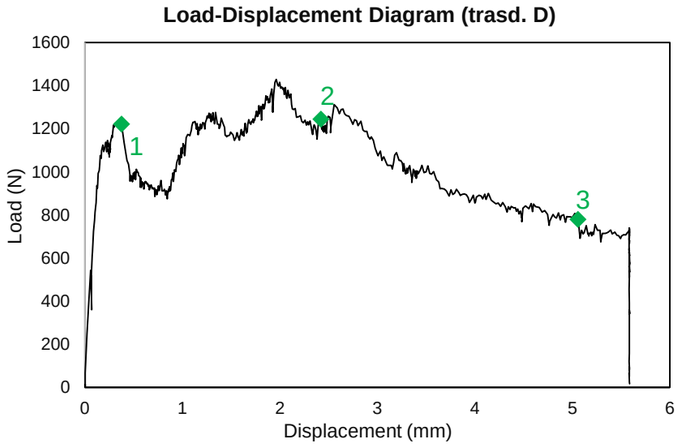

The maximum load reached during the experiment was 1428N. Delamination at the intrados due to the peeling action have had a strong influence on the test result. It was decided to apply four strips of 15cm as anchor perpendicular to the reinforcement direction I the load proximity.

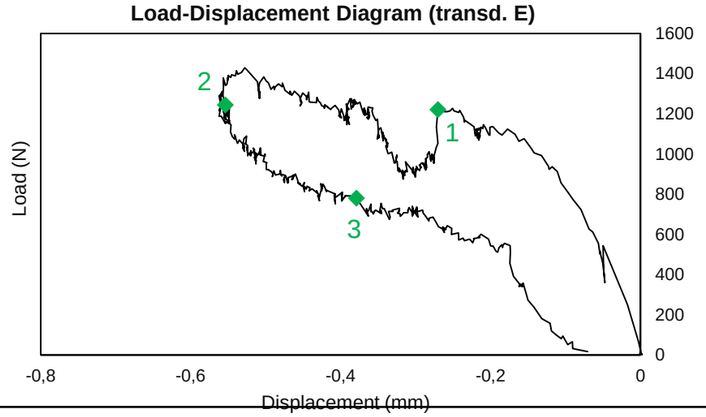

1_Fracture reopening close to the point of application of the load and delamination phenomenon occurs with loos of stiffness

2_second hinge formation on the right half of the arch

3_Hinge at the left support become evident

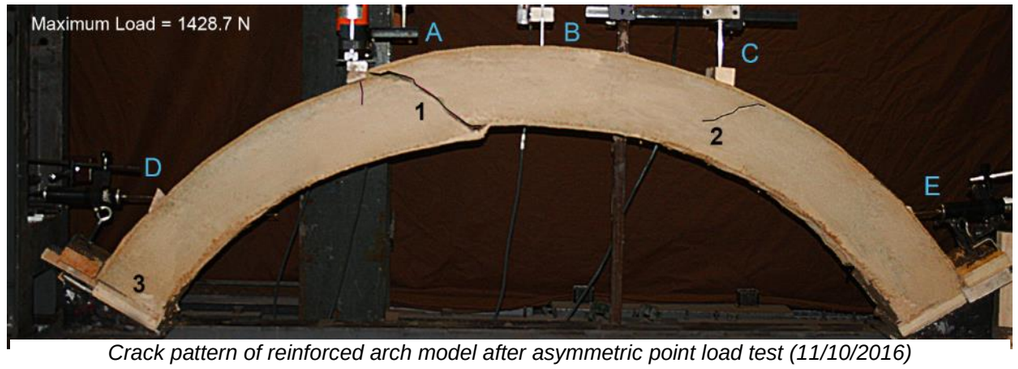

Crack pattern of reinforced arch model after asymmetric point load test (11/10/2016)

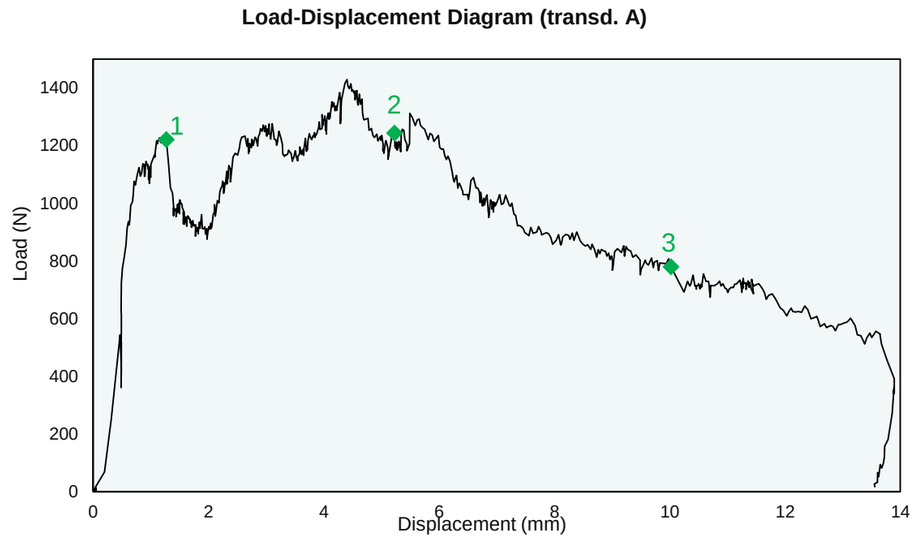

AA3	
Start of realization	29-06-2016
End of realization	6-07-2016
Disarm	23-03-2016
Total dry weight soil (kg)	96
Total water (l)	10.60
Specific weight of the arch (kg/cm³)	0.00217
Reinforcement	
Date of reinforcement application	7-10-2016
Number of wires at the intrados	33
Number of wires at the extrados	34
Average spacing between wires (mm)	4.292
Date of anchor application	11-10-2016
Number of strips	4
Strips width (mm)	150
Test data	
Test date	13-10-2016
Maximum Load (N)	4849

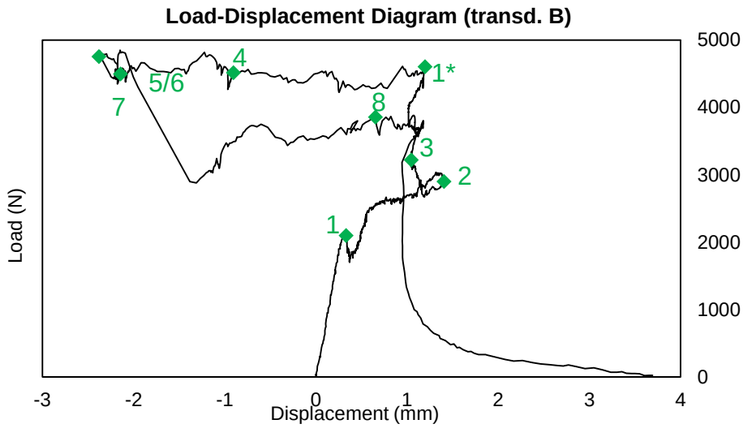

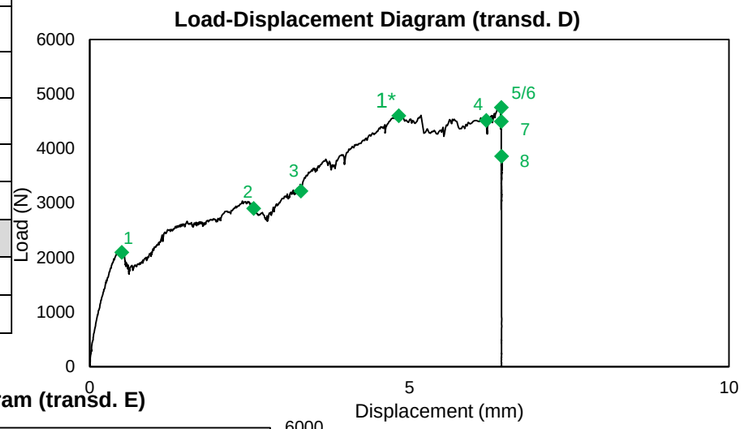

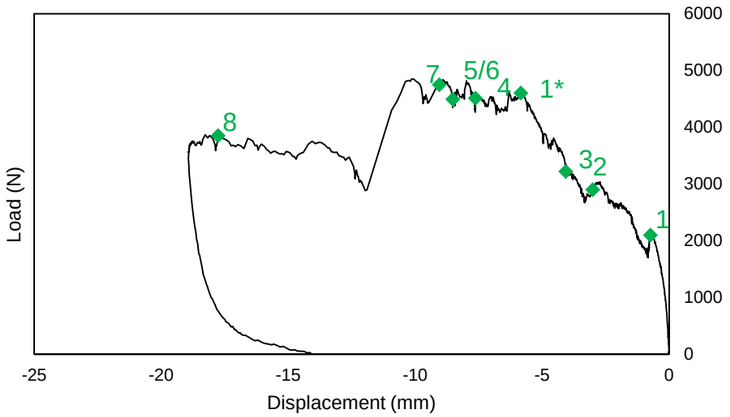

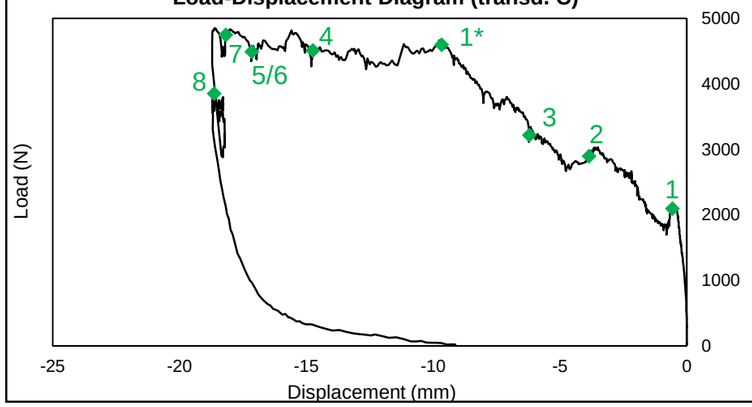

1_ crack formation at the compressed portion (intrados) of the hinge

2_Cracks development (intrados)

3_Compression fracture

1*_Hinge opening with consequent fabric rupture (extrados)

4_Fractures close to the key of the arch (intrados and extrados)

5_Delamination

6_fracture close to the left support

7and 8_ Hinges at supports

The maximum load reached during the experiment was 4849N.

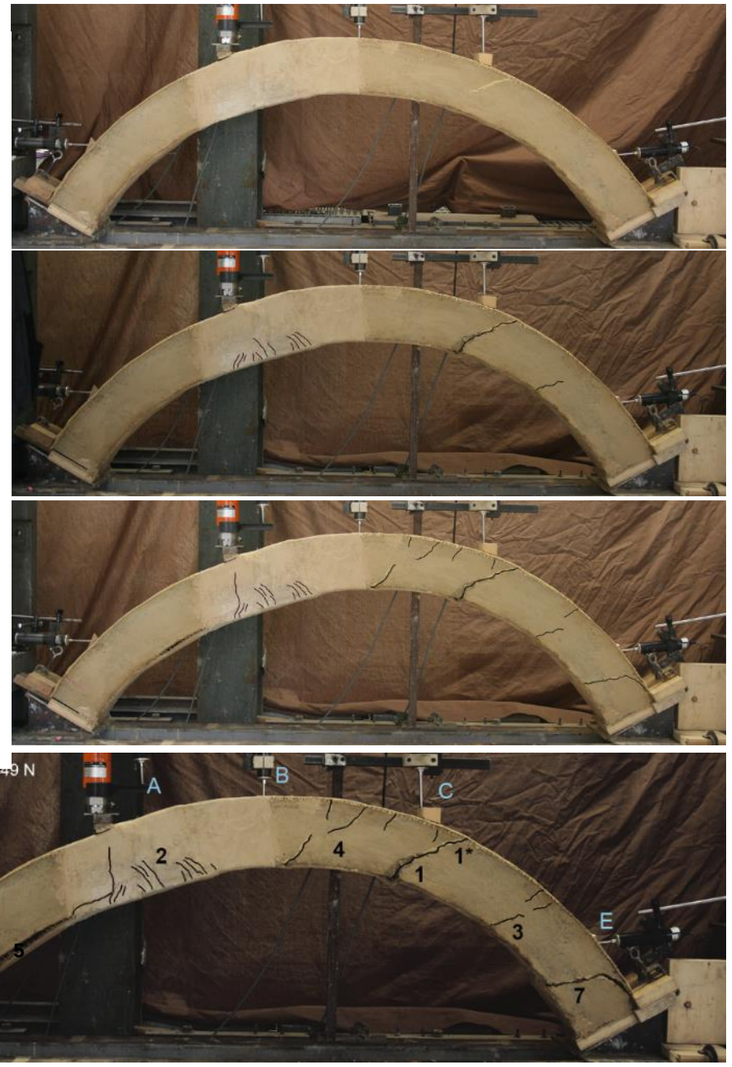

Crack pattern of anchored arch after asymmetric point load test (13-10-2016)

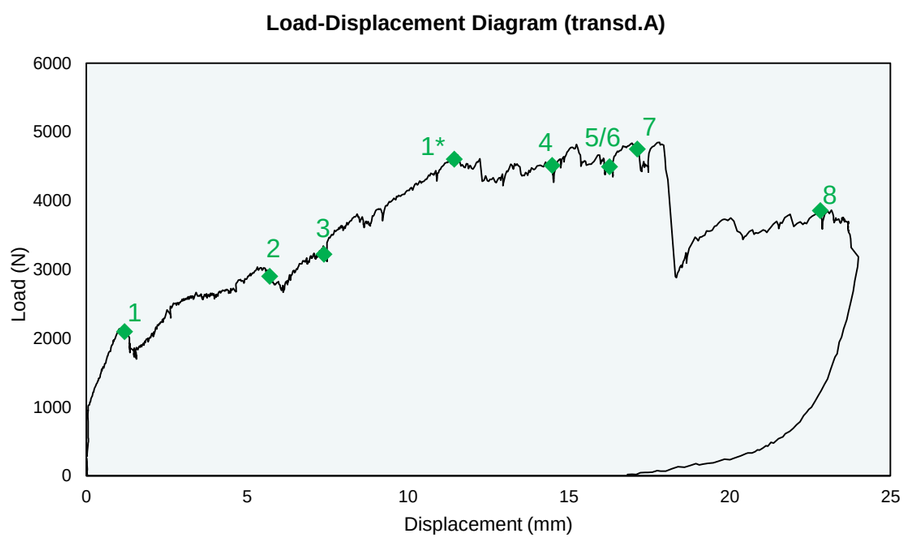

4.4.3.1 Comparison UA3 RA3 and AA3

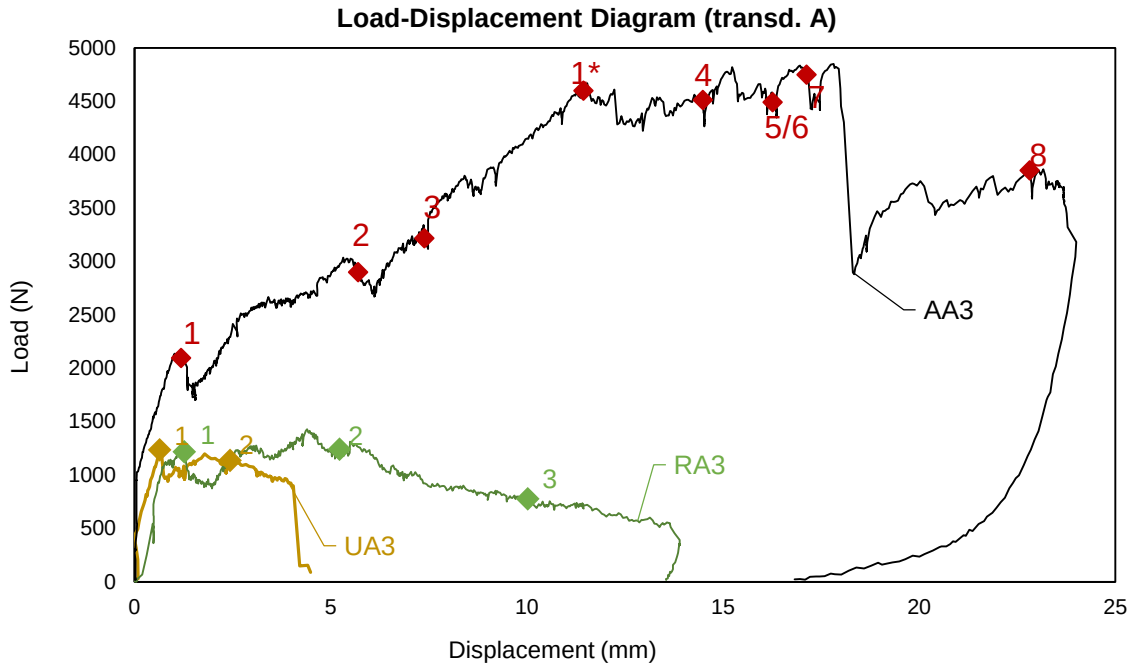

Figure 4.18 – Load displacement curves of unreinforced arch3 in yellow, reinforced arch3 in green and anchored arch3 in black.

The fracture 1 corresponding to the load is characterized by a particularly orientation, with an evident slop respect to the arch cross section. Effectively this fracture had already formed during the curing time and was probably determined by the weakness plane produced during compaction. For some reason, the slope was more marked than in the previous cases. The unreinforced arch developed a mechanism in which the sliding of the fracture 4 initiated. For this reason, the reinforcement applied in the test RA3 was ineffective, as it was subjected to peeling stress from the beginning, and the load increased only by 15%. It was proposed to realize an anchor made of a wrap of fabric put perpendicular to the tensile action of the reinforcement strip.

The occurrence detachment of strengthening material from the support especially concerning arches strengthened at the intrados is a critical problem (Foraboschi, 2004; Valluzzi et al., 2001). In this case a huge component of peeling dictate the failed mechanism. The use of anchor made with the same fabric and applied with the same matrix perpendicular to the reinforcement can be preventing the debonding phenomenon.

The differences regarding the additional use of strips anchor are visible both in term of load capacity and ductility of the structure (Figure 18).

4.5. Global Comparisons

4.5.1 Unreinforced Arches

Three model arches tested without strengthening (UA1, UA2 and UA3) presented a similar structural behaviour, essentially characterized by the development of a four-hinge mechanism.

The relation between vertical load and vertical displacement registered in the load proximity is represented in figure 19 where markers on the curves illustrate the load value corresponding to the hinges except those at the supports, numbered according to the formation sequence.

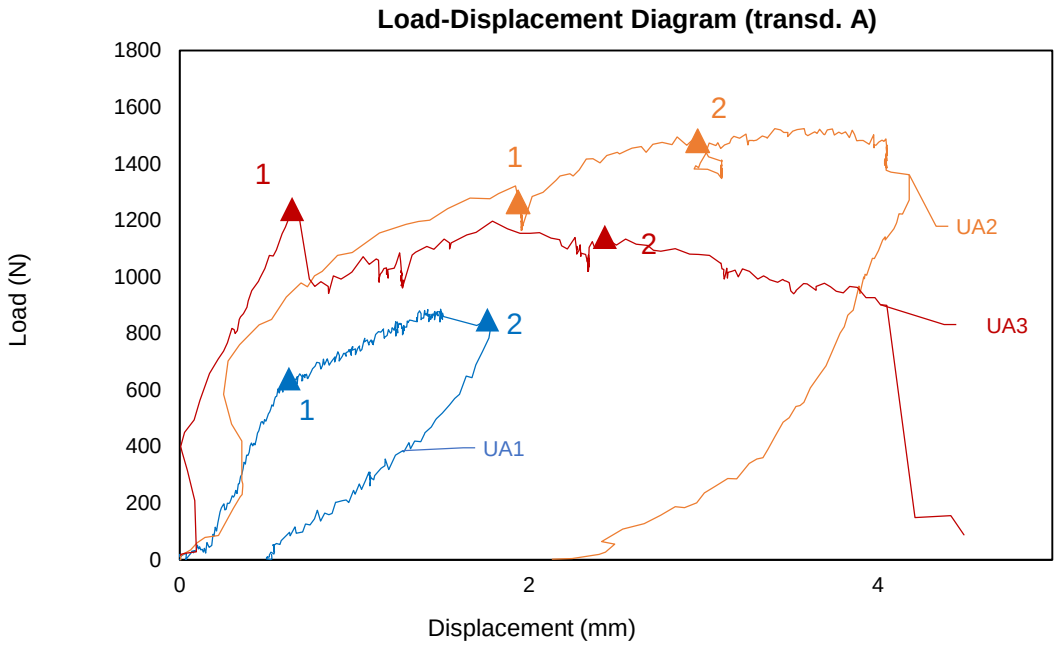

Figure 4.19 – Load displacement curves of unreinforced arch1 in blue, unreinforced arch2 in orange and unreinforced arch3 in red

The hinges at the left support was in each case a starting condition, even if not clearly visible on the third arch. The hinge at the right support in all arches changed its position during the test, from the intrados toward extrados. The first test was stopped before the formation of the fourth hinge. The peak load of each specimen is listed in Table 4.2.

Despite the prepeak stiffness and kinematic resemblance observed in the test UA2 and UA3, differences can be detected in terms of maximum load achieved.

An important feature is the amount of ductility of structure respect to traditional masonry arches. Respect to the collapse load determined with the kinematic theorem, the experimental value obtained by tests UA2 and UA3 is higher. This is expected because the hypothesis of the theory of no tensile strength is conservative.

Specimens	Maximum Load (N)
UA1	885.67
UA2	1524.70
UA3	1237.70
A.V.	1216.02

Table 4.2. Maximum load reached during asymmetric point load tests on the three unreinforced models

4.5.2. Strengthened Arches

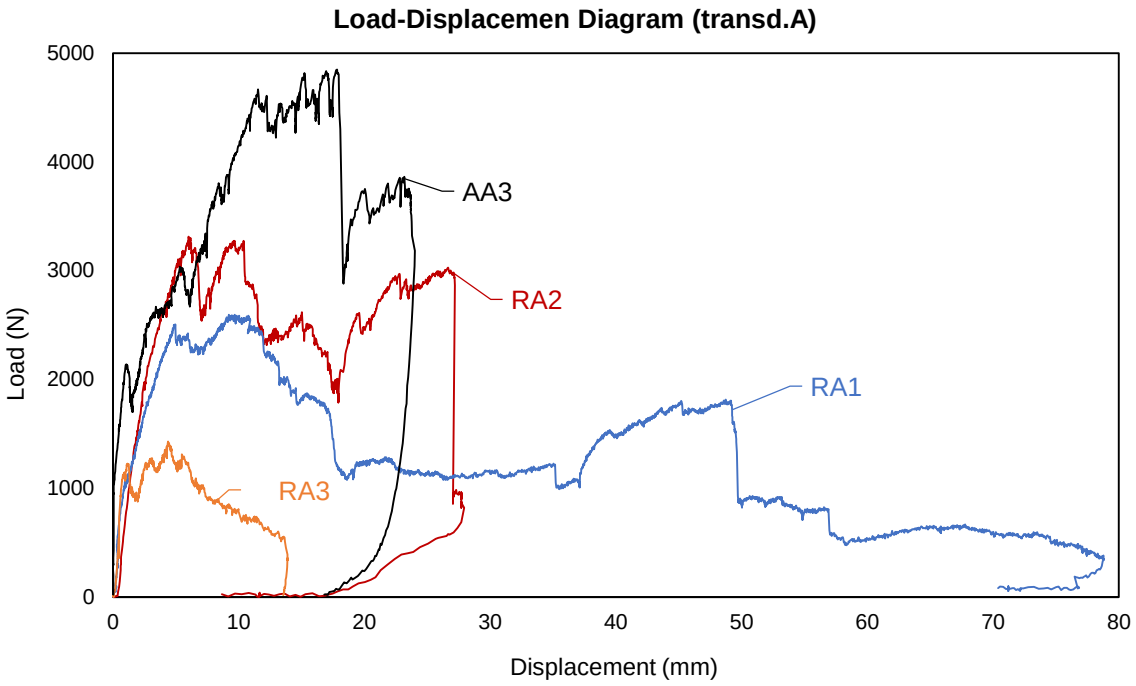

Figure 4.20 – Load displacement curves of reinforced arch1 in blue, reinforced arch2 in red, reinforced arch3 in orange and anchored arch3 in black

Continuous strengthening at intrados and extrados provided an enhance arch behaviour with respect to those unstrengthened and allowed important increase in term of maximum load applied and displacement prior to failure as shown in table 4.3. In the figure 18, the load displacement curves of the three reinforced arch models in comparison with the anchored one are reported. The continuous reinforcement was able to spread the tensile stress and to prevent the four-hinge mechanism. This is what happens while strengthening masonry arches with FRP or FRCM. The failure was led by the detachment of the strip at the intrados. The use of the anchor was able to contrast the debonding.

	Models	Maximum Load (N)	Average values (N)	Strength increase (%)
Unreinforced	UA1	(885.67)	1216.02	-
Unreinforced	UA2	1524.70		
Unreinforced	UA3	1237.70		
Reinforced	RA1	2594.8	2445.16	101%
Reinforced	RA2	3312		
Reinforced	RA3	(1428.7)		
Anchored	AA3	4849	4849	299%

Table 4.3. Experimental results concerning the maximum load achieved and strength increase in comparison to the unreinforced condition, provided by strengthening methods

It was observed that the strengthening method modifies the formation of the hinges (Figure 22), in the hinges sections, which are in combined compressive and bending stresses the resistance depends on the rammed earth compression strength and on the jute fabric tensile strength. The collapse of the structure is due to other mechanisms dependent on the interactions at the local level of the constituent materials.

Figure 4.21 – Hinge at the extrados of strengthened arch

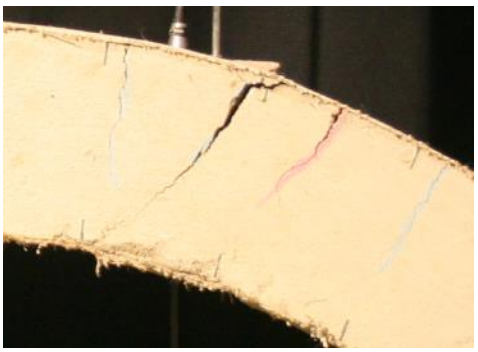

Figure 4.22 – Hinge at the intrados of strengthened arch

Considering the result of the load test on arch2 as the most regular result it is possible to summarize the principle phenomena, which characterized the rammed earth strengthened arches behaviour.

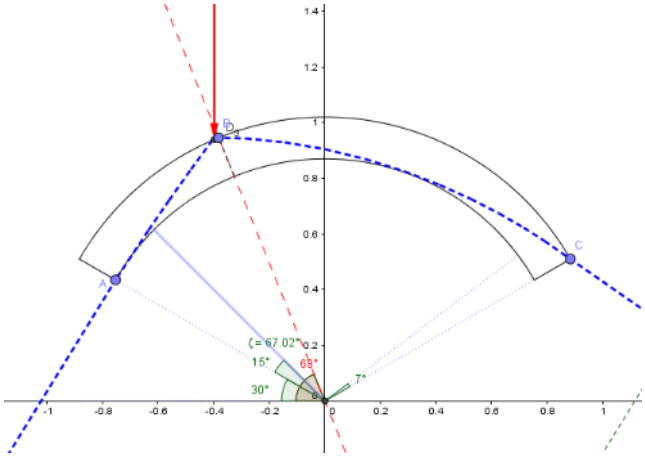

Figure 4.23 Initial condition

Approximately in correspondence of point 1 of the load path, the thrust line of the arch exits from the body of the arch, in the position where the load is applied (Figure 24). Fracture 1 re-opens and the strengthening applied at the intrados begins to act as a restraint to tensile deformation.

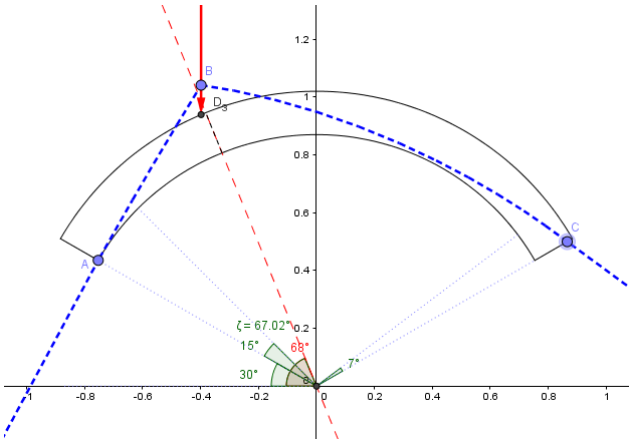

Figure 4.24

Delamination of the reinforcement at the intrados begins. Note that the delamination is not determined by the peeling action but is only facilitated. In fact, the tensile force necessary to delaminate the reinforcement due to peeling action in a curved beam calculated using the equation (4.1) should be definitely higher than the tensile strength of the reinforcement (Figure 25). The equation (4.1) was derived by simple equilibrium condition in Valluzzi et al. (2001) according to the scheme reported in figure 25.

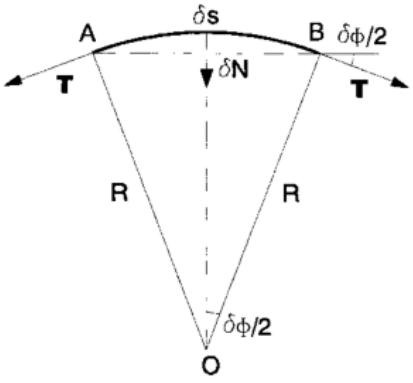

Figure 4.25 Mechanism of Detachment of Laminate from Masonry (Valluzzi 2001)

$$\frac{\delta N}{\delta s} = \frac{T}{R} \qquad (4.1)$$

The beginning of delamination is probably due to the initiation of a tensile fracture in the intrados of the arch and to the deviation of such fracture at the interface between raw earth and fabric. (See interfacial fracture studies of Hutchinson and Suo 1992; Swadener and Liechti 1998.).

Point 2: the trust line exits in correspondence of the second fracture (transducer C) and reinforcement at the extrados begins to act as a constraint.

Point 3: the reinforcement at the intrados after the peak load is delaminated. The delamination of the reinforcement at the intrados, facilitated by the peeling stresses, transforms the reinforced hinge placed next to the point load into a classic hinge and the system becomes similar to the one reported in figure 26.

The third and the fourth hinges form.

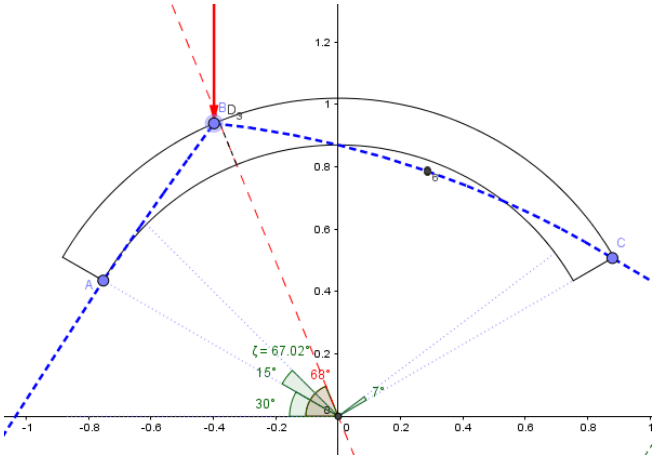

Figure 4.26

The last of the four hinges is placed at the intrados approximately at midspan between the point load and the right springer and the reinforcement at the extrados makes it to behave as a plastic hinge (Figure 22). Knowing the maximum tensile strength of the extrados reinforcement, an approximate evaluation of the plastic moment according to the scheme reported in figure 27 makes it possible to apply the kinematic theorem and to evaluate the collapse load. 3442N is the approximated value of the load obtained not considering the influence of the reinforcement at the intrados, in fact at the ultimate state before collapse the contribution of the fabric at the intrados is negligible (Figure 21). 1055N is the value of jute strenght obtained multiplying the value of the tensile strenght of a yarn (Table 3.3) by the widht of the extrados equal to 145mm.

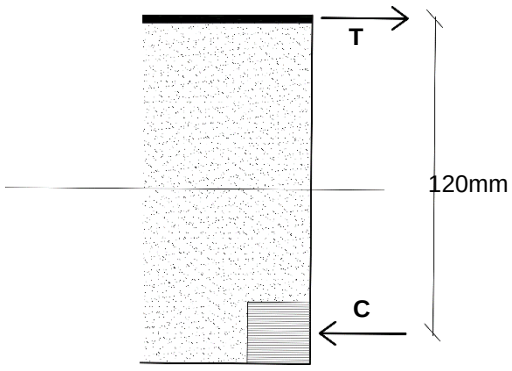

Figure 4.27 Internal forces in a reinforced cross section arch

Note that the resistant moment produced by the reinforcement is an approximated value, being unknown the value of the compressive component C in figure 27 and neglecting the plastic work of the compressive forces. The arm considered is equal to 12mm, measure achieved by the experimental evidences.

4.6 Conclusions

The stability of curved structures under loading condition is strongly dependent on the geometry of the structure and on the constituent material. In particular, the safety condition of the masonry arch is achieved when the line of thrust is kept inside of each section of the arch itself. When the internal force resultant moves out the central core the section partialises and the high deformation phase beings. The presence of reinforcement strips applied at intrados and extrados alters the formation of hinges producing in some cases something that resemble plastic hinges and locally confers tensile strength to the structure. The high mechanical characteristic of the fabric normally employed for strengthening masonry which is characterized by high stiffness and high strength can compromise the global ductility of the structures. In fact, the ultimate strength of the reinforced masonry arches depends on the adhesion between fibers and masonry and the stress component

perpendicular to the interface, which is responsible for the failure, is proportional to the tension in the fibers; it should be better to employ fibers not having a high strength and, at the same time, increase the width of the strips. (Briccoli Bati and Rotunno, 2001; Oliveira et al., 2010; Valluzzi at al., 2001). In the case of jute reinforcement of rammed earth masonry, the exceptional adhesion combined with not very high tensile strength produces interesting results: the intrados hinge distributes the stress on a relatively long length of the arch inducing the material to collaborate to the strength of the arch. The final collapse of this hinge is however, characterized by a “traditional” hinge when the jute fabric at the end fails. The extrados hinge on the contrary is characterized by delamination as in the case of FRP. The presence of anchors can strongly modify this behaviour. The knowledge of parameters determined previously by peeling tests can give useful information to predict the behaviour of reinforced structures.

However, jute is a natural material and its behaviour has to be further investigated in particular with respect to durability. Adaptability to curved surfaces and ease of application make this reinforcement system attractive to be used in strengthening methods.

4.7 Bibliography

Alecci, V., Focacci, F., Rovero, L., Stipo, G., De Stefano, M. 2016. “Extrados Strengthening of Brick Masonry Arches with PBO-FRCM Composites: Experimental and Analytical Investigations.” Composite Structures 149. Elsevier Ltd: 184–96. doi:10.1016/j.compstruct.2016.04.030.

Block, P., Dejong, M., Ochsendorf, J. 2006. “As Hangs the Flexible Line: Equilibrium of Masonry Arches.” Nexus Network Journal 8 (2): 13–24. doi:10.1007/s00004-006-0015-9.

Borri, A., Casadei, P., Castori, G., Hammond, J. 2009. “Strengthening of Brick Masonry Arches with Externally Bonded Steel Reinforced Composites.” Journal of Composites for Construction 13 (August): 468–75. doi:10.1061/(ASCE)CC.1943-5614.0000030.

Borri, A., Castori, G., Corradi, M. 2011. “Intrados Strengthening of Brick Masonry Arches with Composite Materials.” Composites Part B: Engineering 42 (5). Elsevier Ltd: 1164–72. doi:10.1016/j.compositesb.2011.03.005.

Briccoli Bati, S, Fagone, M., Rotunno, T. 2011. “Lower Bound Limit Analysis of Masonry Arches with the CFRP Reinfocements: A Numerical Method.” XX Congresso dell’Associazione Italiana Di Meccanica Teorica Ed Applicata, no. August: 1–10. doi:10.1061/(ASCE)CC.1943-5614.0000350.

Briccoli Bati, S., Rovero. L. 2007. “Towards a Methodology for Estimating Strength and Collapse Mechanism in Masonry Arches Strengthened with Fibre Reinforced Polymer Applied on External Surfaces.” Materials and Structures 41 (7): 1291–1306. doi:10.1617/s11527-007-9328-8.

Briccoli Bati, S., Rotunno, T., "A Composite Material in Glass-Fiber and Cement-Matrix (GFRCM) for Masonry Reinforcement" Fifth international symposium on computer methods in structural masonry, Roma 18-21 Aprile 2001, ed. T. G. Hughes, G. N. Pande Swansea : Computers & Geotechnics 2001 pp. 181-189 ISBN 9780951038024

De Lorenzis, L., Dimitri, R., La Tegola, A. 2007. “Reduction of the Lateral Thrust of Masonry Arches and Vaults with FRP Composites.” Construction and Building Materials 21 (7): 1415–30. doi:10.1016/j.conbuildmat.2006.07.009.

De Lorenzis, L., Zavarise, G. 2010. “Debonding Analysis of Thin Plates from Curved Substrates.” Engineering Fracture Mechanics 77 (16). Elsevier Ltd: 3310–28. doi:10.1016/j.engfracmech.2010.08.013.

Foraboschi, P. 2004. “Strengthening of Masonry Arches With Fiber Reinforced Polymer Strips.” Journal of Composites for Construction 8 (3): 191–202. doi:10.1061/(ASCE)1090-0268(2004)8:3(191).

Heyman, J. 1966. “The Stone Skeleton.” International Journal of Solids and Structures 2 (2): 249–79. doi:10.1016/0020-7683(66)90018-7.

Heyman, J. 1969. “The Safety of Masonry Arches.” International Journal of Mechanical Sciences 11 (4): 363–85. doi:10.1016/0020-7403(69)90070-8.

Heyman J. “The Masonry Arch”. Chichester: Ellis Horwood; 1982.

Huerta S. 2001. “Mechanics of Masonry Vaults: the Equilibrium Approach”. In: Structural analysis of historical constructions. Guimara, 47–70.

Hutchinson, J.W., Suo, Z.1992. “Mixed Mode Cracking in Layered Materials”.. Adv. Appl. Mech. 29: 63-191.

Kooharian, A. 1953. “Limit Analysis of Voussoir (segmental) and Concrete Arches”, Proc. Am.Concr. Inst. 89: 317–328.

Livesley, R.K., “Limit Analysis of Structures Formed from Rigid Blocks”, Int. J. Num. Meth. Eng. 12 (1978) 1853–1871.

Milani, G., Milani, E., Tralli, A. 2009a. “Upper Bound Limit Analysis Model for FRP-Reinforced Masonry Curved Structures. Part I: Unreinforced Masonry Failure Surfaces.” Computers & Structures 87 (23–24). Elsevier Ltd: 1516–33. doi:10.1016/j.compstruc.2009.07.007.

Milani, G., Milani, E., Tralli, A. 2009b. “Upper Bound Limit Analysis Model for FRP–reinforced Masonry Curved Structures. Part II: Structural Analyses.” Computers & Structures 87 (23–24). Elsevier Ltd: 1534–58. doi:10.1016/j.compstruc.2009.07.010.

O’Dwyer, DW. 1999. “Funicular Analysis of Masonry Vaults.” Computers and Structures 73 (1–5): 187–97. doi:10.1016/S0045-7949(98)00279-X.

Oliveira, D. V., Basilio, I., Lourenço, P. B. 2010. “Experimental Behavior of FRP Strengthened Masonry Arches.” Journal of Composites for Construction 14: 312–22. doi:10.1061/(ASCE)CC.1943-5614.0000086.

Papanicolaou, C. G., Triantafillou, T. C., Karlos, K., Papathanasiou, M. 2007. “Textile-reinforced mortar (TRM) versus FRP as strengthening material of URM walls: In-plane cyclic loading.” Materials and Structures 40(10), 1081–1097.

Pippard, A.J.S., Tranter, E., Chitty, L. 1936. “The Mechanics of the Voussoir Arch”. Journal of the ICE, 4:281-307.

Pippard, A.J.S., Chitty, L. 1951. “A Study of the Voussoir Arch”. National Building studies. London

Prota A, Marcari G, Fabbrocino G, Manfredi G, Aldea C. 2006. “Experimental In-plane Behavior of Tuff Masonry Strengthened with Cementitious Matrix-grid Composites”. Journal of Composites for Construction 10(3): 223–33.

Swadener, J.G., Liechti, K.M. 1998. “Asymmetric Shielding in Mixed-Mode Fracture of a Glass/epoxy Interface. J. Appl. Mech. 65:25-29

Valluzzi, M. R., Valdemarca, M., Modena, C. 2001. “Behavior of Brick Masonry Vaults Strengthened By FRP Laminates.” Journal of Composites for Construction 5: 163–69. doi:10.1061/(ASCE)1090-0268(2001)5:3(163).

5 General Conclusions and Outlooks

5.1 Conclusions

A strengthening system to improve the seismic behaviour of rammed earth constructions, both existing and contemporary, is suggested, based on experimental tests and analyses used to validate the technique. The main objective of this research work was to propose a procedure for the measurement of the parameters that influence the adherence of the strengthening package (composed by jute fabric and earth matrix) on rammed earth supports that was as simple as possible and as representative as possible of the ‘‘real’’ behaviour, and to verify the efficiency of the method through a case study.

Materials

The main parameters useful to characterize earth and jute materials were determined and possible procedures of data treatment were proposed.

In the light of geotechnical analyses and mechanical studies conducted on the use of gypsum as a stabilizer, it was observed that the 15% of gypsum powder was the optimal quantitative to reduce the shrinkage of the reinforcement matrix without altering the recyclability of the material. The results obtained from the compression tests with load parallel and perpendicular to the layers showed that the stiffness is influenced by the load direction while the differences in compression strength is within the statistical error. In general, natural materials, especially if rough due to specific processing techniques, deserve particular attention in the tuning of test methods for the definition of mechanical properties, due to the high scattering of results, to the size effects induced by heterogeneities and to the resulting uncertainties. Weibull distribution has proved to be a suitable statistical model to describe the strength of jute yarns. The information obtained with the tests on yarns (warp) revealed more reliable and directly useful to describe the strength of the reinforcement, in fact the weft yarns only contribute to the adhesion of the system, but not to the strength of the reinforcement. Tests on yarns have proved to be simpler and can be recommended as the reference ones in order to evaluate the mechanical and statistical parameters of jute to be employed for the design of strengthening systems.

Adherence

The behaviour and failure mechanism of this natural fiber reinforcement system appeared completely different from those of FRP due to the low tensile strength of the jute fabric and the good adhesion properties of the package to earth substrate. The substantial equality of matrix and masonry substrate gave good compatibility and adhesion of the strengthening

system. Shear tests have proved not to be useful for the determination of the bond strength of jute fabric reinforcement, as bond strength is higher than the load capacity of the fabric. Peeling test actually revealed to be indispensable to achieve information about adhesion capacity. From peeling test results, it was possible to evaluate the bond strength of lap joint. The effective bond length is not a critical parameter and it does not change significantly when varying the Young modulus of the substrate among reasonable values. In the lap joint condition crisis occurred in any case for low tensile resistance of the fabric. The axial stress due to peeling is already substantial for very small angles: with a peel angle of 8° the boundary cleavage has the same influence of the boundary shear. In the design phase it is important to consider that this type of reinforcement works well in the lap joint condition; as it is known, the peeling condition is more severe than the lap joint condition because of the concentration of stress on the delamination line due to the flexibility of the adherent strip. It is necessary to arrange the reinforcement according to the solicitations involved. Furthermore, the small length of adhered reinforcement involved in the process has to be taken into account. On the whole, the knowledge of parameters determined by peeling tests gave useful information to predict the behaviour of reinforced structures.

Case study

In general, the strengthening system studied proved to be compatible to rammed earth because of good adhesion properties and mechanical parameters comparable to the substrate. Indeed the high mechanical characteristic of the fabric normally employed for strengthening masonry which is characterized by high stiffness and high strength can compromise the global behaviour of the structures. The ultimate strength of the reinforced masonry arches depends on the adhesion between fibers and masonry and the stress component perpendicular to the interface, which is responsible for the failure, is proportional to the tension in the fibers; it should be better to employ fibers not having a high strength and, at the same time, increase the width or the thickness of the strips. Adaptability to curved surfaces and ease of application make this reinforcement system attractive to be used in strengthening methods.

Asymmetric load tests on arch models were performed to investigate the effectiveness of the proposed retrofitting technique applied on the curved rammed earth support. The comparative results show that the proposed retrofitting technique significantly increases the load bearing capacity of the rammed earth structure and the maximum displacement in agreement with literature on masonry structures.

The presence of reinforcement strips applied at intrados and extrados altered the formation of hinges producing in some cases something that resemble plastic hinges and locally conferring tensile strength to the structure. In the case of jute reinforcement of rammed earth masonry, the exceptional adhesion combined with not very high tensile strength

produces interesting results: the intrados hinge distributes the stress on a relatively long length of the arch inducing the material to collaborate to the strength of the structure. The final collapse of this hinge is, however, characterized by a “traditional” hinge when the jute fabric at the end fails. The extrados hinge on the contrary is characterized by delamination as in the case of FRP. The presence of anchors can strongly modify this behaviour.

Based on results, it is possible to conclude that the proposed strengthening technique provides a simple and useful measure to strengthen existing rammed earth buildings while minimally increasing the mass of the structure and without altering the recyclability of the material. The proposed retrofitting is easy to implement and cost-effective, it can be readily adopted in the areas where unreinforced rammed earth dwellings are common.

5.2 Outlooks

Further research is necessary to examine in depth the capability of describing the statistical character of test results on jute yarns with different statistical models and could be interesting to deeply analyze the jute stiffness. Moreover the statistical approach must be extended to the definition of the design parameters. In fact, in a successive step it is necessary to define some rules that permit to use the material parameters, whose variability has a definitely statistical behaviour, in a proper way when dealing with the design of a strengthening system for rammed earth constructions.

Nevertheless, the durability of jute fibers combined with earth matrix is neglected in this research work. Jute is a natural material and its behaviour has to be further investigated in particular with respect to durability through durability tests on jute fabric combined with earth matrix. The debonding phenomenon of the reinforcement system at the intrados of the arch should be further investigated

In order to verify the design effectiveness of the strengthening method further case studies should be analyzed and numerical models can be calibrated with the experimental results.